Evolutionary Diversification of Protein Functions: From Translation in Prokaryotes to Innate Immunity in Invertebrates

Dissertation zur Erlangung des
naturwissenschaftlichen Doktorgrades
der Bayerischen Julius-Maximilians-Universitaet Wuerzburg

Vorgelegt von

Carsten D. Prusko
aus
Wuerzburg

Wuerzburg 2006

Evolutionary Diversification of Protein Functions: From Translation in Prokaryotes to Innate Immunity in Invertebrates

Dissertation zur Erlangung des
naturwissenschaftlichen Doktorgrades
der Bayerischen Julius-Maximilians-Universitaet Wuerzburg

Vorgelegt von

Carsten D. Prusko
aus
Wuerzburg

Wuerzburg 2006

Eingereicht am: 08.06.2006

Bei der Fakultaet fuer Chemie und Pharmazie

1. Gutachter: Herr Prof. Dr. H. J. Gross

2. Gutachter: Frau Prof. Dr. H. Beier

der Dissertation

1. Pruefer: Herr Prof. Dr. H. J. Gross

2. Pruefer: Frau Prof. Dr. H. Beier

3. Pruefer: Herr Prof. Dr. J. Tautz

des oeffentlichen Promotionskolloquiums

Tag des oeffentlichen Promotionskolloquiums: 12.07.2006

Doktorurkunde ausgehaendigt am: .....

Erklaerung

Hiermit erklaere ich an Eides statt, dass ich die Dissertation „Evolutionary Diversification of Protein Functions: From Translation in Prokaryotes to Innate Immunity in Invertebrates“ selbstaendig angefertigt und keine anderen als die von mir angegebenen Quellen und Hilfsmittel benutzt habe.

Ich erklaere ausserdem, dass diese Dissertation weder in gleicher oder anderer Form bereits in einem anderen Pruefungsverfahren vorgelegen hat.

Ich habe frueher ausser den mit dem Zulassungsgesuch urkundlich vorgelegten Graden keine weiteren akademischen Grade erworben oder zu erwerben versucht.

Wuerzburg, den 08.06.2006

(Carsten D. Prusko)

Die vorliegende Arbeit wurde am Massachusetts Institute of Technology, Cambridge, USA, von September 2002 bis Maerz 2005, sowie am Institut fuer Biochemie der Bayerischen Julius-Maximilians-Universitaet Wuerzburg von April 2005 bis Juni 2006 unter der Anleitung von Herrn Prof. Dr. Hans-Joachim Gross durchgefuehrt.

Das Arbeiten mit rekombinanter DNA erfolgte entsprechend den Richtlinien zum Schutz vor Gefahren durch *in vitro*-neukombinierte Nucleinsaeuren des BMFT und mit Genehmigung der Zentralen Kommission fuer biologische Sicherheit beim Robert Koch Institut des Bundesgesundheitsamtes.

Dedicated to my Family

ACKNOWLEDGMENTS

Mein ganz besonderer Dank gilt Herrn Prof. Dr. Hans-Joachim Gross fuer seine ausserordentliche Unterstuetzung, seine Geduld und seinen Zuspruch waehrend des Verlaufes meiner Promotion. Durch seinen Einsatz und sein fortwaehrendes Interesse hat er massgeblich zum Erfolg dieser Arbeit beigetragen.

I wish to thank Prof. Dr. U. L. RajBhandary for giving me the opportunity to carry out large parts of this work in his laboratory. I greatly appreciate his support, his scientific training and his way of sharing his enthusiasm for the work, which was a big motivation.

Mein herzlicher Dank gilt Frau Prof. Dr. H. Beier fuer ihr persoenliches Engagement, ihr immerwaehrendes Interesse am Fortgang meiner Arbeit sowie fuer die fachlichen Ratschlaege und stete Bereitschaft zur wissenschaftlichen Diskussion.

Herrn Prof. Dr. J. Tautz moechte ich danken fuer die die Moeglichkeit, meine Arbeit an der Universitaet Wuerzburg fortfuehren zu koennen sowie fuer die finanzielle Unterstuetzung.

Herrn Prof. Dr. U. Fischer moechte ich fuer die Moeglichkeit danken, meine Arbeiten am Institut fuer Biochemie beenden zu koennen.

Bei Herrn Dr. S. Albert moechte ich speziell fuer die Einfuehrung in die Bioinformatik sowie fuer die aeusserst fruchtbare Zusammenarbeit im Laufe des letzten Jahres bedanken.

I am extremely grateful for the support and wonderful environment I got from my lab members at MIT, which was essential for me through my thesis. My special thanks go to Jae, Gayathri, Caroline and Sean for helpful comments and suggestions on this work.

Allen ehemaligen und aktuellen Mitarbeitern der Arbeitskreise Tautz, Rapp und Fischer danke ich fuer die freundliche Atmosphaere und die kollegiale Zusammenarbeit.

Andreas, Flo, Anna und Susanne danke ich fuer ihre Freundschaft und Verbundenheit ueber die Jahre sowie fuer die aufmunternden Worte, welche sicher zum Gelingen dieser Arbeit beigetragen haben.

Mike, Howie and Alex: “Halo it up”! I want to thank you guys for your friendship and support throughout the years as well as for the good times we had at 24/1.

Zum Schluss moechte ich mich von ganzem Herzen bei meiner Mutter und meinem Bruder fuer Ihre Liebe und Unterstuetzung bedanken, ohne die ich es nicht bis hierher geschafft haette.

VITA

Personal Data

- Name: **Carsten Dietmar Prusko**
- Day of birth: **07.05.1977**
- Place of birth: Wuerzburg, Germany
- Marital status: unmarried
- Citizenship: German

Education and military service

- **09/89 – 07/96** Droste-Huelshoff-Gymnasium, Berlin, Allgemeine Hochschulreife (Highschool diploma)
- **09/96 – 07/98** Jagdgeschwader 74 “Moelders”, Neuburg/Donau, Tour of duty

Academic education

- **11/98 – 09/02** **Diploma program**, Department of Biology, University of Wuerzburg, Wuerzburg, Germany
- 06/01 – 08/01 Massachusetts Institute of Technology, Cambridge, USA Research for the diploma thesis in the laboratory of Prof. Dr. U. L. RajBhandary; Title:” Study of the effect of temperature on the initiator activity of mutant *Escherichia coli* initiator tRNA”
- 09/02 Diploma in Biology
- **09/02 – 07/06** **Ph.D. program**, Department of Chemistry, University of Wuerzburg, Wuerzburg, Germany
  Title:” Evolutionary Diversification of Protein Functions: From Translation in Prokaryotes to Innate Immunity in Invertebrates”
- 09/02 – 03/05 Massachusetts Institute of Technology, Cambridge, USA Research for the doctoral thesis in the laboratory of Prof. Dr. U. L. RajBhandary
- 04/05 – 07/06 Institute for Biochemistry, University of Wuerzburg, Research for the doctoral thesis in the laboratory of Prof. Dr. H. Beier

Publications

1. Mayer, C.; Koehrer, C.; Kenny, E.; **Prusko, C.**; and RajBhandary, U. L. (2003), „Anticodon Sequence Mutants of *Escherichia coli* initiator tRNA: Effects of Over-production of Aminoacyl-tRNA Synthetase, Methionyl-tRNA Formyltransferase, and Initiation Factor 2 on Activity in Initiation", *Biochemistry*, Vol. 42, pp 4787-4799

2. Drapeau, M. D.; Albert, S.; Kucharski, R.; **Prusko, C.**; and Maleszka, R., „Evolution of the Yellow/ Major Royal Jelly Protein family and the emergence of social behavior in honeybees", *Genome Research*, submitted

TABLE OF CONTENTS

LIST OF FIGURES AND TABLES

Part I

Tables Pages

Part II

Figures Pages

LIST OF ABBREVIATIONS

2D	two-dimensional
3D	three-dimensional
Å	angstrom
λ	lambda
°C	degrees Celcius
%	percentage
% (w/v)	mass-volume percentage
% (v/v)	volume-volume percentage
µ-	micro-
µg	microgram
µl	microliter
µM	micromolar
A	adenine
A	alanine
A_λ	absorbance at λ wavelength
A. aegypti	*Aedes aegypti*
A. gambiae	*Anophilis gambiae*
A. mellifera	*Apis mellifera*
Aa	amino acid
AA	acrylamide
aaRS	aminoacyl-tRNA synthetase
AcOH	acetic acid
AMP	antimicrobial peptide
Ala	alanine
APS	ammoniumperoxo-disulfate
Asn	asparagines
Asp	aspartic acid
Arg	arginine
ATP	adenosine-5'-triphosphate
B. subtilis	*Bacillus subtilis*
B. mori	*Bombyx mori*
B. stearothermophilus	*Bacillus stearothermophilus*
B.st.	*Bacillus stearothermophilus*
bp	base-pair
BPB	bromphenol blue
BSA	bovine serum albumin
C	carbon
C	cytosine
C	cysteine
cfu	colony forming units
ChEWL	chicken egg-white lysozyme
Ci	Curie
CIP	calf intestine phosphatase
cm	centimeter
cpm	counts per minute
cryst.	crystallized
CTAB	cetyltrimethyl-ammoniumbromide
Cys	cysteine
C-terminal	carboxyl terminal
D	aspartic acid
D. melanogaster	*Drosophila melanogaster*
Da	Dalton
DEAE	diethylaminoethyl
ddH_2O	double distilled water
dH_2O	distilled water
DNA	deoxyribonucleic acid
dNTP	deoxynucleotide-5'-triphosphate
DTT	dithiothreitol
E	glutamic acid
E. coli	*Escherichia coli*
Eco	*Escherichia coli*
ECL	enhanced chemi-luminescent
EDTA	ethylene diamine tetraacetic acid
EF-G	elongation factor G
EF-Tu	elongation factor Tu
EM	electron microscopy
EMSA	electrophoretic mobility shift assay

F	phenylalanine
fAa	formylamino acid
Fig.	figure
fGln	formylglutamine
fIle	formylisoleucine
fMet	formylmethionine
fPhe	formylphenylalanine
fVal	formylvaline
fTHF	N^{10}-formyltetra-hydrofolate
fwr	forward
g	acceleration of gravity
g	gram
G	guanine
G	glycine
GDP	guanosine-5'-diphosphate
GlnRS	glutaminyl-tRNA synthetase
Gln	glutamine
Glu	glutamic acid
Gly	glycine
GTP	guanosine-5'-triphosphate
h	hour(s)
H	histidine
H	hydrogen
^3H	tritium (radioactive hydrogen isotope)
H_2O	water
HEPES	4-(2-hydroxyethyl)-1-Piperazineethane-sulfonic acid
His	histidine
HM	high molecular weight marker
HRP	horseradish peroxidase
I	isoleucine
IF1	initiation factor 1
IF2	initiation factor 2
IF3	initiation factor 3
Ig	immunoglobulin
IgG	immunoglobulin G
Ile	isoleucine
ILM	immuno lectin
IleRS	isoleucyl-tRNA synthetase
IMAC	immobilized metal affinity chromatography
Inj.	injection
IPTG	isopropyl-β-D-thiogalacto-pyranoside
JH	juvenile hormone
k-	kilo-
K	lycine
K_D	binding constant
K_D^{app}	apparent binding constant
k_{on}	association rate constant
k_{off}	dissociation rate constant
kb	kilo base
kDa	kiloDalton
L	liter
L	leucine
LB	Luria-Bertani
Leu	leucine
LPS	lipopolysaccharid
LM	low molecular weight marker
LSC	liquid scintillation counting
Lys	lysine
m-	milli-
M	methionine
M	Molarity (mole/L)
M^{-1}	per molar
M. flavus	*Micrococcus flavus*
mg	milligram
min	minute(s)
MetRS	methionyl-tRNA synthetase

Met	methionine
ml	milliliter
mM	millimolar
mRNA	messenger RNA
MTF	methionyl-tRNA transformylase
MW	molecular weight
n-	nano-
N	number
N	normality
N	asparagines
NAG	N-acetyl-glucosamine
NAM	N-acetyl-muramic acid
nm	nanometer
nM	nanomolar
NMR	nuclear magnetic resonance
nt	nucleotide
N-terminal	amino terminal
O	oxygen
OAc	acetate
p-	pico-
^{32}P	radioactive phosphor isotope
P	proline
pAb	polyclonal antibody
PAMP	pathogen associated molecular pattern
PAGE	polyacrylamide gel electrophoresis
PCR	polymerase chain reaction
Pell.	pellet
PGN	peptidoglycan
PGRP	peptidoglycan recognition protein
PGRP-L	long PGRP
PGRP-S	short PGRP
pH	negative base-10 logarithm of proton concentration
Phe	phenylalanine
PheRS	phenylalanyl-tRNA synthetase
pM	picomolar
PMSF	phenylmethyl-sulphonylfluoride
PNK	polynucleotide kinase
PO	phenoloxidase
PPO	prophenoloxidase
ppA	PPO-activating enzyme
Pro	proline
PRR	pattern-recognition receptor
psi	pounds per square inch
PTC	peptidyltransferase center
PTH	peptidyl-tRNA hydrolase
PVDF	polyvinylidinedifluride
Q	glutamine
R	arginine
RBS	ribosomal binding site
rev	reverse
RF1	release factor 1
RF2	release factor 2
RF3	release factor 3
RNA	ribonucleic acid
rpm	revolutions per minute
RRF	ribosome recycling factor
rRNA	ribosomal RNA
RNase	ribonuclease
RU	response unit
s	seconds
s^{-1}	per second
S	serine
^{35}S	radioactive sulfur isotope
SAP	shrimp alkaline phosphatase
SD	Shine-Dalgarno

SDS	sodiumdodecylsulfate
SelB	selenocysteinyl-tRNA-specific elongation factor
Ser	serine
SPR	surface plasmon resonance
Sup.	supernatant
T	thymine
T	threonine
T	temperature
T_m	melting temperature
TCA	trichloroacetic acid
TEMED	*N*,*N*,*N*',*N*'-tetra-methylethylene-diamine
Thr	threonine
Tris	trishydroxyl-methylaminomethane
tRNA	transfer RNA
$tRNA_x$	tRNA isoacceptor x
$tRNA^{fMet}$	initiator tRNA
$tRNA^{XXX}$	amino acid XXX accepting elongator tRNA
Trp	tryprophane
Tyr	tyrosine
U	unit
U	uracil
UTR	untranslated region
UV	ultra violet
v	volume
V	Volts
V	valine
Val	valine
ValRS	valyl-tRNA synthetase
vol.	volume
w	weight
W	tryptophane
w/	with
w/o	without
XCFF	xylene cyanol
Y	tyrosine

Part I

tRNA-protein interactions in the initiation of protein synthesis in Escherichia coli

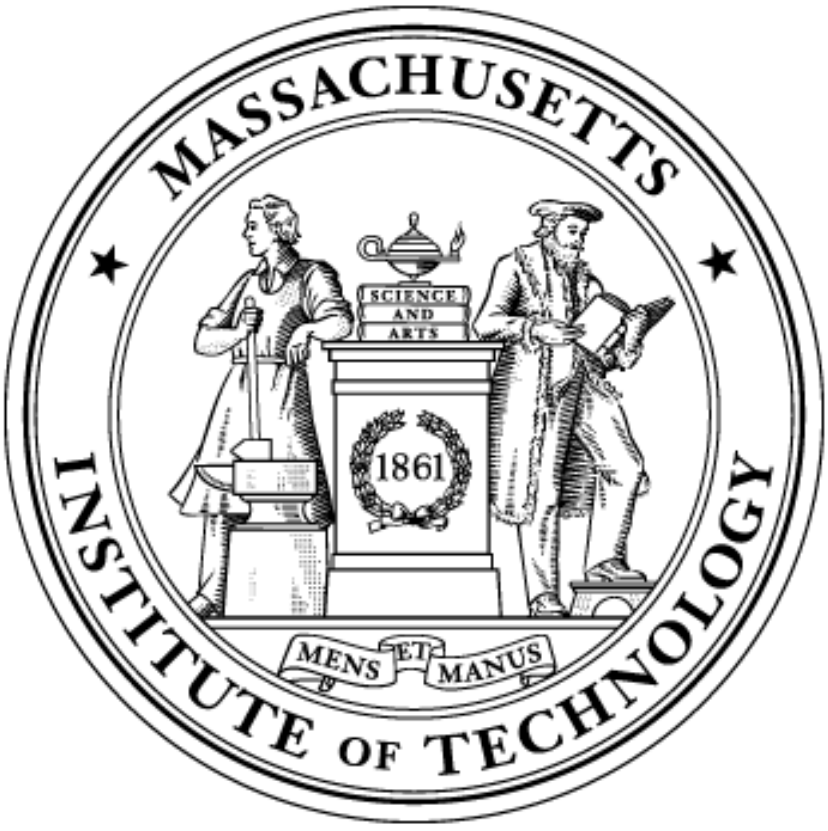

Chapter I

General introduction

1.1. The central dogma of molecular biology

The genome of an organism is the whole genetic information of an organism that is transmitted between generations. The term was first coined, in 1920, by Hans Winkler (Winkler, 1920). Although species may be completely different on a phenotypic level, the fundamental genetic principles are conserved (Cromie *et al.*, 2001; Lander *et al.*, 2001). In 1970, Nobel Laureate Francis Crick postulated the classical "central dogma of molecular biology" which describes the flow of genetic information from DNA to protein (Crick, 1970). The DNA (deoxyribonucleic acid) functions as the elementary template carrying the essential genetic code for every organism. The code is organized in so-called triplets or codons, comprised of three nucleotides coding specifically for a single amino acid (Matthaei and Nirenberg, 1961; Nishimura *et al.*, 1965). The genetic information is mediated through the transcription of the DNA into messenger RNA (ribonucleic acid, mRNA) that is processed and then translated into protein.

1.2. The translation process

Translation is the process by which the genetic information delivered as transcribed mRNA is translated into an active protein or an inactive precursor protein. This occurs on large macromolecular ribonucleoprotein complexes named ribosomes. The ribosome catalyses peptide bond formation between amino acids and synthesizes polypeptides based on the genetic information encoded on the mRNA. In general, translation can be divided into four consecutive stages: initiation, elongation, termination and the recycling of the ribosome to enter a new cycle of translation.
In the following sections the event of translation initiation in bacteria will be dissected by giving detailed structural and functional descriptions of the individual components. Finally a more general overview of the elongation, termination and ribosome recycling phases will be given.

1.3. Initiation of translation in prokaryotes

Translation initiation occurs in three steps and involves three initiation factors, namely IF1, IF2 and IF3. Mediated by initiation factors IF1 and IF3, mRNA and IF2, in a ternary complex with GTP and initiator tRNA (fMet-tRNA^{fMet}), bind to the 30S ribosomal subunit in an unknown and possibly random order, thereby forming a relatively unstable 30S pre-initiation complex. The Shine-Dalgarno (SD) sequence of canonical mRNAs interacts with the anti-SD sequence of the 16S ribosomal RNA (rRNA) (Yusupova *et al.*, 2001), adjusting the initiation codon in the ribosomal P-site. Positioning of the initiator tRNA in the P-site of the ribosome is promoted by IF2 (Gualerzi and Pon, 1990) and involves a three step process that are designated codon-independent binding, codon-dependent binding and fMet-tRNA adjustment (Tomsic *et al.*, 2000). The binding of fMet-tRNA is further stabilized by IF3 that also confers proofreading capability by destabilizing mismatched codon-anticodon interaction (Gualerzi *et al.*, 1977). The pre-initiation complex then undergoes a rate-limiting conformational change that promotes codon-anticodon interaction, forming the more stable 30S initiation complex (Pon and Gualerzi, 1984). In a process that is preceded by IF3 release, the 50S ribosomal subunit joins the 30S initiation complex in a manner that stimulates IF2 to hydrolyze its bound GTP to GDP and inorganic phosphate. This irreversible reaction conformationally rearranges the 30S subunit and releases IF1 and IF2, forming the 70S initiation complex ready for the repetitive cycles of polypeptide chain elongation (1.9.).

1.4. The ribosome

As mentioned above, ribosomes are large ribonucleoprotein complexes that are the catalyst of protein synthesis, highly conserved within all kingdoms of life. Approximately two-third of the ribosome consists of RNA and one-third consists of proteins. All ribosomal functions rely in large measures – in some cases entirely – on rRNA. In particular, rRNA is responsible for catalyzing peptide bond formation (Khaitovich *et al.*, 1999; Nissen *et al.*, 2000), contributes to mRNA decoding and to mRNA and tRNA translocation after peptide bond formation (Ogle and Ramakrishnan, 2005; Schmeing *et al.*, 2003), the ribosome is thus a ribozyme (Steitz and Moore, 2003). All ribosomes are composed of two subunits of unequal size (Fig. 1-1). Each

subunit possesses three binding sites for tRNA, designated the A (aminoacyl), which accepts incoming aminoacylated tRNA; P (peptidyl), which holds the tRNA with the nascent peptide chain; and E (exit), which holds the deacylated tRNA before it leaves the ribosome.

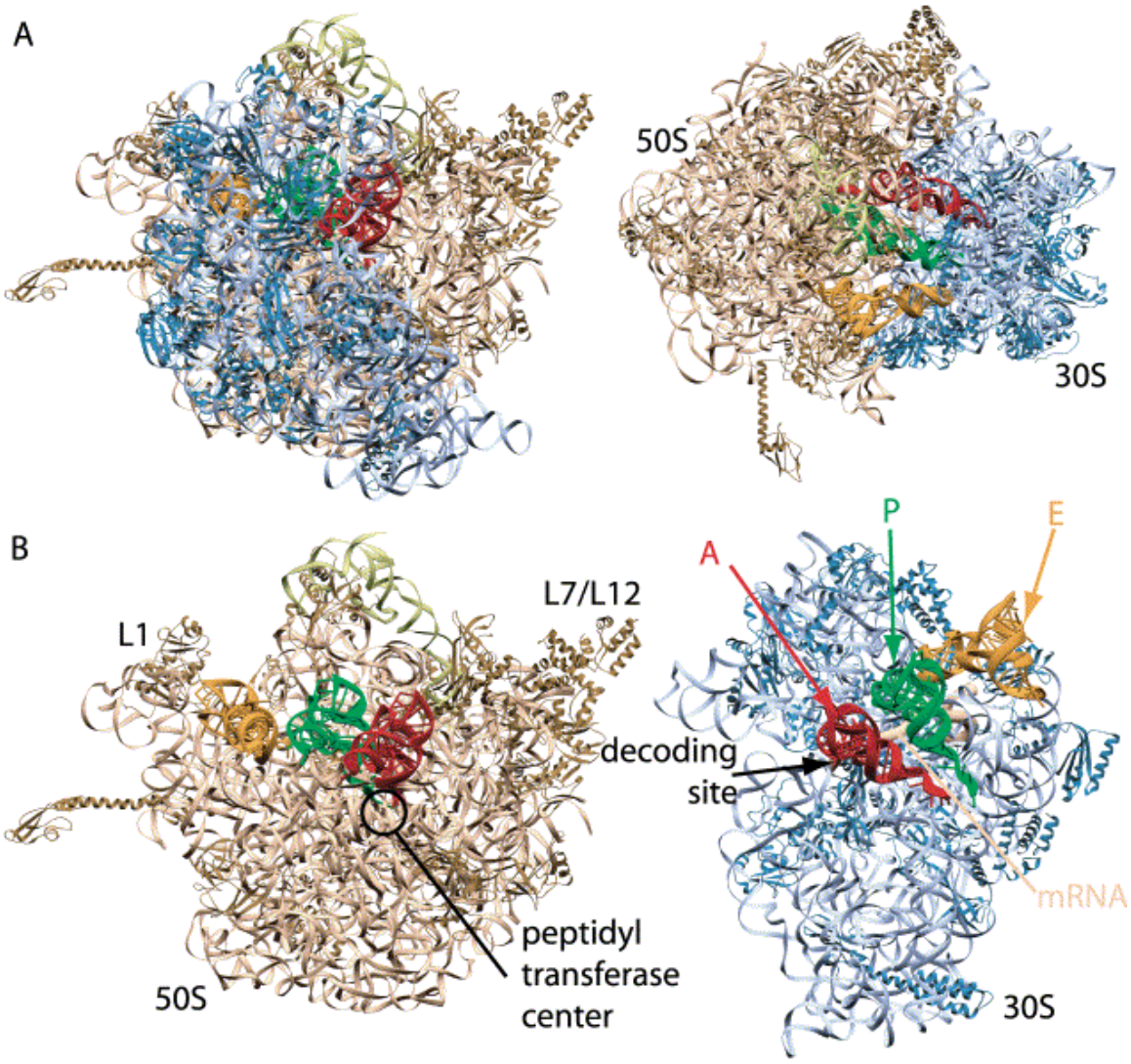

Fig. 1-1: Crysal structure of the bacterial ribosome

The structure of the 70S ribosome is shown (from Ramakrishnan, 2002). A) Two views of the 70S ribosome complexed with mRNA and tRNA (Yusupov et al., 2001), with the "top" view on the left and the view from the 30S side on the right. B) Exploded view of the 50S (left) and 30S (right) subunits in the 70S ribosome, showing the locations of A-, P-, and E-site tRNAs

In bacteria the small and large subunit are defined as 30S and 50S, respectively, based on their relative sedimentation rate. Once they are associated they form the

intact 70S ribosome. The small subunit is composed of 21 proteins and one RNA molecule of approximately 1500 nucleotides, sedimenting at 16S. The 16S rRNA forms four secondary structure domains (Noller and Woese, 1981), thereby determining the shape of the subunit (Schluenzen *et al.*, 2000; Wimberly *et al.*, 2000). Based on its overall structure the subunit can be divided into an upper third, called the head, that is connected by the neck to the body, composed of shoulder, platform, and base. A protrusion at the base is called the spur. The large subunit is composed of two rRNAs, sedimenting at 23S and 5S, and 34 proteins. The 23S rRNA (~ 2900 nucleotides) contributes six of the seven secondary-structure domains (Noller *et al.*, 1981), whereas the 5S rRNA (~ 120 nucleotides) is regarded as the seventh domain of the subunit. The 50S subunit consists of a round base with three protuberances called the L1 protuberance, the central protuberance, and the L7/L12 stalk. A tunnel, 100Å long and 15Å in diameter (Nissen *et al.*, 2000), extends from the region containing the A- and P-sites to the part of the large subunit from which the newly assembled polypeptide chain exits the ribosome.

There is a clear division of labor between the two subunits (Ramakrishnan, 2002). The small subunit binds the mRNA and the anticodon loop and stem of tRNA, and contributes to the fidelity of translation by monitoring the base pairing between the codon and the anticodon, a process known as decoding. During decoding, the selection of the correct tRNA is controlled by a combination of two mechanisms. The first is a steric recognition of the geometry of codon-anticodon base pairing, thereby discriminating against mismatches (Potapov, 1982). Recent crystallographic studies (Ogle *et al.*, 2001; Ogle *et al.*, 2003) showed that the binding of mRNA and cognate tRNA in the A site induces a conformational change in the conserved nucleotides A1492 and 1493 of helix 44 of 16S RNA, thereby causing the conserved base G530 to switch from *syn* to *anti* conformation. In their new conformation, A1493 directly interacts with the first base pair of the codon-anticodon helix, whereas A1492 and G350 tightly pack into the second base pair. The result of these induced changes is that the first two base pairs are closely monitored by the ribosome, in a way that allows discrimination between base pairing and mismatch. The third base pair or "wobble", however, is not monitored therefore accommodating for other base pairing geometries (Ramakrishnan, 2002). The second mechanism, often termed "kinetic proofreading", involves a stabilizing interaction between elongation factor Tu (EF-Tu), bound to aminoacyl-tRNA and GTP, and the ribosome (Pape *et al.*, 1999). The initially labile binding complex becomes stabilized as a result of the above described

conformational change. As a consequence the ribosome triggers the GTPase activity of EF-Tu (Rodnina *et al.*, 1995) resulting in the dissociation of the factor in its GDP bound state and a repositioning of the aminoacyl-tRNA, thereby promoting peptide bond formation. In case of incorrect base pairing, the ternary complex will dissociate from the ribosome more rapidly than either GTP hydrolysis or peptide bond formation can occur (Pape *et al.*, 1999). Therefore, there is no doubt that the ribosome plays a major roll in selectivity of tRNA (Ramakrishnan, 2002).

The large ribosomal subunit on the other end is mainly responsible for the peptide bond formation and protein release (Monro, 1967). The peptidyl transfer reaction, by which the α-amino group of an A-site tRNA attacks the carbonyl group of the peptidyl group which is attached to the P-site bound tRNA, occurs in the peptidyltransferase center (PTC). The PTC is located at the base of a cleft that binds the acceptor ends of the tRNA. It consists of some ribosomal proteins and the ribosomal RNA. In resent years crystallographic and biochemical studies have shown that the peptidyl transferase center comprised mainly of the 23S ribosomal RNA (Ban *et al.*, 2000; Nissen *et al.*, 2000; Spahn *et al.*, 2000) making the PTC a classical ribozyme (Steitz and Moore, 2003).

Although both subunits display individual functions and activities, protein synthesis only occurs in the context of a full constituted 70S ribosome. Upon 70S assembly the two subunits remain loosely associated through large numbers of intermolecular bridges, giving the ribosome its flexible character necessary to perform its task during elongation (Yusupov *et al.*, 2001). It was early proposed that both subunits are in motion and shift relatively to each other during translation (Bretscher, 1968), and that this mobility is an essential part of the mechanism of translocation (Spirin, 1969). Recent advances in X-ray crystallography made available high-resolution structures of intact 70S ribosome (Schuwirth *et al.*, 2005; Vila-Sanjurjo *et al.*, 2003; Yusupov *et al.*, 2001) giving new insight into the structural rearrangement during subunit association and elongation, respectively.

1.5. The messenger RNA

Translation is usually initiated by binding of the 30S ribosome to mRNA thereby selecting for a start codon. A highly conserved initiation codon is AUG, coding for the amino acid methionine. AUG is the most common start codon due to its ability to form the most stable interaction with the CAU anticodon in initiator tRNA (Mayer *et al.*, 2003). Weaker pairing with fMet-tRNA^{fMet} is part of the reason why translation is

less efficient when alternative start codons replace AUG. In *Escherichia coli* 83% of the genes use AUG as start codon, GUG and UUG occur at frequencies of 14% and 3%, respectively (Blattner *et al.*, 1997). The exceptional AUU start codon is only found in two genes of *E. coli* and has shown to have very low efficiency in initiation (Sussman *et al.*, 1996). One of these genes encodes the potentially toxic protein poly(A) polymerase (*pcnB*), which explains why translation must be restrained (Binns and Masters, 2002). The other encodes initiation factor 3 (*infC*).

Bacterial mRNAs are normally polycistronic messages, coding for more than one protein, and possess therefore multiple signals for initiation and termination. Thus, the correct selection of the initiation codon is of high importance since it sets the reading frame for the rest of the translation process. A major role in the selection process plays the 16S ribosomal RNA. A part of the mRNA that is covered by the ribosome in the initiation phase is located within the 5' untranslated region (5'UTR) upstream of the putative start codon and is called ribosomal binding site (RBS) (Steitz, 1969). The RBS contains a purine-rich sequence, known as Shine-Dalgarno (SD) sequence, which is complementary to, and base pairs with, a sequence near the 3' end of the 16S RNA (anti-SD) (Shine and Dalgarno, 1974; Steitz and Jakes, 1975). *E. coli* mRNAs have the SD sequence GGAGG positioned 7± nucleotides upstream of the start codon. In general the optimal spacing depends on exactly which bases at the 3' end of 16S RNA (3'-AUUCCUUCCAC…-5') participate in the interaction (Chen *et al.*, 1994). In most mRNAs, the standard 4 to 5 base pair SD interaction is strong enough to mediate efficient translation. However, a stronger-than-normal SD interaction does help, when the start codon is not AUG (Weyens *et al.*, 1988), or the initiation site is masked by secondary structure (de Smit and van Duin, 1994). Secondary structures are important regulatory elements in polycistronic mRNAs. They prevent translation initiation at AUG codons other than the putative initiation codon by sterically hindering binding of the 30S subunit. Interestingly, elongating 70S ribosomes display the remarkable ability to penetrate base paired structures (Lingelbach and Dobberstein, 1988; Sorensen *et al.*, 1989), thereby allowing initiation in the context of coupled translation (Kozak, 2005). Besides the SD sequence, A-rich motifs were frequently observed near the initiation site, especially between the SD and initiation codon, pinpointing towards a requirement of adenosines at particular positions for ribosomal binding (Chen *et al.*, 1994). Mutational analysis, however, did not reveal any significant effect on initiation efficiency (Ringquist *et al.*, 1992). Thus, it was proposed that these motifs might

play an important role in minimizing secondary structures (Kozak, 1999), thereby stimulating translation initiation.

Besides canonical mRNAs that contain the above described 5'UTR elements, bacteria also possess leaderless mRNA, albeit rare, with no more than ~40 identified in bacteria (Moll *et al.*, 2002). In leaderless mRNA the SD interaction is precluded because the mRNA starts at, or a few nucleotides 5' upstream of the initiation codon. Thus, binding to the ribosome involves probably a mechanism that is somewhat different from binding of canonical mRNA. One difference is that binding of leaderless mRNA is dependent on the presence of initiator tRNA, whereas canonical mRNAs bind independently of the initiator tRNA (Benelli *et al.*, 2003). A growing body of evidence supports the idea of a novel pathway in which translation of leaderless mRNAs begins with a 70S ribosome. It was shown that leaderless mRNA binds preferentially and more stably to 70S ribosome compared to 30S subunit (O'Donnell and Janssen, 2002; Udagawa *et al.*, 2004), and that chemically cross-linked 70S ribosomes were able to initiate leaderless but not canonical mRNAs (Moll *et al.*, 2004). These results rationalize the effects of initiation factors, where translation of leaderless mRNA is inhibited by IF3, which promotes 70S dissociation, and augmented by IF2, which stabilizes binding of fMet-tRNA^{fMet} (Grill *et al.*, 2000; Grill *et al.*, 2001; Tedin *et al.*, 1999).

1.6. The initiator tRNA

A central role in protein synthesis play small RNA molecules, so-called transfer RNAs (tRNAs), which serve as adaptor molecules that are loaded with their individual amino acid. tRNAs decode the message of mRNA by Watson-Crick base pairing between the codon on the mRNA and a complementary region on the tRNA, the anticodon (Clark *et al.*, 1968; Goodman *et al.*, 1968). The pairing of the mRNA codon to the tRNA anticodon is independent of the nature of the amino acid attached to the tRNA (Chapeville *et al.*, 1962), in other words, misacylation of a tRNA unavoidably leads to incorporation of a wrong amino acid into the protein. Therefore, the accuracy of the aminoacylation reaction, ensured by the aminoacyl-tRNA synthetase (aaRS), is of first importance in all living cells. For each of the 21 universal amino acids exists at least one tRNA as well as one cognate aminoacyl-tRNA synthetase (McClain, 1993; Schimmel, 1989). tRNAs display a distinct secondary and tertiary structure (Holley *et al.*, 1965; Rich and Kim, 1978). The cloverleaf fold, universal in

all cellular tRNAs, has three stem and loop regions, namely D-, T-, and anticodon region, a variable loop and acceptor stem with a single stranded N-C-C-A 3'-end. The defined structure of the tRNA enables them to interact very specifically with the components of the protein synthesis machinery.

In translation there are two different classes of tRNA required: i) the initiator tRNA that is used exclusively for the initiation step inserting methionine at the N-terminal end of a protein and ii) the elongator tRNAs that are used for insertion of amino acids into internal peptidic linkages (Kozak, 1983). In bacteria and in eukaryotic organelles such as mitochondria and chloroplasts, the initiator tRNAs are used as formylmethionyl-tRNA (Marcker and Sanger, 1964). In the *E. coli* genome two genes encode for initiator tRNA ($tRNA^{fMet}$) (Ikemura and Ozeki, 1977). The major fraction of cellular initiator tRNA ($tRNA_1^{fMet}$) is encoded by the *metZ* gene. Three identical copies of the gene occur in tandem repeats within the operon know as metZ operon (Kenri *et al.*, 1994). A relatively small fraction of $tRNA^{fMet}$ ($tRNA_2^{fMet}$) is encoded by the *metY* gene, located at the beginning of the *nusA/infB* operon (Ikemura and Ozeki, 1977; Ishii *et al.*, 1984).

During the initiation phase of translation the initiator tRNA is positioned at the P-site of the small subunit, whereas the elongator tRNAs are excluded from such binding. The discrimination of methionine-isoaccepting initiator and elongator tRNAs by the protein synthesis machinery is based mainly on structural differences. The initiator tRNA determinants are located in the anticodon stem, the acceptor stem, and the dihydrouridine (D)-stem (Fig. 1-2). A key feature of initiator tRNA shared by prokaryotes and eukaryotes are three highly conserved consecutive G:C base pairs found in the anticodon stem (Sigler, 1975; Sprinzl *et al.*, 1987). Mutational analysis of the anticodon stem region of *E. coli* $tRNA^{fMet}$ where one, two, or all three base pairs were changed to that of methionine-accepting elongator tRNA showed that these G:C base pairs are important for binding of $tRNA^{fMet}$ to the P-site of the ribosome (Seong and RajBhandary, 1987). X-ray crystallography suggests that the three G:C base pairs contribute to the unique structure of the anticodon loop (Woo *et al.*, 1980), thereby favoring P-site binding through a better fit. On the other hand alteration of the G:C base pairs to that of elongator $tRNA^{Met}$ favors A-site binding, enabling the initiator tRNA to act as elongator (Seong and RajBhandary, 1987). The observed structural uniqueness of the anticodon region of initiator tRNA was further confirmed by S1-nuclease mapping of *E. coli* $tRNA^{fMet}$ and $tRNA^{Met}$ (Seong and RajBhandary, 1987; Wrede *et al.*, 1979). Furthermore, it was shown that the three

G:C base pairs are important for IF3 recognition (Hartz *et al.*, 1990), whereas the binding to IF2 is not affected by changes (Seong and RajBhandary, 1987).

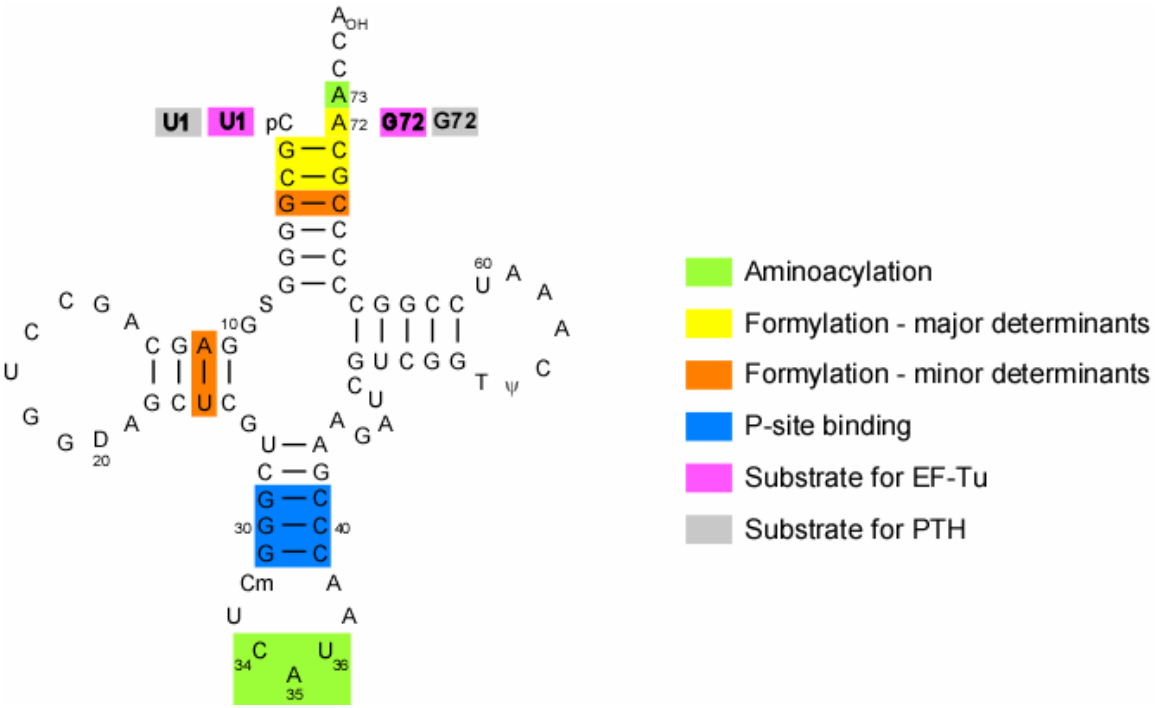

Fig. 1-2: Cloverleaf representation of *E. coli* initiator tRNA^{fMet}

The regions important for tRNA identity are highlighted. Details are given in the text. Modified figure from Mayer *et al.*, 2001.

Both, methionine-isoaccepting inititator and elongator tRNAs are aminoacylated by methionyl-tRNA synthetase (MetRS). MetRS interacts with part of the acceptor stem and the anticodon loop of the tRNA. The major determinant for MetRS in tRNA^{Met} binding is the anticodon. Extensive biochemical analyses have shown that the cytosine at the anticodon wobble position (C34) primarily determines the identity of methionine-isoaccepting tRNAs (Muramatsu *et al.*, 1988; Schulman and Pelka, 1988), and that the other two anticodon bases A35 and U36 are the second most important identity elements (Ghosh *et al.*, 1990). These findings were confirmed by recent crystallographic data of MetRS from *Aquifex aeolicus*, giving further insight into the mechanism of anticodon recognition by MetRS (Nakanishi *et al.*, 2005). A minor determinant is nucleotide A73, often call discriminator base, in the acceptor stem of methionyl-isoaccepting tRNAs as revealed by *in vitro* and *in vivo* analyses of mutant *E. coli* inititor tRNA (Lee *et al.*, 1992). Based on their results Lee and

coworkers concluded that the discriminator base rather contributes to the structure and flexibility of the 3' end of the acceptor stem than being involved in a direct interaction with MetRS.

Another structural feature in bacterial initiator tRNA is a conserved mismatch at the end of the acceptor stem between the 5' terminal nucleotide C1 and the corresponding nucleotide on the 3' site A72 (Delk and Rabinowitz, 1974; Dube *et al.*, 1968). The lack of a Watson-Crick base pair is important for specifying several distinctive properties. The mismatch is important for formylation of the initiator tRNA by methionyl-tRNA transformylate (MTF) (Lee *et al.*, 1992; Lee *et al.*, 1991). The enzyme catalyzes the transfer of a formyl group from N^{10}-formyltetrahydrofolate to the α-amino group of the methionine attached to $tRNA^{fMet}$. Formylation of Met-$tRNA^{fMet}$ is important for protein synthesis in eubacteria. Mutant initiator tRNAs defective in formylation are extremely poor in initiation of protein synthesis (Varshney and RajBhandary, 1992). Crystallographic studies of MTF in complex with fMet-$tRNA^{fMet}$ showed that the mismatch provides a 5-nucleotide long single-stranded acceptor arm on the 3'-end of the tRNA that is just long enough to reach the active site of MTF (Schmitt *et al.*, 1998). In addition to its requirement for MTF interaction, the mismatch has a function as negative determinant for EF-Tu and peptidyl-tRNA hydrolase (PTH), an enzyme which is responsible for hydrolyzing the ester linkage in N-aminoacyl-tRNA and peptidyl-tRNAs that have dissociated from the ribosome (Lee *et al.*, 1992; Schulman and Pelka, 1975). The absence of a base pair between nucleotide 1 and 72 prevents the aminoacylated initiator tRNA from binding to elongation factor EF-Tu (Seong *et al.*, 1989; Seong and RajBhandary, 1987), and protects fMet-$tRNA^{fMet}$ against hydrolytic cleavage by PTH.

Another structural feature unique in bacterial, mitochondrial, and chloroplast initiator tRNAs is a purin 11:pyrimidine 24 base pair instead of a pyrimidine 11:purin 24 base pair found in elongator tRNAs (Rich and RajBhandary, 1976). It was shown that the A11:U24 base pair plays a minor role in the interaction of MTF and fMet-$tRNA^{fMet}$ in *E. coli* (Lee *et al.*, 1991). Mutation of A11:U24 to C11:G24 results in a lower binding affinity towards MTF, however, when 3 of 4 base pairs in the D-stem including the A11:U24 base pair base pairs are mutated to sequences similar to that of *E. coli* $tRNA^{Gln}$ and yeast $tRNA^{Tyr}$ no effect on formylation is observed. Thus, it is suggested that a change of the A11:U24 base pair alters the local structure of the D-stem rather than affecting a direct interaction with MTF.

1.7. The initiation factor IF2

IF2 is the largest of three initiation factors. It is encoded by the *infB* gene that is part of the polycistronic *nusA/infB* operon. Transcription of *nusA/infB* operon occurs primarily from a promoter separated by three genes upstream from *infB*. This promoter is autogenously controlled by the translational product of *nusA* (Nakamura *et al.*, 1985; Plumbridge *et al.*, 1985). Three isoforms of IF2, i.e. IF2-α (97.3 kDa), IF2-β (79.7 kDa), and IF2-γ (78.8 kDa), exist in *E. coli* and other members of the family Enterobacteriaceae (Laursen *et al.*, 2002; Nyengaard *et al.*, 1991). The three isoforms are translated from three independent but in-frame translational start sites of the *infB* mRNA. Therefore, IF2-β and IF2-γ differ from IF2-α only by the absence of the first 157 and 164 amino acid residues, respectively (Mortensen *et al.*, 1995). It was shown that the presence of both the large and the smaller isoforms is required for optimal growth (Sacerdot *et al.*, 1992). In case of optimal growth conditions the cellular content of IF2-β and IF2-γ is close to the level of IF2-α (Howe and Hershey, 1983), however, the ratio of IF2-β and IF2-γ to IF2-α increases as a response to cold shock (Giuliodori *et al.*, 2004).

Based on interspecies homology IF2 can be divided into a conserved C-terminal region and a less highly conserved N-terminal region. Furthermore, biochemical and immunological studies led to a six-domain structural model of *E. coli* IF2 (Mortensen *et al.*, 1998) (Fig. 1-3A). The N-terminal region of IF2 is highly variable in both primary structure and length, and can be divided into three separate domains. Domain I contains a small subdomain, termed IF2N, of approximately 50 residues, found in all bacteria and some plastide IF2s. The structure of the subdomain has been solved by NMR spectroscopy and displays homology to the stem contact fold domains of methionyl- and glutaminyl-tRNA synthetases and the B5 domain of phenylalanine-tRNA synthetase (Laursen *et al.*, 2003). However, no specific function has been assigned to the IF2N domain. The IF2N domain is connected to the conserved C-terminal domains by a highly flexible linker region (Laursen *et al.*, 2004). Macromolecular interactions of the domains of the N-terminal region have been demonstrated only in *E. coli*, where a fragment consisting of the combined domains I and II, but not a fragment of isolated domain I, binds to the 30S ribosomal subunit (Moreno *et al.*, 1999; Moreno *et al.*, 1998). Furthermore, it was observed that domains I and II of *E. coli* IF2 interact with the *infB* mRNA (Laursen *et al.*, 2002). However, the functional importance of the N-terminal region remains

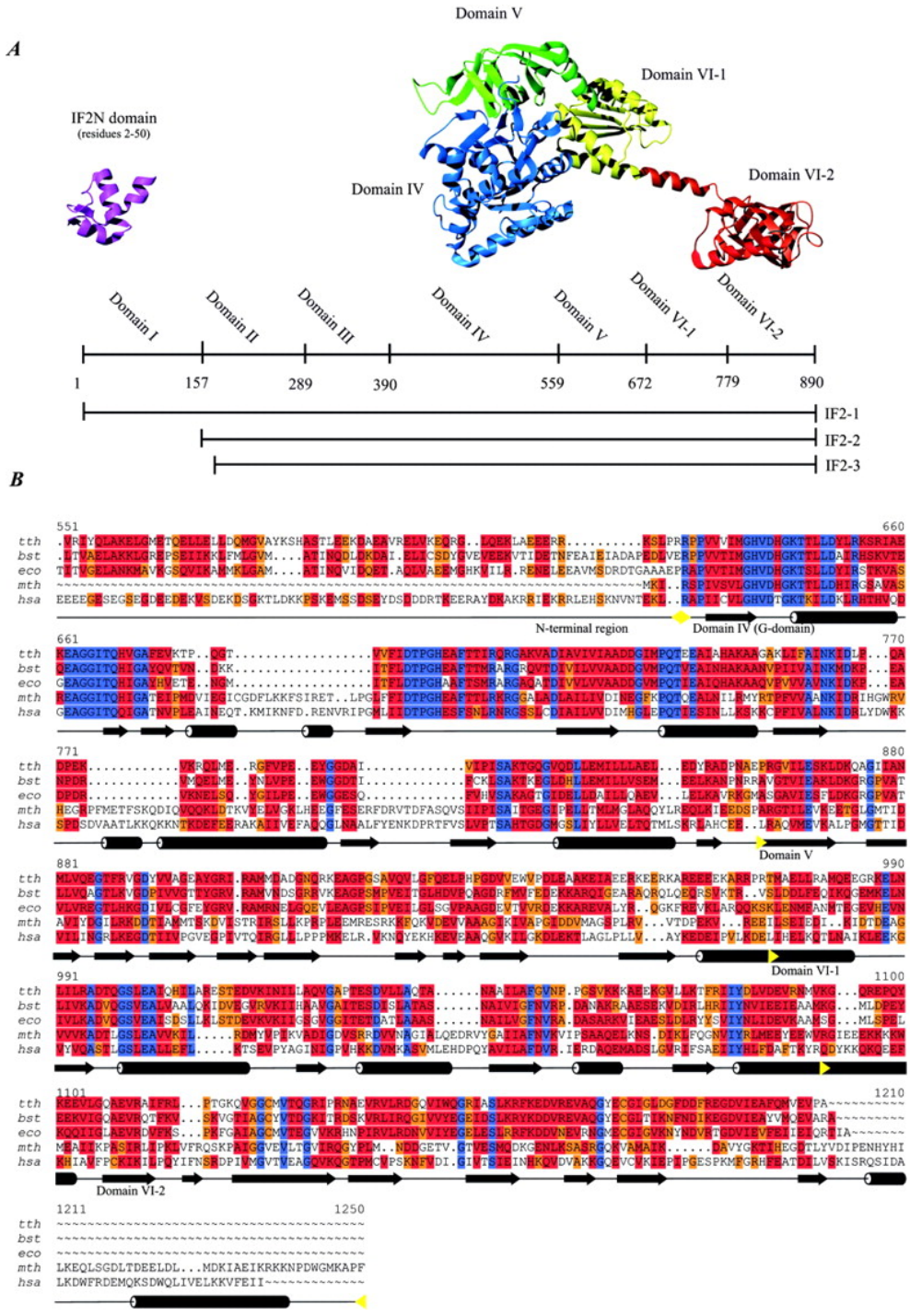

Fig. 1-3: IF2 and structural homologues

A) Schematic representation of the E. coli IF2 primary structure. The domain boundaries and the lengths of the three IF2 isoforms are indicate. Ribbon diagrams of the structure of the IF2N domain from E. coli and the IF2 homologue aIF5B from M. thermoautotrophicum are shown. The E. coli domain nomenclature is used. B) Sequence alignment of selected bacterial IF2 and archaeal and eukaryotic homologues (figure from Laursen et al., 2005).

unsolved. The conserved C-terminal region of the protein consists of domains IV to VI (Mortensen *et al.*, 1998). Although no direct tertiary-structure information is available for domains IV to VI of *E.coli* IF2, the structure of the homologous protein aIF5B from the archaeon *Methanobacterium thermoautotrophicum* has been solved by X-ray crystallography (Roll-Mecak *et al.*, 2000). Based on amino acid sequence homology a similar structure was predicted for the C-terminal domains of *E. coli*. The N-terminal Domain VI represents a GTP binding motif, which is shared with four other proteins involved in translation, i.e. EF-Tu, EF-G, RF3, and SelB (Rodnina *et al.*, 2000; Vetter and Wittinghofer, 2001). Adjacent to the G-domain is a β-barrel (domain V) and an αβα-structure (domain VI-I) that is connected via a long α-helix ending with a second β-barrel (domain VI-II).

There are several functions attributed to IF2. One of the main properties is the recognition and binding of fMet-tRNA^{fMet}, and the stimulation of binding of the latter to the ribosomal P-site. The direct mechanism of this process is still unknown and discussed controversially. One hypothesis is that IF2 in complex with the initiating 30S ribosomal subunit helps select the fMet-tRNA over other tRNAs (Gualerzi and Pon, 1990). Combined *in vitro* and *in vivo* studies using mutant initiator tRNAs, however, support the view that IF2 acts as a carrier of fMet-tRNA to the 30S ribosome (Mangroo and RajBhandary, 1995; Wu and RajBhandary, 1997), much as EF-Tu does for aminoacyl-tRNAs to the 70S ribosome (Kozak, 1999). Formation of the binary complex is strongly dependent on the formylation of Met-tRNA^{fMet} (Sundari *et al.*, 1976) but independent of GTP (Pon *et al.*, 1985). It was shown that IF2 will form a complex with the initiator tRNA or any other aminoacyl-tRNA as long as the amino group of the amino acid attached is acylated (e.g. formylgroup or acylgroup) (Leon *et al.*, 1979). Thus, the presence of an N-blocked amino acid such as formylmethionine is an important determinant for IF2 binding of fMet-tRNA (Sundari *et al.*, 1976). Furthermore, *in vivo* and *in vitro* experiments have shown that the binding affinity of IF2 towards the initiator tRNA is affected by the nature of the amino acid attached to tRNA^{fMet} (Mayer *et al.*, 2003). In these studies IF2 displayed a high preference for formyl-methionine compared to weak binding and poor initiation efficiency when formyl-glutamine was attached to tRNA^{fMet}.

On a structural basis the binding of IF2 to fMet-tRNA^{fMet} has been studied extensively by mutagenesis as well as Raman and NMR spectroscopy (Guenneugues *et al.*, 2000; Krafft *et al.*, 2000; Meunier *et al.*, 2000; Misselwitz *et al.*, 1999). The main interaction involves the most C-terminal domain VI-II and the acceptor end of fMet-

$tRNA^{fMet}$. Binding studies revealed that the acceptor hexanucleotide CAACCA-fMet has almost the same affinity for IF2 as the intact fMet-tRNA (Guenneugues *et al.*, 2000). Concerning IF2, a combination of NMR spectroscopy and genetic approaches identified functionally essential residues of *Bacillus stearothermophilus* IF2 involved in the interaction with fMet-$tRNA^{fMet}$, i.e. C668, K699, R700, Y701, K702, E713, C714, and G715 (Guenneugues *et al.*, 2000; Spurio *et al.*, 2000). Cross-linking experiments further indicated interactions between residues N611 to R645 (domain V) of *E. coli* IF2 and the T-stem of fMet-$tRNA^{fMet}$ as well as residues W215 to R237 (domain II) and the anticodon stem of the initiator tRNA (Wakao *et al.*, 1989; Yusupova *et al.*, 1996). Finally, fMet-$tRNA^{fMet}$ protects a position in domain V of *B. stearothermophilus* IF2 agains digestion by trypsin (Severini *et al.*, 1992).

The role of the GTPase activity of IF2 has been a matter of debate for decades. The crucial importance of GTP hydrolysis in translation initiation and its direct relation to cell viability have been shown by several studies of G-domain mutants of IF2 (Laalami *et al.*, 1994; Larigauderie *et al.*, 2000; Laursen *et al.*, 2003; Luchin *et al.*, 1999). Hydrolysis of GTP has been suggested to be important for the release of IF2 from the 70S initiation complex (Lelong *et al.*, 1970; Lockwood *et al.*, 1972), and for the adjustment of the initiator tRNA in the ribosomal P-site (La Teana *et al.*, 1996). A recent study of initiation complex formation by using stopped-flow experiments with light scattering showed that the GTP-bound form of IF2 accelerates association of the ribosomal subunits and that GTP hydrolysis accelerates ejection of IF2 from the 70S (Antoun *et al.*, 2003). Comparison of the aIF5B structure in the GDP and GTP forms indicated that a sizable conformational change in the switch 2 region of the active site on the G-domain occurs upon GTP binding (Roll-Mecak *et al.*, 2000). Antoun and coworkers further showed that the GTP-bound form of IF2 is strongly stabilized by fMet-$tRNA^{fMet}$. Based on these findings a two-conformation model was proposed: one conformation with high affinity to GTP and the 50S subunit promoting 70S complex formation, and the GDP conformation with low affinity to GTP and 50S subunit resulting in a rapid dissociation of the factor form the post-initiation ribosome. Despite new insights further studies are needed to achieve a detailed understanding of the role of GTP hydrolysis in the translation initiation event.

In terms of ribosomal interaction, IF2 is the only initiation factor that displays a relatively high and specific affinity for both ribosomal subunits. Using various truncation mutants of IF2 in binding reactions with 30S and 50S subunits, Moreno and coworkers delineated the specific domains of IF2 responsible for binding of the

ribosomal subunits (Moreno *et al.*, 1999; Moreno *et al.*, 1998). Accordingly, the G-domain and domain III of IF2 interact with the 50S subunit, while portions of domain II, as well as the N-terminal domain interact with the 30S subunit. A more detailed topographical localization of IF2 on the 70S ribosome was obtained by cleavage of ribosomal RNA using chemical nucleases tethered to cysteine residues at specific sites of IF2 (Marzi *et al.*, 2003). No cleavage of the rRNA was observed when IF2 was bound to 30S ribosomal subunits or to the complete 30S initiation complex. However, 16S rRNA was cleaved when IF2 was bound to the 70S initiation complex. The result indicated a delocalization of IF2 during the transition from the 30S to the 70S initiation complex, promoted through the hydrolysis of GTP. The overall idea of intra- and intermolecular rearrangements of IF2 in complex with the ribosome found further support by cryo-electron microscopy of a reconstituted *E. coli* 70S initiation complex (Allen *et al.*, 2005).

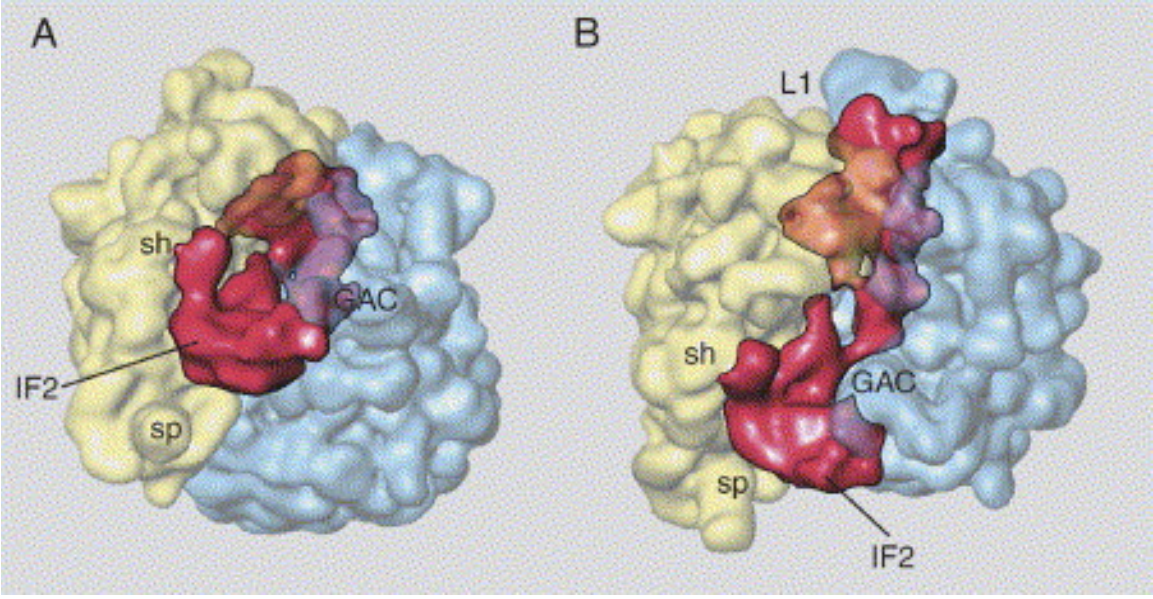

Fig. 1-4: Cryo-EM structure of the GDPNP-stalled *E. coli* 70S ribosome with IF2

A) In this view, the N-terminal domains of IF2 are in the foreground. These interact with the 50S subunit (blue) at the GTPase-associated center (GAC) and with the 30S subunit (yellow) over a large surface on the intersubunit side of the shoulder (sh). B) The initiation complex has, with respect, to A), been rotated by ~45° around a horizontal axis and ~30° around the long axis of the ligand density. Additional labelled features also indicated the spur of the 30S (sp) subunit and the L1 stalk (L1) (figure from Allen *et al.*, 2005).

1.8. The initiation factors IF1 and IF3

IF1 is the smallest of the three bacterial initiation factors with a molecular mass of 8.2 kDa in *E. coli*. It is encoded by the infA gene (Sands *et al.*, 1987). The transcription is not physically linked to any other genes and is controlled by two promoters leading to monocistronic mRNAs (Cummings *et al.*, 1991). The protein product is a small β barrel RNA-binding protein consisting of five β strands and a loop connecting strands 3 and 4 containing a short 3_{10} helix endowed with high flexibility (Sette *et al.*, 1997). IF1 contains a highly conserved oligonucleotide binding fold that can bee found in other RNA binding proteins. Proteins with IF1-like structure and function are present in all three kingdoms of life.

The binding of IF1 to the 30S ribosomal subunit has been extensively mapped by biochemical and NMR analyses (Celano *et al.*, 1988; Sette *et al.*, 1997). The data indicate that IF1 binds in a cleft between the 530 loop and helix 44 of 16S RNA and ribosomal protein S12. These findings were further supported by X-ray crystallography of the IF1-30S complex from *Thermus thermophilus* (Carter *et al.*, 2001). The crystal structure shows that IF1 binds the A-site of the 30S subunit, thereby preventing A-site binding of tRNAs during translation initiation. The interaction is mainly electrostatic, involving the positively charged surface of IF1 and the two abovementioned ribosomal structures. The location of IF1 on the ribosomal subunit rationalizes the effect of protection towards chemical modification of nucleotides A1492, A1493 and G350 (Moazed *et al.*, 1995). Mutational analysis showed that the C1408-G1494 base pair and the three adenosines A1408, A1492, and 1493 are required for optimal binding (Dahlquist and Puglisi, 2000). Furthermore, the crystal structure provided new insight into the mechanism of action of IF1. Upon binding, IF1 inserts the loop containing residues 17 to 25 into helix 44 of the small subunit, thereby causing bases A1492 and 1493 to flip out in a non-stacked conformation and inducing a conformational change over a long distance of the subunit. It is though that this conformational change represents the transition state in the equilibrium between subunit association and dissociation (Ramakrishnan, 2002).

Several functions have been attributed to IF1. It affects the dissociation and association kinetics of 70S ribosomes (Dottavio-Martin *et al.*, 1979), primarily through the stimulating effect on the activity of IF2 and IF3 (Pon and Gualerzi, 1984). On the one hand it favors ribosome dissociation activity of IF3 and stimulates the affinity of IF2 for the ribosome by favoring its binding to the 30S subunit.

Interaction between IF2 and the ribosomal subunit is favored when IF1 is bound, and the release of IF2 is indirectly promoted when IF1 is ejected. It is thought that the influence of IF1 on the affinity of IF2 for the ribosomal subunit is either a result of a physical contact between the two factors as suggested by cross-linking studies (Boileau *et al.*, 1983) and phylogenetic comparisons (Choi *et al.*, 2000), or more indirectly where IF1 ejection induces a conformational change of the 30S subunit thereby weakening the interaction of IF2 with the 70S initiation complex (Stringer *et al.*, 1977).

Another factor required for initiation is IF3. Although not universally conserved, the 20.4 kDa large protein is essential for cell viability in *E. coli* (Olsson *et al.*, 1996; Sacerdot *et al.*, 1982). The 180 amino acid long initiation factor is encoded by the *infC* gene that is part of the *infC-rpmI-rplT* operon coding also for the two ribosomal proteins L35 and L20 (Lesage *et al.*, 1990). The genes are transcribed by four promoters and terminated by two transcriptional terminators. At the translational level, the expression of IF3 underlies an autoregulatory mechanism. The initiation codon on the infC mRNA is the unusual AUU codon. IF3 disfavors initiation at non-cognate initiation codons and hence represses the expression of its own gene (Butler *et al.*, 1986). IF3 is composed of two structural domains of approximately equal size (Biou *et al.*, 1995; Fortier *et al.*, 1994; Garcia *et al.*, 1995). The two domains, called IF3N and IF3C, are separated by a long and flexible linker (Hua and Raleigh, 1998; Moreau *et al.*, 1997). It was shown that the ~ 45Å lysine-rich linker is essential for IF3 function, but its length and chemical composition can be varied without altering IF3 activity (de Cock *et al.*, 1999). The IF3N domain consists of a globular α/β-fold, with helix α1 packed against a mixed five-strand β-sheet. This fold is followed linker helix α2, which connects IF3N with IF3C. IF3C consists of a two-layer α/β sandwich fold composed of a four-strand mixed β-sheet packed against two parallel α-helices. Both domains have the ability to move (Moreau *et al.*, 1997) and bind to the 30S ribosomal subunit (Sette *et al.*, 1999).

IF3 performs several different functions. First, its binding to the 30S subunit prevents association of the ribosomal subunits by blocking binding of the 50S (Grunberg-Manago *et al.*, 1975). This essential function ensures a free pool of 30S subunits thereby stimulating 30S initiation complex formation, the rate limiting step in translation. Second, IF3 is involved in the adjustment of the mRNA from the standby site to the decoding P-site of the 30S subunit (Lesage *et al.*, 1990), thereby stimulating the rapid formation of codon-anticodon interaction at the P-site (Gualerzi

et al., 1977; Wintermeyer and Gualerzi, 1983). Third, it controls initiation fidelity by monitoring the codon-anticodon interaction, thereby promoting dissociation of initiation complexes with an incorrectly bound non-initiator tRNA (Hartz *et al.*, 1990; Hartz *et al.*, 1989) and complexes with triplets other than AUG, GUG and UUG in the ribosomal P-site (Haggerty and Lovett, 1997; Meinnel *et al.*, 1999; Sussman *et al.*, 1996). The mechanism by which IF3 facilitates its fidelity function is of controversial debate. One model suggest that IF3 directly inspects the codon-anticodon base pair and/or anticodon stem loop of P-site bound tRNA (Hartz *et al.*, 1990; Meinnel *et al.*, 1999), whereas the other proposes a more indirect inspection by factor-induced conformational change of the 30S subunit (Pon and Gualerzi, 1974; Pon *et al.*, 1982). The idea of a more indirect interaction finds further support by data obtained from cryo-electron microscopy (McCutcheon *et al.*, 1999) and X-ray crystallography (Pioletti *et al.*, 2001). Both studies show that the location of IF3 on the 30S subunit is too far away from the ribosomal decoding site and the anticodon stem of P-site bound tRNA to enable any physical contact with either structure. In addition, a direct interaction is rather difficult since the codon-anticodon interaction and the anticodon stem are buried within the 30S structure (Cate *et al.*, 1999). Finally, a role of IF3 in ribosome recycling was proposed. It was observed to enhance the dissociation of deacylated tRNAs from post-termination complexes and to dissociate 70S ribosomes into subunits (Hirokawa *et al.*, 2002; Karimi *et al.*, 1999).

All functions of the native IF3 can be accomplished by the isolated IF3C domain *in vitro*, while the IF3N domain probably serves the purpose of modulating the thermodynamic stability of IF3-30S complexes (Petrelli *et al.*, 2001). Although no autonomous function could be attributed to IF3N, Petrelli and coworkers observed that the ribosome affinity of the IF3C domain is lowered by two orders of magnitude in the absence of IF3N. Site-directed mutagenesis was used to map the active site of the IF3C domain (Petrelli *et al.*, 2003). It revealed that arginines at positions 99, 112, 116, 147, and 168 are important for the binding to the 30S ribosomal subunit. The ability of IF3 to dissociate the ribosome into subunits was affected mainly by mutations of R112 and R147. The stimulation of dissociation of pseudo-initiation complex, with non-initiator tRNA bound, was mainly affected by mutations of R99 and R112, whereas dissociation of non-canonical initiation complexes, with initiation codons other than AUG, GUG, and UUG, was no affected by any abovementioned mutations. Stimulation of translation initiation was mainly affected by mutations of arginine residues 116 and 129. Finally, the repositioning of the mRNA from the

standby site to the P-decoding site was affected weakly by mutations of R129, R131, R133, R147, and R169, indicating that IF3C contains two active surfaces, one embedded in the 30S subunit and the other facing the mRNA (Petrelli *et al.*, 2003).

1.9. Elongation, termination and ribosome recycling

Once the 70S initiation complex is formed the ribosome is ready for the repetitive cycles of elongation, a process in which one amino acid after the other is attached to the nascent polypeptide chain. The ribosome elongates the polypeptide chains in a three-stage reaction cycle. Aminoacyl-tRNA is delivered to the ribosome in a ternary complex with elongation factor Tu (EF-Tu) and GTP. The stepwise movement of aminoacyl-tRNA from EF-Tu into the ribosomal A-site entails a number of intermediates (Rodnina *et al.*, 2005). The ribosome recognizes the correct aminoacyl-tRNA through shape discrimination of the codon-anticodon duplex, and regulates the rates of GTP hydrolysis by EF-Tu and aminoacyl-tRNA accommodation in the A-site by an induced fit mechanism (Rodnina and Wintermeyer, 2001). The ribosome-dependent GTP hydrolysis triggers a large conformational change in EF-Tu that promotes the dissociation of the factor from the ribosome. Following release, EF-Tu·GDP becomes regenerated to EF-Tu·GTP by guanine exchange factor EF-Ts (Rodnina and Wintermeyer, 2001). The release of EF-Tu leads to repositioning of aminoacyl-tRNA in the A-site promoting the rapid catalysis of peptide bond formation. The polypeptide chain that was attached to the tRNA in the P-site is transferred through a nucleophilic displacement to the amino group of the 3’ linked aminoacyl-tRNA in the A-site. Once the peptide bond formation has occurred, tRNAs and mRNA are translocated through coupled movements on the ribosome. This process involves the translocation of peptidyl-tRNA from the A-site to the P-site. During the movement, the mRNA is carried along with the tRNA, and deacylated tRNA dissociates from the P-site via the exit (E)-site (Wintermeyer *et al.*, 2004).
Translocation requires the elongation factor G (EF-G) that binds the ribosome in a complex with GTP. Several mechanisms for translocation have been proposed. According to the classical model binding of EF-G induces the translocation of the peptidy-tRNA from the A-site to the P-site. This step is followed by GTP hydrolysis resulting in the release of EF-G·GDP from the ribosome (Inoue-Yokosawa *et al.*, 1974). Footprinting experiments on 16S and 23S ribosomal RNA were used to examine the occupancy of the tRNA binding sites and led to a two-step hybrid site

model by Moazed and Noller (Moazed and Noller, 1989; Moazed and Noller, 1989). It was shown that the CCA end of peptidyl-tRNA moves spontaneously from the P-site to the E-site of 23S rRNA upon peptide bond formation, while remaining in the P-site with respect to 16S rRNA. This results in a hybrid site of binding, called the P/E-site. The same occurs for aminoacyl-tRNA in the A-site leading to a A/P-hybrid site. This spontaneous shift was shown to be independent of factors and GTP, respectively. In the following EF-G and GTP-dependent step, both tRNAs and mRNA move relatively to 16S rRNA, leading to a non-hybrid state of the tRNAs. The hybrid site model implies that there is relative motion between the 50S and 30S subunit during translocation, a fact that has been discussed earlier. A more controversial model for translocation was proposed by Rodnina and coworkers (Rodnina *et al.*, 1997). The so-called motor model is based on steady state kinetic experiments showing that GTP hydrolysis occurs before translocation and accelerates translocation more than 50-fold relative to that of non-hydrolysable analogs. It was suggested that a conformational transition in EF-G itself is in some way coupled to translocation. Instead of viewing EF-G as a small G-protein, where the action, here translocation, is carried out by the factor in its active GTP form followed by dissociation of the inactive GDP form, EF-G was suggested to act as a motor protein where the energy of hydrolysis is channeled into the translocation event. Finally, a combination of cryo-electron microscopy and biochemical analysis led to a more dynamic neoclassical model (Zavialov *et al.*, 2005) where the ribosome plays a pivotal role as guanine-nucleotide exchange factor. It was suggested that EF-G enters the pre-termination ribosome in the GDP-favoring form, and that EF-G·GDP drives the ribosome from its relaxed state with full binding sites for three tRNAs to a twisted conformation with hybrid sites for two tRNAs. Furthermore it is thought that the ribosome-dependent exchange of GDP to GTP promotes a switch of the EF-G conformation that brings the ribosome from the trans-termination state to the post-termination state, thereby completing the translocation event.

The elongation cycle is repeated until the entire coding sequence of the mRNA is translated and a termination codon appears in the decoding site. The final step in protein synthesis is the hydrolysis of the ester bond that connects the peptide chain with the tRNA in the P-site and subsequent release of the finished protein (Zavialov *et al.*, 2001). This is facilitated by one of the class-I release factors RF1 or RF2 (Kisselev *et al.*, 2003), which recognize the stop codons UAG, UAA and UGA, UAA, respectively. Binding of a class-I release factor to a stop codon in the ribosomal A-

site triggers hydrolysis. Genetic and biochemical studies indicate that a universally conserved Gly-Gly-Gln (GGQ) motif interacts with the peptidy-transferase center on the 50S ribosomal subunit, thereby inducing protein release from the ribosome (Kisselev *et al.*, 2003; Mora *et al.*, 2003; Zavialov *et al.*, 2002). Furthermore, two variants of another motif of bacterial release factors were identified. Pro-Ala-Thr (PAT) in RF1 and Ser-Pro-Phe (SPF) in RF2 that recognize stop codons by direct interaction with the mRNA in the decoding site. Taken together, these experiments suggest that termination of protein synthesis requires that each of the release factors can interact simultaneously with the two functional centers on the ribosome. Although the structure of RF2 is of compact nature (Vestergaard *et al.*, 2001) that would make a simultaneous interaction with both peptidy-transferase center and decoding site impossible, cryo-EM studies of RF2 in pre- and post-termination complexes with the ribosome revealed an open conformation for RF2 that allows the GGQ motif to reach the PTC, and at the same time the SPF motif to contact the stop codon (Rawat *et al.*, 2003). Thus it was hypothesized that binding of the SPF motif to the cognate stop codon in the decoding site unfolds the structure of the factor, thereby allowing the GGQ motif to make contact with the PTC. After the peptide release the class-I release factor is removed from the ribosome with the help of a class-II release factor, the G-protein RF3 (Freistroffer *et al.*, 1997). Free RF3 in the GDP form enters the ribosome, and GDP on RF3 dissociates rapidly when the post-termination complex contains a class-I release factor (Zavialov *et al.*, 2001) which leads to a stable complex. Upon release of the peptide chain from the P-site bound tRNA, GTP can rapidly bind to RF3 and promotes dissociation of the class-I release factor (Zavialov *et al.*, 2002). It was proposed that RF3 in the GTP form drives the ribosome into the same conformation as does EF-G·GTP, resulting in a ribosomal state with strong binding to RF3·GTP and low affinity for RF1 or RF2 that leads to a rapid dissociation of the class-I RFs from the ribosome (Zavialov and Ehrenberg, 2003). The following hydrolysis of GTP dissociates the class-II release factor.

The final step in protein synthesis is the disassembly of the post-termination complex whereby the ribosome is situated on the mRNA with the termination codon in the A-site and a deacylated tRNA on either P- or E-site (Kaji *et al.*, 1998). The 70S ribosomes are dissociated into the 30S and 50S subunits by cooperative action of ribosome recycling factor (RRF), EF-G, and IF3. However, the exact mechanism for this event remains obscure. Based on its crystal structure it has been proposed that RRF is a structural and functional mimic of tRNAs (Selmer *et al.*, 1999). It was

thought that recycling of post-termination ribosomes is similar to translocation carried out by EF-G. Accordingly, the action of EF-G could bring RRF into the P-site thereby displacing the deacylated tRNA from the P-site to the E-site, which then dissociates rapidly from the ribosome. However, chemical footprinting and cryo-EM studies of RRF·ribosome complexes showed that RRF does not bind to the A-site (Agrawal *et al.*, 2004; Lancaster *et al.*, 2002). Instead a mechanism was proposed where the ribosome acts as a guanine-nucleotide exchange factor for EF-G (Zavialov *et al.*, 2005). Exchange of GDP to GTP on EF-G leads to an altered conformation of RRF in such a way that favors binding of both factors to the 50S subunit rather than 70S ribosome, thereby splitting the ribosomal subunits apart. Further, it was shown that IF3 stabilizes the dissociation by binding to the transiently formed 30S subunit, preventing re-association back to 70S ribosomes (Hirokawa *et al.*, 2005). This three-factor-dependent stable dissociation of ribosomes into subunits completes the ribosome cycle and the resulting subunits are ready for the next round of translation.

Chapter II

Role of the acceptor stem of E. coli initiator tRNA in the interaction with initiation factor 2

2.1. Introduction

The process of translation initiation in bacteria involves the formation of the 30S·mRNA·fMet-tRNA initiation complex. Complex formation is facilitated by the three initiation factors IF1, IF2, and IF3. To ensure that all tRNAs other than the initiator tRNA are excluded from this process of initiation, several quality control checkpoints are used. The first occurs at the stage of aminoacylation where the aminoacyl-tRNA synthetase primarily distinguishes tRNAs based on their anticodons. Only tRNA with the correct anticodon will be charged with the cognate amino acid. The next proofreading step occurs at the stage of formylation. Initiator tRNA is discriminated by methionyl-tRNA transformylase which requires the tRNA to have a mismatch or weak base pair in the acceptor stem between nucleotides 1 and 72 (Lee *et al.*, 1992). Furthermore, MTF recognizes the amino acid attached to the tRNA in a hierarchy of preferences with the highest affinity for methionyl-tRNA^{fMet} (Li *et al.*, 1996; Mayer *et al.*, 2003). The last checkpoint involves binding of fMet-tRNA to IF2, which selects the initiator tRNA by recognition of the formylated α-amino group (Sundari *et al.*, 1976) and the amino acid attached to the tRNA (Mayer *et al.*, 2003). It has been shown that IF2 only requires a short fragment of the 3' acceptor end of the initiator tRNA for interaction (Guenneugues *et al.*, 2000). The hexanucleotide CAACCA-fMet has almost the same affinity for IF2 as intact fMet-tRNA. Although cross-linking experiments indicated interactions of IF2 with the T-stem and the anticodon stem of fMet-tRNA (Wakao *et al.*, 1989; Yusupova *et al.*, 1996), it was not clear whether IF2 recognizes any distinct feature of the main body of the tRNA. Studies of real-time binding of Escherichia coli IF2 to the mutant initiator tRNA G72, in which the highly conserved CxA mismatch between nucleotides 1 and 72 was changed to a strong C1:G72 base pair, showed a poorer binding of IF2 to the mutant initiator tRNA (Mayer *et al.*, 2003). Mutation of A72 to G72 resulted in a 7-fold lower association rate constant, followed by a rapid dissociation and/or major conformational change of the complex between IF2 and mutant G72 (Fig. 2-1),

suggesting that i) the C1xA72 mismatch or ii) the nature of the nucleotide at position 72 might be important for IF2 recognition.

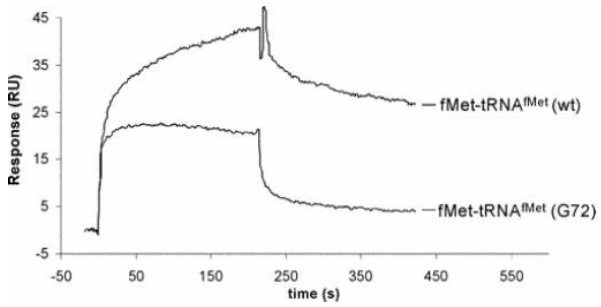

Fig. 2-1: Comparative binding of fMet-tRNA^{fMet} and fMet-tRNA^{fMet} (G72)

Typical sensograms obtained with 1 µM injections of the tRNAs injected across an IF2-coupled sensor chip surface are shown as overlay plot (from Mayer *et al.*, 2003)

The aim of the presented work involves the understanding of the molecular basis of IF2 interaction with the acceptor stem of the initiator tRNA. Specifically, we wanted to investigate whether the poor binding of the G72 mutant to IF2 is due to the loss of direct interaction with the C1 and/or A72 or whether IF2, like MTF, is sensitive to the presence of a strong base pair at this position. To accomplish this, a set of mutant *E. coli* $tRNA_2^{fMet}$ were used (Fig. 2-2). The U1 mutant (C1→U1) should reveal whether IF2 interacts directly with C1 and/or A72, while the U1G72 double mutant (C1xA72→U1G72) should indicate whether the mismatch between positions 1 and 72 is important for IF2 binding. To investigate the role of the "discriminator" base A73, another set of mutant was used. The G73 mutant (A73→G73) and the two double mutants G72C73 and G72U73 (A73→C73 and A73→U73, respectively, coupled to an A72→G72 mutation) are also shown in figure 2-2.

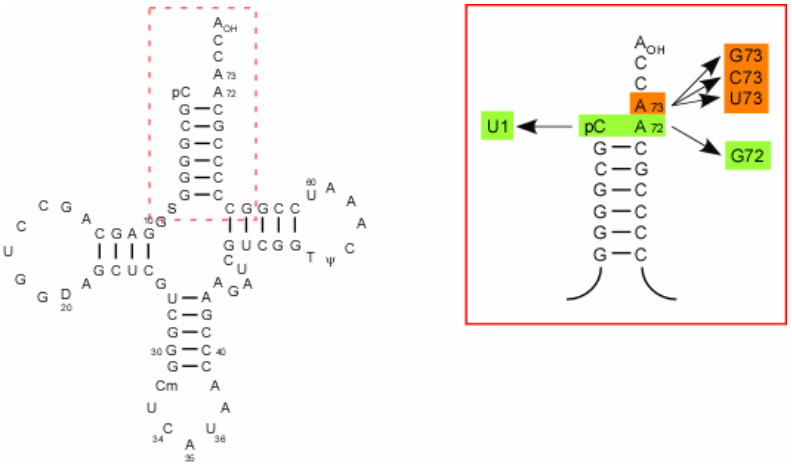

Fig. 2-2: Clover leaf structure of *E. coli* initiator tRNA^{fMet}

Boxed area represents the acceptor stem with the sites of mutations indicated by arrows.

2.2. Material

2.2.1. Chemicals

Acrylamide/Bis premixed powder	BioRad Laboratories Inc., Hercules, CA
Adenosine triphosphate	Sigma-Aldrich Corp., St. Louis, MO
Ampicillin	Roche Diagnostics Corp., Indianapolis, IN
Agarose	GIBCO, Invitrogen Corp., Grand Island, NY
Arabinose	Sigma-Aldrich Corp., St. Louis, MO
Bacto-Agar	DIFCO, BD Bioscience, San Jose, CA
Bacto-Nutrient Broth	DIFCO, BD Bioscience, San Jose, CA
Bacto-Trypton	DIFCO, BD Bioscience, San Jose, CA
Bacto-Yeast-Extract	DIFCO, BD Bioscience, San Jose, CA
Casamino Acid	DIFCO, BD Bioscience, San Jose, CA
Complete Mini protease inhibitor	Roche Diagnostics Corp., Indianapolis, IN
Cytosine triphosphate	Sigma-Aldrich Corp., St. Louis, MO
Guanosine triphosphate	Sigma-Aldrich Corp., St. Louis, MO
Kanamycin	Sigma-Aldrich Corp., St. Louis, MO
Isopropyl-β-D-thiogalactopyranoside	Roche Diagnostics Corp., Indianapolis, IN
L-glutamine	Sigma-Aldrich Corp., St. Louis, MO
L-isoleucine	Sigma-Aldrich Corp., St. Louis, MO
L-methionine	Sigma-Aldrich Corp., St. Louis, MO
L-phenylalanine	Sigma-Aldrich Corp., St. Louis, MO
L-valine	Sigma-Aldrich Corp., St. Louis, MO
Phenol, cryst.	Roche Diagnostics Corp., Indianapolis, IN
Trichloroacetic Acid	Mallinckrodt Baker Inc., Phillipsburg, NJ
Thymine triphosphate	Sigma-Aldrich Corp., St. Louis, MO
TriReagent®	Sigma-Aldrich Corp., St. Louis, MO

2.2.2. Radiochemicals

Adenosine-5'-γ-[^{32}P] triphophate (specific activity: 6000 Ci/ mmole)	PerkinElmer Life Sciences Inc., Boston, MA
L-[^{35}S]-methionine (specific activity: 1000 Ci/mmole)	PerkinElmer Life Sciences Inc., Boston, MA
L-[^{3}H]-glutamine (specific activity: 30-60 Ci/mmole)	PerkinElmer Life Sciences Inc., Boston, MA
L-[^{3}H]-isoleucine (specific activity: 77 Ci/mmole)	Amersham Biosciences Corp., Piscataway, NJ

L-[^{3}H]-phenylalanine (specific activity: 118 Ci/mmole)	Amersham Biosciences Corp., Piscataway, NJ
L-[^{3}H]-valine (specific activity: 46 Ci/mmole)	Amersham Biosciences Corp., Piscataway, NJ

2.2.3. Oligodeoxyribonucleotides

All oligodeoxyribonucleotides were acquired from Operon Biotechnologies Inc., Huntsville, AL

Oligonucleotide	Sequence of Oligonucleotide	Description
CP_fMet1_5539	5′- ACCGACGACCTTCGGGT -3′	*nt 40-56 of $tRNA_2^{fMet}$
UV5G	5′- GAACCGACGATCTTCGG -3′	*nt 39-55 of $tRNA_1^{fMet}$
BSIF2_F_BamHI	5′- GGCAGGATCCAAAATGCGTGTGTACGAA -3′	PCR primer
BSIF2_R_KPNI	5′- GGCAGGTACCTGCCCGAGCCACTTCCTG -3′	PCR primer

*oligonucleotide for use in Northern blot analysis; indicated is the position of sequence complementary within the tRNA of interest;

2.2.4. Enzymes, Proteins and Antibodies

ANTIBODIES

α-*Eco* IF2 pAb (rabbit)	Dr. John Hershey, UCD, Davis, CA
α-His4 pAb (mouse)	Amersham Biosciences Corp., Piscataway, NJ
ECL anti-rabbit (sheep), HRP-linked	Amersham Biosciences Corp., Piscataway, NJ
ECL anti-mouse (sheep), HRP-linked	Amersham Biosciences Corp., Piscataway, NJ

ENZYMES AND PROTEINS

*Bam*HI	New England Biolabs, Beverly, MA
Bovine Serum Albumin Standard	Pierce Biotechnology Inc., Rockford, IL
Bovine Serum Albumin (Fraction V)	Roche Diagnostics Corp., Indianapolis, IN
*Bpm*I	New England Biolabs, Beverly, MA
Calf Intestinal Phosphatase	New England Biolabs, Beverly, MA
Glutaminyl-tRNA synthetase (*Eco*)	Dr. Sean Kennedy, MIT, Cambridge, MA
*Hin*dIII	New England Biolabs, Beverly, MA
*Kpn*I	New England Biolabs, Beverly, MA
Methionyl-tRNA synthetase (*Eco*)	Dr. Alexei Stortchevoi, MIT, Cambridge, MA
Methionyl-tRNA formyltransferase (*Eco*)	Dr. Alexei Stortchevoi, MIT, Cambridge, MA

*Nco*I	New England Biolabs, Beverly, MA
Nuclease P1	Roche Applied Science, Indianapolis, IN
Proteinase K	Boehringer Mannheim GmbH, Mannheim, Germany
*Pvu*I	New England Biolabs, Beverly, MA
Quick DNA Ligase	New England Biolabs, Beverly, MA
Ribonuclease A	Sigma-Aldrich Corp., St. Louis, MO
Shrimp Alkaline Phosphatase	Roche Diagnostics Corp., Indianapolis, IN
S100 extract ValRS enriched	Dr. Xin-Qi Wu, MIT, Cambridge, MA
T4 DNA Ligase	New England Biolabs, Beverly, MA
T4 Polynucleotide Kinase	New England Biolabs, Beverly, MA
$Vent_R$ DNA Polymerase	New England Biolabs, Beverly, MA
PROTEIN MARKERS	
BenchMark™ Pre-stained Protein Ladder	Invitrogen Corp., Carlsbad, CA

2.2.5. Plasmids

Plasmids	Description	Marker	Reference
pUC13/ trnfM	wild-type $tRNA_2^{fMet}$ gene cloned in pUC13	Ampicillin	Gite and RajBhandary, 1997
pTZ19R/ trnfMG73	pUC derived plasmid bearing the gene for the mutant $tRNA_2^{fMet}$ G73	Ampicillin	Lee *et al.*, 1992
pTZ19R/ trnfMG72U73	pUC derived plasmid bearing the gene for the mutant $tRNA_2^{fMet}$ G72U73	Ampicillin	Lee *et al.*, 1992
pBR322/ trnfMG72C73	Mutant $tRNA_2^{fMet}$ G72C73 gene cloned in pBR322	Tetracyclin	Lee *et al.*, 1992
pBR322/ trnfMU1	mutant $tRNA_2^{fMet}$ U1 gene cloned in pBR322	Tetracyclin	Lee *et al.*, 1991
pBR322/ trnfMU1G72	mutant $tRNA_2^{fMet}$ U1G72 gene cloned in pBR322	Tetracyclin	Lee *et al.*, 1991
pRSVCATam1.2.5/ trnfMU35A36	pBR322 derived plasmid bearing the genes for the CAT reporter and the mutant initiator $tRNA_2^{fMet}$ (U35A36)	Ampicillin	Varshney *et al.*, 1991
pQE30	Vector for high-level expression of N-terminally 6x His-tagged proteins	Ampicillin	*Qiagen Inc.*
pQE-IF2	Expresses IF2-α of *E. coli* in frame with a N-terminal tag of $MRGSH_6$ (IF2-αHis6)	Ampicillin	Mayer *et al.*, 2003
pQE30-BstIF2	Expresses IF2 of *B. stearothermophilus* in frame with a N-terminal tag of $MRGSH_6$ (BSIF2-His6)	Ampicillin	*This Thesis*

2.2.6. Bacterial strains

Strain	Genotype / details	Reference
B105	*met*Y locus expressing $tRNA_1^{fMet}$, r_B^- m_B^- *gal*$^-$ *recA*$^+$	Mandal and RajBhandary, 1992
CA274	H*fr*, *lac*Z125am, *trp*A49am, *rel*A1, *spo*T1	Brenner and Beckwith, 1965
JM109	*end*A1, *gyr*A96, *hsd*R17(r_k^- m_k^+), *mcr*B$^+$, *rec*A1, *rel*A1, *sup*E44, *thi*-1, ∆(lac-proAB), F'[*traD36, proAB, lacI*^{q}*Z∆M15*]	Yanisch-Perron *et al.*, 1985
XL-1 Blue	*end*A1, *gyr*A96, *hsd*R17(r_k^- m_k^+), *lac*, *rec*A1, *rel*A1, *sup*E44, *thi*-1, F'[*pro*AB, *lac*I^{q}Z∆M15, Tn10 (Tet^r)]	Bullock *et al.,* 1987
M15 (pREP4)	*lac*$^-$, *ara*$^+$, *gal*$^+$, *rec*A$^+$, *uvr*$^+$, *lon*$^+$, F$^-$, *mtl*$^-$, *thi*$^-$, pREP4kan^r	Villarejo and Zabin, 1974

2.2.7. Material for Chromatography

Diethylaminoethyl cellulose (DE52)	Whatman Int. Ltd., Maidstone, England
Sephadex™ G-25 Quick spin columns	Roche Diagnostics Corp., Indianapolis, IN
Sephacryl™ 200HR	Amersham Biosciences Corp., Piscataway, NJ
TALON™ Metal Affinity resin	BD Bioscience Clontech, Palo Alto, CA
Thin layer chromatography sheet (13255 Cellulose)	Eastman Kodak Company, Rochester, NY

2.2.8. Analytical Kits

QIAprep Spin Miniprep Kit	Qiagen Inc., Valencia, CA
QIAquick Gel Extraction Kit	Qiagen Inc., Valencia, CA
QIAquick PCR Purification Kit	Qiagen Inc., Valencia, CA
Quick Start Bradford 1x Dye Reagent	BioRad Laboratories Inc., Hercules, CA
Western Lightning® Western Blot Chemiluminescence Reagent	Perkin Elmer Life Sci., Boston, MA

2.2.9. Instruments and additional equipment

CENTRIFUGES

Clinical Centrifuge Model CL	International Equipment, Needham, MA
Microcentrifuge	Brinkham, New York, NY
µSpeedFuge SFR13K	Savant Instruments Inc., Farmingdale, NY
Sorvall RC-3B	Kendro Laboratory Products, Asheville, NC

Sorvall RC 5C plus	Kendro Laboratory Products, Asheville, NC
Sorvall Ultra 80	Kendro Laboratory Products, Asheville, NC

EQUIPMENT

ChemiImager™	AlphaInnotech Corporation, San Leandro, CA
Centricon® Centrifugal Filter Units	Millipore Corp., Billerica, MA
Bio-Dot™ apparatus	BioRad Laboratories Inc., Hercules, CA
Electrophoresis System, vertical	Owl Separation Systems, Portsmouth, NH
Electrophoresis System, horizontal	Owl Separation Systems, Portsmouth, NH
Fraction collector	Gilson, Middleton, WI
Hoefer Blotting tank	Hoefer Inc., San Francisco, CA
Hoefer Electroblot apperatus	Hoefer Inc., San Francisco, CA
Hybond-N^+® membrane	Amersham Biosciences Corp., Piscataway, NJ
Immobilon-P® membrane	Millipore Corp., Billerica, MA
Liquid Scintillation Counter (1217 RACKBETA)	PerkinElmar Life Sci., Downers Grove, IL
Mini-PROTEAN 3® Cell	BioRad Laboratories Inc., Hercules, CA
MF-Millipore Membrane (HAWP)	Millipore Corp., Billerica, MA
Slide-A-Lyzer® Dialysis Cassettes	Pierce Biotechnology Inc., Rockford, IL
SpectraPor® 6 Dialysis Membranes	Spectrum Labs, Rancho Domingues, CA
Speed Vac Concentrator	Savant Instruments Inc., Farmingdale, NY
Spectrophotometer (HP 845x UV-Visible System)	Hewlett Packard, Palo Alto, CA
PhosphorImager (Typhoon™ 9400 scanner)	Amersham Biosciences Corp., Piscataway, NJ
Peristaltic pump P-3	Buchler Instruments, Kansas City, MO
DNA Engine® Peltier Thermal Cycler (PTC-200™)	MJ Products, BioRad Laboratories Inc., Waltham, MA
UV Stratalinker® 2400	Stratagene Inc., La Jolla, CA
X-ray film X-Omat™ AR	Eastman Kodak Company, Rochester, NY
X-ray film BioMax™ MR	Eastman Kodak Company, Rochester, NY

COMPUTER SOFTWARE

AlphaEase™ Software	AlphaInnotech Corporation, San Leandro, CA
Image Quant™ TL Software	Amersham Biosciences Corp., Piscataway, NJ
Sigma Plot® 8.0	Systat Software Inc., Point Richmond, CA
MS Excel	Microsoft Corp., Redmond, WA

2.3. Methods

2.3.1. Nucleic Acids

2.3.1.1. Separation of nucleic acids by gel electrophoresis

2.3.1.1.1. Agarose gel electrophoresis

Agarose gel electrophoresis is a simple and highly efficient method for separating, identifying, and purifying 0.5- to 25-kb DNA fragments (Sambrook and Russell, 2001). In general agarose gel electrophoresis is employed to check the progress of restriction enzyme digestion, to quickly determine the yield and purity of DNA isolation and PCR reaction, and to size fractionated DNA molecules. The procedure of agarose gel electrophoresis can be divided into three stages: 1) a gel is prepared with an agarose concentration appropriate for the size of the DNA fragments to be separated. Most agarose gels are made between 0.7% and 2%, where a 0.7% gel will show good separation (resolution) of large DNA fragments (0.8- to 12-kb) and a 2% gel will show good resolution for small fragments (0.2- to 1-kb); 2) the DNA samples are loaded into the sample well and the gel is run at a voltage and time period, that will achieve optimal separation. The DNA fragments migrate in the electrical field at a rate that is inversely proportional to the logarithm of the number of base pairs; and 3) the gel is stained or visualized directly, if ethidium bromide has been incorporated into the gel and electrophoresis buffer, by illumination with UV light. Ethidium bromide intercalates between GC-pairs and fluoresces following excitation.

10x TBE

		[g/L]
Tris	890 mM	107.8
H_3BO_4	890 mM	55.02
Na_2EDTA	20 mM	7.44
ddH_2O	ad 1000 ml	

5x DNA-loading buffer

Glycerin (86%)	50%
Na_2EDTA (0.5 M)	25 mM
XCFF (1%)	0.03%
BPB (1%)	0.03%
ddH_2O	ad 10 ml

The agarose (% (w/v) = gel concentration) was boiled in 50 ml of 0.5% TBE buffer. After cooling the solution to 60°C ethidium bromide was added to a final

concentration of 0.5 µg/ ml. The gel was poured into the gel chamber containing the comb, and after solidification the gel was placed into the electrophoresis apparatus filled with 0.5% TBE buffer and ethidium bromide at the same 0.5 µg/ml concentration. The comb was removed and the samples, supplemented with 5x DNA-loading buffer, were applied to the wells. Gels were normally run at 60 to 80 volts.

2.3.1.1.2. Polyacrylamide gel electrophoresis (PAGE)

Polyacrylamide gel electrophoresis offers high resolution of low molecular weight nucleic acids. Polyacrylamide gels provide somewhat better resolution as well as significantly higher capacity compared to agarose gels. Depending on the pore size of the gel (3.5% to 20% polyacrylamide), a separation from 10 to 1000 bp can be achieved. A polyacrylamide gel is formed by the polymerization of acrylamide monomers into long chains, which are further covalently cross-linked, most commonly by N,N'-methylenebisacrylamide. Polymerization of a polyacrylamide gel is initiated by free radicals provided by ammonium peroxo-disulfate and stabilized by TEMED. The pore size of a polyacrylamide gel is determined by the total percentage of acrylamide (the sum of weights of the acrylamide monomer and cross-linker). Two types of polyacrylamide gels are used: 1) a non-denaturing polyacrylamide gel is used for separation of double-stranded DNA and RNA molecules based on their native intra- and intermolecular interaction; 2) a denaturing polyacrylamide is used for separation of single-stranded DNA and RNA molecules. It contains 7M urea which prevents base pairing and the formation of secondary structures, therefore separating the nucleic acids based solely on size.

2.3.1.1.2.1. Non-denaturing PAGE

Non-denaturing polyacrylamide gels can be used for the separation of transfer RNAs based on the fact that the tRNAs present in a cell differ in size and nucleic acid composition, thereby displaying distinct secondary and tertiary structures (Seong and RajBhandary, 1987).

Analytical and preparative gels were prepared by horizontally pouring the ice cold gel solution between two glass plates (40x20 cm) separated by spacers of 0.07 to 0.15 cm, followed by the insertion of appropriate sized combs. Polymerization was allowed to occur between 2 and 12 h at room temperature. The gels were mounted onto a vertical electrophoresis system, electrophoresis buffer was TBE and pre-electrophoresis was done for 1 h at 300 V at room temperature. Samples were

prepared by addition of 2x PAGE-loading buffer and applied onto the gel. Electrophoresis was carried out for 24 to 48 h at 350 V at room temperature until the bromphenol blue dye reached the bottom of the gel.

Gel solution	**12 %**	**15 %**
	per 150 ml	
AA:Bis (19:1) 40%	45 ml	56.25 ml
10x TBE	15 ml	15 ml
ddH_2O	90 ml	78.75 ml
TEMED	225 µl	225 µl
APS (10%)	360 µl	360 µl

2x PAGE loading buffer	
Glycerol	30%
TBE	2x
XCFF	0.1%
BPB	0.1%
ddH_2O	ad 10 ml

2.3.1.1.2.2. Denaturing PAGE

Denaturing polyacrylamide gel was prepared by horizontally pouring the ice cold gel solution between two glass plates (40x20x0.04 cm gel dimensions). After insertion of the appropriate sized comb, the gel was allowed to polymerize for at least 4 h. The gel was mounted onto a vertical electrophoresis system, the comb was gently removed and the wells were thoroughly flushed with electrophoresis buffer (TBE). The gel was pre-run for 1 h at 1300 V at room temperature. Samples were prepared by addition of 2x denaturing loading buffer and applied to the gel. Electrophoresis was carried out for 4 h at 1300 V at room temperature.

Denaturing gel solution		
		Per 40 ml
Urea	7M	16.8 g
AA:Bis (19:1) 40%	8%	8 ml
10x TBE	1x	4 ml
ddH_2O		ad 40 ml
TEMED		70 µl
APS (10%)		150 µl

2x denaturing loading buffer	
Urea	7M
TBE	2x
XCFF	0.1%
BPB	0.1%
ddH_2O	ad 10 ml

2.3.1.1.2.3. Acid urea PAGE

Acid urea polyacrylamide gels are basically denaturing gels run at acidic pH that allows the separation of tRNA in their deacylated, aminoacylated, and formylated forms (Ho and Kan, 1987; Varshney *et al.*, 1991). Acid urea gel analyses were performed according to Varshney et al. (Varshney *et al.*, 1991). A 6.5% acid urea polyacrylamide gels were prepared by horizontally pouring the ice cold gel solution between two glass plates (40x20x0.04 cm gel dimensions). Following insertion of the appropriate sized comb, the gel was allowed to polymerize for at least 4 hours before use. The gel was mounted onto a vertical electrophoresis system, the comb was gently removed, and the wells were thoroughly flushed with electrophoresis buffer (0.1 M sodium acetate, pH 5.0). The gel was pre-run for 1 h at 4°C and 400 V. Samples were prepared by addition of 2x AU loading buffer to 5 µl of reaction samples containing 0.02 to 0.04 A_{260} units of $tRNA^{fMet}$. 5 µl were loaded onto the acid urea polyacrylamide gel and electrophoresis was carried out overnight at 4°C and 500 V until the bromphenol blue dye reached the bottom of the gel.

Acid Urea gel solution

		per 40 ml
Urea	7 M	16.8 g
AA:Bis (19:1) 40%	6.5%	6.5 ml
NaOAc (1M) pH 5.0	0.1 M	4 ml
ddH_2O		ad 40 ml
TEMED		70 µl
APS (10%)		150 µl

2x acid urea (AU) loading buffer

Urea	7 M
NaOAc	0.2 M, pH 5.0
XCFF	0.05%
BPB	0.05%
ddH_2O	ad 10 ml

2.3.1.2. Localization of tRNAs by Northern hybridization

Once RNA molecules are separated by gel electrophoresis they can be further analyzed by Northern hybridization. The hybridization step allows the identification of RNA blotted and immobilized on a nylon membrane with a radioactive or otherwise labelled nucleic acid probe.

2.3.1.2.1. 5'-[^{32}P]-labelling of oligodeoxyribonucleotides

Probes used for northern hybridization were chemically synthesized oligodeoxyribonucleotides that were radioactively labelled at the 5'-end. The synthetic oligonucleotides possess a free 5'-hydroxyl group where the terminal phosphate group of γ-[^{32}P]-ATP can be attached enzymatically using T4 polynucleotide kinase (PNK).

15 pmoles of oligonucleotide were added to 1x T4-PNK buffer (70 mM Tris-HCl, pH 7.6, 10 mM $MgCl_2$, 5 mM dithiothreitol) in a final volume of 45 µl. The mixture was incubated for 10 min at 65°C and immediately chilled on ice. 5 pmoles of γ-[^{32}P]-ATP (specific activity: 6000 Ci/mmole) and 20 units of T4 polynucleotide kinase were added and the mixture was incubated for 30 min at 37°C. For enzyme inactivation the reaction was further incubated for 20 min at 65°C, quick frozen and subsequently stored at -20°C. Before use in a Northern hybridization the 5'-[^{32}P]-labelled oligonucleotides were heated for 10 min at 100°C.

2.3.1.2.2. Transfer and Northern hybridization

The portion of the gel which contained the tRNAs of interest was electroblotted onto a Hybond-N^+ membrane in transfer buffer containing 10 mM Tris·Acetate (pH 7.8), 5 mM sodium acetate and 0.5 mM ethylenediaminetetraacetic acid using a Hoefer Electroblot apparatus for 20 min at 10 V followed by 2 h at 40 V at 4°C. The tRNA was cross-linked to the membrane using a UV Stratalinker® 2400 with default settings. The blot was pre-hybridized for 2 h at 42°C in pre-hybridization solution. Thereafter, hybridization was performed for 24 h at 42°C in hybridization solution containing 0.3 nM of a 5'-[^{32}P]-labelled oligodeoxyribonucleotide probe complementary to a nucleotide sequence of the tRNA of interest. Finally, the membrane was washed 1x 30 min in 6x SSC at room temperature. Autoradiograms were prepared by either using X-Omat AR X-ray films or storage phosphor autoradiography and read using a Typhoon 9400 scanner.

10x Transfer Buffer

		per 2000 ml
Tris	100 mM	24.23 g
NaOAc	50 mM	8.20 g
EDTA (0.5 M)	5 mM	20 ml
AcOH		→ pH 7.5
ddH_2O		ad 2000 ml

20x SSC solution

		per 1000 ml
NaCl	3 M	175.32 g
Sodium citrate	0.3 M	88.23 g
AcOH		→ pH 7.0
ddH_2O		Ad 1000 ml

100x Denhardt's solution

		per 100 ml
Ficoll (type 400)	2% (w/v)	2 g
PVP 40	2% (w/v)	2 g
BSA (Frac. V)	2% (w/v)	2 g
ddH_2O		ad 100 ml

solution was filter sterilized and stored at -20°C

Pre-hybridization solution

		per 30 ml
20x SSC	6x	9 ml
100x Denhardt's	10x	3 ml
SDS (20%)	0.5%	0.75 ml
ddH_2O		17.25

Hybridization solution

		per 25 ml
20x SSC	6x	7.5 ml
SDS (20%)	0.1%	125 µl
ddH_2O		17.35 ml

Hybridization solution was preheated at 42°C

2.3.1.2.3. Removal of oligodeoxyribonucleotides from the membrane

Following hybridization it was often necessary to further analyze the blot using a different radioactively labelled probe. For this purpose the membrane was stripped as recommended by the manufacturer by washing the membrane several times in boiling stripping solution (0.1x SSC, 0.1% SDS). The membrane was checked for complete removal of probe by autoradiography prior to a new round of hybridization.

2.3.1.3. Isolation of nucleic acids from aqueous solutions

2.3.1.3.1. Ethanol precipitation of nucleic acids

Addition of ethanol allows quantitative precipitation of nucleic acids from aqueous solutions. It disrupts the hydrate shell of nucleic acids and promotes binding of monovalent cations Li^+, Na^+, and NH_4^+ to the negatively charged phosphate groups. Furthermore at slight acidic pH some phosphate groups become protonated. The loss of repulsive forces results in the aggregation and precipitatin of the nucleic acids.
Nucleic acids were precipitated by addition of one-tenth volume of 3M NaOAc or LiOAc (pH 5.2) and two to three volumes of ice cold absolute ethanol to the aqueous solution, followed by thorough mixing and incubation at 0 to -80°C. The precipitate was collected by centrifugation at 15,000x*g* for 30 min at 4°C. A subsequent wash with ice cold 70% ethanol, followed by brief centrifugation, removed residual salt and moisture. After drying the pellet, the nucleic acids were resuspended in appropriate volumes of ddH_2O or buffer and if necessary stored at -20°C

2.3.1.3.2. Isopropanol precipitation of nucleic acids

Isopropanol is an effective alternative to ethanol and has the avantage of precipitating nucleic acids at lower volumes. Nucleic acids were precipitated by addition of one-tenth volume of 3M NaOAc and one volume of isopropanol to the aqueous solution. Following mixing and incubation at room temperature for 10 min, nucleic acids were pelleted by centrifugation at 15,000x*g* for 30 min at 4°. Isopropanol and salt were removed by several washes of the pellet with ice cold 70% ethanol. After the washing step pellets were further processed as described above.

2.3.1.3.3. Quantification of nucleic acids by spectrophotomerty

Nucleic acids absorb UV light of 250 to 270 nm wavelength, with a maximum at 260nm and thus can be quantified spectrophotometrically. The reading at 260nm allows calculation of the concentration of nucleic acids in solution. An A_{260} unit of 1 corresponds to approximately 50 µg/ml for double-stranded DNA and 40 µg/ml for single-stranded DNA and RNA. The ratio between readings at 260 nm and 280 nm provides an estimate for the purity of the nucleic acid. DNA and RNA preparations free of protein and phenol have A_{260}/A_{280} ratios of 1.8 and 1.95, respectively.

2.3.1.4. Isolation and purification of DNA from bacteria

2.3.1.4.1. Isolation of plasmid DNA

Isolation of plasmid DNA from bacterial cells was carried out by using a Qiaprep® Spin Miniprep Kit from Qiagen following the manufacturer's instructions. The principle of the method is based on alkaline lysis of bacterial cells (Birnboim and Doly, 1979). Briefly, the preparation allows for the precipitation of contaminating proteins, lipids, and chromosomal DNA, and the subsequent binding of aqueous plasmid DNA onto silica in the presence of high salt.

2.3.1.4.2. Isolation of genomic DNA

Genomic DNA from *Bacillus stearothermophilus* was isolated according to Current Protocols in Molecular Biology, Unit 2.4: Preparation of Genomic DNA from Bacteria (Ausubel, 2001).

B. stearothermophilus was grown in 10 ml of nutrient broth for 48 h at 55°C. 1.5 ml was taken and cells were pelleted by centrifugation for 2 min in a microcentrifuge. The cell pellet was resuspended in 582 µl of TE buffer (pH 7.4), followed by the addition of 15 µl of 20% SDS and 3 µl of proteinase K (20 mg/ml). After incubation for 1 h at 37°C, 100 µl of 5M NaCl were added, followed by the addition of 80 ml of a CTAB/NaCl solution (10% CTAB in 0.7 M NaCl). The mixture was further incubated for 10 min at 65°C. 0.7 ml of chloroform/isoamyl alcohol (24:1) was added, thoroughly mixed and centrifuged for 5 min using a microcentrifuge. The aqueous layer was transferred into a fresh tube and an equal volume of phenol/chloroform/isoamyl alcohol (25:24:1) was added. After separating the layers by centrifugation, the aqueous layer was transferred into a fresh tube and nucleic acids were precipitated by the addition of 0.6 volume of isopropanol. The DNA precipitate was pelleted by centrifugation and washed with 70% ethanol. Finally the pellet was dried and dissolved in 50 µl of TE buffer (pH 7.4).

2.3.1.5. Amplification of DNA by polymerase chain reaction

The polymerase chain reaction (PCR) is a rapid procedure for *in vitro* enzymatic amplification of a specific segment of DNA. The enzyme that facilitates this reaction is a thermo-stabile DNA polymerase. The PCR requires a three-step cycling process: 1) thermal denaturation of double-stranded DNA, 2) annealing of the primers, and 3)

primer extension. Denaturing is carried out at 94°C and separates the complementary strands of the DNA thus preparing them for the annealing step. The primers are attached to the dissociated DNA strands. Primers are single-stranded oligonucleotides that are complementary to one of the original DNA strands, to either the 5'- or the 3'-side of the sequence of interest. For annealing, a temperature is chosen that is 3 to 5°C lower than the T_m of the matrix/oligonucleotide hybrid. Once annealing has occurred, the DNA polymerase catalyzes the synthesis of a new strand of DNA by adding nucleotides complementary to those in the unpaired DNA strand onto the annealed primer. The optimal temperature for DNA polymerase is between 72 to 78°C. In theory, the number of DNA strands doubles upon completion of each cycle. Typically between 25 and 30 cycles were run to obtain the desired amplified product.

2.3.1.5.1. The polymerase chain reaction

For amplification of DNA, $Vent_R$ DNA Polymerase from New England Biolabs has been used throughout the course of this work. PCR was carried out using a DNA Engine® Peltier Thermal Cycler from MJ Products.

Amplification of DNA by PCR

components	[µl]	final concentration
Plasmid DNA (~30 ng/µl)	1	~30 ng
5'- primer (10 µM)	2	0.2 µM
3'- primer (10 µM)	2	0.2 µM
$MgSO_4$ (100 mM)	2	2 mM
dNTP-mix (10 mM)	2	0.2 mM
10x Vent Pol Buffer	10	1x
$Vent_R$ Polymerase (2 U/µl)	0.7	1.4 U
ddH_2O	79.8	
Final volume	100	

In the cases where genomic DNA was used as template DNA, 100 to 500 ng DNA was added to the reaction. Reactions without DNA template were always performed as negative controls. For standard amplification of DNA following program was used:

Standard PCR program for amplification of DNA

	Step	Temperature	Time	Cycle(s)
1	denaturing	95°C	5 min	1
2	denaturing	95°C	0.5 min	
	annealing	T_M-3-5°C	1.5 min	25-30
	elongation	72°C	3 min*	
3	completion	72°C	10 min	1
4	storage	4°C	hold	

*1 min per 1000 bp of DNA sequence of interest was used for calculating the duration of the elongation cycle based on the average processivity of the polymerase.

The basic melting temperature T_m of the primers was calculated based on the formular T_m= (wA+xT)· 2 + (yG+zC)·4, where w, x, y, and z are the numbers of bases A, T, G, and C in the sequence, respectively.

2.3.1.5.2. Analysis and purification of PCR products

After completion of PCR aliquots (5 to 10 µl) were taken, supplemented with 5x DNA-loading buffer and analyzed by agarose gel electrophoresis (2.3.1.1.1.). After confirmation of the desired product, the remaining reaction was purified by reversal binding of DNA to a silica matrix using a *QIAquick PCR Purification Kit*. In case of contamination by nonspecific PCR products the remaining reaction was subjected to preparative agarose gel electrophoresis. The DNA fragment of interest was excised and recovered from the gel by using a *QIAquick Gel Extraction Kit* following the instructions of the manufacturer.

2.3.1.6. Cloning of DNA

Unless specified otherwise, for cloning, methods outlined by Sambrook *et al*. were used (Sambrook and Russell, 2001).

2.3.1.6.1. Preparation of cloning vectors from plasmid DNA

Most restriction endonucleases specifically recognize 4 to 8 base pair long sequences in double-stranded DNA molecules. These sequences are cleaved by the restriction enzyme generating either blunt or cohesive ends, so-called sticky ends, where the digested DNA molecule possesses at each end a short single-stranded overhang. During the course of this work restriction enzymes were used that generate sticky ends.

Linearized cloning vectors were prepared by restriction digestion of 5 to 10 µg of plasmid DNA using appropriate restriction endonucleases.

Preparative restriction digestion of plasmid DNA

components	[µl]	final concentration
plasmid DNA (5-10 µg)	variable	0.1 to 0.3 µg/µl
10x reaction buffer	3	1x
Restriction enzyme (10-20 U)	3	30 to 60 U
ddH_2O	ad 30	
Final volume	30	

The temperature and duration of incubation as well as the reaction buffer were dependent on the restriction enzyme used in each case. For double digestions using two restriction enzymes simultaneously, conditions were chosen so as to ensure activity of both enzymes. In this case the reaction volume was increased to 50 µl. The extent of digestion was analyzed by agarose gel electrophoresis (2.3.1.1.1.).

2.3.1.6.2. Dephosphorylation of linearized plasmids by alkaline phosphatase

In order to prevent re-ligation of linearized vectors the 5'-phosphate residues were hydrolyzed by calf intestine phosphatase (CIP) (Ausubel, 2001). In general, CIP (20 U) was added directly to the restriction digestion reactions after 2 h of incubation and the mixture was further incubated for 1 h at 37°C. After the reactions were complete, the digested and dephosphorylated vectors were isolated by gel

electrophoresis on a preparative 0.5% agarose gel (w/v). The desired DNA fragments were excised and recovered by using a *QIAquick Gel Extraction Kit*.

2.3.1.6.3. Generation of PCR products with cohesive ends

For directed ligation of PCR products into linearized vector, PCR products were digested with appropriate restriction enzymes to generate single-stranded overhangs complementary to those in the vector. PCR primers were usually designed in such a way that the desired PCR product contained specific restriction site at each end. Restriction digest was carried out as described in section 2.3.1.6.1., followed by purification of the reactions by using a *QIAquick PCR Purification Kit*.

2.3.1.6.4. Ligation of DNA

Ligation of DNA is the process in which linear DNA fragments are joined together. The enzyme T4 DNA ligase catalyzes the formation of a phosphodiester bond between juxtaposed 5' phosphate and 3' hydroxyl termini in duplex DNA or RNA. The enzyme joins blunt end and cohesive end termini as well as repair single stranded nicks in duplex DNA, RNA or DNA/RNA hybrids. Sticky-end ligation has the advantage of a directed insertion of a desired DNA fragment (e.g. PCR products) into a linearized vector, based on the complementarity of overhangs generated by digestion with two restriction endonucleases.

For effective ligation insert DNA was added to the reaction in a 5 to 10-fold molar excess over the linearized vector (approx. 0.05 pmol vector to 0.5 pmol insert).

Ligation of DNA fragments with cohesive ends

components	[µl]	final concentration
DNA fragment	variable	Approx. 100 ng
Dephosphorylated vector	1	Approx. 100 ng
10x T4-DNA-ligase buffer	2	1x
T4-DNA-ligase (20 U/µl)	1	20 U
ddH_2O	ad 20	
Final volume	20	

In general ligation reactions were incubated for 12 to 16h at 14°C. Following incubation 10 µl were directly used for transformation of competent cells (2.3.1.6.5.2.).

2.3.1.6.5. Transformation of bacterial cells

Bacterial transformation is the process by which bacterial cells take up naked DNA molecules. If the foreign DNA has an origin of replication recognized by the host cell DNA polymerase, the bacteria will replicate the foreign DNA along with their own DNA. When transformation is coupled with antibiotic selection techniques, bacteria can be induced to uptake certain DNA molecules, and those bacteria can be selected for that incorporation. Bacteria which are able to uptake DNA are called "competent" and are made so by treatment with calcium chloride in the early log phase of growth. The bacterial cell membrane is permeable to chloride ions, but is non-permeable to calcium ions. As the chloride ions enter the cell, water molecules accompany the charged particle. This influx of water causes the cells to swell and is necessary for the uptake of DNA. The exact mechanism of this uptake is unknown. It is known, however, that the calcium chloride treatment has to be followed by heat treatment. The procedure for preparation of competent cells and transformation is based on the protocol by Hanahan (Hanahan, 1983).

2.3.1.6.5.1. Preparation of competent cells

Cells from a frozen stock of the desired *E. coli* strain were streaked out on Luria-Bertani (LB) agar plates and grown overnight at 37°C. A single colony was picked and used to inoculate 10 ml of SOB-medium and cells were grown overnight with agitation at 37°C. 1 ml of the primary culture was used to inoculate 100 ml of SOC-medium in a 1 L flask. The cells were grown with shaking at 37°C until the culture reached an optical density at A_{600} of 0.5. 2 x 50 ml were transferred into ice cooled 50 ml falcon tubes and cells were chilled on ice for 15 min. The cells were pelleted by centrifugation at 5,000 rpm for 10 min at 4°C (Sorvall RC-3B/H6000A). The cells were resuspended in 83 ml of buffer RF1 and incubated on ice for 1 h. After further centrifugation the cells were resuspended in 20 ml buffer RF2 and incubated on ice for 15 min. 700 µl of DTT solution (2.2 M DTT, 10 mM KOAc) were added and cells were further chilled on ice for 10 min. Finally, 200 µl aliquots of competent cells were dispensed into ice cooled 1.5 ml reaction tubes, quick frozen, and stored at -80°C. All steps were performed aseptically.

The efficiency of competent cells was measured by transforming them with a standard amount of pUC19 plasmid DNA (1-10 ng). The transformation efficiency is expressed as colony forming units per microgram DNA (cfu/µg). A transformation efficiency of 10^7 to 10^9 is normally obtained using this procedure.

SOC-medium		**SOB-medium**	
NaCl	10 mM	NaCl	5 mM
KCl	2.5 mM	KCl	2.5 mM
Bacto-Trypton	2% (w/v)	Bacto-Trypton	2% (w/v)
Bacto-Yeast Extract	0.5% (w/v)	Bacto-Yeast Extract	0.5% (w/v)
	-autoclaved-		
	Solutions were sterile filtrated, then added		
$MgSO_4$ (1 M)	10 mM	$MgSO_4$ (1 M)	10 mM
$MgCl_2$ (1 M)	10 mM	$MgCl_2$ (1 M)	10 mM
$CaCl_2$ (5 M)	50 mM		
Glucose (1 M)	20 mM		

RF1 solution	
	Final concentration
RbCl	100 mM
$MnCl_2$	50 mM
KOAc	30 mM
$CaCl_2$	10 mM
Glycerol	15% (v/v)
ddH_2O	→pH 5.8 w/ AcOH

- Solutions were sterile filtrated; stored at 4°C –

RF2 solution	
	Final concentration
RbCl	10 mM
MOPS	10 mM
$CaCl_2$	75 mM
Glycerol	15% (v/v)
ddH_2O	→pH 6.8 w/ NaOH

- Solutions were sterile filtrated; stored at 4°C –

2.3.1.6.5.2. Transformation of competent cells

200 µl of competent cells were thawed on ice. 1 to 10 ng of plasmid DNA or 10 µl of a ligation reaction were added. The cell suspensions were gently mixed and chilled on ice for 40 min. The cells were incubated for 60 s at 42°C and kept on ice for further 10 min. 800 µl of SOB-media were added and the cells were incubated under shaking for 30 to 60 min at 37°C. Finally, 100 and 500 µl of the cells were plated out on LB agar plates containing the appropriate antibiotic as selection marker and the plates were incubated overnight at 37°C. Colonies of transformants were picked for further analysis or stored for several weeks at 4°C.

2.3.1.7. Sequencing of DNA

Throughout the course of this work, DNA was sequenced by automated sequencing using the Applied Biosystems 3730 capillary DNA sequencer (Applied Biosystems Inc., Foster City, CA) at the MIT CCR HHMI Biopolymers Laboratory, Massachusetts Institute of Technology, employing the manufacturer's Big Dye Terminator Cycle Sequencing Reaction Mix.

2.3.1.8. Purification of transfer RNA

2.3.1.8.1. Organisms and culture

Escherichia coli B105 containing pUC19 or pBR322 and derivatives thereof were grown in LB broth supplemented with 100 µg ampicillin per ml and 5 µg tetracyclin per ml, respectively.

2.3.1.8.2. Overexpression and isolation of total RNA

A primary culture (20 ml) was used to inoculate 1 to 2 L LB broth and the culture was grown overnight at 37°C. The next day the culture was aliquoted by transferring it to 1 L centrifuge bottles. The cells were pelleted by centrifugation at 3,000 rpm for 15 min at 4°C (Sorvall RC-3B/H6000A), resuspended in 10% sucrose, transferred to a 250 ml centrifuge tube and subsequently centrifuged for 10 min at 4°C at 3,000 rpm. After determining the net wet weight, the cell pellet was quick frozen or used immediately for further proceedings.

The pellet was resuspended in 1.4 ml extraction buffer per gram wet weight. 1 volume of water-saturated unbuffered-phenol was added to the cell suspension and the mixture was nutated for 2 to 3 h at 4°C. By centrifugation for 30 min at 10,000x*g* at 4°C (Sorvall RC 5C plus/SLA-1500) the aqueous phase containing the nucleic acid was separated from the organic phase and transferred into a fresh tube. The phenol phase was re-extracted by addition of ½ volume of extraction buffer and centrifugation at 10,000x*g* for 20 min. The aqueous layers were combined and the nucleic acids were precipitated overnight at 4°C in the presence of 0.3 M sodium acetate (pH 5.2) and 2 volumes of ethanol. Subsequently the pellet was dissolved in 1 to 2 ml of buffer WB1 and the concentration of the total RNA was determined by spectrophotometry.

Extraction buffer	
Tris·HCl, pH 7.5	10 mM
Na_2EDTA	5 mM

Buffer WB1	
Tris·HCl, pH 7.5	10 mM
Na_2EDTA	1 mM
NaCl	200 mM

2.3.1.8.3. Preparation of total tRNA pool

The total RNA sample was applied to a diethylaminoethyl cellulose (DE52) column pre-equilibrated with buffer WB1. The column was washed with 3 bed volumes of the same buffer. By using buffer EB1 (described below) the tRNA was eluted from the column (flowrate: 0.1-0.2 ml/min) and 2 ml fractions were collected. The absorbance at 260 nm was determined and fractions with absorbance at 260 nm were pooled. Total tRNA was precipitated overnight at 4°C by addition of 2 volumes of ethanol. The tRNA was pelleted by centrifugation at 10,000x*g* for 45 min at 4°C, washed with ice cold 70% ethanol and dissolved in 50-100 µl of TE buffer (described below). After determining the absorbance at 260 nm, the total tRNA sample frozen and stored at –20°C. Aliquots were used to test the activity and the overexpression level of the $tRNA_2^{fMet}$ wild-type and mutants by performing aminoacylation assays (2.3.1.8.5.) and running analytical 15% non-denaturing polyacrylamide gels (40x20x0.15 cm gel dimension; 2.3.1.1.2.1.).

Buffer EB1	
Tris·HCl, pH 7.5	10 mM
NaCl	1 M

TE buffer	
Tris·HCl, pH 7.5	10 mM
Na_2EDTA	1 mM

2.3.1.8.4. Isolation of $tRNA^{fMet}$ species

Total tRNA samples were subjected to preparative polyacrylamide gel electrophoresis (12% acrylamide/bisacrylamide in 1x TBE, 40x20x0.15 cm gel dimension). The wells were formed with wide slot combs capable of taking up to 500 µl of sample volume. After 1 h pre-electrophoresis at 300 V, 20-50 A_{260} units of total tRNA were applied per slot and electrophoresis was performed at 350 V until the bromphenol dye reached the bottom of the gel. The $tRNA_2^{fMet}$ band was located by UV-shadowing and excised from the gel. The gel pieces were crushed and the tRNA was eluted overnight at 4°C by addition of 1.5x volume of buffer EB2 with agitation. The slurry was settled by short centrifugation. The supernatant was transferred into a fresh tube and replaced by 1 volume of fresh buffer EB2. After elution for additional 8h the supernatants were combined and loaded onto a 1.5 ml DE52 column, equilibrated with buffer WB2, with a flow rate of 0.1 to 0.2 ml/h. The column was washed with 10 bed volume of the same buffer. The tRNA was eluted with buffer EB3 and 1 ml fractions were collected. The absorption at A_{260} was measured and the tRNA containing fractions were pooled, followed by ethanol precipitation (without addition of sodium acetate) overnight at 4°C. The pellet obtained by centrifugation (45 min at 10,000g at 4°C) was dissolved in 100 to 200 µl TE buffer and the amount of tRNA was estimated spectrophotometrically after which the sample was stored at -20°C.

Buffer EB2	
Tris·HCl, pH 7.5	20 mM
LiCl	100 mM

Buffer WB2	
Tris·HCl, pH 7.5	100 mM
LiCl	100 mM

Buffer EB3	
Tris·HCl, pH 7.5	100 mM
LiCl	1 M

2.3.1.8.5. Aminoacylation assays

2.3.1.8.5.1. Testing quality of [^{35}S]-methionine

0.1 µl of L-[^{35}S]-methionine was spotted on a cellulose thin layer chromatography sheet (13255 Cellulose) and chromatography was performed using isobutyl alcohol, acetic acid and H_2O (3:1:1) as solvent to separate methionine from its oxidized form. The radioactive spots were visualized by autoradiography. The spots of methionine and methionine sulfoxide were excised from the TLC sheet and were quantitated by liquid scintillation counting (1217 Rackbeta LSC). The percentage of non-oxidized methionine was calculated by counts per minute $(cpm)_{MET}$ over cpm_{TOTAL} (cpm_{TOTAL} represents the radioactivity of the entire lane). The percentage of non-oxidized methionine was used as a correction factor for calculating the methionine-acceptance in an aminoacylation assay since methionyl-tRNA synthetase can only utilize the non-oxidized form in its reaction.

2.3.1.8.5.2. Methionine accepting tRNA^{fMet}

0.05-0.1 A_{260} units of wild-type tRNA^{fMet} were used for aminoacylation. Aminoacylation buffer 1 (10x: 1.5 M NH_4Cl, 100 mM $MgCl_2$, 100 µg/µl BSA, 1 mM Na_2EDTA, 200 mM imidazole·HCl, pH 7.6), 2 mM of ATP, 83µM L-[^{35}S]-methionine (specific activity 6.48 x 10^3 cpm/pmol) and 2.5 µl of MetRS (1.54 x 10^{-6} U/µl) were added per reaction. The mixture was incubated at 37°C. 5 µl aliquots were taken at various time points and spotted onto 3MM Whatman filter paper (soaked in 10% TCA/ 2% casamino acid). The filters were washed for 10 min in ice cold 10% TCA/ 2% casamino acids, 3x 15 min in ice cold 5% TCA and finally in ice cold 96% ethanol. Subsequently the filters were dried at 75°C and the acid-precipitable counts were determined by Liquid Scintillation Counting (LSC).

10x Aminoacylation buffer 1	
Imidazole·HCl, pH 7.6	200 mM
NH_4Cl	1.5 M
$MgCl_2$	100 mM
Na_2EDTA	1 mM

2.3.1.8.5.3. Glutamine accepting $tRNA^{fMet}$

The reactions contained 30 mM HEPES-KOH (pH 7.4), 10 mM magnesium acetate, 10 mM KCl, 2 mM ATP, 50 µM L-[^{3}H]-glutamine (specific activity 1.12 x 10^4 cpm/pmol), 0.05 to 0.1 A_{260} unit of glutamine accepting $tRNA_2^{fMet}$ and 22 µg of *E. coli* GlnRS enriched S100 protein extract. Standard procedure was carried out as described above (2.3.1.8.5.2.).

10x Aminoacylation buffer 2	
HEPES·KOH, pH 7.4	300 mM
$MgCl_2$	100 mM
KCl	100 mM

2.3.1.9. 5'-end radiolabelling of tRNA

2.3.1.9.1. Labelling and purification of labelled tRNA

5'-[^{32}P]-end labelling of tRNA was carried out by dephosphorylation and subsequent phosphorylation of the tRNA by polynucleotide kinase (PNK) (Silberklang *et al.*, 1977).

0.15 A_{260} unit of wild-type $tRNA_2^{fMet}$ and 0.1 A_{260} unit of each mutant $tRNA_2^{fMet}$ were denatured in 1x SAP buffer (10x: 0.5 M Tris·HCl, pH 7.6, 50 mM MgCl) for 1 min at 65°C. To dephosphorylate the tRNA, 2.5 U of Shrimp alkaline phosphatase were added for a final reaction volume of 25 µl and subsequently incubated for 1 h at 37°C, followed by heat inactivation at 65°C for 20 min. Radiolabelling of the 5'-end of the dephosphorylated tRNA was carried out using a PNK reaction mixture containing dephosphorylated tRNA, 1x SAP buffer, 5 mM DTT, 12.7 µM ATP, 0.66 µM γ-[^{32}P]-ATP and 25 U of PNK. The mixture was incubated for 30 min at 37°C followed by heat inactivation of the enzyme as described earlier. The tRNA was extracted twice with phenol/chloroform (saturated with 10 mM sodium acetate), followed by one chloroform/isoamyl alcohol extraction. The tRNA was ethanol precipitated for 20 min on dry ice. The pellet was washed twice with 70% ethanol and dissolved in 5 µl of TE buffer (pH 7.4). The 5'-[^{32}P]-end labelled tRNA was purified by gel electrophoresis on an 8% polyacrylamide gel (40x20x0.04 cm) containing 7 M urea and TBE buffer. Following pre-electrophoresis for 1 h at 1300 V at room temperature

in TBE, samples were loaded and electrophoresis was carried out for 4 h at 1300 V. The tRNA was located by autoradiography and passively eluted from the gel slice by shaking for 12 h at 4°C into TE buffer (pH 8). The slurry was settled by short centrifugation. The supernatant was transferred into a fresh tube and replaced by 1 volume of fresh buffer twice. The supernatants were combined and loaded onto a DE52 cellulose column, equilibrated with buffer WB2. The column was washed extensively with the same buffer in order to remove all residual urea. The tRNA was eluted with elution buffer EB3 with a flow rate of 0.1 ml/h. 100 µl fractions were collected. Fractions containing radiolabelled tRNA were combined, 0.2 A_{260} unit of unlabelled tRNA was added and ethanol precipitation was performed. The pellet was washed with 96% ethanol and dissolved in TE buffer (pH 7.4).

2.3.1.9.2. Analysis of 5'-[^{32}P]-end labelled tRNA

Analysis of the 5'-[^{32}P]-end labelled tRNA was performed using a modified protocol described by Silberklang et al.(Silberklang *et al.*, 1979).

The reaction (5 µl) contained a 1 µl aliquot of denatured 5'-[^{32}P]-labelled tRNA and 1 µg of nuclease P1 (1 mg/ml) in 50 mM ammonium acetate. For the preparation of the UV markers 20 µg of carrier yeast tRNA were digested with 2 µg of nuclease P1. The mixture was incubated for 5 hours at 37°C. Cerenkov counting of the enzymatic digested radiolabelled tRNA was performed and 30,000 cpm were added to 2.5 µl of the carrier tRNA digest. The mixture was dried under vacuum. Ammonium acetate was removed by dissolving the pellet in 5 µl of H_2O and subsequently the pellet was dried under vacuum, which was repeated 5 times. The final pellet was dissolved in 2 µl of H_2O and 1 µl was spotted onto a TLC sheet (13255 Cellulose). Chromatography in the first dimension was carried out in solvent 1 containing isobutyric acid, concentrated ammonium hydroxide and H_2O (66/1/33). After drying overnight at room temperature the second dimension was run in solvent 2 containing 0.1 M sodium phosphate (pH 6.8), ammonium sulfate and n-propyl alcohol (100/60/2; v/w/v). The plate was dried and autoradiography was performed. The UV markers were detected by UV shadowing.

2.3.1.10. Preparative aminoacylation and formylation of 5'-[^{32}P]-end labelled tRNA^{fMet}

2.3.1.10.1. Preparation of formyltetrahydrofolate (fTHF)

fTHF is stored in HCl as N^5,N^{10} –methenyl form and has to be converted to its N^{10} –formyl and active form just prior to use by incubation in 40 mM imidazole·HCl (pH 8.0) at 37°C for 10 min.

2.3.1.10.2. Preparation of formylaminoacyl-tRNA^{fMet}

(A) *Methionine accepting tRNA$_2^{fMet}$*: 5'-[^{32}P]-labelled tRNA was renatured in the presence of 10 mM $MgCl_2$ by incubation in aminoacylation buffer 1 (composition see 2.3.1.8.5.2.) in a total volume of 50 µl. The mixture was incubated for 2 min at 55°C, transferred to 37°C for 15 min and kept at room temperature for 15 min. A 100 µl reaction, containing the renatured tRNA, 4 mM ATP, 1 mM L-methionine, aminoacylation buffer 1, 10 µg BSA and 18.3 µg or 36.6 µg *E. coli* MetRS for wild-type and mutant tRNA^{fMet} G72 or mutants G73 and G72C73, respectively, was incubated for 20 min at 37°C. 45 µl of 1.1 mM *N*^{10}-formyltetrahydrofolate (330 µM final concentration, activated prior to use), as well as 2.6 µg (for tRNA$_2^{fMet}$ wild-type), 5.3 µg (for mutants G73 and G72C73) or 10.6 µg (for mutant G72), respectively, of a histidine tagged version of *E. coli* MTF, were added to the aminoacylation reactions and further incubation was carried out for 30 min at 37°C. The reaction mixtures were extracted with phenol/chloroform (equilibrated with 10 mM NaOAc, pH 5.2) twice, followed by one extraction with chloroform. The tRNA was precipitated in the presence of 0.3 M sodium acetate (pH 5.2) and 2 volumes of 96% ethanol. After centrifugation the pellets were washed with ice cold 70% ethanol, vacuum dried and dissolved in 50 µl of 5 mM sodium acetate (pH 5.2). tRNAs were separated from small contaminating molecules by size exclusion using G-25 Sephadex Quick spin columns. The recovered tRNA was ethanol precipitated; pellets were washed with 70% ethanol and dissolved in 50 µl of 5 mM sodium acetate (pH 5.2). Spectrometric analysis at A_{260} was carried out and small aliquots were taken for further analysis of the samples by acid urea gel. Finally the samples were aliquoted, quick frozen and stored at -20°C until further use.

(B) *Glutamine accepting tRNA$_2^{fMet}$*: 5'-[^{32}P]-labelled mutant tRNA$_2^{fMet}$ U35A36 was renatured in aminoacylation buffer 2 (composition see 2.3.1.8.5.3.) following the

same procedure as described above. Aminoacylation reaction was carried out for 20 min at 37°C in 100 µl containing 30 mM HEPES·KOH (pH 7.4), 10 $MgCl_2$, 10 mM KCl, 2 mM ATP, 5 mM DTT, 1 mM L-glutamine, 100 µg BSA/ ml and 22.5 µg histidine tagged *E. coli* GlnRS. The formylation reaction was initiated by the addition of N^{10}-formyltetrahydrofolate (330 µM final concentration) and 2.6 µg of *E. coli* MTF and was further incubated for 30 min at 37°C for completion. Purification of the reaction product was done as described above (2.3.1.10.2.).

2.3.1.11. Preparation of 3'-end radiolabelled formylaminoacyl-tRNA^{fMet}

2.3.1.11.1. Aminoacylation and Formylation

(A) *wild-type initiator* $tRNA_2^{fMet}$: Generation of formylated tRNA was adapted from Mayer et al. (Mayer *et al.*, 2003). First, 2 A_{260} units of purified $tRNA_2^{fMet}$ were renatured in the presence of 10 mM $MgCl_2$ by incubation of the tRNA in 25 µl of aminoacylation buffer 1 (see 2.3.1.8.5.2.) for 2 min at 55°C, 15 min at 37°C and finally for 15 min at room temperature. Aminoacylation reaction was carried out in 100 µl containing aminoacylation buffer 1, 2 mM ATP (pH 7.0), 0.1 µg BSA, 100 µM (specific activity: 40.8 Ci/mmol) or 250 µM (specific activity: 5.85 Ci/mmol) L-[S^{35}]-methionine and 22 µg of histidine tagged MetRS. The reaction mixture was incubated at 37°C for 20 min. 35 µg of histidine tagged MTF were added together with N^{10}-formyltetrahydrofolate (330 µM final concentration, activated prior to use). The reaction was incubated further at 37°C for 30 min. The incubation mixture was extracted two times with phenol/chloroform (equilibrated with 10 mM sodium acetate, pH 5.2), followed by one extraction with chloroform. The tRNA in the final aqueous supernatant was precipitated in the presence of 0.3 M sodium acetate (pH 5.2) and 2 volumes of ethanol. After precipitation the tRNA was dissolved in 10 mM sodium acetate (pH 5.2) and dialyzed 3x 1 h against 10 mM sodium acetate (pH 5.2) and 1 M NaCl, followed by 2x 1 h against 10 mM sodium acetate (pH 5.2) and 1 h against 5 mM sodium acetate. The tRNA was again precipitated in the presence of 0.3 M sodium acetate (pH 5.2) by 2 volumes of ethanol. After centrifugation, the tRNA was dissolved in 5 mM sodium acetate (pH 5.2).

(B) *mutant initiator* $tRNA_2^{fMet}$ *G72*: 2 A_{260} unit of purified tRNA was renatured, aminoacylated and formylated as described in (A).

(C) *mutant initiator* $tRNA_2^{fMet}$ *U35A36*: 2 A_{260} units of purified tRNA was renatured in 16 µl of aminoacylation buffer 2 (see 2.3.1.8.5.3.) as described in (A). Aminoacylation reaction was carried out in 200 µl containing aminoacylation buffer 2,

2 mM ATP (pH 7.0), 5 mM dithiotreitol, 0.8 U pyrophosphatase, 200 µM L-[^{3}H]-glutamine (specific activity: 3.4 Ci/mmol) 15 µg of histidine-tagged GlnRS. The reaction mixture was incubated at 37°C for 20 min, followed by addition of 35 µg of His-tagged MTF and N^{10}-formyltetrahydrofolate solution (330 µM final concentration). The reaction was continued at 37°C for 30 min.
Extraction, precipitation and dialysis of mutant $tRNA_2^{fMet}$ were performed as described (A). The extent of aminoacylation and formylation of all species was confirmed by acid urea gel electrophoresis and Northern blot analysis. Concentration of tRNA was determined by A_{260} measurements.

2.3.1.11.2. Alkaline-treatment and chromatographic analysis

2 µl of the final samples (~ 200,000 cpm) and an equal volume of 0.1 N of sodium hydroxide were incubated at 37°C for 1 h. 2 µl were spotted on a cellulose Thin Layer Chromatography sheet (13255 Cellulose) and chromatography was performed for 2 h using a solvent containing n-butanol, pyridine, acetic acid and water (30:20:6:24). Subsequently, the sheet was air dried and autoradiography was performed using Kodak BioMax™ MR x-ray films.

2.3.2. Proteins and Enzymes

2.3.2.1. Characterization of proteins

2.3.2.1.1. Concentration and buffer exchange of protein samples

Purification of proteins and protein extracts often entails several steps that require different buffer conditions, e.g. different pH and salt concentration, step-specific chemical compounds that interfere in the downstream procedure. During preparative work it is also often necessary to concentrate diluted samples in order to proceed to the next step. The following methods have been applied throughout this work.

2.3.2.1.1.1. Dialysis

For dialysis either Slide-A-Lyzer® Dialysis Cassettes or SpectraPor® 6 Dialysis Membranes with the appropriate cut-offs have been used. Dialysis membranes were prepared by boiling the tubings in 2% (w/v) disodium carbonate and 1 mM disodium ethylenediaminetetraacetic acid (pH 8), followed by rinsing them several times in distilled water. The membranes were boiled in 1 mM disodium ethylene-

diaminetetraacetic acid (pH 8), allowed to cool and were finally stored in ethanol at 4°C. Before use, the tubings were washed with distilled water.
Dialysis was carried out in a volume that exceeded the sample volume by 100-fold.

2.3.2.1.1.2. Ultrafiltration

Centricon® Centrifugal filter units YM-30 and YM-50 with 30 and 50 kD cut-off, respectively, were used for efficient concentration and desalting of small volume (max. 1 ml) as well as removal of contaminating proteins of lower molecular weight. The samples were applied to the filtration units and centrifuged at 5,000x*g* and 4°C. The retentates were washed several times with the desired buffer, recovered and processed further.

2.3.2.1.2. Quantitation of proteins in aqueous solutions

2.3.2.1.2.1. Protein quantitation by Bradford assay

The assay is based on the observation that the absorbance maximum for an acidic solution of Coomassie Brilliant Blue G-250 shifts from 465 nm to 595 nm when binding to arginine and aromatic residues of a protein occurs (Bradford, 1976). Both hydrophobic and ionic interactions stabilize the anionic form of the dye, causing a visible color change. The assay is useful since the extinction coefficient of a dye-albumin complex solution is constant over a 10-fold concentration range. The protein concentration of a test sample is determined by comparison to that of a series of protein standards known to reproducibly exhibit a linear absorbance profile in this assay.

Measurement of unknown protein concentration:
Measurements of protein concentration were performed using Bradford dye reagent from BioRad Laboratories. 1 ml of Bradford reagent was added to 10 µl of protein solution. After incubation for 5 min the absorbance at 595 nm was measured. Standard curves were created by assaying BSA solutions of known protein amount ranging from 1 to 10 µg.

2.3.2.1.2.2. Protein quantitation by UV absorbance

Proteins in solution absorb ultraviolet light with absorbance maxima at 280 and 215 nm. Amino acids with aromatic rings such as phenylalanine, tryptophan and tyrosine

are the primary reason for the absorbance peak at 280 nm. Peptide bonds are primarily responsible for the peak at 215 nm. Secondary, tertiary, and quaternary structure all affect absorbance, therefore factors such as pH, ionic strength, etc. can alter the absorbance spectrum. For most proteins, UV-light absorption allows detection of concentration down to 100 µg/ml. Since protein samples can contain nucleic acid that absorb at 260 nm as well as 280 nm, Warburg and Christian (Warburg and Christian, 1942) derived an equation that correct for this contamination:

$$[\text{Protein}]\ (\text{mg/ml}) = 1.55 \times A_{280} - 0.76 \times A_{260}$$

Measurement of protein solutions:
Concentration of proteins in aqueous solutions was determined by measuring the absorption of UV-light at 260 nm and 280 nm.

2.3.2.1.3. Electrophoretic separation of proteins

Polyacrylamide gel electrophoresis can be used to separate complex mixtures of proteins. A common method for separating proteins is a discontinuous polyacrylamide gel electrophoresis under denaturing conditions, that is, in the presence of sodium dodecyl sulfate (SDS) (Laemmli, 1970). A discontinuous SDS-polyacrylamide gel consists of an upper stacking gel (pH 6.8) which concentrates the proteins and a lower resolving gel (pH 8.8) which separates the proteins. The separation is based on the fact that SDS, an anionic detergent, binds to the amino acid residues of the proteins, disrupting the secondary and tertiary structure and conferring a net negative charge on all the proteins, making the linearized polypeptide chains migrate in an electric field on the basis of their size. The electrophoretic mobility of a protein in the gel is inversely proportional to the logarithm of its mass. Protein separation by SDS-PAGE can be used to estimate relative molecular mass, to determine the relative abundance of major proteins in a sample, and to determine the distribution of proteins among fractions. The purity of protein samples can be assessed and the progress of a fractionation or purification procedure can be followed.

2.3.2.1.3.1. SDS-polyacrylamide gel electrophoresis

Throughout the course of this study protein samples were subjected to SDS-polyacrylamide gel electrophoresis using a 12% polyacrylamide gel and a Mini-PROTEAN 3 Cell slab gel system from Biorad Laboratories.
First, the resolving gel was poured vertically between two bottom sealed glass plates, followed by carefully pouring double distilled water on top of the gel solution. After polymerization of the resolving gel, the water was removed and the stacking gel was poured on top the resolving gel. An appropriate comb was applied and the stacking gel was allowed to polymerize. The ready-to-use gel was clamped into the clamping frame and electrode assembly fold, and placed into the buffer tank. The apparatus was filled with electrophoresis buffer, the comb was removed and the wells were thoroughly flushed with buffer. Protein samples were prepared by addition of 2x SDS-loading buffer and heating the samples for 3 min at 100°C. The samples were loaded onto the gel along with a BenchMark™ Pre-stained Protein Ladder as molecular mass marker. The apparatus was attached to a power-supply and electrophoresis was started at 60 V. After the BPB dye moved into the resolving gel, the voltage was increased to 120 V. Electrophoresis was continued until the BPB dye reached the bottom of the gel.

Solutions were prepared according to Sambrook *et al.* (Sambrook and Russell, 2001)

Resolving gel (12%)	
	per 15 ml
AA:Bis (29:1) 30%	6 ml
Tris·HCl, 1.5 M (pH 8.8)	3.8 ml
ddH_2O	4.9 ml
SDS (10%)	150 µl
APS (10%)	150 µl
TEMED	6 µl

Stacking gel (5%)	
	per 5 ml
AA:Bis (29:1) 30%	0.83 ml
Tris·HCl, 1 M (pH 6.8)	0.63 ml
ddH_2O	3.4 ml
SDS (10%)	50 µl
APS (10%)	50 µl
TEMED	5 µl

2x SDS-loading buffer	
Tris·HCl, pH 6.8	100 mM
SDS	4% (w/v)
Glycerol	17% (v/v)
2-mercaptoethanol	0.1% (v/v)
BPB	0.1% (w/v)

Electrophoresis buffer	
Tris base	25 mM
Glycine	250 mM
SDS	0.15% (w/v)

2.3.2.1.3.2. Staining of proteins in gels

Proteins can easily and rapidly be located by Coomassie Brillinat Blue staining. Detection of protein bands depends on nonspecific binding of the dye, Coomassie blue R, to proteins. The detection limit is 100ng/ protein band.

Following gel electrophoresis, gels were incubated in staining solution for 1h at room temperature with shaking. Thereafter, they were destained with methanol/acetic acid destaining solution with shaking until blue protein bands appeared against a clear background. For preservation, the gels were rinsed for several minutes in a 10% glycerol/water solution placed between two sheets of cellophane on a gel drying apparatus or subjected to air drying at 37°C.

Staining solution	
Methanol	45% (v/v)
Acetic acid	10% (v/v)
Coomassie blue R	0.05% (w/v)
ddH_2O	45%

Destaining solution	
Methanol	45% (v/v)
Acetic acid	10% (v/v)
ddH_2O	45%

2.3.2.1.3.3. Densitometric analysis of protein gels

Spot densitometry of Coomassie stained SDS-polyacrylamide gels was performed using a ChemiImager™. Scans were evaluated with the AlphaEase™ Software according to the application note provided by the manufacturer.

2.3.2.1.4. Western blot analysis

Proteins that were separated by SDS-polyacrylamide gel electrophoresis can be further analyzed by immunoblotting, often referred to as Western blotting (Towbin *et al.*, 1979). As a first step, the proteins are electrophoretically transferred in a tank or a semidry transfer apparatus to a nitrocellulose, PVDF, or nylon membrane. The transferred proteins are immobilized on the surface of the membrane providing access for reaction with immunodetection reagents. In the second step, a primary antibody (polyclonal or monoclonal) is used to identify specific antigens. The membrane is washed and the antibody-antigen complexes are identified with with a secondary antibody. This secondary antibody is specific an anti-IgG antibody (e.g. sheep anti-mouse IgG) and is coupled to horseradish peroxidase (HRP) or alkaline phosphatase enzymes. Chromogenic or luminescent substrates are used to visualize the activity carried by the secondary antibody.

2.3.2.1.4.1. Transfer and immunodetection

After separation by SDS-polyacrylamide gel electrophoresis, proteins were transferred onto an Immobilon-P® membrane using a Hoefer blotting tank. The transfer was carried out for 2 h at 65 V at 4°C in ½ Towbin buffer containing 10% methanol.

After the successful transfer, the membrane was washed twice for 10 min in PBS and was blocked overnight in blocking buffer. The membrane was briefly rinsed in PBS, and incubated for 2 to 4 h at room temperature in blocking buffer containing the primary antibody (α-*Eco*IF2 Ig (rabbit), 1:20,000; or α-His4 Ig (mouse), 1:2,500). Subsequently the membrane was washed 3 times for 10 min with washing buffer followed by incubation with the secondary antibody for 1h at room temperature (anti-rabbit Ig (sheep), HRP-linked, 1:5,000; or anti-mouse Ig (sheep), HRP-linked, 1:7500 in blocking buffer). Finally the membrane was washed once again, excess liquid removed, and detection of the antibody coupled peroxidase was performed with an ECL oxidase/luminol reagent kit. The signals were detected by autoradiography using X-Omat AR X-ray films.

½ Towbin buffer	
Tris	12 mM
Glycine	96 mM

5x PBS	
	per 1000 ml
Na_2HPO_4	41.15 g
NaH_2PO_4	10.2 g
NaCl	20 g
ddH_2O	→ pH7.4

Wash buffer	
PBS	1x
Tween 20	0.1% (v/v)
Non-fat dry milk	0.25% (w/v)

Blocking buffer	
PBS	1x
Tween 20	0.1% (v/v)
Non-fat dry milk	1% (w/v)

2.3.2.1.4.2. Stripping of Western membranes

Following immunodetection the Western membrane can be reused for probing with a different primary antibody. This requires the removal of the previous antibody, known as stripping. For stripping the membrane was incubated in stripping solution for 30 min at 50°C, followed by rinsing the membrane several times in PBS. A new round of immunodetection was initiated by incubating the membrane in blocking buffer and further continued as described in 2.3.2.1.4.1.

Stripping solution	
Tris·HCl, pH 6.8	62.5 mM
SDS	2% (v/v)
2-mercaptoethanol	100 mM

2.3.2.1.5. Purification of proteins by conventional Chromatography

2.3.2.1.5.1. Purification by Metal-Chelate Affinity Chromatography

Immobilized metal affinity chromatography (IMAC) is used primarily in purification of recombinant proteins engineered to have six consecutive histidine residues on either

the amino or carboxy terminus. This is achieved by using the natural tendency of histidine to chelate divalent metals such as Ni^{2+} or Co^{2+}. Under conditions of physiological pH (~pH 7), histidine binds by sharing electron density of the imidazole nitrogen with the electron-deficient orbital of transition metals. Elution of polyhistidine-tagged proteins occurs in a competitive manner in the presence of moderate concentrations of imidazole (in the elution buffer) that is identical to the histidine side chain. For purification of recombinant polyhistidine-tagged proteins a cobalt-based IMAC resin (TALON™ Metal Affinity resin from BD Bioscience Clontech) was chosen. Compared to nickel-based IMAC resins, that often exhibit an undesirable tendency to bind unwanted host proteins containing exposed histidine residues, a cobalt-based IMAC resin displays an enhanced selectivity for polyhistidine-tagged proteins, thus reducing the affinity for host proteins. Prior to sample application the IMAC resin was equilibrated with binding buffer (see section 2.3.2.2.2.) according to the instructions of the manufacturer.

2.3.2.1.5.2. Purification by Gel-Filtration Chromatography

Gel filtration separates proteins solely on the basis of differences in molecular size. Separation is achieved using a porous matrix to which the molecules, for steric reasons, have different degrees of access. Smaller molecules have greater access and larger molecules less. The matrix is packed into a chromatographic column, the sample mixture applied, and the separation accomplished by passing an aqueous buffer (the mobile phase) through the column. Protein molecules that are confined in the volume outside the matrix beads will be swept through the column by the mobile phase and the sample is thus eluted in decreasing order of size. The protein fractions eluted are detected by UV measurement and fractions are collected for subsequent analysis and further preparation steps.

Throughout the course of this study Sephacryl™ 200HR from Amersham Biosciences Corp. was used as matrix for gel filtration chromatography. Prior to sample application the matrix was equilibrated by passing 10 fold bed volume of appropriate buffer through the column. Specific conditions are given in detail in the section were gel filtration chromatography was applied.

2.3.2.1.5.3. Purification by Ion-Exchange Chromatography

Ion-exchange chromatography separates biomolecules on the basis of surface charge. Charged groups on the surface of a protein interact with oppositely charged

groups immobilized on the ion-exchange medium. The charge of a protein depends on the pH of its environment. The pH at which the net charge of a protein is zero, i.e. where the numbers of positive charges equals the numbers of negative charges, is known as the isoelectric point (pI). When the operating pH is greater than the pI, the protein will have a net negative charge, and should bind to anion-exchange media, which are positively charged. When the operating pH is less than the pI, the protein will have a net positive charge, and should bind to cation-exchange media, which are negatively charged.

For preparation of protein extracts applying ion-exchange chromatography diethylaminoethyl cellulose (DE52) from Whatman Int. Ltd. was used as anion-exchange media. The DE52 cellulose was prepared by equilibrating the pre-swollen resin with the appropriate equilibration buffer (further specified in section 3.3.2.1.) according to the instructions of the manufacturer.

2.3.2.2. Recombinant expression and purification of *Escherichia coli* initiation factor 2

2.3.2.2.1. Organisms and culture

E. coli strain JM109, transformed with the plasmid pQE-IF2 (Mayer *et al.*, 2003) was grown in LB broth supplemented with 200 µg ampicillin per ml.

2.3.2.2.2. Recombinant expression and purification of *E. coli* IF2

The recombinant host, carrying pQE-IF2, was grown in 10 ml LB broth overnight at 37°C. The primary culture was used to inoculate 1 L of LB broth and the culture was grown with shaking at 37°C to A_{600} of 0.6. Recombinant expression of N-terminally histidine tagged IF2α was induced by 1 mM IPTG and cells were grown for further 4 h at 37°C. Subsequently the cells were pelleted, washed once with 100 ml of 20 mM Tris·HCl (pH 7.5), 5 mM $MgCl_2$ and stored at –20°C. Induction and overexpression were analyzed by SDS-PAGE.

Cells were thawed on ice and resuspended in 25 ml of cold buffer XP. The buffer was supplemented with 4 tablets of EDTA-free Complete Mini protease inhibitor in order to reduce proteolytic cleavage of the N-terminal fragment. Cells were disrupted by two passages through a French pressure cell (15,000 psi) at 4°C and cell debris was removed by centrifugation at 10,000x*g* at 4°C. The purification was carried out using

the TALON™ Metal Affinity resin according to the manufacturer's batch-gravity flow purification protocol. The clarified lysate was added to 20 ml of Talon-slurry (50% in buffer XP) and binding of histidine tagged protein was allowed to proceed for 30 min at 4°C, followed by centrifugation for 5 min at 1,000x*g*. After 3 cycles of washing with 5 volumes of buffer XP for 10 min, the slurry was transferred to a column and washed with 10 bed volumes of buffer XP10. Bound protein was eluted with buffer XP100. 5 ml fractions were collected and aliquots of the fractions were analyzed by SDS-PAGE. The protein containing fractions were pooled and repeatedly (8x) passed through through a Centricon® YM-50 filtration unit by centrifugation at 5,000x*g* for 1 h at 4°C until the entire sample was applied. The concentrated supernatant was re-diluted with buffer PW and centrifuged again. The protein was recovered from the filter unit and dialyzed against buffer PS. Finally the protein concentration was determined using Bradford binding-dye assay (2.3.2.1.2.1.) and histidine tagged *E. coli* IF2α was stored at -20°C. Prior to use in electrophoretic mobility shift assay (EMSA) and filter binding assay IF2 dilutions were prepared based on the fraction of full-length IF2 in the protein sample, obtained from densitometry measurements of Coomassie stained SDS-gels.

Buffer XP	
Tris·HCl, pH 8.0	20 mM
NaCl	500 mM
PMSF	1 mM
2-mercaptoethanol	10 mM

Buffer XP10	
Tris·HCl, pH 8.0	20 mM
NaCl	500 mM
PMSF	1 mM
2-mercaptoethanol	10 mM
Imidazole·HCl, pH 7.6	10 mM

Buffer XP100	
Tris·HCl, pH 8.0	20 mM
NaCl	500 mM
PMSF	1 mM
2-mercaptoethanol	10 mM
Imidazole·HC', pH 7.6	100 mM

Buffer PW	
Tris·HCl, pH 8.0	20 mM
NaCl	300 mM
PMSF	1 mM
2-mercaptoethanol	10 mM

Buffer PS	
Tris·HCl, pH 8.0	20 mM
NaCl	200 mM
2-mercaptoethanol	10 mM
Glycerol	50%

2.3.2.3. *Bacillus stearothermophilus* IF2

2.3.2.3.1. Organisms and culture

B. stearothermophilus (Cat. #7953; American Type Culture Collection, Manassas, VA, USA) was cultured at 55°C in nutrient broth. *Escherichia coli* XL1-blue, harboring plasmid pQ30/BSIF2, was grown at 37°C in LB broth supplemented with 100 µg ampicillin per ml. *E. coli* M15 containing the plasmid pREP4 and transformed with pQE-BSIF2 was cultured at 37°C in LB broth supplemented with 100 µg ampicillin per ml and 30 µg kanamycin per ml.

2.3.2.3.2. Isolation of DNA

Genomic DNA from *Bacillus stearothermophilus* was isolated as described in section 2.3.1.4.2. The plasmid pQE30 and its derivative were propagated in *E. coli* XL1-blue and isolated with QIAprep miniprep method. Qiagen's gel extraction kit was used to isolate DNA fragments from agarose gels.

2.3.2.3.3. Cloning of *B. stearothermophilus infB* gene

Unless specified otherwise, for cloning, methods outlined in section 2.3.1.6. were used. The entire *B. stearothermophilus infB* gene (Brombach *et al.*, 1986) was amplified by PCR from genomic DNA using $Vent_R$ DNA Polymerase and employing 5'-GGCAGGATCCAAAATGCGTGTGTACGAA and 5'-GGCAGGTACCTGCCCGAGCCACTTCCTG as forward and reverse primers, respectively. The first and last 21 nucleotides of the reading frame of *B. stearothermophilus infB* were used to design the primers. The forward primer also contained a *Bam*HI site that overlapped with the *infB* start codon, while the reverse primer also contained a *Kpn*I site. The restriction sites were later used for cloning the gene into the expression vector pQE30. The PCR amplified *inf*B gene product was purified using QIAquick PCR purification kit and subjected to restriction

digest using *Kpn*I and *Bam*HI restriction enzymes. Subsequently the 2.1 kb fragment was cloned into pQE30. After transformation into *E. coli*, XL1-blue positive clones were screened by digestion of isolated plasmid DNA with *Nco*I restriction enzyme. The cloned region was further sequenced by automated sequencing using the Applied Biosystems 3730 capillary DNA sequencer (Applied Biosystems Inc., Foster City, CA) at the MIT CCR HHMI Biopolymers Laboratory, Massachusetts Institute of Technology, employing the manufacturer's Big Dye Terminator Cycle Sequencing Reaction Mix.

2.3.2.3.4. Recombinant expression and purification of *B. stearothermophilus* IF2

The pQE30 clones containing the intact reading frame of *B. stearothermophilus infB* were transformed into *E. coli* M15/pREP4 expression system (Qiagen Inc.). The constructs produced IF2 with an N-terminal histidine tag. The recombinant host, carrying pQE30-BstIF2, was grown in 10 ml LB broth supplemented with 100 µg ampicillin per ml and 30 µg kanamycin per ml at 37°C for 12 h, which was used as inoculum for 1 L of LB broth containing the same antibiotics. The culture was incubated with shaking at 37°C, and when culture at A_{600} of 1.0, IF2 expression was induced with 1 mM IPTG. After 2 h of further incubation, the culture was centrifuged and cells were washed with 20 mM Tris·HCl (pH 7.5), 5 mM $MgCl_2$. Following further centrifugation the cell pellet was quick frozen and stored at -20°C until further use.
The cells were thawed on ice in the presence of 25 ml buffer XP containing 5 tablets of EDTA-free Complete Mini protease inhibitor and were disrupted by passage through a French pressure cell at 10,000 psi at 4°C. The lysate was clarified by centrifugation at 10,000x*g* for 30 min at 4°C. The supernatant was further diluted to a final volume of 100 ml with buffer XP containing 2 tablets of Complete Mini protease inhibitor. The whole mixture was applied to 10 ml of TALON™ Metal Affinity resin pre-equilibrated with buffer XP. Binding of histidine tagged protein was allowed for 20 min at 4°C. The slurry was settled by centrifugation, washed 4x with buffer XP and loaded onto a column (40x1 cm). After further washes with buffer XP10, bound protein was eluted with buffer XP100. 4 ml fractions were collected and analyzed by SDS-PAGE. Protein-containing fractions were pooled and volume was reduced by passage through Centricon YM-30 filtration units. The concentrated sample (1 ml) was loaded by gravity flow onto a 100 cm by 1 cm Sephacryl-200HR column pre-equilibrated with buffer XP. Buffer was passed through the column at a flow rate of

0.35 ml/min using a peristaltic pump. 1 ml fractions were collected by a fraction collector and were analyzed by Bradford binding dye assay and SDS-PAGE. Fractions containing full-length IF2 were pooled, concentrated by passage through Centricon YM-30 filtration units and subsequently dialyzed against buffer PS. Finally the protein concentration was determined using Bradford binding-dye assay (2.3.2.1.2.1.) and the sample was stored at -20°C.

2.3.3. tRNA binding assays

2.3.3.1. Electrophoretic Mobility Shift Assay

2.3.3.1.1. General experimental setup

Pre-reaction mixtures (9 µl) containing IF2 (5 µM to 0.01 µM dilution series) 20 mM Tris·HCl (pH 7.4), 20 mM NaCl, 1 mM DTT and 1.25 µM yeast $tRNA^{Tyr}$ were incubated for 10 min on ice. Binding reactions were initiated by the addition of 1 µl of 5'-^{32}P-labelled formylaminoacyl-tRNA (0.2 µM) and were allowed to reach equilibrium by incubation for further 15 min on ice. Reactions containing *Bacillus stearothermophilus* IF2 were incubated at room temperature (Wu and RajBhandary, 1997).

2 µl of loading buffer (50% glycerol, 0.05% bromphenol blue) were added and the reaction mixtures were applied onto a 6% polyacrylamide gel (19:1; 20x20x0.07 cm gel dimension). The electrophoresis buffer was 0.5x TBE. Pre-electrophoresis was done for 1 h at 4°C and 100 V. Electrophoresis was carried out at 150 V for 2 h at 4°C. The gel was fixed in 10% methanol/10% acetic acid, dried and exposed. The amounts of free formylaminoacyl-tRNA and the bound formylaminoacyl-tRNA were determined using a Typhoon™ 9400 PhosphorImager with Image Quant software.

2.3.3.1.2. Calculations of K_D

For calculation of K_D, IF2 concentrations were plotted as X axis (in µM) and the fraction of formylaminoacyl-tRNA in complex as Y axis. K_D values for the IF2·formylaminoacyl-tRNA complexes, involving wild-type initiator $tRNA_2^{fMet}$ and the mutant initiator $tRNA_2^{fMet}$ were calculated by Sigma Plot® from the curve fit based on the equation for one site saturation ligand binding:

$$y = \frac{B_{\max} \cdot x}{K_d + x}$$

2.3.3.2. RNase protection assay

The protocol is a modification of the methods described by LaRiviere *et al.* (LaRiviere *et al.*, 2001) and Stortchevoi *et al.* (Stortchevoi *et al.*, 2003).

2.3.3.2.1. General experimental setup

First, 3 µl of diluted samples of IF2 (diluted serially from 50 µM to 10 µM, see experimental setup) were added to 24 µl of a pre-mixture containing 22.5 mM Tris·HCl (pH 7.4), 1.25 mM of $MgCl_2$, 1.25 mM dithiothreitol and 1.5 µM yeast $tRNA^{Tyr}$. The binding reactions were started by addition of 3 µl of ^{3}H- or ^{35}S- labelled formylaminoacyl-tRNA (400 nM in 5 mM NaOAc, pH 5.2) and the mixtures (30 µl) were incubated for 20 min on ice to allow the reactions to reach equilibrium. 10 µl of RNase A solution (concentrations shown below) were added. The reaction was incubated on ice for a certain time (see experimental setup) and stopped by addition of 10 µl of 50% ice cold TCA, followed by 5 µl of 1 mg/ml solution of total *E. coli* tRNA. The samples were filtered under vacuum through a sheet of Millipore membrane (HAWP, 0.45 µm) mounted on a Bio-Dot™ apparatus. The membrane was washed three times with 200 µl each of 5% TCA, removed from the apparatus and rinsed in ice cold 96% ethanol for additional 5 min. Subsequently, the membrane was air dried at room temperature and membrane fragments corresponding to individual samples were excised and transferred into scintillation vials for liquid scintillation counting.

2.3.3.2.2. Measurements of off rates of IF2·formylaminoacyl-tRNA complexes

The incubation mixture (100 µl) contained 5 µM IF2 and 40 nM formylaminoacyl-tRNA in binding buffer. The mixture was incubated for 30 min on ice and treated with 20 µl of RNase A (3.75 ng/µl). 20 µl aliquots were taken out at 5, 10, 20, 30 and 60

s and were transferred to a well, on a 96-well assay plate, containing 20 µl of ice cold 20% TCA. Further steps were carried out as described in 2.3.3.2.1.

2.3.3.2.3. Effect of IF2 concentration on protection against RNase cleavage

In a 30 µl reaction, 1 µM or 5 µM IF2 were incubated either with 40 nM fMet-tRNA (wild-type) or 40 nM fGln-tRNA (mutant U35A36) for 20 min on ice. 0.025 µg of RNase A (in 10 µl) was added and the reaction was stopped after 30 s. Further steps as described in 2.3.3.2.1.

2.4. Results

2.4.1. Purification of wild-type and mutant initiator $tRNA_2^{fMet}$

Binding studies of complex formation between bacterial IF2 and wild-type and mutant initiator tRNA from *E. coli* required large quantities of pure initiator tRNA. The *E. coli* genome encodes two different initiator tRNA ($tRNA^{fMet}$) (Ikemura and Ozeki, 1977). The major fraction of cellular initiator tRNA ($tRNA_1^{fMet}$) is encoded by the *metZ* gene (Kenri *et al.*, 1994) while a relatively small fraction of initiator $tRNA^{fMet}$ ($tRNA_2^{fMet}$) is encoded by the *metY* gene (Ikemura and Ozeki, 1977; Ishii *et al.*, 1984). The two isoacceptor $tRNA^{fMet}$ species differ in a single nucleotide at position 46. $tRNA_1^{fMet}$ has m^7G, whereas $tRNA_2^{fMet}$ has A (Dube *et al.*, 1969; Egan *et al.*, 1973). All mutants used in this study are derivatives of the latter species and were expressed recombinantly in the *E. coli* strain B105, a strain where the *metY* locus specifies $tRNA_1^{fMet}$, resulting in the lack of the $tRNA_2^{fMet}$ species (Mandal and RajBhandary, 1992).

Further purification of wild-type $tRNA_2^{fMet}$ and mutants thereof is primarily based on the ability to separate $tRNA_2^{fMet}$ from all other tRNAs on a non-denaturing poly-acrylamide gel (Seong and RajBhandary, 1987). The individual steps in purification are illustrated in figure 2-3. The initiator tRNAs were overexpressed in *E. coli* strain B105 by culturing cells overnight at 37°C. The cells were harvested and total RNA was obtained by extraction with water- or Tris-saturated phenol (2.3.1.8.2.). Phenol extraction was carried out for several hours with shaking at 4°C. The aqueous phase containing nucleic acid was separated from the organic phase by centrifugation and

nucleic acids recovered by ethanol precipitation. Following phenol extraction, large

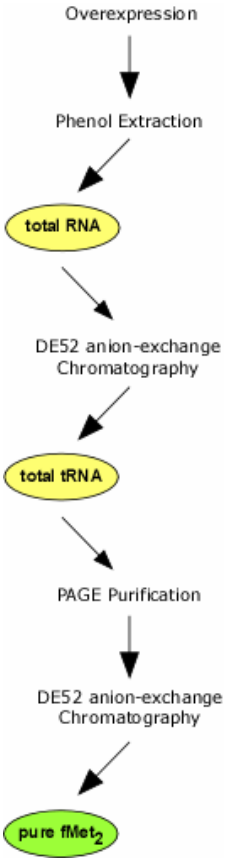

Fig. 2-3:
Flowscheme of steps involved in purification of *E.coli* $tRNA_2^{fMet}$

ribosomal RNA (rRNA) and contaminating DNA molecules were removed by anion-exchange chromatography (2.3.1.8.3.). The total RNA sample was applied to a DE52 column and extensively washed. tRNA molecules were eluted from the column in the presence of 1 M sodium chloride, while the larger and highly negatively charged rRNA molecules remained tightly bound to the DE52 matrix. After the tRNA containing fractions were pooled, the total tRNA was precipitated, dissolved in appropriate buffer and sample concentrations were determined. In the next step, $tRNA_2^{fMet}$ was separated from $tRNA_1^{fMet}$ and other tRNA by polyacrylamide gel electrophoresis under non-denaturing conditions (2.3.1.8.4.). $tRNA_2^{fMet}$ is one of the fastest migrating tRNA under these conditions (Fig. 2-4B). As mentioned above *E. coli* B105 does not contain any endogenous $tRNA_2^{fMet}$, which makes this strain suitable for expression of mutant $tRNA_2^{fMet}$ completely free of contamination by wild-type $tRNA_2^{fMet}$. Typically 20 to 50 A_{260} units of total tRNA were loaded onto a preparative 12% polyacrylamide gel and subjected to electrophoresis (2.3.1.1.2.1.).

Following gel electrophoresis tRNAs were located on the gel by UV-shadowing as shown in figure 2-4. Wild-type and mutant tRNAs (here: G73, G72C73, and G72U73, respectively) showed high expression levels, confirming results obtained by aminoacylation assays of total tRNA samples (see Table 2-1). The tRNA of interest was excised from the gel avoiding any contamination by other tRNAs and recovered from the gel. The combined elution fractions were applied to a small DE52 anion-exchange column in order to concentrate the tRNA by subsequent column elution and ethanol precipitation. Finally the tRNA was taken up in appropriate storage buffer and the highly enriched tRNA tested for its methionine and glutamine acceptance by

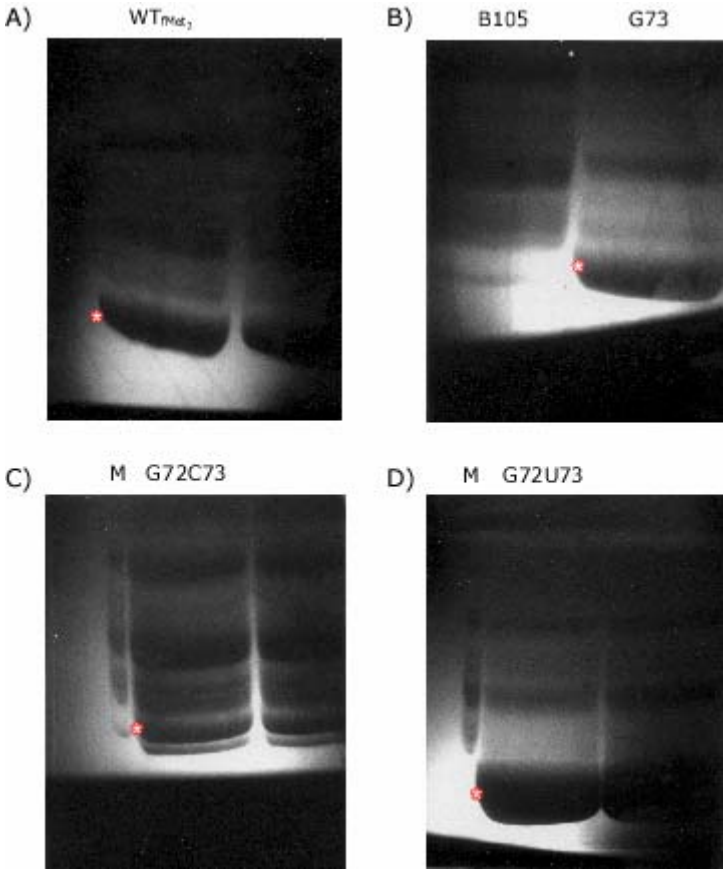

Fig. 2-4: Detection of separated tRNA by UV shadowing

tRNA species were separated on a preparative 12% polyacrylamide gel (2 slots, 40x20x0.15 cm gel dimension). The star indicates the band of interest. A) 20 A_{260} units of $tRNA_2^{fMet}$ Wild-type enriched total tRNA were applied to each well. B) 50 A_{260} units of G73 enriched total tRNA as well as 10 A_{260} units of total tRNA obtained from *E. coli* B105 were loaded onto the gel; C) 50 A_{260} of G72C73 enriched total tRNA were applied; M, 0.5 A_{260} total tRNA obtained from *E. coli* B105; D) 50 A_{260} units of total tRNA enriched with G72C73 were applied onto the gel. M, total tRNA obtained from *E. coli* B105, 0.5 A_{260} units were applied.

aminoacylation assays (2.3.1.8.5.). The percentage of acceptance for its cognate amino acid indicates the overall purity of a tRNA batch. The progression in purifying wild-type and mutant $tRNA_2^{fMet}$ is summarized in table 2-1. Besides determining the purity by ways of aminoacylation assays the highly enriched tRNAs were further analyzed for the presence of $tRNA_1^{fMet}$ by analytical polyacrylamide gel electrophoresis and subsequent Northern blot analysis (2.3.1.2). 0.15 A_{260} units of total tRNA and final sample of wild-type and mutant $tRNA_2^{fMet}$ were loaded onto a 15% analytical polyacrylamide gel. After electrophoresis the gel was stained with ethidium bromide and the separation pattern was documented. Subsequently, the

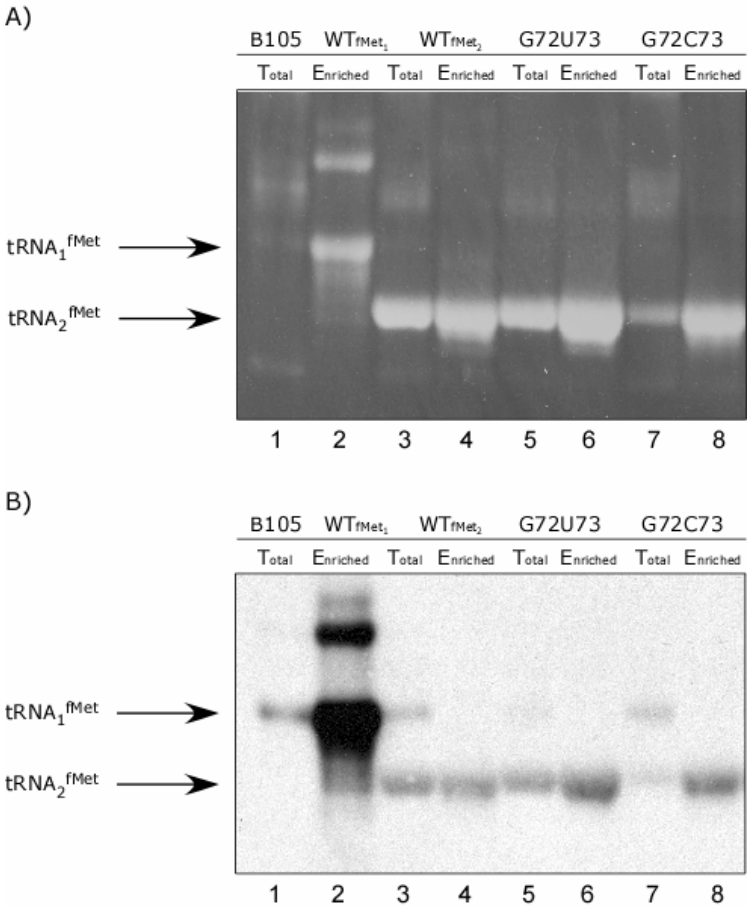

Fig. 2-5: PAGE and Northern blot analysis of purified wild-type and mutant *E. coli* $tRNA_2^{fMet}$ G72U73 and G72C73

tRNAs were separated on an analytical 15% non-denaturing polyacrylamide gel. 0.15 A_{260} units of total and enriched tRNA of each tRNA species were applied. A) tRNAs were detected by ethidium bromide (0.5 ug per ml); B) Northern blot analysis. The blot was hybridized with 5'-^{32}P-labelled oligonucleotides complementary to $tRNA_1^{fMet}$: 5'- ACCGACGACCTTCGGGT -3'.

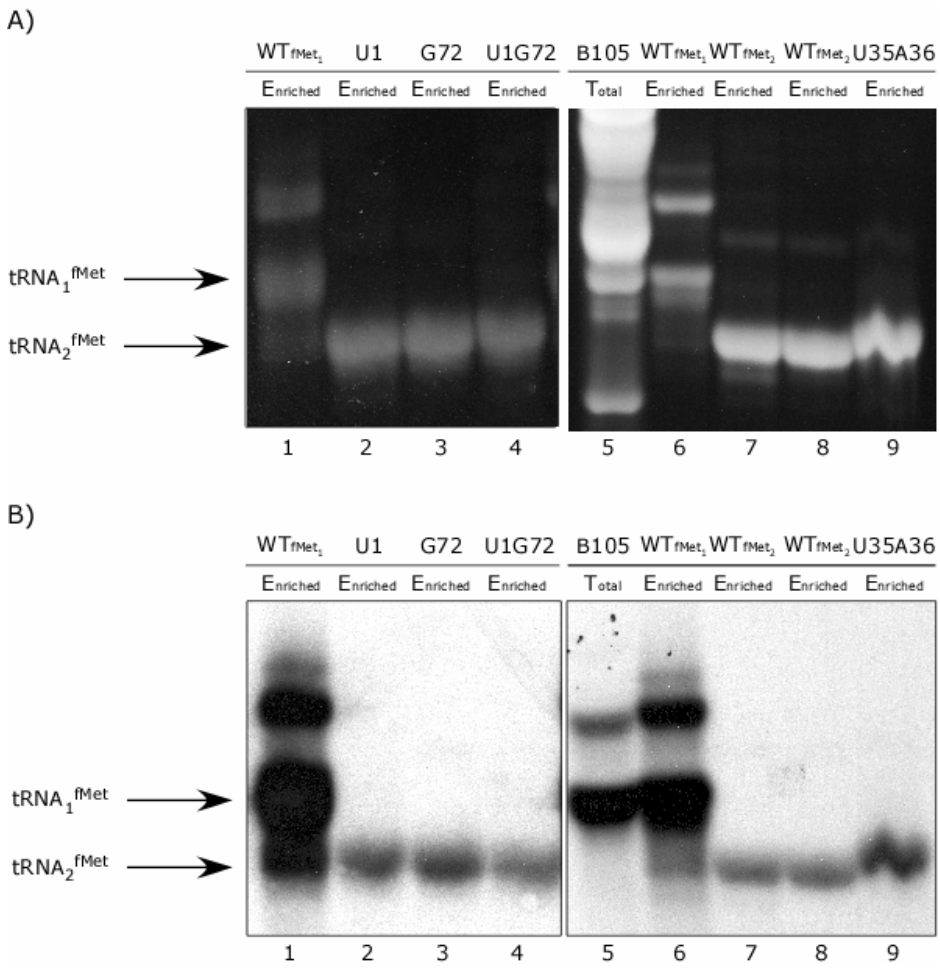

Fig. 2-6: PAGE and Northern blot analysis of purified wild-type and mutant *E. coli* $tRNA_2^{fMet}$ U1, G72, U1G72, and U35A36

tRNAs were separated on an analytical 15% non-denaturing polyacrylamide gel. 0.15 A_{260} unit of total and enriched tRNA of each tRNA species was applied. A) tRNAs were detected by ethidium bromide (0.5 ug/ml); B) Northern blot analysis. The blot was hybridized with 5'-^{32}P-labelled oligonucleotides complementary to $tRNA_1^{fMet}$: 5'- ACCGACGACCTTCGGGT -3'.

tRNAs were transferred from the gel onto a Hybond-N^+ membrane by electroblotting. After successful transfer, the tRNAs were cross-linked to the membrane and subjected to pre-hybridization. In the hybridization step, the membrane was probed with an oligonucleotide complementary to the sequence between nucleotides 39 to 55 of $tRNA_1^{fMet}$. Hybridization was carried out for 24 h at 42°C. The membrane was washed in SSC and autoradiography was performed. Figures 2-5 and 2-6 show the results of the polyacrylamide gels stained with ethidium bromide (A) and Northern blot analysis (B) of purified wild-type and mutant $tRNA_2^{fMet}$. Along with the purified

tRNAs, total tRNA from untransformed B105 and partially purified $tRNA_1^{fMet}$ were loaded onto the gels as markers. Although the sequences of $tRNA_1^{fMet}$ and $tRNA_2^{fMet}$ only differ at position 46, both display different mobilities in non-denaturing polyacrylamide gels, which allows the distinct identification by Northern blot analysis of any contamination by $tRNA_1^{fMet}$ in the purified tRNA batches. Comparison of total tRNA samples and $tRNA_1^{fMet}$ marker with the corresponding samples of highly enriched $tRNA_2^{fMet}$ indeed shows that all purified tRNA batches were free of any contamination by isoacceptor $tRNA_1^{fMet}$. Therefore the methionine acceptance solely accounts for wild-type $tRNA_2^{fMet}$ and mutants.

$tRNA_2^{fMet}$	$tRNA_2^{fMet}$ in total tRNA [%]	Quantity of purified $tRNA_2^{fMet}$ *(total tRNA applied [A_{260} unit])*	Purity of $tRNA_2^{fMet}$ [%]
Wild-type	**~ 32**	**12.7 A_{260} units** *(120)*	**97.4**
G73	**~ 23**	**13.9 A_{260} units** *(100)*	**84.3**
G72U73	**~ 36**	**25.1 A_{260} units** *(100)*	**99.7**
G73C73	**~ 18**	**6.9 A_{260} units** *(150)*	**84.2**
U1	**N/D**	**9.9 A_{260} units** *(200)*	**89.3**
G72	**N/D**	>100 A_{260} units[a]	**99.4**
U1G72	**N/D**	**5.4 A_{260} units** *(120)*	**87.5**
U35A36	**~ 15**	**6.8 A_{260} units** *(140)*	**98.2**

Table 2-1: Compilation of purified *E. coli* wild-type and mutant initiator tRNA

Amounts of tRNAs were determined by spectrophotometry at 260 and 280 nm readings and are defined as A_{260} units (1 A_{260} unit equals 40 µg of tRNA). Purity of tRNA corresponds to acceptance of the appropriate amino acid as determined by aminoacylation assay.[a] Laboratory stock.

Overall, wild-type and mutant $tRNA_2^{fMet}$ were obtained in sufficient amounts and purity for their use in electromobility shift and filter binding assays. Throughout the course of this study it was necessary to purify several other batches of wild-type and mutant $tRNA_2^{fMet}$ with approximately the same yield and purity as described above. In case of mutants G73 and G72C73, which had only purities of 84.3 and 84.2 %, respectively, aliquots of aminoacylation reaction were analyzed by acid urea gel and found to be fully aminoacylated (2.4.2.). Furthermore they were radioactively labelled with ^{32}P at the 5'-end, subjected to nuclease P1 digestion and analyzed by

2D thin-layer chromatography (2.3.1.9.2.). Based on co-migration of UV-markers the positions of the four major mononucleotides pA, pG, pU, and pC were localized on the TLC sheet after chromatography. Autoradiography of the plates revealed in all cases a single spot, which was identified to be nucleotide cytidine (Fig. 2-7B/C). Since the initiator tRNA is the only tRNA in *E. coli* that possesses a cytosine at position 1 it was concluded that batches of mutant $tRNA_2^{fMet}$ G73 and G72C73 were purified to homogeneity (purity >95%).

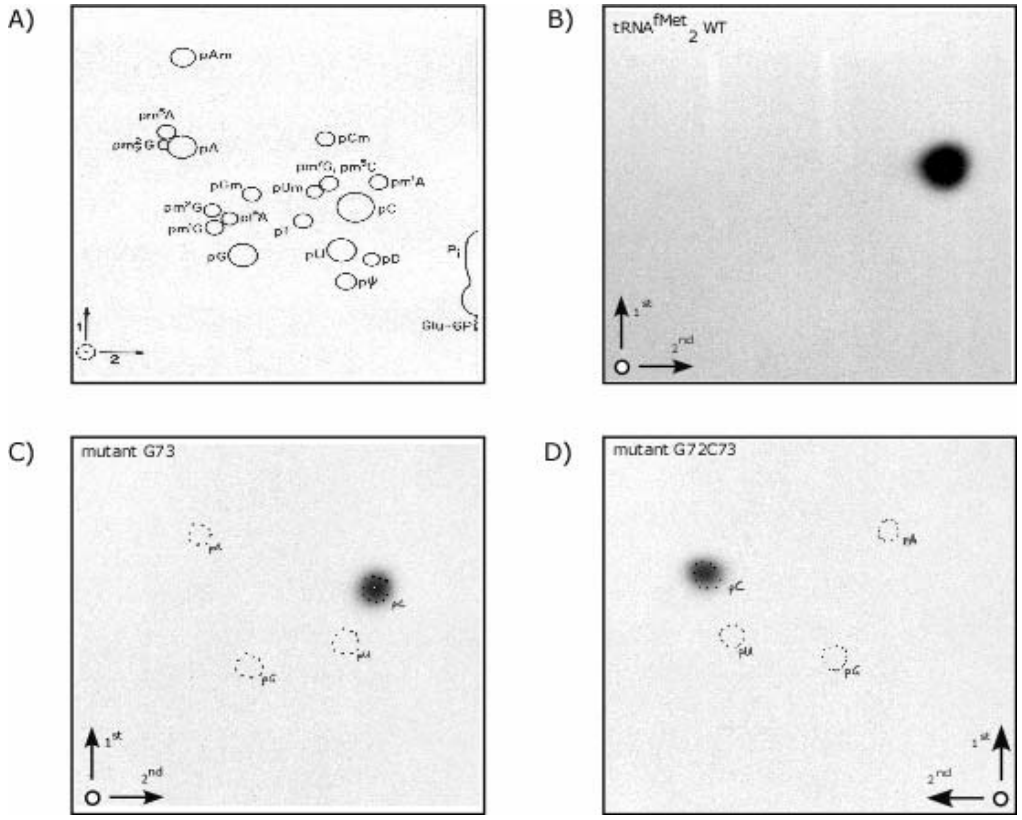

Fig. 2-7: 5' analysis of ^{32}P-labelled tRNA.

5'-[^{32}P]-tRNA were digested with nuclease P1, mixed with UV markers and subjected to 2D thin-layer chromatography. Autoradiography of TLC is shown; A) schematic illustration of the mobility of mononucleotides; B) wild-type $tRNA_2^{fMet}$; C) mutant $tRNA_2^{fMet}$ G73; D) mutant $tRNA_2^{fMet}$ G72C73.

2.4.2. Preparation of radiolabelled formylaminoacyl-tRNA^{fMet}

2.4.2.1. Preparation of 5'-[^{32}P]-labelled formylaminoacyl-tRNA^{fMet}

For their use as substrate in electrophoretic mobility shift assay to investigate the effect of mutations on IF2·fMet-tRNA, formylaminoacyl-tRNA^{fMet} labelled with ^{32}P had

to be prepared. Preparation of 5'-[^{32}P]-labelled formylaminoacyl-tRNA^{fMet} can be divided into two main parts: i) radioactive labelling, and ii) quantitative aminoacylation and formylation. Each part consists of several steps, which are illustrated in figure 2-8.

5'-[^{32}P]-labelling of tRNA is based on the principle of dephosphorylation by shrimp alkaline phosphatase (SAP) and subsequent phosphorylation using polynucleotide kinase (PNK) as described by Silberklang *et al.* (Silberklang *et al.*, 1977). Since both

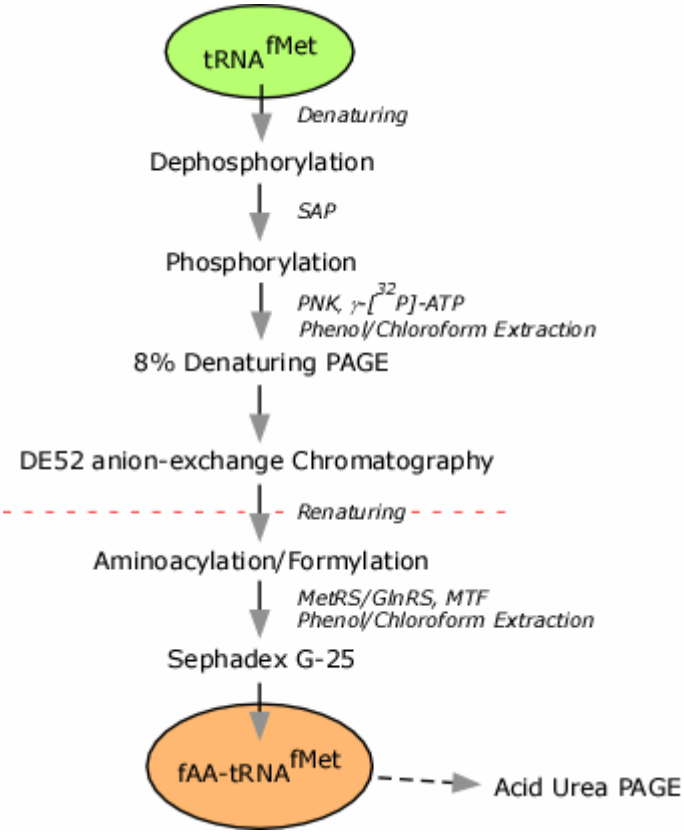

Fig. 2-8:
Flowscheme of preparation of 5'[^{32}P]-labelled formyl-aminoacyl-tRNA

enzymes favor single stranded DNA or RNA substrates, the tRNA was partially denatured by heat treatment before addition of SAP. In the following reaction, SAP removed the 5' phosphate group from cytosine at position 1. After incubation for 1 h at 37°C the enzyme was heat inactivated for 20 min at 65°C. ^{32}P was enzymatically attached to the dephosphorylated cytosine by PNK in the presence of γ-[^{32}P]-adenosine triphosphate. The labelling reaction was restricted to 30 min at 37°C due to the nuclease activity from the enzyme. The reaction was stopped and enzymes were removed by phenol/chloroform extraction, and the tRNA in the combined

aqueous phases was ethanol precipitated. Intact tRNA was separated from degradation products and ATP by gel electrophoresis under denaturing conditions. The intact tRNA was located on the gel by autoradiography and eluted from the excised gel piece. In order to remove any contamination by urea, which would inhibit the following aminoacylation reaction, the ^{32}P-labelled tRNA was applied to a DE52

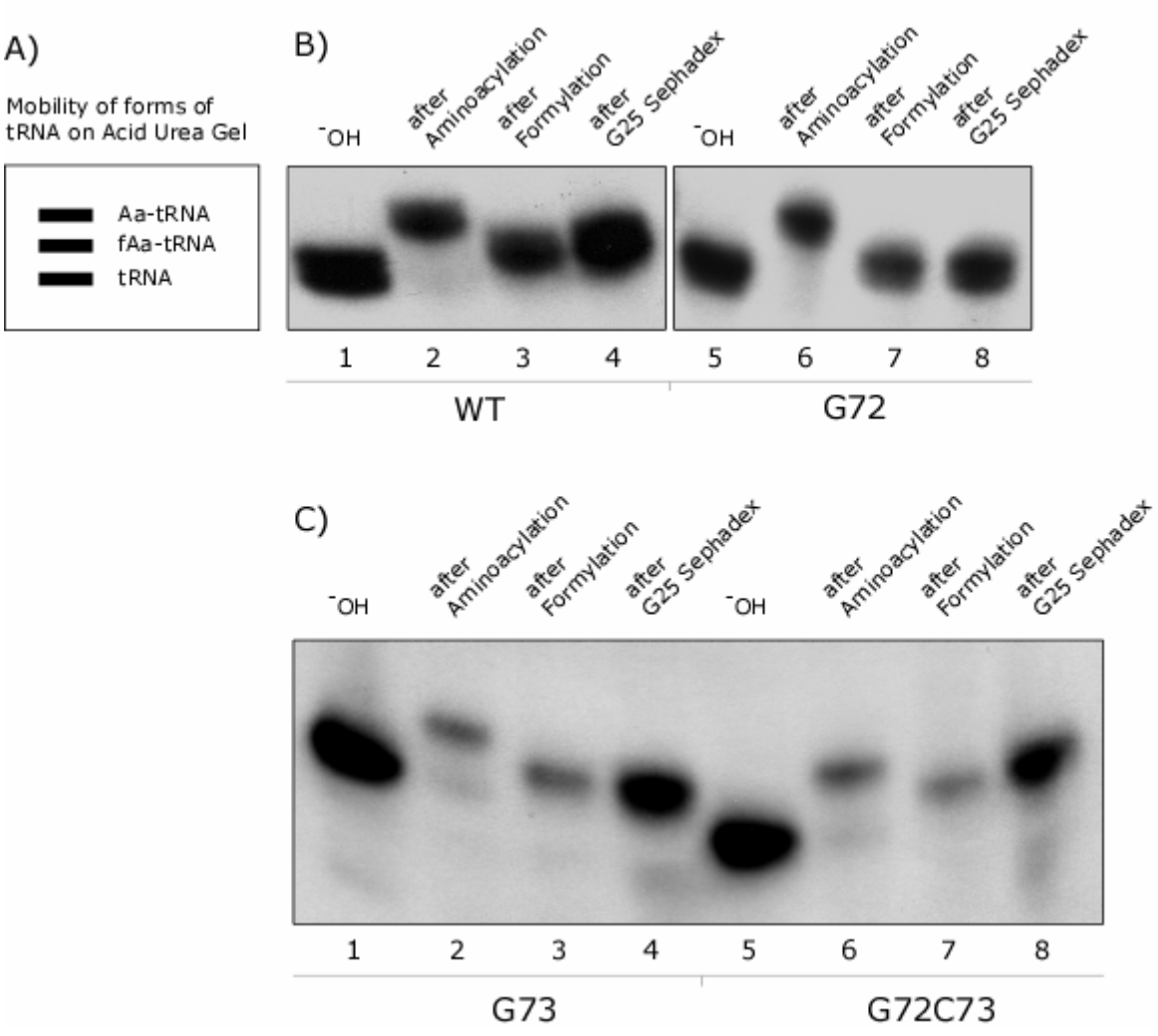

Fig. 2-9: Preparation of 5'-[32P]-labelled fMet-tRNA$_2^{fMet}$ wild-type and acceptor stem mutants

The figure shows an autoradiography of a 6.5% acid urea polyacrylamide gel. Samples included 0.1 A_{260} units of carrier tRNA. -OH: samples were treated with 0.1 M Tris·HCl (pH 9.5) for 30 min at 37°C; A) schematic illustration of the mobility of uncharged and charged forms of tRNAs on an acid urea gel; B) wild-type and mutant tRNA$_2^{fMet}$ G72; C) mutant tRNA$_2^{fMet}$ G73 and G72C73.

column and thoroughly washed. The eluted tRNA was collected by ethanol precipitation in the presence of non-radioactive tRNA of the same species. As the tRNA was recovered in a denatured form, it had to be renatured prior to its use in aminoacylation and formylation reactions. Renaturing of tRNA was facilitated in aminoacylation buffer containing 10 mM $MgCl_2$, since $MgCl_2$ can have a stimulating effect on tRNA folding. The tRNA was subsequently aminoacylated and formylated by its cognate aminoacyl-tRNA synthetase and methionine transformylase, respectively. Since it has been shown that the G73 and G72C73 mutants are poor substrates for methionyl-tRNA synthetase and mutant G72 a very poor substrate for MTF (Lee *et al.*, 1992), amounts of respective enzyme were increased in each case. Reactions

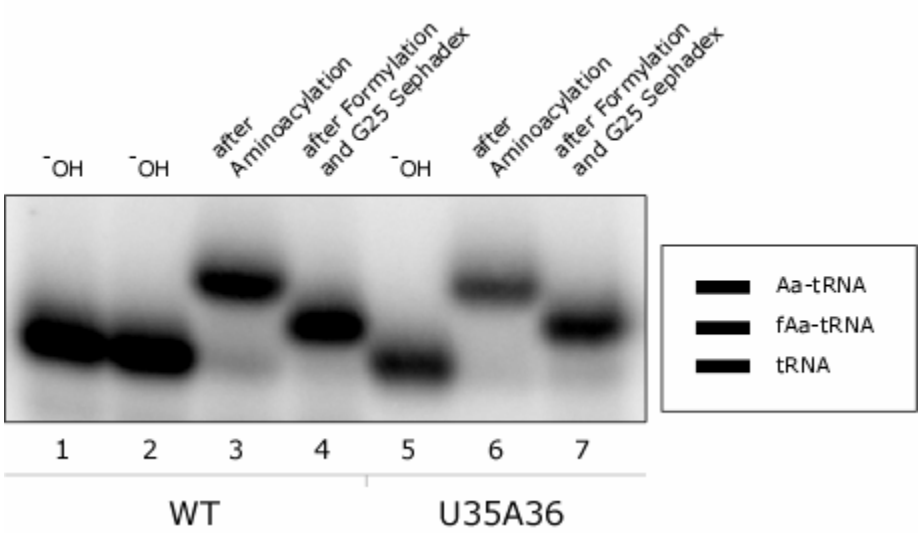

<u>Fig. 2-10:</u> Preparation of 5'-[32P]-labelled fMet-tRNA$_2^{fMet}$ wild-type and mutant U35A36

The figure shows an autoradiography of a 6.5% acid urea polyacrylamide gel. Samples included 0.1 A_{260} units of carrier tRNA. -OH: samples were treated with 0.1 M TrisHCl (pH 9.5) for 30 min at 37° C.

were stopped and enzymes were removed by phenol/chloroform extraction under acidic conditions. Formylaminoacyl-tRNA was recovered from the aqueous phase by ethanol precipitation and applied to Sephadex G-25 spin columns to remove small molecules such as amino acids and ATP. After a final ethanol precipitation, the pellets were dissolved in sodium acetate and samples were analyzed by acid urea gel electrophoresis (Fig. 2-9 and Fig. 2-10).

Analysis of samples taken during the preparation of 5'-[^{32}P]-labelled formylaminoacyl-tRNA^{fMet} by acid urea gel electrophoresis showed that all tRNAs were

quantitatively aminoacylated and formylated. In some cases, the final sample contained negligible traces of uncharged tRNA (Fig. 2-9C, lanes 4 and 8; Fig. 2-10, lane7) as determined by phosphor imaging. During the course of this study several batches of wild-type and mutant ^{32}P-labelled formylaminoacyl-tRNAs had to be prepared with similar results.

2.4.2.2. Preparation of 3'-end radiolabelled formylaminoacyl-tRNA^{fMet}

For their use in RNase protection assay it was necessary to radiolabel the tRNA at the 3' end. This was facilitated by using radio-labeled amino acid such as ^{35}S-methionine in case of wild-type and mutant tRNA^{fMet} G72 or ^{3}H-glutamine in case of mutant initiator U35A36. Preparative aminoacylation and subsequent formylation was carried out at 37°C for 20 min and 30 min, respectively. Figure 2-11 shows the general procedure. After the aminoacylation and formylation reactions, excess of

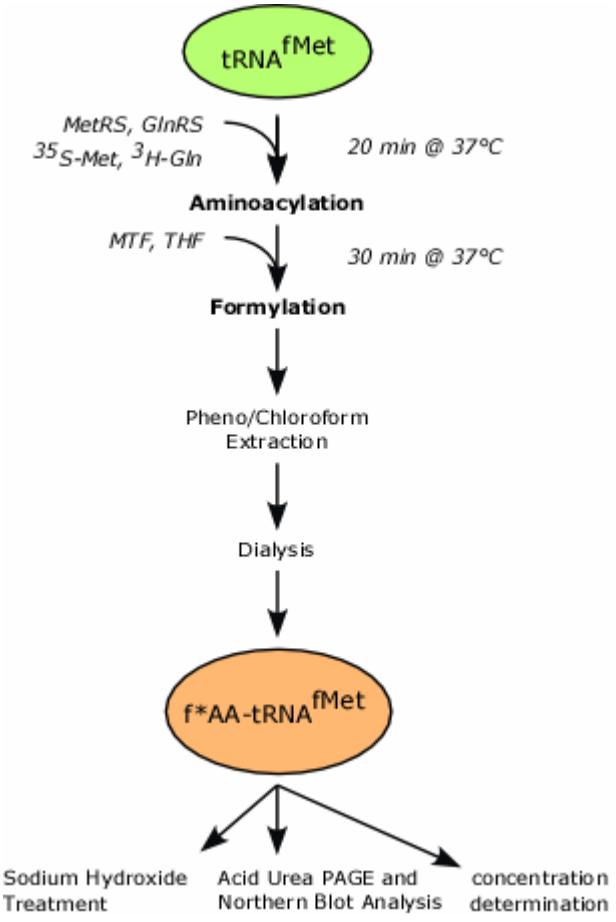

Fig. 2-11:
Flowscheme of preparation of 3'-radiolabelled fAa-tRNA

enzymes were removed by phenol/chloroform extraction under acidic conditions. Subsequently, extensive dialysis was performed in order to remove excess amounts of small molecules like amino acids and ATP, followed by ethanol precipitation. Final samples were analyzed by acid urea gel electrophoresis and Northern blot analysis (Fig. 2-12). Wild-type and mutant $tRNA_2^{fMet}$ G72 and U35A36 were quantitatively aminoacylated and formylated.

Another approach to analyze the formylation level of ^{35}S-methionylated tRNA is by alkaline treatment of the samples followed by thin layer chromatography, which will separate L-formylmethionine from L-methionine. The result of this experiment is shown in figure 2-13. There is a clear separation of formylmethionine from methionine. The use of 0.1 N sodium hydroxide (final concentration) efficiently hydrolyzed the radioactive amino acid from the 3' end of the tRNA. In all tRNA samples the hydrolyzed amino acid has a different mobility than the ^{35}S-Met marker (Fig. 2-13compare lanes 2, 3, 6 and 7 with lanes 1 and 5) indicating that all of the aminoacylated tRNA became quantitatively formylated by MTF. The appearance of additional spots when using 0.1 N Tris·HCl at pH 9.0 (Fig. 2-13, lane 4) can be

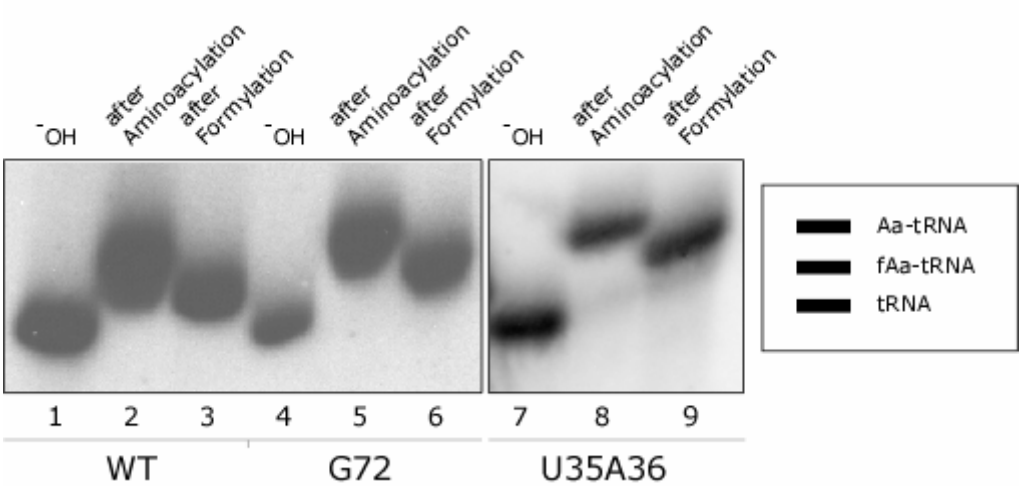

Fig. 2-12: Preparation of 3'-radiolabelled formylaminoacyl-$tRNA_2^{fMet}$

Progression of aminoacylation and formylation of wild-type and mutant tRNAs were analyzed by acid urea gel and Northern blot analysis. Aliquots from each reaction step were taken and added to 2x acid urea loading buffer containing 0.025 A_{260} units of yeast $tRNA^{Tyr}$ as carrier. The blot was hybridized with 5'-^{32}P-labelled oligonucleotides complementary to $tRNA_2^{fMet}$: 5'- GAACCGACGATCTTCGG -3'; -OH: samples were treated with 0.1 M TrisHCl (pH 9.5) for 30 min at 37°C.

explained by the fact that Tris not only facilitates hydrolysis by deprotonation of H_2O, but also reacts directly with the amino acid attached to the 3'-end of the tRNA, thereby forming a formylmethionine·Tris amide.

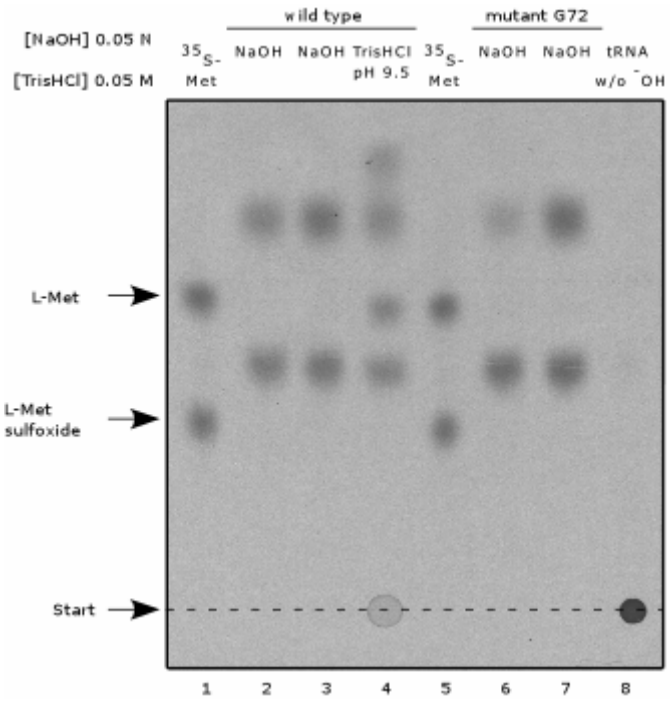

Fig. 2-13:

Alkaline treatment of f[^{35}S]-methionylated tRNA

Samples were incubated in the presence of either 0.05 N NaOH or 0.05 M Tris·HCl (pH 9.5) for 1 h at 37°C. 200,000 cpm of reaction and ^{35}S-Met marker were spotted. Autoradiography was performed using Kodax BioMax™ MR film.

2.4.3. Recombinant expression and purification of *E. coli* IF2

2.4.3.1. Induced expression of recombinant *E. coli* IF2

Binding studies of complex formation between *E. coli* IF2 and wild-type and mutant initiator tRNA required the purification of large amounts of IF2. This was achieved by expression of a recombinant version of IF2, which contains a N-terminal polyhistidine tag, and subsequent purification of the protein by metal-affinity chromatography.

A primary culture of *E. coli* strain JM109 transformed with plasmid pQE-IF2 (Mayer *et al.*, 2003) was used to inoculate 2x 500 ml of LB broth supplemented with ampicillin. The cultures were grown to a culture A_{600} of 0.6 and expression of recombinant *E. coli* IF2 was induced by the addition of IPTG. After further incubation of cultures at 37°C for 4 h the levels of expression were analyzed by SDS-polyacrylamide gel electrophoresis (Fig. 2-14). Samples of IPTG induced cultures (Fig. 2-14, lanes 5 to 8) showed accumulations of a protein of appropriate size, indicated by black arrow, compared to the sample of uninduced culture (Fig. 2-14, lane 9). It also appeared

that expression levels already reached saturation after 3 h post-induction since no increase of protein amounts could be observed after further incubation. Typically 3 to 4 g of cell pellets were obtained from a 1 L culture.

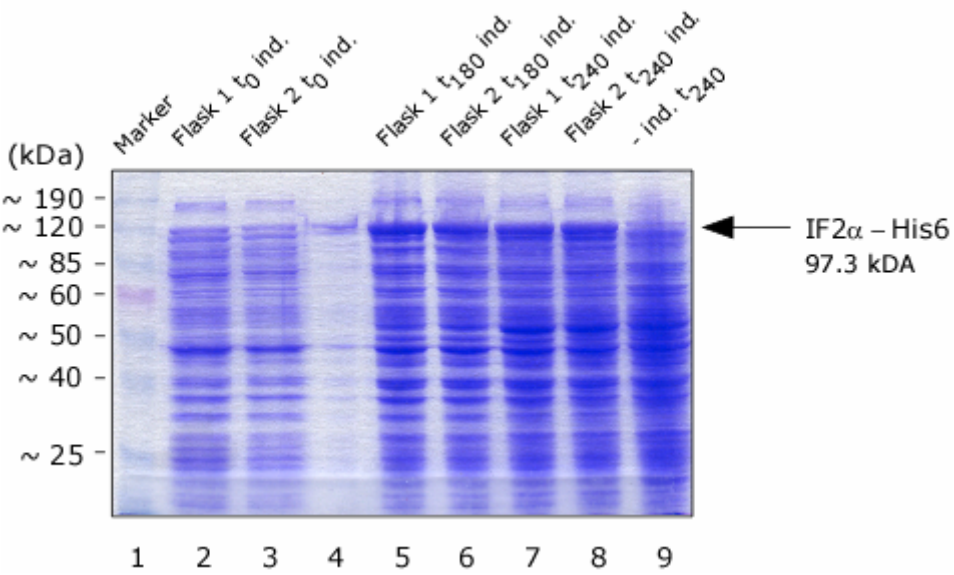

Fig. 2-14: Induced expression of recombinant *E. coli* IF2

Coomassie stained 10% SDS-PAGE is shown. 1 ml aliquots of cultures were taken at 0 h, 3 h, and 4 h post-induction. Cell pellets were resuspended in SDS-loading buffer and samples were boiled for 5 min. t_x refers to post-induction time [min].

2.4.3.2. Purification of recombinant *E. coli* IF2

Construction of proteins expressed with a terminal polyhistidine-tag allows a direct purification of the recombinant protein by metal affinity chromatography (2.3.2.1.5.1.). The *E. coli infB* gene was cloned such that gene expression led to a recombinant protein possessing a polyhistidine tag at the N-terminus (Mayer *et al.*, 2003). Due to the fact that some amounts of IF2 are proteolytic cleaved upon cell lysis, resulting in a 65 kDa C-terminal fragment, a polyhistidine tag at the N-terminus enables the purification of full-length IF2, thereby separating it from the cleavage product. Purification of *E. coli* IF2 was performed according to the protocol of Mayer *et al.* (Mayer *et al.*, 2003). The steps involved in purification are illustrated in figure 2-15. After cells were disrupted by passage through a French pressure cell, clarified lysate was applied to the cobalt-based TALON™ Metal Affinity resin. Histidine tagged IF2 was bound to the matrix by "batch-gravity flow" followed by extensive

washes. The resin was transferred to a column and was washed again in the presence of 10 mM imidazole in order to remove nonspecifically bound proteins. Elution of bound IF2 occurred in a buffer containing 100 mM imidazole until no more

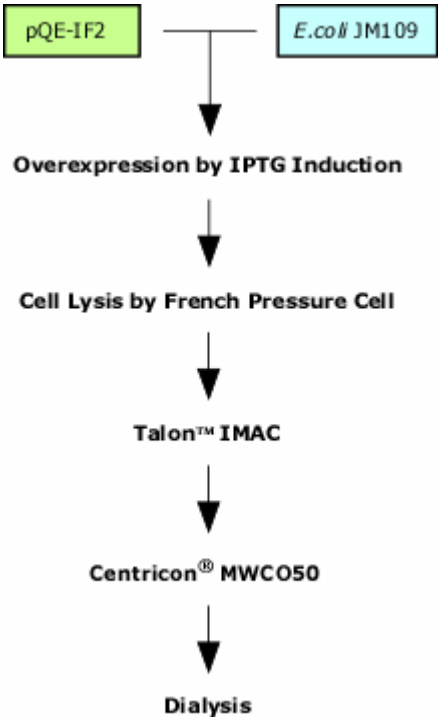

Fig. 2-15: Flowscheme of purification of *E. coli* IF2

Shown is a schematic illustration of the steps involved in purification of recombinant *E. coli* IF2 expressed in *E. coli* JM109 cells.

protein was detected in the fractions as determined by Bradford binding-dye assay (2.3.2.1.2.1.). The fractions were analyzed by SDS-polyacrylamide gel electrophoresis and pooled based on the ratio of full-length IF2 to contaminating fragments. The sample was subjected to ultrafiltration using Centricon® Centrifugal filter units with a 50 kDa cut-off. Finally the recovered protein was dialyzed against storage buffer and stored at -20°C. The progression of purification was analyzed by SDS-PAGE and Western blot analysis (Fig. 2-16). The clarified lysate (Fig. 2-16, lane 2) showed high proteolytic cleavage of *E. coli* IF2 despite the addition of protease inhibitors at high concentrations. However, almost the entire 65 kDa C-terminal cleavage product was successfully removed after metal affinity chromatography. The fragment hardly bound to the affinity resin and was washed off in the presence of 10 mM imidazole (Fig. 2-16, lanes 4 and 5). Negligible traces were detectable when large amounts of the purified IF2 (4 µg) were loaded onto the gel (Fig. 2-16, lanes 8 and 9). The only contamination which remained in the eluate was a small N-terminal

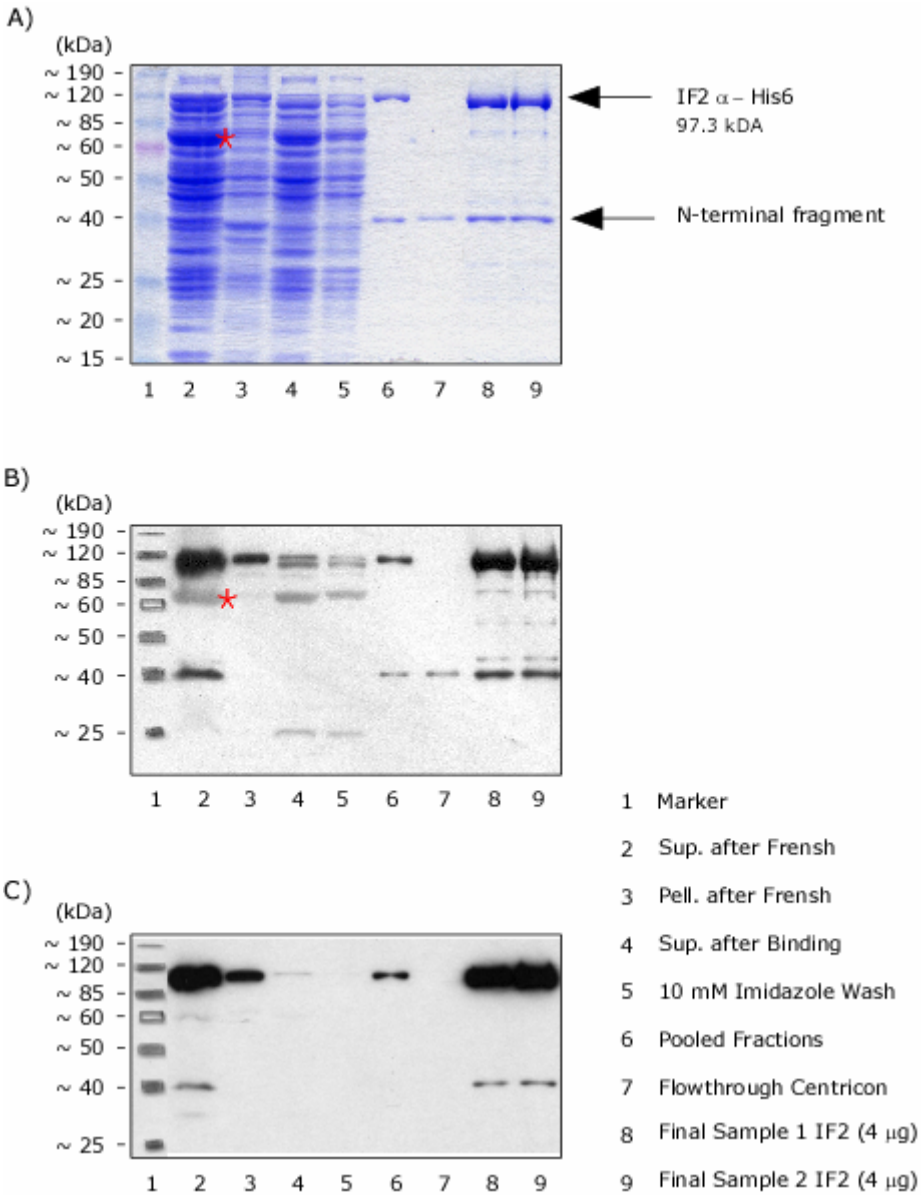

Fig. 2-16: Purification of recombinant *E. coli* IF2

Progression of IF2 purification analyzed by SDS-polyacrylamid gel electrophoresis and Western blotting; Red star indicates a 65 KDa C-terminal cleavage product of IF2 A) 10% SDS-PAGE of protein samples taken during the IF2 purification procedure. Lanes 2 and 3 show samples after cell lysis using a Frensh pressure cell and lane 4 to 6 during the TALON™ purification. Lanes 7 to 9 show samples taken during and after Centricon® purification. B) Western blot analysis of a 10% SDS-PAGE loaded with the same samples as in A. The blot was probed against IF2 using a polyclonal antibody. C) Western blot analysis of a 10% SDS-PAGE loaded with the same samples as in A. The blot was probed against tetra-histidine using a monoclonal antibody.

fragment (as indicated by western blot analysis; Fig. 2-16C, lanes 8 and 9). Repeated passage through Centricon® Centrifugal filter units removed it to some

extend (Fig. 2-16A, lane 7). Since the C-terminal domain of IF2 contains all molecular determinants necessary and sufficient for recognition and binding of fMet-tRNA, the N-terminal cleavage product was considered not to interfere in the following binding studies (Misselwitz *et al.*, 1997; Spurio *et al.*, 2000). Purification of *E. coli* IF2 yielded on average 8 mg of protein from 1L cultures. The purity of full-length IF2 determined by densitometric analysis (2.3.2.1.3.3.) was 75 to 80%. The concentrations of IF2 used in the binding assays were adjusted accordingly.

2.4.4. Cloning, expression and purification of recombinant *B. stearothermophilus* IF2

2.4.4.1. Cloning of *B. stearothermophilus infB* gene

IF2 from the gram$^+$ bacterium *B. stearothermophilus* has been used in several studies investigating recognition and binding of *E. coli* fMet-tRNA (Misselwitz *et al.*, 1997; Spurio *et al.*, 2000; Wu and RajBhandary, 1997).

The advantage of utilizing *B. stearothermophilus* IF2 lies in the termal stability compared its *E. coli* counterpart. For recombinant expression of the *Bacillus* protein in *E. coli* a construct had to be generated following the cloning strategy illustrated in figure 2-17. Genomic DNA isolated from *B. stearothermophilus* was used to amplify the *infB* gene by polymerase chain reaction. The PCR product was purified by QIAquick PCR purification kit and subsequently digested with the appropriate restriction enzymes for cloning into the expression vector pQE30. The expression vector was chosen to produce *B. stearothermophilus* IF2 with an N-terminal polyhistidine tag. After ligation and transformation of *E. coli* XL1-blue, clones were screened for the presence of the insert by digestion of isolated plasmid DNA with restriction endonuclease *NcoI*. Both, vector and insert DNA contain one recognition site for this enzyme, thus digestion of positive constructs should lead to 3.4 kb and 2.3 kb fragments. Positive clones were identified and the integrity of the recombinant *infB* gene was confirmed by automated sequencing. The construct was used for transformation of *E. coli* M15 containing the repressor plasmid pREP4 (Qiagen), that ensures tight regulation of gene expression.

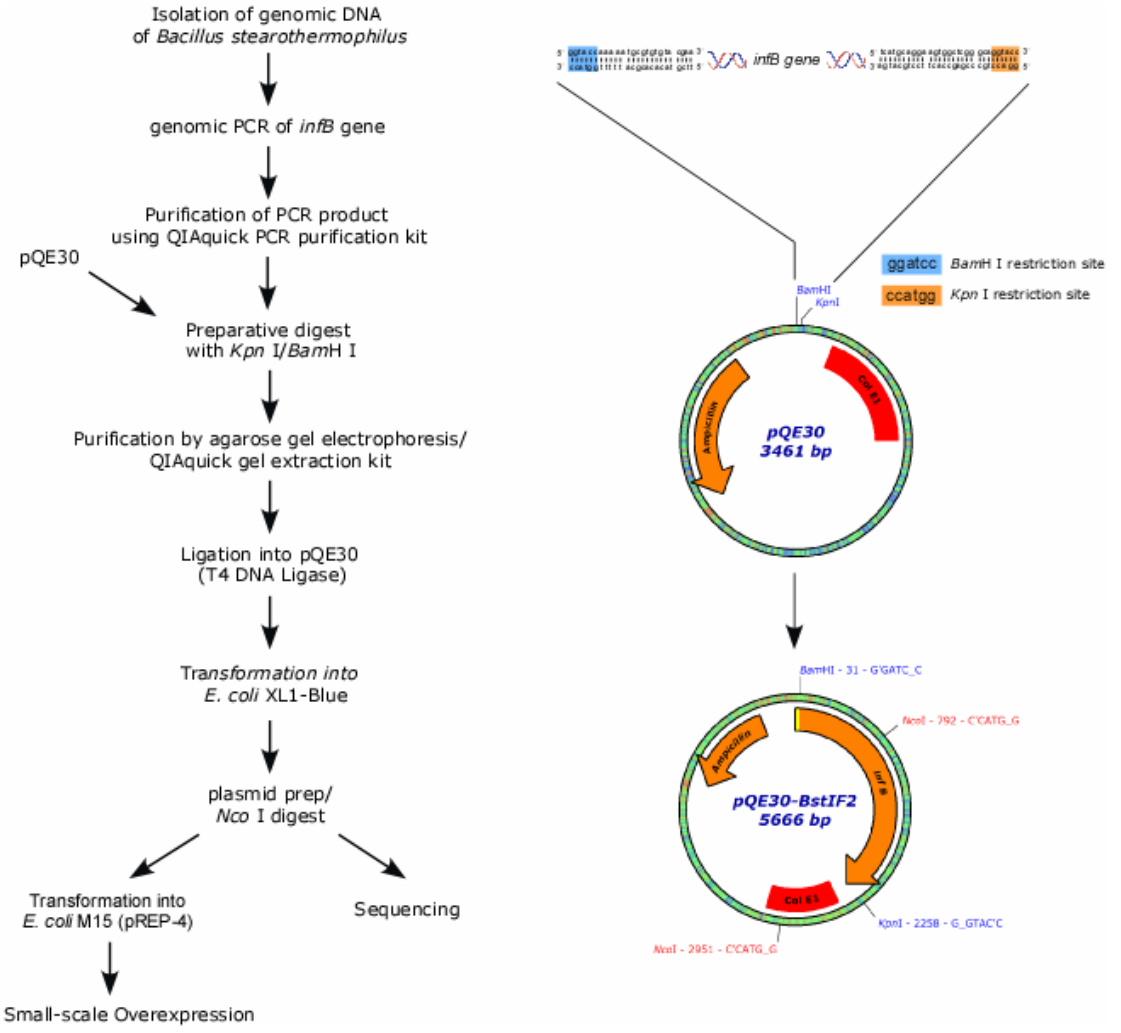

Fig. 2-17: Strategy for cloning of *B. stearothermophilus* IF2

Shown is a schematic illustration of the steps involved in cloning the *infB* gene of *B. stearothermophilus* into the expression vector pQE30.

2.4.4.2. Induced expression of recombinant *B. stearothermophilus* IF2

E. coli M15 cells containing plasmids pQE30-BstIF2 and pREP4 were cultured in 50 ml of LB broth supplemented with ampicillin and kanamycin until the culture reached an A_{600} of 0.5. The culture was split in half and IPTG was added to one of the two subcultures. The cultures were further grown for 4.5 h. Aliquots were taken and expression of recombinant *B. stearothermophilus* IF2 was analyzed by SDS-polyacrylamide gel electrophoresis (2.3.2.1.3.) and Western blotting (2.3.2.1.4.). Addition of IPTG induced the expression of a protein with a molecular weight of ≤ 85

kDa (Fig. 2-18A, lanes 6 to 9). The theoretical molecular weight of the 756 amino acid long recombinant IF2 is 83.2 kDa. As expected, blotting and immuno-detection using a monoclonal antibody directed against a tetra-histidine epitope identified the histidine tagged *B. stearothermophilus* IF2 (Fig. 2-18B). Analysis of expression levels (Fig. 2-18, lanes 6 to 9) showed that the amounts of expressed IF2 do not saturate.

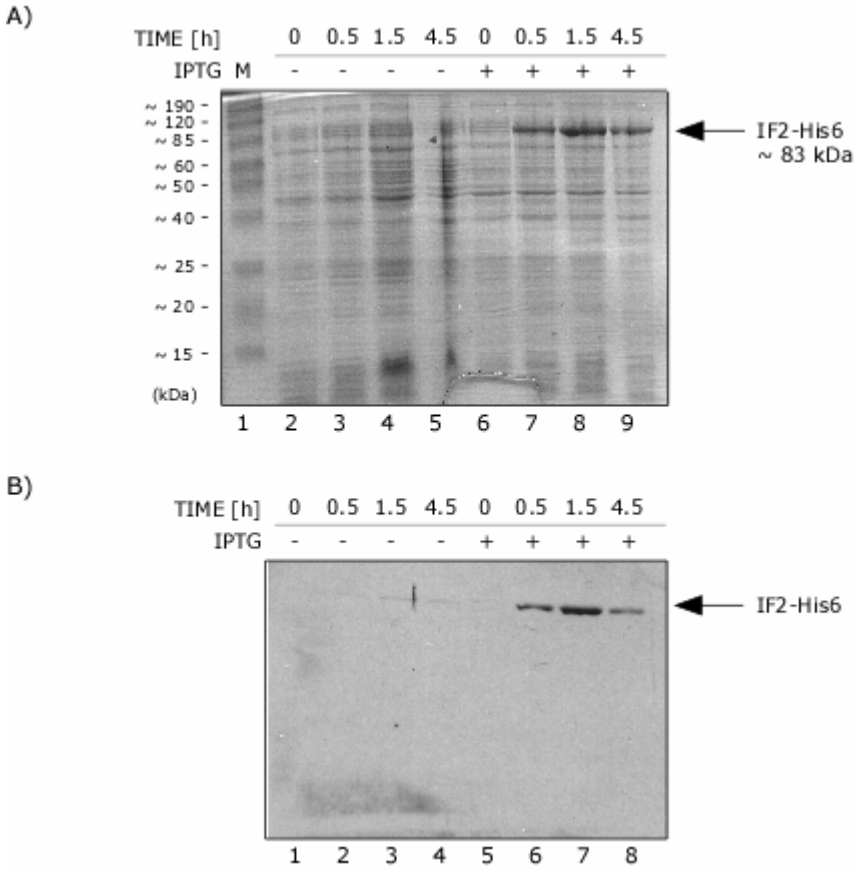

Fig. 2-18: Induced expression of *B. stearothermophilus* IF2 (small scale)

25 ml cultures of *E. coli* M15/pREP4 cells transformed with plasmid pQE30-BstIF2 were grown to an A_{600} of 0.5. Recombinant expression of *B. stearothermophilus* IF2 was induced by addition of IPTG (1 mM final concentration). 1 ml aliquotes were taken at various time points post-induction. Samples were analyzed by SDS-polyacrylamide gel electrophoresis and Western blotting: A) Coomassie stained 10% SDS-PAGE; B) Western blot analysis of a 10% SDS-PAGE loaded with the same samples as in A. The blot was probed against tetra-histidine using a monoclonal antibody.

Within the first 1.5 h post-induction the levels of IF2 increased, however, a decrease in IF2 amounts was observed after further 3 h of incubation. Based on these findings, an A_{600} of 0.8 to 1.0 and incubation time following induction of 2 h were

chosen to obtain maximum expression of *B. stearothermophilus* IF2 for large scale purification (2.3.2.3.4.).

2.4.4.3. Purification of recombinant *B. stearothermophilus* IF2

A 10 ml primary culture of *E. coli* M15/pREP4 transformed with pQE30-BstIF2 supplemented with ampicillin and kanamycin was used to inoculate 1 L LB broth supplemented with the same antibiotics. Once the culture reached A_{600} of 1.0, expression was induced by the addition of IPTG. After further 2 h of growth the cells were harvested and further processed. A schematic overview of the purification procedure is shown in figure 2-19.

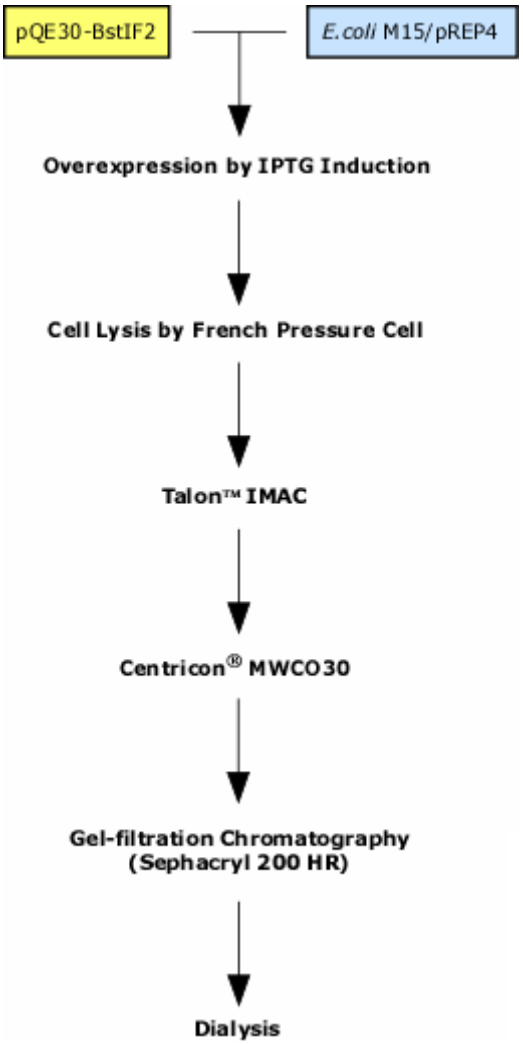

Fig. 2-19: Flowscheme of purification of *B. stearothermophilus* IF2

Shown is a schematic illustration of the steps involved in purification of recombinant *B. stearothermophilus* IF2 expressed in *E. coli* M15/pREP4 cells.

The cells were lysed by passage through a French pressure cell and the clarified lysate was applied to a TALON™ metal affinity resin. Polyistidine tagged IF2 was bound to the matrix by "batch-gravity flow" followed by extensive washes. The resin was transferred to a column, washed again and bound IF2 was elution in the presence of 100 mM imidazole. Due to the high proteolytic cleavage of *B. stearothermophilus* IF2, various degradation products co-eluted with the full-length

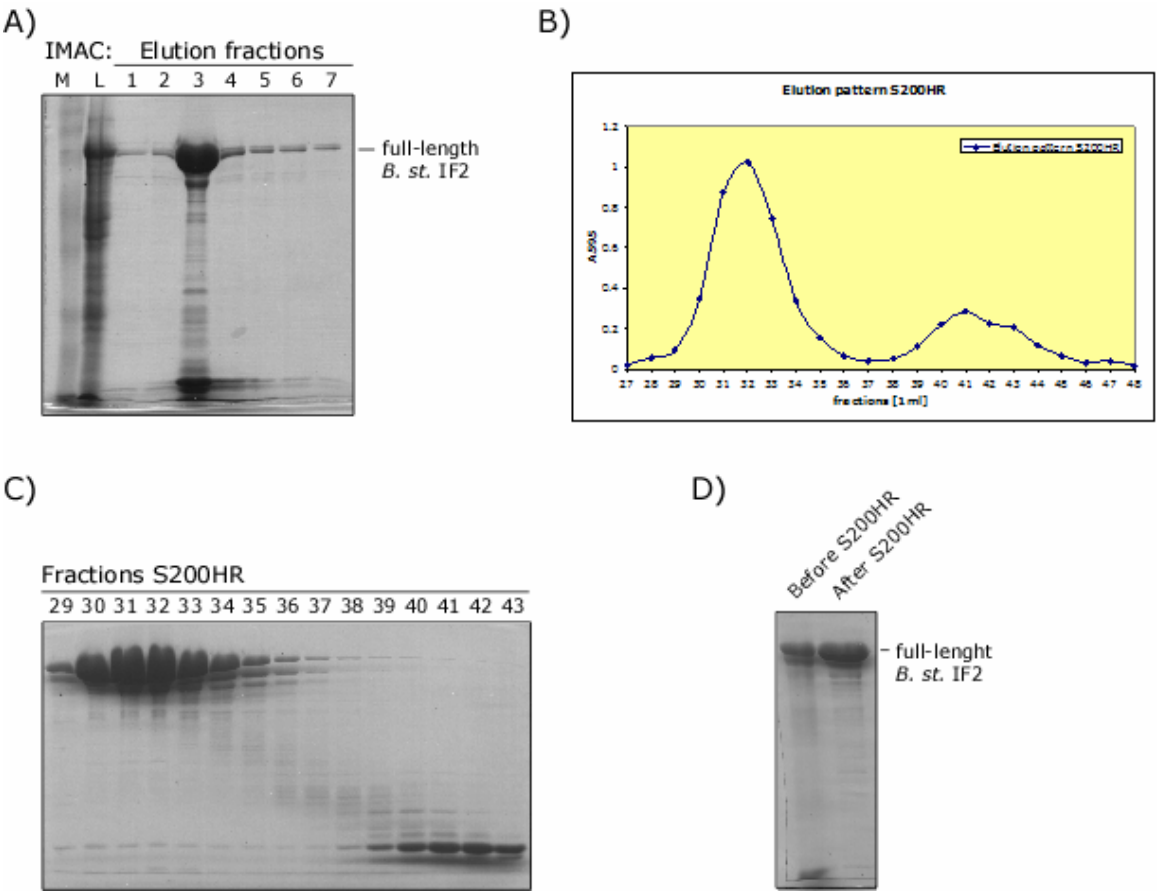

Fig. 2-20: Purification of *B. stearothermophilus* IF2

Cells were grown at 37°C to an A_{600} of 1.0 and recombinant expression was induced by addition of IPTG (1 mM, final concentration). Incubation was further continued for 2 h at 37°C; A) TALON purification: collected fractions during imidazole elution were analyzed on a 10% SDS-polyacrylamid gel stained with Coomassie blue; M: protein marker, L: cell lysate after French pressure cell; B) Gel-filtration: Elution pattern; fractions were analyzed for the presence of protein by Bradfort binding-dye assay; C) Gel-filtration: Elution pattern: protein containing fractions were further analyzed by 10% SDS-PAGE; D) Gel-filtration: Fractions containing full-length *B. stearothermophilus* IF2 were pooled and concentrated, finally analyzed by SDS-polyacrylamid gel electrophoresis.

protein (Fig. 2-20A), pooled fractions were concentrated by ultrafiltration and subjected to gel-filtration using a Sephacryl™ 200HR matrix. Full-length IF2 was successfully separated from the predominant ~15 kDa cleavage product as shown in figures 2-20B and C. Based on the extend of contamination fractions 29 to 33 were pooled. The protein was concentrated, dialyzed against storage buffer (2.3.2.2.2.) and stored at -20°C. From a 1 L culture (7 g of cell mass) ~18 mg of *B. stearothermophilus* IF2 was obtained with an overall purity of 90% as determined by densitometric analysis (2.3.2.1.3.3.). The concentrations of IF2 used in electrophoretic mobility shift assay (EMSA) were adjusted accordingly.

2.4.5. Binding of IF2 to acceptor stem mutants of initiator tRNA^{fMet}

EMSA and filter binding assays, as well as a real-time binding assays using surface plasmon resonance (SPR, BIACORE) are often used techniques for determining kinetic parameters (binding constant K_D, association rate constant k_a, and dissociation rate constant k_d) of complex formation. Although using filter binding assays would be a simple technique for determining K_D, its use in the case of the *E. coli* IF2·fMet-tRNA^{fMet} complex is limited, due to the weakness of the complex *in vitro* (K_D ~ 1 µM; (Mayer *et al.*, 2003)). EMSA was chosen as the primary method for determining the binding constant K_D as it has been shown that the polyacrylamide gels stabilize the complexes, allowing measurement of K_D (Wu and RajBhandary, 1997).

2.4.5.1. EMSA of *E. coli* IF2 and fMet-tRNA$_2^{fMet}$ complex formation

EMSA was used to analyze the complex formation between *E. coli* IF2 and *E. coli* wild-type fMet-tRNA$_2^{fMet}$, as well as the mutants G72, G73, and G72C73. Complex formation between wild-type or mutant fMet-tRNA$_2^{fMet}$ and purified IF2 was initiated by addition of 5'-[^{32}P]-labelled fMet-tRNA to reactions containing various concentrations of IF2 (2.3.3.1.1.). The reactions were allowed to reach equilibrium and loaded onto a 6% polyacrylamide gel. Polyacrylamide gel electrophoresis facilitates the separation of unbound tRNA from tRNA·protein complex, since a complex migrates slower through a polyacrylamide gel than unbound tRNA. Therefore the assay allows one to determine the amount of tRNA bound by the protein as a function of protein concentration. Due to the polyacrylamide gel the

complex is stabilized, thus, the bands observed represent the fraction of bound and unbound tRNA present before the electrophoresis. Autoradiography was performed,

A)

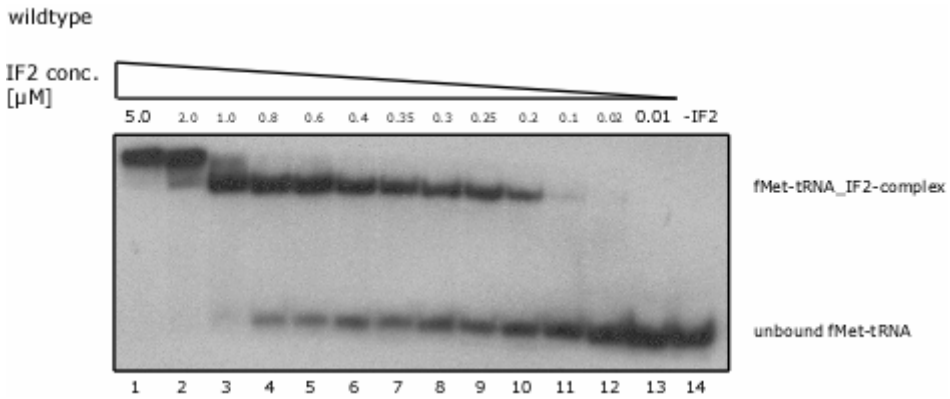

B)

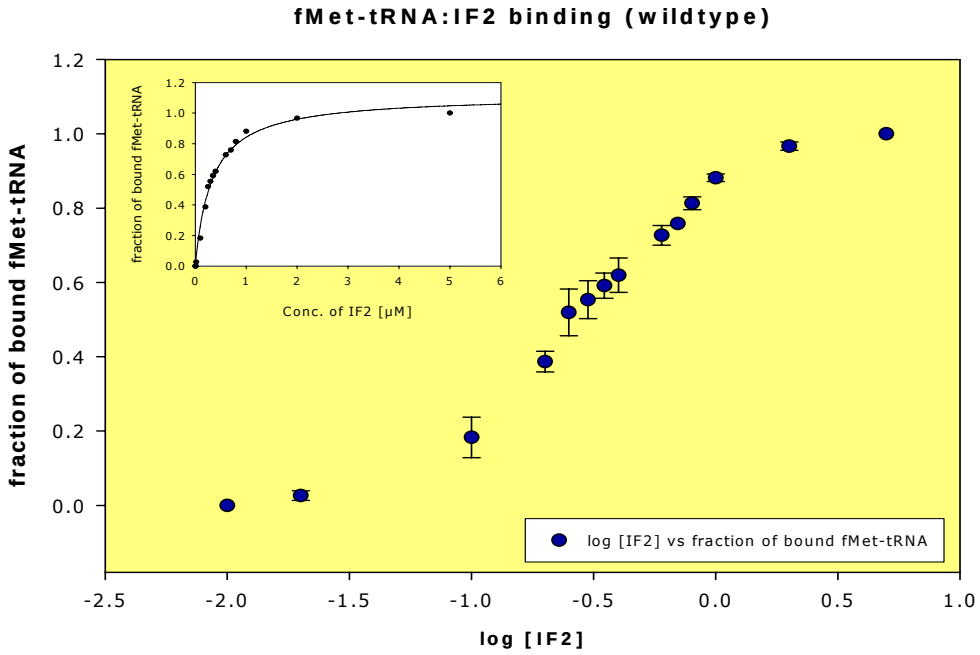

Fig. 2-21: Binding of *E. coli* IF2 to initiator fMet-tRNA (wild-type)

Electrophoretic mobility shift assay for the formation of IF2·fMet-tRNA wild-type complex. The amount of tRNA was 0.02 µM. The amount of *E. coli* IF2 varied from 0.01 to 2 µM. The free and bound fMet-tRNA were separated by PAGE; A) Autoradiography of a 6% polyacrylamide gel; B) Equilibrium binding curve for the interaction of IF2 with fMet-tRNA^{fMet} (wt). The inset shows curve fitting using a model for one site saturating ligand binding.

A)

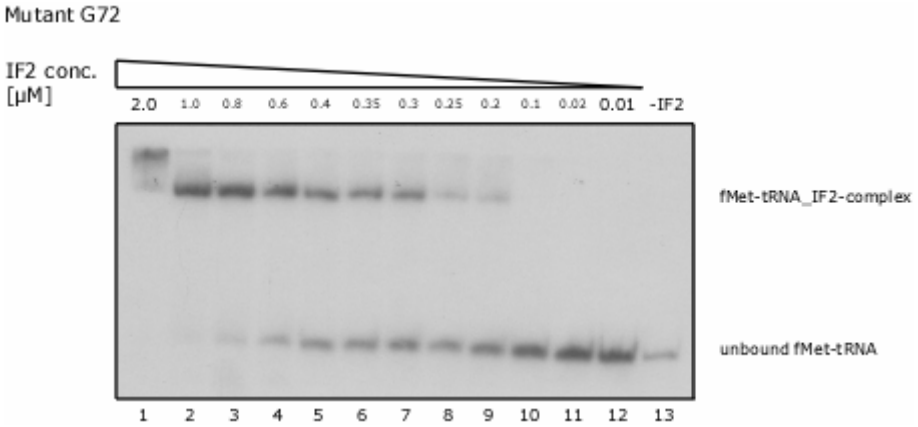

B)

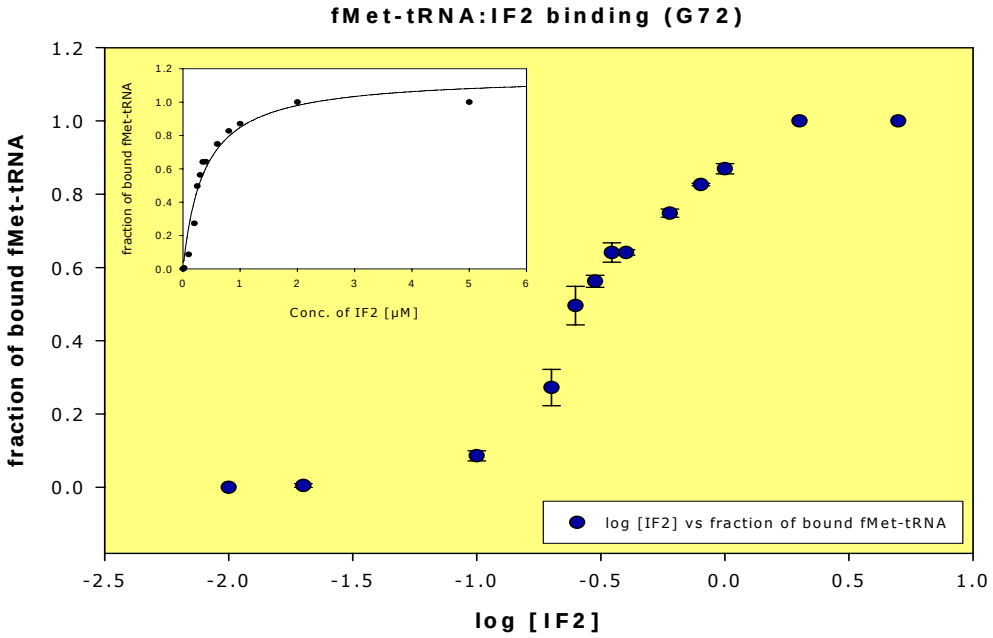

Fig. 2-22: Binding of *E. coli* IF2 to initiator fMet-tRNA (G72)

Electrophoretic mobility shift assay for the formation of IF2·fMet-tRNA G72 complex. The amount of tRNA was 0.02 µM. The amount of *E. coli* IF2 varied from 0.01 to 2 µM. The free and bound fMet-tRNA were separated by PAGE; A) Autoradiography of a 6% polyacrylamide gel; B) Equilibrium binding curve for the interaction of IF2 with fMet-tRNA^{fMet} (G72). The inset shows curve fitting using a model for one site saturating ligand binding.

fMet-tRNA	K_D^{app} [nM]
wild-type	325.2 ± 27.6[a]
G72	369.1 ± 64.2[b]
G73	486.4 ± 65.8[b]
G72C73	470.6 ± 77.1[b]

Table 2-2: Equilibrium dissociation constants of IF2·fMet-tRNA complexes

[a] Average of 5 separate measurements; [b] Average of 3 separate measurements.

and EMSA were analyzed by phosphor imaging. For calculation of K_D, IF2 concentrations were plotted against the fraction of fMet-tRNA in complex (Fig. 2-22 (wild-type) and Fig. 2-23 (mutant G72)). K_D values of wild-type and mutants G72, G73, and G72C73 were obtained from curve fitting, presented in table 2-2. For the IF2·wild-type complex an apparent K_D of 325.2 nM ± 27.6 was calculate while the IF2·G72 complex had an apparent K_D of 369.1 nM ± 64.2. Similar results were obtained from binding reactions using a different batch of IF2. In the case of the IF2·G73 and IF2·G72C73 complexes, curve fitting estimated apparent K_D values of 486.4 ± 65.8 nM and 470.6 nM ± 77.1, respectively. Comparison of the binding constants to that of IF2·wild-type complex (K_D^{app} of 325.2) revealed a slight increase in K_D of less than 1.5 fold. Despite the slight increase in K_D^{app}, the results indicated that IF2 had almost the same binding affinity for these mutant tRNAs. In order to explain these unexpected results, EMSA was repeated by assaying the complex formation between fGln-tRNA^{fMet} and uncharged tRNA^{fMet}. Binding studies have shown that fGln-tRNA^{fMet} and uncharged tRNA^{fMet} are very poor substrates for IF2, compared to fMet-tRNA^{fMet} (Mayer *et al.*, 2003; Sundari *et al.*, 1976; Wu and RajBhandary, 1997). Since Wu and coworkers applied EMSA as their primary technique, we expected to obtain similar results. However, analysis of the three complexes revealed no differences in IF2 affinity for fMet-tRNA and fGln-tRNA (Fig. 2-23). Despite the 2-fold weaker binding of uncharged tRNA, the experiment showed that the assay was not sensitive enough to investigate the effect of acceptor stem mutations on IF2 binding affinity.

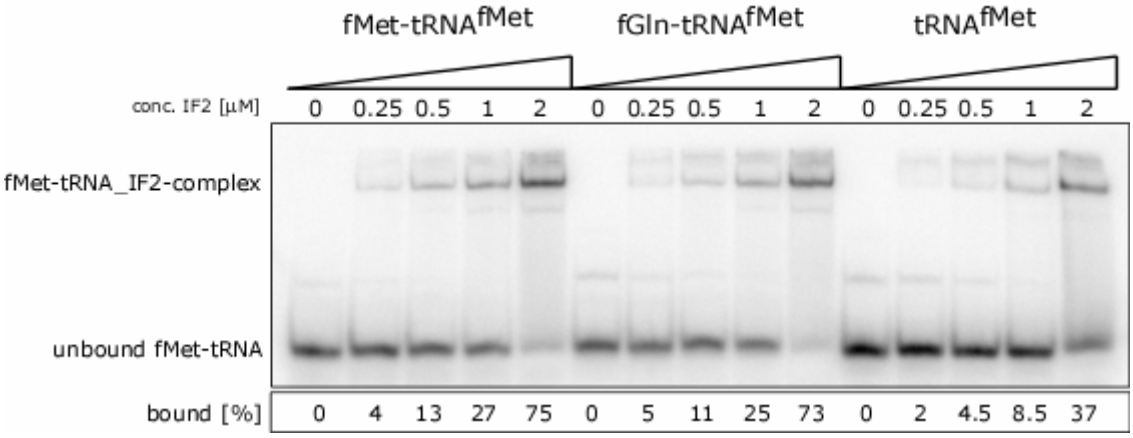

Fig. 2-23: Binding of *E. coli* IF2 to initiator fMet-tRNA, fGln-tRNA, and tRNA

Electrophoretic mobility shift assay for the formation of IF2·formylaminoacyl-tRNA complexes. The amount of tRNA was 0.02 µM. The amount of *E. coli* IF2 varied from 0.25 to 2 µM. The free and bound fMet-tRNA were separated on a 6% polyacrylamide gel.

2.4.5.2. RNase protection analysis

RNase protection assays are a commonly used technique for determining kinetic parameters such as equilibrium dissociation constant K_D and dissociation rate constant k_{off}, of various protein·tRNA interactions (LaRiviere *et al.*, 2001; Stortchevoi *et al.*, 2003; Szkaradkiewicz *et al.*, 2000). It is based on the principle that a protein interacting with its primary substrate protects the latter against digestion by ribonucleases. The ribonuclease actively competes with the protein for substrate, therefore it is possible to compare formation and stability of protein·substrate complexes. Binding of fGln-tRNA^{fMet} to initiation factor 2 has been shown to be 10- to 30-fold weaker than the affinity of IF2 towards fMet-tRNA^{fMet} (Mayer *et al.*, 2003; Wu and RajBhandary, 1997). Although IF2 displays high specificity for the wild-type initiator tRNA, the binding is thought to be weak (~1 µM), which is also reflected in its fast dissociation rate of 0.0295 s^{-1} (Mayer *et al.*, 2003). Therefore, in order to use RNase protection assays to analyze the interaction of IF2 with acceptor stem mutants of the initiator tRNA, the appropriate concentration of RNase A suitable for protection of the wild-type fMet-tRNA^{fMet} by IF2 needed to be determined by titration of RNase A from 0.5

A)

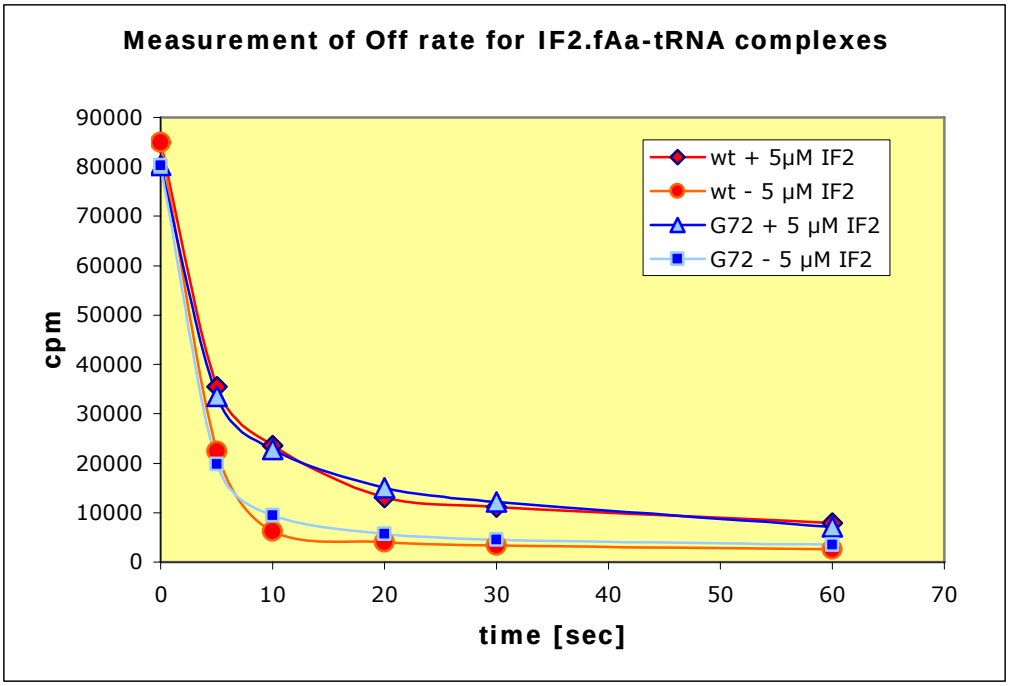

B)

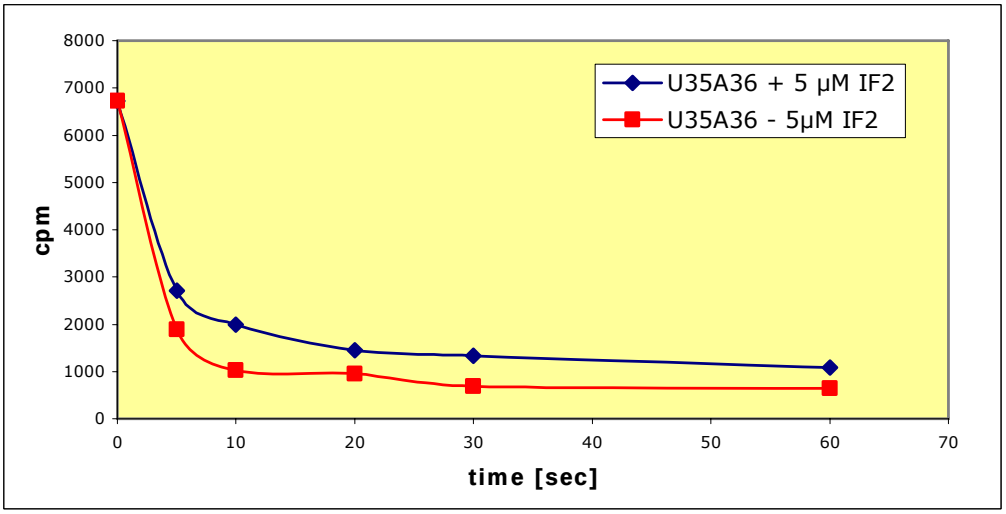

<u>Fig. 2-24:</u> Measurement of Off rates for IF2·formylaminoacyl-tRNA complexes

5 µM IF2 and 40 nM of [^{35}S]- or [^{3}H]-formylaminoacyl-tRNAs in 100 µl were incubated for 20 min on ice. After addition of RNase A, 20 µl aliquots were taken at each time point and transferred to 20 µl of ice cold 20% TCA. TCA precipitable counts are plotted. A) wild-type and mutant IF2·fMet-tRNA G72 complexes. B) mutant IF2·fGln-tRNA U35A36 complex.

A)

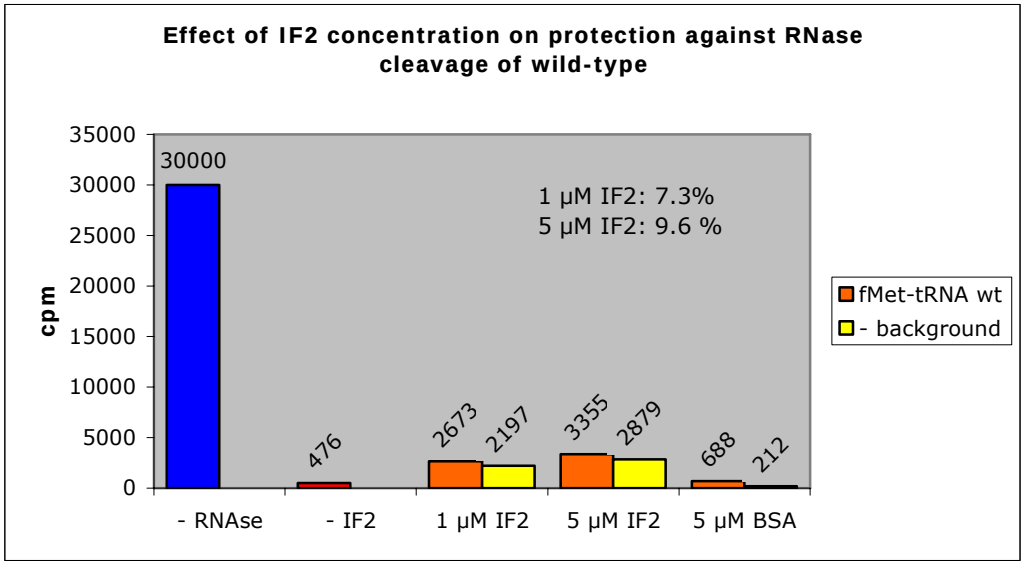

B)

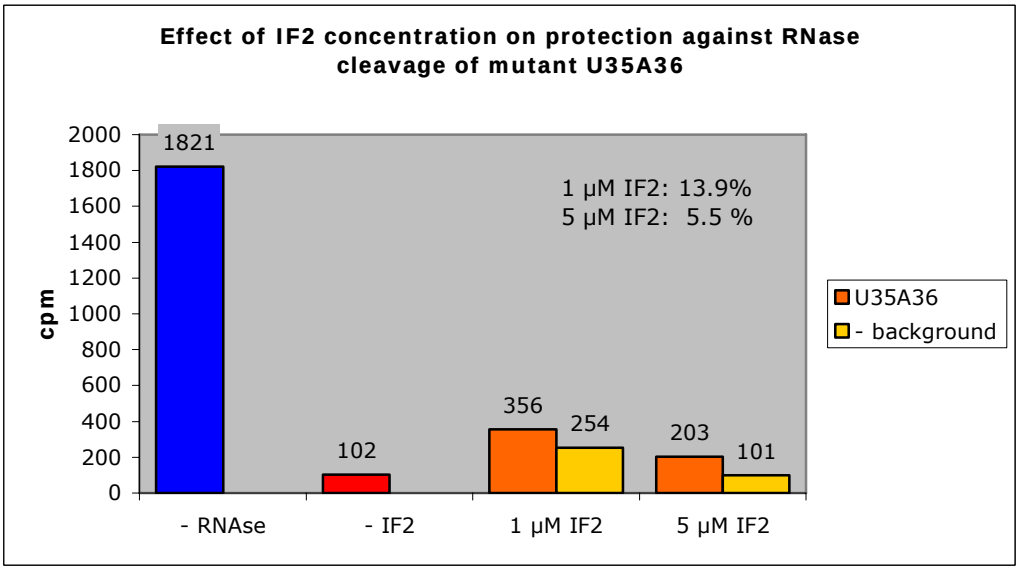

Fig. 2-25: Effect of IF2 concentration

RNase Protection assays were performed in the presence of 1 µM or 5 µM IF2. TCA precipitable counts are plotted. A) wild-type IF2·fMet-tRNA complex. B) mutant IF2·fGln-tRNA U35A36 complex.

to 50 ng. 25 ng of RNase A was chosen, due to a feasible protection, relative to background level. The stability of the IF2·fMet-tRNA^{fMet} wild-type complex was further investigated by carrying out a time course where aliquots were taken at various time

points after addition of RNase A. In addition, mutant initiator tRNAs G72 and U35A36 were also assayed. Since IF2 has a 10 to 30 fold lower affinity for fGln-tRNA^{fMet} (U35A36) than for fMet-tRNA^{fMet} wild-type, this mutant was chosen to be a suitable control for the sensitivity of the assay. IF2 and formylaminoacyl-tRNA (^{35}S- or ^{3}H-labelled) were incubated on ice to allow the binding reaction to reach equilibrium. RNase A was added and the reaction was further incubated. The reaction was stopped by addition of TCA and TCA precipitable material was collected by nitrocellulose filtration followed by liquid scintillation counting. Figures 2-25A and 2-25B show the dissociation of the IF2·formylaminoacyl-tRNA complexes. Within 5 seconds more than 50 percent of the wild-type, G72 and U35A36 complexes dissociated. If one subtracts the background levels, the percentage drops even below 20%. It is notable, that although a higher IF2 concentration was used in this experiment (5 µM), less then 10% of the wild-type fMet-tRNA was protected by IF2 after 30 s. Due to the fact that similar protection was observed at 1 µM IF2, the initial experiment was repeated using 1 µM and 5 µM IF2 at 25 ng of RNase (Fig. 2-25). Varying the concentration of IF2 had only a marginal effect on the protection of wild-type fMet-tRNA. The use of mutant U35A36 as substrate resulted in 14% protection at 1 µM IF2 compared to 5.5 % at the higher concentration (Fig. 2-25B).

2.4.5.3. EMSA of *B. stearothermophilus* IF2 and formylaminoacyl-tRNA$_2^{fMet}$ complex formation

As mentioned above, Wu and RajBhandary had performed EMSA to investigate the effect of the amino acid attached to the initiator tRNA on IF2 binding (Wu and RajBhandary, 1997). They used IF2 from the thermo-stable organism *B. stearothermophilus*. In general it is thought that the IF2 is more stable compared to IF2 from *E. coli*. The *infB* gene of *B. stearothermophilus* was therefore cloned, and the protein expressed in *E. coli* and purified to homogeneity (2.4.4.). The ability of purified *B. stearothermophilus* IF2 to discriminate between fMet-tRNA^{fMet} and fGln-tRNA^{fMet} (Wu and RajBhandary, 1997) was tested by EMSA (2.3.3.1). Analysis of binding reactions containing either fMet-tRNA^{fMet}, fGln-tRNA^{fMet} or uncharged tRNA^{fMet}, however, did not result in any clear discrimination as shown in figure 2-26. Similar to *E. coli* IF2, no difference was observed between fMet-tRNA^{fMet} and fGln-tRNA^{fMet}, and only a slight decrease in binding of uncharged tRNA^{fMet} compared to the aminoacylated and formylated tRNAs was detectable.

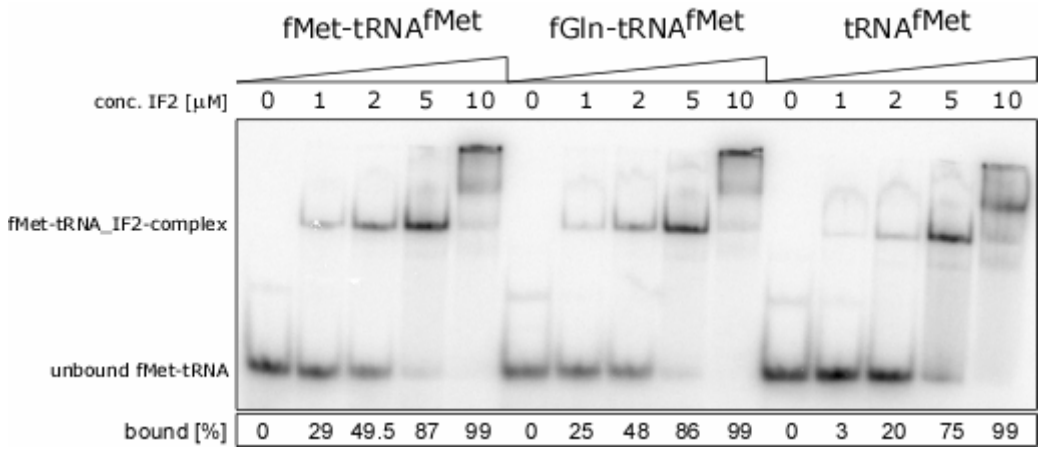

Fig. 2-26: Binding of *B. stearothermophilus* IF2 to initiator formylaminoacyl-tRNA

Electrophoretic mobility shift assay for the formation of IF2·formylaminoacyl-tRNA complex. The amount of tRNA was 0.02 µM. The amount of B. stearothermophilus IF2 varied from 1 to 10 µM. The free and bound formylaminoacyl-tRNA were separated on a 6% polyacrylamide gel.

2.5. Discussion

IF2 represents an important checkpoint in the initiation of translation. It binds initiator tRNA and positions it over the initiation codon in the ribosomal P-site, in a GTP-dependent manner (Gualerzi and Pon, 1990). It has been suggested that a 90 amino acid C-terminal subdomain (domain IV) of *B. stearothermophilus* and a similar domain in *Thermus thermophilus* IF2 (Szkaradkiewicz *et al.*, 2000) contains all molecular determinants necessary and sufficient for recognition and binding of the initiator tRNA (Misselwitz *et al.*, 1997; Spurio *et al.*, 2000). Despite advances in crystallographic techniques in the past years, there is no conclusive structural information on how IF2 recognizes the initiator tRNA. Based on biochemical experiments over decades, it was thought that in eubacteria, the primary determinant for the recognition of the initiator tRNA by IF2 is a formylated α–amino group (Sundari *et al.*, 1976), a feature also found in initiator tRNA from mitochondria and chloroplasts (Liao and Spremulli, 1991; Lucchini and Bianchetti, 1980). Recently, combined *in vitro* and *in vivo* studies has suggested a hierarchy of IF2 preference for the identity of the amino acid attached to the initiator tRNA in the following order, fMet > fVal > fIle > fPhe > fGln (Mayer *et al.*, 2003; Wu and RajBhandary, 1997).

NMR analysis of the 90 amino acid fragment of *B. stearothermophilus* in the presence of fMet or methionine indicated a specific, although weak, interaction with fMet, but not methionine (Guenneugues *et al.*, 2000). In addition, it has been suggested that the CAACCA-fMet portion of the initiator tRNA is all that is needed for binding to IF2. This observation was further supported by cryo-electron microscopy of a reconstituted *E. coli* 70S initiation complex (Allen *et al.*, 2005). The obtained model suggested that domain IV of IF2 interacts only with a single-stranded portion of the tRNA. Although there is some evidence that the interaction is extended to the minor groove of the TΨC stem and loop of $tRNA^{fMet}$ based on the protection of fMet-tRNA by IF2 against enzymatic cleavage (Wakao *et al.*, 1989), it is not clear whether IF2 recognizes and interacts with the main body of the tRNA. Studies of real-time binding of *E. coli* IF2 using a mutant initiator tRNA, in which the highly conserved CxA mismatch between nucleotides 1 and 72 was changed to a strong base pair C1:G72, have suggested that the mismatch might also be an important determinant for IF2 recognition of fMet-tRNA (Mayer et al., 2003). In this study, IF2 displayed low binding affinity for the G72 mutant fMet-tRNA, lowering the association rate constant by 7 fold (4.16×10^3 M^{-1} s^{-1}) compared to the wild-type fMet-tRNA (2.94×10^4 M^{-1} s^{-1}), suggesting that i) the C1xA72 mismatch or ii) the nature of the nucleotide at position 72 might be important for IF2 recognition (Mayer et al., 2003). The decrease in Response Unit (RU) values during later time points (>50 s) of the association curve of the G72 mutant was interpreted as being due to either a major conformational change in the IF2·fMet-complex, rapid dissociation of the complex, or both. To gain further insight into the molecular basis of this phenomenon, electrophoretic mobility shift assays (EMSA) and RNase protection experiments were performed. Although filter binding assays would have been a simple technique to determine the binding constant K_D, its can not be used in the case of the *E. coli* IF2·fMet-tRNA complex, because the complex is weak. Based on protection experiments (Petersen *et al.*, 1979) and real-time binding experiments (Mayer *et al.*, 2003) an apparent K_D of 1 µM was determined for wild-type IF2·fMet-tRNA complex.

Since polyacrylamide gel stabilizes complexes, EMSA was used as the first approach to determine K_D values for acceptor stem mutant of initiator tRNA. Results obtained from EMSA for IF2 binding of wild-type and mutant initiator tRNAs G72, G73, and G72C73, indicated no significant difference in binding (2.4.5.1., Table 2-2). To verify this result and to challenge the sensitivity of the assay, the binding affinity of IF2 towards $fGln\text{-}tRNA^{fMet}$ and uncharged tRNA was analyzed. As mentioned above IF2

has a hierarchy of preference for the identity of the amino acid attached to the initiator tRNA. Binding of fGln-tRNA by IF2 has been shown to be 10 to 30 fold weaker than the affinity of IF2 towards fMet-tRNA (Mayer *et al.*, 2003; Wu and RajBhandary, 1997). In addition, Mayer and coworkers showed that uncharged initiator tRNA is hardly bound by IF2. However, analyses of these complexes by EMSA did not reveal any significant discrimination by IF2 (Fig. 2-23), suggesting that either the chosen conditions or the experimental setup were not suitable for assaying the IF2·formylaminoacyl-tRNA^{fMet} interaction. The effect of binding inhibition by low amounts of $MgCl_2$ and moderate amounts of monovalent cations (>50 mM) (Sundari *et al.*, 1976) was taken into account when constituting the appropriate binding buffer. Binding of *E. coli* IF2 to wild-type and mutant fMet-tRNA^{fMet} was carried out under conditions used by Mayer and co-worker in their real-time binding experiment (Mayer *et al.*, 2003). Therefore, potential interference in binding due to buffer components can be ruledout.

As a second approach complex formation was also analyzed by RNase protection assay, a commonly used technique to determine kinetic parameters of protein·tRNA binding (LaRiviere *et al.*, 2001; Stortchevoi *et al.*, 2003; Szkaradkiewicz *et al.*, 2000). It is based on the principle that a protein interacting with its primary substrate protects the latter against digestion by ribonuclease. The ribonuclease competes with IF2 for formylaminoacyl-tRNA, therefore, formylaminoacyl-tRNA that dissociates from IF2 will also be rapidly digested by RNase A, allowing one to measure the k_{off} rates. The weak interaction between IF2 and the wild-type initiator tRNA is reflected in the fast dissociation rate of 0.0295 s^{-1} (Mayer *et al.*, 2003). Thus, the observation that within 5 seconds more than 60 percent of the wild-type, G72 and U35A36 complexes had been dissociated was not a surprise (Fig. 2-14). By subtracting background levels, the percentage of protection drops below 20%. This is a clear indication that the dissociation rates are very fast. The time period between addition of RNase and withdrawing of the first aliquot, was the limiting factor in the characterization of wild-type and mutant *E. coli* IF2·formylaminoacyl-tRNA complexes. Furthermore, increasing IF2 concentrations by 5 fold did not result in a significant increase in protection (Fig. 2-25). In the case of fGln-tRNA the protection levels dropped even further. The observation that IF2 shows nonspecific interactions with other tRNA or itself, resulting in a super shift in EMSA at higher concentrations (Fig. 2-21A, lane 1), could explain the results above. These nonspecific interactions

with other IF2 or tRNA molecules might decrease the affinity towards its primary substrate or reduce the effective concentration of IF2.

Previous IF2-tRNA binding studies, including the work from Wu and RajBhandary, have used IF2 from the organism *B. stearothermophilus* for EMSA and RNase protection assays (Spurio *et al.*, 2000; Szkaradkiewicz *et al.*, 2000; Wu and RajBhandary, 1997). With binding studies using IF2 from *B. stearothermophilus*, the reaction buffer contains higher concentrations of $MgCl_2$ and monovalent cations compared to conditions suitable for *E. coli* IF2. An increased concentration of these cations could therefore reduce nonspecific interactions and result in distinct discrimination by IF2 for the wild-type and mutant tRNA substrates. EMSA was performed in the presence of either fMet-tRNA^{fMet}, fGln-tRNA^{fMet}, or uncharged tRNA, using the buffer conditions described by Wu and RajBhandary (Wu and RajBhandary, 1997). Unfortunately, no distinct differences were observed between IF2 binding to fMet-tRNA^{fMet} and fGln-tRNA^{fMet} (Fig. 2-26), suggesting an inherent problem in the experimental setup. The principle of the experimental design is based on the Michaelis-Menten equation, where the equilibrium constant K_d is the concentration of the protein (IF2), at which 50% of the substrate (formylaminoacyl-tRNA) is bound under conditions where the concentration of free protein exceeds 90%. Wu and RajBhandary followed a different approach (Wu and RajBhandary, 1997), where the protein concentration remained constant and the substrate was titrated, thus using a more sophisticated calculation of K_D. The advantage is that IF2 concentrations remain low, thereby avoiding possible nonspecific interactions at higher concentrations of IF2 that may interfere in binding as discussed above. Therefore, the experimental setup outlined by Wu and RajBhandary is a worth-while alternative to investigating the effect of mutations in the accepter stem of initiator tRNA in recognition and binding by IF2.

In addition to real-time binding data obtained by Mayer and co-workers (Mayer *et al.*, 2003), there are several other indications that the mismatch at the end of the initiator tRNA is important for a proper interaction with IF2. *In vivo* studies have shown that mutant initiator tRNAs carrying a U1G72 wobble base pair at positions 1-72, combined with changes in the anticodon loop was half as efficient in initiation upon IF2 overproduction, as a mutant initiator tRNA only having the anticodon mutations (Thanedar *et al.*, 2000). It was suggested that the two tRNAs have different affinities towards IF2. Thus, it can be speculated that the presence of a base pair alters the conformation of the acceptor stem and arm. Indeed, analysis of

acceptor stem mutants of *E. coli* initiator tRNA by nuclear magnetic resonance revealed that the unique arrangement of the mismatch causes a distinctly different orientation of the single-strand terminus compared to mutants with regular 1-72 base pairs (Zuleeg *et al.*, 2000). Based on the structural model of wild-type $tRNA^{fMet}$ it has been suggested that an unusual inter-strand stacking between C1 and A73 causes the distinct orientation of the single-stranded terminus and that reorientation has to occur upon complex formation with an interacting protein. Therefore interactions between nucleotides at position 1 and 72 due to base pairing disfavor an easy displacement of nucleotide 1 on the one hand and the single-strand terminus on the other hand, thereby preventing a local conformational flexibility and deformability of the latter. The importance of the flexibility of the single-strand terminus has been shown for the interaction of initiator tRNA with MTF (Lee *et al.*, 1992; Lee *et al.*, 1993). Although a single hexanucleotide mimicking the single-strand terminus displays almost the same binding affinity as the intact wild-type initiator tRNA towards IF2 (Guenneugues *et al.*, 2000), structural changes at the end of the intact tRNA, thereby altering the local conformation, could affect a proper binding by IF2. It might well be that flexibility of the single-strand terminus is also required to fit into the binding pocket of IF2.

To further investigate the role of the mismatch of initiator tRNA in binding by IF2 electrophoretic mobility shift assays should be repeated by following the protocol of Wu and RajBhandary (Wu and RajBhandary, 1997). Furthermore, IF2 complex formation of wild-type and mutant initiator tRNAs should be analyzed by real-time binding using BIACORE as it has been used previously (Mayer *et al.*, 2003).

Chapter III

The effect of the amino acid attached to the E. coli initiator tRNA on the hydrolytic activity of peptidyl-tRNA hydrolase

3.1. Introduction

In general, protein synthesis is initiated with methionine in eukarya and archiae or its derivate formylmethionine in eubacteria and eukaryotic organelles such as mitochondria and chloroplasts (Kozak, 1999). Of the two species of methionine tRNA present in these organisms, the initiator tRNA is used for the initiation of protein synthesis whereas the elongator tRNA is used for the insertion of methionine into internal peptide linkages. Because of its unique function, the initiator tRNA possesses many highly specific properties that are different from those of elongator tRNAs (Mayer *et al.*, 2001). These elements that are critical for the identity of the initiator tRNA are mostly clustered in the acceptor stem and anticodon stem. One feature important for specifying three of its four distinct properties is a base mismatch conserved at the end of the acceptor stem in all bacterial and organelle initiator tRNA. The mismatch has been shown to be important in formylation of the methionine attached to the initiator tRNA by methionyl-tRNA transformylate (MTF) (Lee *et al.*, 1992; Lee *et al.*, 1991) and is suggested to play a role in recognition by IF2 (Mayer *et al.*, 2003). In addition to its requirement for MTF interaction, the mismatch also functions as a negative determinant for elongation factor Tu (EF-Tu) (Seong *et al.*, 1989; Seong and RajBhandary, 1987) and peptidyl-tRNA hydrolase (PTH) (Lee *et al.*, 1992; Schulman and Pelka, 1975). PTH is an enzyme which hydrolyzes N-blocked aminoacyl- and peptidyl-tRNA to facilitate tRNA recycling (Lee *et al.*, 1992; Schulman and Pelka, 1975). The absence of a base pair between nucleotide 1 and 72 protects fMet-tRNA^{fMet} against hydrolytic cleavage by PTH. Although sequence and structural feature of the initiator tRNA might be primary determinants for the interaction of MTF, IF2, EF-Tu, and PTH, there is increasing evidence that the amino acid attached to the initiator tRNA may also play an important role in recognition and discrimination of aminoacylated tRNA by these proteins (LaRiviere *et al.*, 2001; Mayer *et al.*, 2003; Stortchevoi *et al.*, 2003;

Thanedar *et al.*, 2000; Wu and RajBhandary, 1997). In bacteria, tRNAs subsequent to their aminoacylation are bound and inspected by MTF and EF-Tu in a competitive manner. Even though the mismatch at the end of the acceptor stem is the most important identity element for *E. coli* MTF, ample *in vitro* and *in vivo* evidence suggest a hierarchy of preference for the attached amino acid, in the following order Met > Gln > Phe > Ile > Val > Lys (Mayer *et al.*, 2003). The preference of *E. coli* MTF for methionine is even more pronounced in the bovine mitochondrial MTF, where the amino acid is the most important identity element on the initiator tRNA (Takeuchi *et al.*, 2001). The crystal structure of *E. coli* MTF·fMet-tRNA complex showed that the methionine binding cavity consists of a cluster of hydrophobic side chains and holds the methionine moiety of Met-tRNA in place but does not make any specific contact with it, allowing alternate amino acids (Schmitt *et al.*, 1998). Selectivity of the tRNA backbone and amino acid may have evolved to improve the translational accuracy by reducing the delivery of misacylated tRNAs to the ribosome. An important role in this process is played by EF-Tu, which acts as a carrier for aminoacyl-tRNA. EF-Tu was generally thought of as a nonspecific tRNA-binding protein because it binds every elongator aminoacyl-tRNA with approximately the same affinity (Janiak *et al.*, 1990; Louie and Jurnak, 1985). However, EF-Tu binds certain tRNAs esterified with noncognate amino acid differently than it binds the corresponding correctly aminoacylated tRNA (LaRiviere *et al.*, 2001). LaReviere and coworkers showed that the thermodynamic contribution of the amino acid and the tRNA backbone to the overall binding affinity is independent of each other and compensates for one another when the tRNA is correctly aminoacylated. It was suggested that a "tight" amino acid such as glutamine is correctly esterified to the comparatively "weak" $tRNA^{Gln}$, whereas a "weak" amino acid such as alanine is correctly esterified to the comparatively "tight" $tRNA^{Ala}$. On this basis, the low affinity of EF-Tu toward methionylated initiator tRNA compared to methionylated elongator species can be explained due to the fact that both methionine and the $tRNA^{fMet}$ are "weak" binders. Once the initiator tRNA has escaped binding by EF-Tu and becomes formylated by MTF, it is bound by IF2 and positioned at the ribosomal P site. For several decades it was thought that the primary determinant for recognition and binding by IF2 is an N-blocked amino acid (Leon *et al.*, 1979; Sundari *et al.*, 1976). Recent *in vitro* and *in vivo* studies showed that IF2 has a higher preference for formylmethionine compared to other formylated amino acids (Mayer *et al.*, 2003; Wu and RajBhandary, 1997). As with MTF a hierarchy of preferred amino acid was observed for IF2 as well, in the

following order fMet > fVal > fIle > fPhe > fGln, indicating that the role of methionine has evolved in such a way that it is favored for initiation of protein synthesis. In line with these findings are the results obtained from *in vivo* studies showing that PTH hydrolyses the ester linkage of fGln-tRNA^{fMet} and not that of fMet-tRNA^{fMet} which appears to be completely resistant to PTH (Thanedar *et al.*, 2000). So far it was thought that the resistance of initiator tRNA is due to the presence of a 5'-terminal phosphate at the end of a fully base-paired acceptor stem. This is the only determinant for the hydrolase activity, therefore the absence of a base pair at position 1-72 protects fMet-tRNA^{fMet} against hydrolytic cleavage by PTH. This raises the question whether PTH also has a hierarchy of preferences for the amino acid attached to initiator tRNA with methionine being the poorest substrate? The work presented in this chapter is an attempt to answer this question by *in vitro* analysis of the substrate specificity of PTH using wild-type and mutant initiator tRNA aminoacylated with methionine, glutamine, valine, isoleucine, and phenylalanine, respectively (Fig. 3-1).

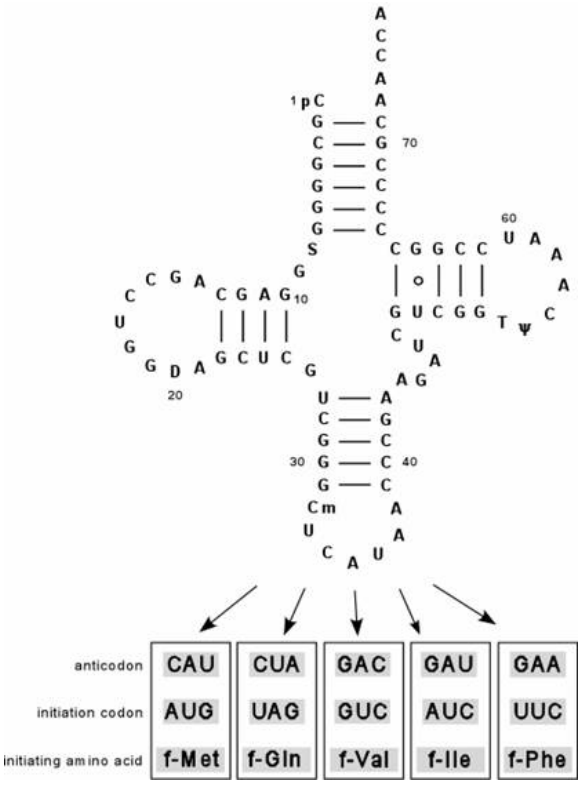

Fig. 3-1: Schematic representation of *E. coli* initiator tRNA

Cloverleaf structure of wild-type initiator tRNAs. Codon and cognate anticodon mutations that initiate translation with amino acids other than methionine are presented in boxes.

3.2. Material

If not further specified chemicals and equipment have been used as listed under section 2.2.

3.2.1. Oligodeoxyribonucleotides

All oligodeoxyribonucleotides were acquired from Operon Biotechnologies Inc., Huntsville, AL.

Oligonucleotide	Sequence of Oligonucleotide	Description
CP_fMet1_5539	5'-ACCGACGACCTTCGGGT-3'	*nt 39-55 of $tRNA_1^{fMet}$
UV5G	5'-GAACCGACGATCTTCGG-3'	*nt 40-56 of $tRNA_2^{fMet}$
CK 42	5'-TACCAGGCTGCTCCAC-3'	*nt 7-22 of $tRNA^{fMet}$
SHtr 28	5'-CCGACGATCTTCGGGTTGTCAG-3'	*nt 32-53 of $tRNA_2^{fMet}$
SHtr 34	5'-TCGGGTTTAGACCCGAC-3'	*nt 26-43 of $tRNA^{fMet}$
CP_Tyr_1025	5'-CCTTTGGCCGCTCGGG-3'	*nt 10-25 of $tRNA^{Tyr}$
trnfMG34C36fwr	5'- TTGCCATGGTTCAGGCGCGGGG -3'	PCR fwr primer G34C36
trnfMG34C36rev	5'-AGATAAGCTTAAACCCCGATAAATCGGGGC -3'	PCR rev primer G34C36
pBADseq	5'-GTGTCTATAATCACGGCAGAAAAGTCC-3'	MCS of pBAD

*oligonucleotide for use in Northern blot analysis; indicated is the position of sequence complementary within the tRNA of interest;

3.2.2. Plasmids

Plasmids	Description	Marker	Reference
pUC13/ trnfM	wild-type $tRNA_2^{fMet}$ gene cloned in pUC13	Ampicillin	*Gite and RajBhandary*, 1997
pRSVCATam1.2.5/ trnfMU35A36	pBR322 derived plasmid bearing the genes for the CAT reporter and the mutant initiator $tRNA_2^{fMet}$ (U35A36)	Ampicillin	*Varshney et al.*, 1991
pBR322/ trnfMG72U35A36	pBR322 plasmid bearing the gene for mutant initiator $tRNA_2^{fMet}$ (G72/U35A36)	Ampicillin	*Seong et al.*, 1989
pRSVCATI1.2.5/ trnfMG34	pBR322 derived plasmid bearing the genes for the CAT reporter and the mutant initiator $tRNA_2^{fMet}$ (G34)	Ampicillin	*Wu et al.*, 1996
pRSVCATF1.2.5/ trnfMG34A36	pBR322 derived plasmid bearing the genes for the CAT reporter and the mutant initiator $tRNA_2^{fMet}$ (G34A36)	Ampicillin	*Mayer et al.*, 2003

pRSVCATV1.2.5/ trnfMG34C36	pBR322 derived plasmid bearing the genes for the CAT reporter and the mutant initiator $tRNA_2^{fMet}$ (G34C36)	Ampicillin	*Wu et al.*, 1996
pBAD	Vector for controlled gene expression, containing the arabinose-inducible *araBAD* promoter (P_{BAD}) and regulator (AraC) of *E. coli*	Ampicillin	*Guzman et al.*, 1995
pBAD/ trnfMG34C36	pBAD derived plasmid bearing the gene for the mutant initiator $tRNA_2^{fMet}$ (G34C36)	Ampicillin	*This work*
pBAD/ trnfMU35A36	pBAD derived plasmid bearing the gene for the mutant initiator $tRNA_2^{fMet}$ (U35A36)	Ampicillin	*Lab stock*
pET3-glnS	pET3 transcription vector, bearing the *E. coli glnS* gene, for high overexpression of *E. coli* glutaminyl-tRNA synthetase	Ampicillin	*Weygand-Durasevic et al.*, 1993
pKS21	pKS vector bearing the *E. coli ileS* gene, for overxpression of *E. coli* isoleucyl-tRNA synthetase	Ampicillin	*Shiba and Schimmel,* 1992
pB1	Plasmid carrying the *E. coli pheS* gene, for overexpression of *E. coli* phenyl-tRNA synthetase	Ampicillin	*Plumbridge et al.,* 1980
pQE30	Vector for high-level expression of N-terminally 6xHis-tagged proteins	Ampicillin	*Stueber et al*. 1990
pQE-PTH	PCR-generated BamH I/Hind III fragment of the *E. coli pth* gene cloned into the MCS of pQE30; overexpression of peptidyl-tRNA hydrolase with N-terminal 6xHis-tag	Ampicillin	*This work*

3.2.3. Bacterial strains

Strain	Genotype / details	Reference
B105	*metY* locus expressing $tRNA_1^{fMet}$, r_B^- m_B^- *gal*$^-$ *recA*$^+$	*Mandal and RajBhandary*, 1992
BL21 (DE3) pLysS	F-, *omp*T, *hsd*S_β(r_β-m_β-), *dcm*, *gal* (*λcIts857 ind*I *sam7 nin*5 *lac*UV5-T7) *pLys*S (*cm*^{r})	*Studier et al.*, 1990
CA274	H*fr*, *lac*Z125am, *trp*A49am, *rel*A1, *spo*T1	*Brenner and Beckwith*, 1965
DH5α	*deo*R, *end*A1, *gyr*A96, *hsd*R17(r_k^- m_k^+), *rec*A1, *rel*A1, *supE*44, *thi*-1, ∆(*lac*ZYA-argFV169), φ80*lac*Z∆M15, F$^-$	*Hanahan*, 1983
M15 (pREP4)	*lac*$^-$, *ara*$^+$, *gal*$^+$, *rec*A$^+$, *uvr*$^+$, *lon*$^+$, F$^-$, *mtl*$^-$, *thi*$^-$, pREP4kan^r	*Villarejo and Zabin*, 1974
MV1184	*ara*$^+$, ∆(*lac*-proAB), *rps*L, *thi* (φ80*lac*Z∆M15), ∆(*srl-rec*A)306:: Tn10(*tet*^{r})/F'[*tra*D36, *pro*AB$^+$, *lac*I^q, *lac*Z∆M15]	*Hanahan*, 1983
TK2	*metZΔ2 (Cm^R)*	*Kenri et al.*, 1991
XL-1 Blue	*end*A1, *gyr*A96, *hsd*R17(r_k^- m_k^+), *lac*, *rec*A1, *rel*A1, *sup*E44, *thi*-1, F'[*pro*AB, *lac*I^{q}Z∆M15, Tn10 (Tet^r)]	*Bullock et al.*, 1987

3.3. Methods

3.3.1. Nucleic Acids

3.3.1.1. Recombinant expression and purification of transfer RNA

3.3.1.1.1. Organisms and culture

E. coli B105, CA274, and TK2 transformed with pUC19 derived plasmids were grown in LB broth supplemented with 100 µg ampicillin per ml.

3.3.1.1.2. Purification of transfer RNA

Purification of *E. coli* $tRNA_2^{fMet}$ and mutants thereof was in general performed as described in 2.3.1.8. with the exception of PAGE purifiying mutants G34, G34C36, and G34A36 on a 15% polyacrylamide gel.

3.3.1.1.3. Aminoacylation assays

3.3.1.1.3.1. Glutamine accepting $tRNA_2^{fMet}$ U35A36 and G72/U35A36

The reactions contained aminoacylation buffer 2, 2 mM ATP, 50 µM L-[^{3}H]-glutamine (specific activity: 1.12 x 10^4 cpm/pmol), 0.05 to 0.1 A_{260} unit of glutamine accepting $tRNA_2^{fMet}$ and 22 µg of *E. coli* S100 protein extract enriched in GlnRS. The mixture was incubated at 37°C. 5 µl aliquots were taken at various time points and spotted onto 3MM Whatman filter paper (soaked in 10% TCA/ 2% casamino acid). The filters were washed for 10 min in ice cold 10% TCA/ 2% casamino acid, then 3x 15 min in ice cold 5% TCA and finally in ice cold 96% ethanol. Subsequently the filters were dried at 75°C and the acid-precipitable counts were determined by Liquid Scintillation Counting (LSC).

10x Aminoacylation buffer 2	
HEPES·KOH, pH 7.4	300 mM
$MgCl_2$	100 mM
KCl	100 mM

3.3.1.1.3.2. Isoleucine accepting $tRNA_2^{fMet}$ G34

0.1 A_{260} unit of purified mutant $tRNA_2^{fMet}$ G34 was incubated at 37°C in 30 µl of a mixture containing aminoacylation buffer 3, 2 mM ATP, 50 µM isoleucine (specific activity: 12.6 x 10^3 cpm/pmol) , 5 mM DTT, and 17 µg of S100 protein extract enriched in IleRS. Standard procedure was carried out as described above.

10x Aminoacylation buffer 3	
HEPES·KOH, pH 7.4	300 mM
$MgCl_2$	100 mM

3.3.1.1.3.3. Phenylalanine accepting $tRNA_2^{fMet}$ G34A36

0.1 A_{260} unit of partially purified mutant $tRNA_2^{fMet}$ G34A36 was incubated at 37°C in 30 µl of a mixture containing aminoacylation buffer 3, 2 mM ATP, 50 µM phenylalanine (specific activity: 13 x 10^3 cpm/pmol) , 5 mM DTT, and 30 µg of S30 protein extract enriched in PheRS. Standard procedure was carried out as described above.

3.3.1.1.3.4. Valine accepting $tRNA_2^{fMet}$ G34C36

0.1 A_{260} unit of partially purified mutant $tRNA_2^{fMet}$ G34C36 was used for aminoacylation. Aminoacylation buffer 1, 2 mM ATP, 83 µM L-valine (specific activity: 10.2 x 10^3 cpm/pmol) and 10 µg of S100 enriched in ValRS were added per 30 µl reaction. The mixture was incubated at 37°C. Standard procedure was carried out as described above.

10x Aminoacylation buffer 1	
Imidazole·HCl, pH 7.6	200 mM
NH_4Cl	1.5 M
$MgCl_2$	100 mM
Na_2EDTA	1 mM

3.3.1.2. Preparation of 3'-end radiolabelled formylaminoacyl-tRNA^{fMet}

Radioactively labelled formylaminoacyl-tRNAs were prepared by aminoacylation using radioactive amino acids and subsequent formylation following the protocol as described in 2.3.1.11.1.

3.3.1.3. Cloning and recombinant expression of mutant tRNA$_2^{fMet}$ G34C36

3.3.1.3.1. Cloning of mutant tRNA$_2^{fMet}$ G34C36 gene

Unless specified otherwise, methods outlined in section 2.3.1.6. were used for cloning. The gene of *E. coli* tRNA$_2^{fMet}$ bearing mutations in the anticodon sequence (C34→G34 and U36→C36) was amplified by PCR from plasmid pRSVCATV1.2.3/trnfMG34C36 (Mayer *et al.*, 2003) using 5'-TTTGCCATGGTTCAGGCGCGGGG-3' as the forward primer and 5'-AGATAAGCTTAAACCCCGATAAATCGGGGC-3' as the reverse primer. The forward primer included the first 23 nucleotides of the *E. coli trnfM* gene and contained a *Nco*I restriction site at the 5'-end. The reverse primer was complementary to a sequence upstream of the transcriptional terminator sequence of the *trnfM* gene containing a *Hin*dIII restriction site. The restriction sites were later used in cloning the gene into MCS of the pBAD vector upstream of the arabinose-inducible *araBAD* promoter (P_{BAD}). The PCR product was purified using QIAquick PCR purification kit and subjected to restriction digest using *Nco*I and *Hin*dIII restriction enzymes. Subsequently the 238 nucleotide long fragment was cloned into pBAD. The cloned region was sequenced by automated sequencing using the Applied Biosystems 3730 capillary DNA sequencer (Applied Biosystems Inc., Foster City, CA) at the MIT CCR HHMI Biopolymers Laboratory, Massachusetts Institute of Technology, employing the manufacturer's Big Dye Terminator Cycle Sequencing Reaction Mix.

3.3.1.3.2. Induction of recombinant expression of tRNA$_2^{fMet}$ G34C36

Cells from *E. coli* strain TK2 transformed with plasmid pBAD/trnfMG34C36, were grown in 5 ml LB broth supplemented with 100 µg ampicillin per ml at 37°C until the A_{600} reached 0.5 to 1.0. Expression of mutant tRNA$_2^{fMet}$ G34C36 was induced by addition of arabinose at concentrations ranging from 0.05% to 0.5% (w/v). After

further incubation for 6 h at 37°C, cells were harvested and total RNA was isolated as described below.

3.3.1.3.3. Isolation of total RNA using TriReagent®

Cells from a 5 ml culture were pelleted by centrifugation (Clinical Centrifuge Model CL) and resuspended in 500 µl of TriReagent®. The cell lysate was passed several times through a pipette and the homogenate was incubated at room temperature for 5 min followed by the addition of 100 µl chloroform/ isoamyl alcohol (24:1). The suspension was kept at room temperature for additional 2 min, and subjected to centrifugation for 15 min at 12,000x*g* and 4°C (µSpeedFuge SFR13K). The aqueous layer was transferred to a fresh tube and RNA was ethanol precipitated on dry ice for 20 min. After further centrifugation the pellet was washed several times with ice cold 70% ethanol and dissolved in 100 µl of 5 mM NaOAc (pH 5.0).

3.3.2. Proteins and Enzymes

3.3.2.1. Preparation of *E. coli* protein extracts containing recombinant *E. coli* aminoacyl-tRNA synthetases

3.3.2.1.1. Organisms and culture

E. coli strains BL21(DE3) pLysS, MV1184 and CA274 transformed with plasmids pET3-glnS, pKS21 and pB1, respectively, were cultured at 37°C in LB broth supplemented with 100 µg ampicillin per ml.

3.3.2.1.2. Preparation of S100 extract containing recombinant *E. coli* glutaminyl-tRNA synthetase

In the construct pET3-*glnS* the recombinant *glnS* gene is under the control of the T7 RNA polymerase promoter, thus the expression of GlnRS is dependent on the presence of the T7 RNA polymerase. BL21(DE3) pLysS transformed with pET3-*gln*S (Weygand-Durasevic *et al.*, 1993) was grown in 10 ml LB broth supplemented with ampicillin overnight at 37°C and was used to inoculate 1 L of LB broth supplemented with the same antibiotic. The culture was incubated with shaking at 37°C until the culture grew to an A_{600} of 0.6. The expression of the T7 RNA polymerase was induced upon the addition of 1 mM IPTG. After 4 hours of further growth, the culture was

centrifuged and the cell pellet was washed with buffer containing 20 mM Tris·HCl (pH 7.5) and 5 mM $MgCl_2$. After further centrifugation, the cells were resuspended in 20 ml of buffer TM, and passed through a French pressure cell twice at 10,000 psi. The lysate was centrifuged for 30 min at 27,000x*g* at 4°C. The supernatant was subjected to ultracentrifugation for 1 h at 100,000x*g*. The S100 supernatant was loaded onto a 10 ml DE52 column pre-equilibrated with wash buffer XW at 4°C with a flow rate of 0.5 ml/min. Upon loading, the column was washed with 50 ml of wash buffer. The proteins bound to the column were eluted with buffer XE at a flow rate of 0.5 ml/min. 3 ml fractions were collected and protein containing fractions were pooled (determined by dye-binding assay). The extract was dialyzed against extract storage buffer. Finally, the protein concentration was determined and the S100 extract was stored at –20°C. Aminoacylation assay was performed to test the activity of the extract using total tRNA enriched with $tRNA_2^{fMet}$ mutant U35A36.

Buffer TM	
Tris·HCl, pH 7.5	10 mM
$MgCl_2$	2 mM
DTT	2 mM
PMSF	2 mM

Buffer XW	
KH_2PO_4, pH 7.5	20 mM
$MgCl_2$	1 mM
DTT	2 mM
Glycerol	10%

Buffer XE	
KH_2PO_4, pH 6.5	250 mM
$MgCl_2$	1 mM
DTT	2 mM
Glycerol	10%

Buffer XS	
KH_2PO_4, pH 7.5	10 mM
DTT	2 mM
Glycerol	50%

3.3.2.1.3. Preparation of S100 extract containing recombinant *E. coli* isoleucyl-tRNA synthetase

E. coli MV1184 harboring plasmid pKS21 (Shiba and Schimmel, 1992) was grown in 10 ml of LB broth supplemented with ampicillin at 37°C for 12 h. This 10 ml culture was used as inoculum for 1 L LB broth supplemented with ampicillin. The culture was

grown with shaking until it reached an A_{600} of 0.6 and expression of isoleucyl-tRNA synthetase was induced by 1 mM IPTG. After 4 h of incubation, the cells were harvested and an IleRS enriched S100 protein extract was prepared as described in section 3.2.3.1.2. Aminoacylation assay was performed to test the activity of the extract using total tRNA enriched with $tRNA_2^{fMet}$ mutant G34.

3.3.2.1.4. Preparation of S30 extract containing recombinant *E. coli* phenylalanyl-tRNA synthetase

E. coli CA274 transformed with plasmid pB1 (Plumbridge *et al.*, 1980) was grown in 10 ml of LB broth supplemented with 100 µg ampicillin per ml overnight at 37°C and was used to inoculate 1 L of LB broth. The culture was grown for 12 to 14 hours with shaking at 37°C since pB1 constitutively expresses the genes *pheS* and *pheT,* which code for the two subunits of *E. coli* phenylalanyl-tRNA synthetase. The cells were further process as described in section 3.2.3.1.2. except that the ultracentrifugation step was omitted. An aminoacylation assay was performed to test the activity of the extract using total tRNA enriched with $tRNA_2^{fMet}$ mutant G34A36.

3.3.2.2. Cloning and recombinant expression of *E. coli* peptidyl-tRNA hydrolase

3.3.2.2.1. Organisms and culture

E.coli M15, containing the pREP4 construct for *lac* repression was transformed with pQ30-*pth* was grown in LB broth supplemented with 100 µg ampicillin per ml and 30 µg kanamycin per ml.

3.3.2.2.2. Cloning of *E. coli pth* gene

Unless otherwise specified, cloning methods outlined in section 2.3.1.6. were used. A DNA fragment containing the *E. coli pth* gene, obtained from a laboratory stock, was digested with *Bam*HI and *Hin*dIII. After gel purification the fragment was ligated using T4 DNA Ligase into the expression vector pQE30, digested with the same restriction enzymes. The generated plasmid pQE30-*pth* which was subsequently transformed into *E. coli* M15/pREP4 produced PTH with an N-terminal polyhistidine tag. Plasmid DNA were isolated from single colonies and were analyzed for the

presence of the insert. Positive colonies were used to analyze the expression levels of recombinant PTH upon IPTG induction.

3.3.2.2.3. Recombinant overexpression and purification *E. coli* PTH

The recombinant host, carrying pQE30-*pth*, was grown in 10 ml LB broth, supplemented with 100 µg ampicillin per ml and 30 µg kanamycin per ml at 37°C for 12 h, which was used as inoculum for 1 L of LB broth containing the same antibiotics. The culture was incubated with shaking at 37°C, and expression of PTH was induced by 1 mM IPTG when the culture reached an A_{600} of 0.6. After further 4 h of incubation, the culture was centrifuged and the cell pellet was washed with a buffer containing 20 mM Tris·HCl (pH 7.5) and 5 mM $MgCl_2$. Cells were pelleted again, quickly frozen and stored at -80°C.

Cells were thawed on ice in the presence of 25 ml of ice cold buffer XPE supplemented with 4 tablets of EDTA-free Complete Mini protease inhibitor. Cells were disrupted by passage through a French pressure cell at 10,000 psi twice and the lysate was centrifuged at 10,000x*g* for 30 min at 4°C. The supernatant was applied to 20 ml of TALON™ Metal Affinity resin pre-equilibrated with buffer XPE. The mixture was nutated for 30 min at 4°C, followed by centrifugation for 5 min at 700x*g*. Supernatant was discarded and the Talon resin was washed 3 times with 5 volumes of buffer XPE. The slurry was transferred to a column and washed with 10 volumes of buffer XPE10. Subsequently, his-tagged PTH was eluted with buffer XPE100 in 5 ml fractions. Protein-containing fractions were pooled and dialyzed against XPS buffer. Finally the protein concentration of the PTH batch was determined using Bradford binding-dye assay (2.3.2.1.2.1.) and the protein stock was stored at -20°C.

Buffer XPE	
Tris·HCl, pH 8.0	2 mM
NaCl	100 mM
PMSF	0.5 mM
2-mercaptoethanol	10 mM

Buffer XPE10	
Tris·HCl, pH 8.0	2 mM
NaCl	100 mM
PMSF	0.5 mM
2-mercaptoethanol	10 mM
Imidazole, pH 7.6	10 mM

Buffer XPE100	
Tris·HCl, pH 8.0	2 mM
NaCl	100 mM
PMSF	0.5 mM
2-mercaptoethanol	10 mM
Imidazole, pH 7.6	100 mM

Buffer XPS	
HEPES·KOH, pH 7.5	20 mM
KCl	150 mM
PMSF	0.5 mM
2-mercaptoethanol	10 mM
Glycerol	50%

3.3.3. Peptidyl-tRNA hydrolase activity assay

2 µl of formylaminoacyl-tRNA (2.5 µM to 80 µM) were added to 27 µl of premix (20 mM HEPES·KOH, pH 7.2, 10 mM $MgCl_2$, 25 mM KCl, 10 mM 2-mercaptoethanol, 100 µg/ml BSA). The mixture was pre-incubated for 10 min 37°C and 5 µl were withdrawn and spotted onto a 3MM Whatman filter saturated with 10% TCA and 2% casamino acid. The reaction was initiated by the addition of 30 nM of PTH (1 nM final concentration) and further incubated at 37°C. At various time points 5 µl aliquots were spotted onto 3MM Whatman filters saturated with 10% TCA and 2% casamino acid. The filters were allowed to dry for 1 minute and were further stored in ice cold 10% TCA and 2% casamino acid. The filters were washed 3x 10 minutes in ice cold 5% TCA and 2x 5 minutes in ice cold 100% ethanol. Finally, the filters were dried and TCA precipitable material was determined by liquid scintillation counting (LSC).

3.4. Results

3.4.1. Purification of anticodon mutants of initiator tRNA

The mutant initiator tRNAs G34, G34C36, G34A36, and U35A36 have been shown to be aminoacylated with isoleucine, valine, phenylalanine, and glutamine, respectively (Mayer *et al.*, 2003). This allows us to investigate the role of the amino acids attached to the initiator tRNA in hydrolytic activity of peptidy-tRNA hydrolase, since the tRNA backbone remains the same. In order to obtain large quantities of purified mutant $tRNA_2^{fMet}$, tRNAs were overexpressed in *E. coli* strains B105 and CA274. Following overnight growth at 37°C, cells were harvested and total RNA was obtained by phenol extraction under acidic conditions. Large rRNA molecules were removed by anion-exchange chromatography. Total tRNA samples of anticodon

mutants were analyzed on a 15% non-denaturing polyacrylamide gel (Fig. 3-2). Wild-type and mutant initiator tRNA U35A36 migrated as expected (Fig. 3-2, lanes 2 and 3). On the other hand mutants G34, G34C36, and G34A36 display a slower mobility on a non-denaturing polyacrylamide gel, indicating a different conformation of these mutants compared to that of the wild-type initiator tRNA. Due to their distinct conformations, the three mutants migrate in close distance to wild-type isoacceptor 1 ($tRNA_1^{fMet}$). Thus the original protocol for subsequent PAGE purification was slightly modified by increasing the percentage of polyacrylamide from 12% to 15% to achieve better separation. While a 12% non-denaturing polyacrylamide gel was sufficient for purification of mutants U35A36 and G72/U35A36, adequate separation of mutant $tRNA_2^{fMet}$ G34 was only achieved using a 15% polyacrylamide gel.

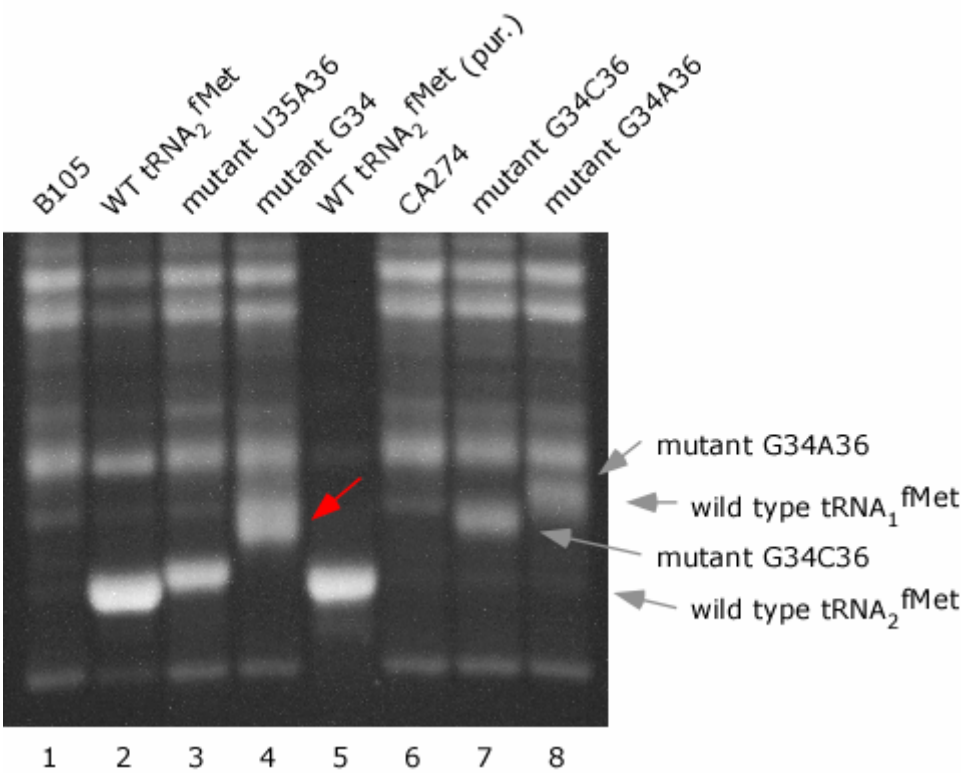

Fig. 3-2: Migration pattern of anticodon mutants on non-denaturing PAGE

Total tRNA was isolated from *E. coli* strains B105 (lanes 1 to 4) and CA274 (lanes 6 to8) under acidic conditions and purified by anion-exchange chromatography. Strains were transformed with plasmid for overexpression of wild-type and mutant $tRNA_2^{fMet}$ bearing mutations in the anticodon, respectively. 0.2 A_{260} units of total tRNA were loaded onto a 15% analytical non-denaturing polyacrylamide gel. The gel was stained with 0.5 µg ethidium bromide per ml. Band indicated by red arrow corresponds to mutant $tRNA_2^{fMet}$ G34.

In case of mutants G34C36 and G34A36 material obtained after PAGE purification contained wild-type $tRNA_1^{fMet}$ as it was determined by aminoacylation assay in the presence of methionine and MetRS (data not shown). Due to the fact that both $tRNA_2^{fMet}$ mutants were not highly expressed as compared to wild-type $tRNA_2^{fMet}$ (Fig. 3-2, compare lanes 7 and 8 to lane 2) careful excision form the gel to avoid contamination of $tRNA_1^{fMet}$ yielded only small amounts of partially purified tRNA. Following PAGE purification and subsequent anion-exchange chromatography the purity of tRNA batch was determined by aminoacylation assays (3.2.2.1.3.). Yield and purity of obtained batches of mutant initiator tRNA are compiled in table 3-1.

$tRNA_2^{fMet}$	**LB cultures** [liters]	**Total tRNA** [A_{260} unit]	**Total tRNA applied** [A_{260} unit]	$tRNA_2^{fMet}$ **recovered** [A_{260} unit]	**Purity** [%]
U35A36	4	419	140	14	>98
G72/U35A36	2	220	100	12.5	>98
G34	3	500	420	19.6	>95
G34C36	2	535	200	~2	~60%
G34A36	3	932	200	~3	~75%

Table 3-1: Compilation of purified *E. coli* initiator tRNA anticodon mutants

Amounts of tRNAs were determined by spectrophotometry at 260 and 280 nm readings and are defined as A_{260} units (1 A_{260} unit equals 40 µg of tRNA). Purity of tRNA corresponds to acceptance of the appropriate amino acid as determined by aminoacylation assay.

3.4.2. Expression of mutant initiator tRNA in *E. coli* strain TK2

As described above, migration of anticodon mutants G34, G34C36, and G34A36 is different from that of wild-type $tRNA_2^{fMet}$. They migrate in close distance to the $tRNA_1^{fMet}$ species which makes it very difficult to PAGE purify sufficient amounts of mutant tRNA free of contamination of $tRNA_1^{fMet}$. To overcome this obstacle we obtained mutant *E. coli* strain TK2 from the laboratory of Professor Y. Kano, Japan, in which the *met*Z gene, encoding $tRNA_1^{fMet}$, was replaced by the chloramphenicol-resistance gene (Kenri *et al.*, 1991). Due to the lack of $tRNA_1^{fMet}$ this strain was thought to be suitable for overexpression and purification of anticodon mutants. Competent cells of *E. coli* TK2 were prepared and transformed with plasmids pRSVCATV1.2.5./trnfMG34C36 (bearing the gene for mutant G34C36) and

pRSVCATF1.2.5./trnfMG34A36 (bearing the gene for mutant G34A36) (2.3.1.6.5.). Other than for pRSVCATF1.2.5/trnfMG34A36, transformation of pRSVCATV1.2.5./ trnfMG34C36 did not result in any transformants. Neither did transformation of *E. coli* strains B105, XL-1 Blue, and DH5α. Colonies were only obtained for *E. coli* CA274, a strain that originally has been used for overexpression of anticodon mutants (3.4.1.). These and similar observations made by colleagues (personal communication) indicate that expression of mutant $tRNA_2^{fMet}$ G34C36, which is charged with valine (Wu and RajBhandary, 1997), is toxic to certain *E. coli* strains. However, the molecular basis of this phenomenon is unknown.

3.4.2.1. Cloning and induced expression of mutant $tRNA_2^{fMet}$ G34C36

Expression of mutant $tRNA_2^{fMet}$ G34C36 from plasmid pRSVCAT1.2.5./trnfMG34C36 is under the control of the *trnfM* promoter leading to constitutive expression of the tRNA. Since the constitutive expression of mutant G34C36 seems to have a negative effect on cell viability of *E. coli* strain TK2, it was decided to put the mutant *trnfM* gene under the control of an inducible promoter like the *ara*BAD promoter (PBAD). Therefore, the mutant *trnfM* gene including the downstream region containing the transcriptional terminator was cloned into the expression vector pBAD-mycHis (3.3.1.3.) following the cloning strategy outlined in figure 3-3. Besides the inducible *ara*BAD promoter, the vector encodes for the regulatory protein AraC, which ensures tight regulation of expression of potentially toxic genes. The desired coding region of the mutant *trnfM* gene was amplified by polymerase chain reaction (PCR) using plasmid pRSVCATV1.2.5./trnfMG34C36 as template. The forward primer was designed in such a way that the gene was amplified without the tRNA promoter. The PCR product was subjected to restriction digestion using *Nco*I and *Hin*dIII restriction endonucleases, gel purified and subsequently cloned into the multiple cloning site of vector pBAD-mycHis digested with the enzymes. Plasmid DNA was isolated from *E. coli* XL1-blue transformants and the presence of the insert was screened for by restriction digestion using *Pvu*I and *Bpm*I. Three fragments were expected in cases where the vector contains the insert. Several positive constructs were identified and the integrity of the mutant *trnfM* gene was confirmed by automated sequencing (data not shown). Subsequently the expression of the mutant $tRNA_2^{fMet}$ was tested. Cells of *E. coli* XL1-blue harboring plasmids pBAD, pBAD/trnfMG34C36 and pBAD/trnfMU35A36, respectively, were grown in 5 ml LB broth supplemented with ampicillin at 37°C to a culture A_{600} of 0.5. Expression of mutant tRNAs was induced

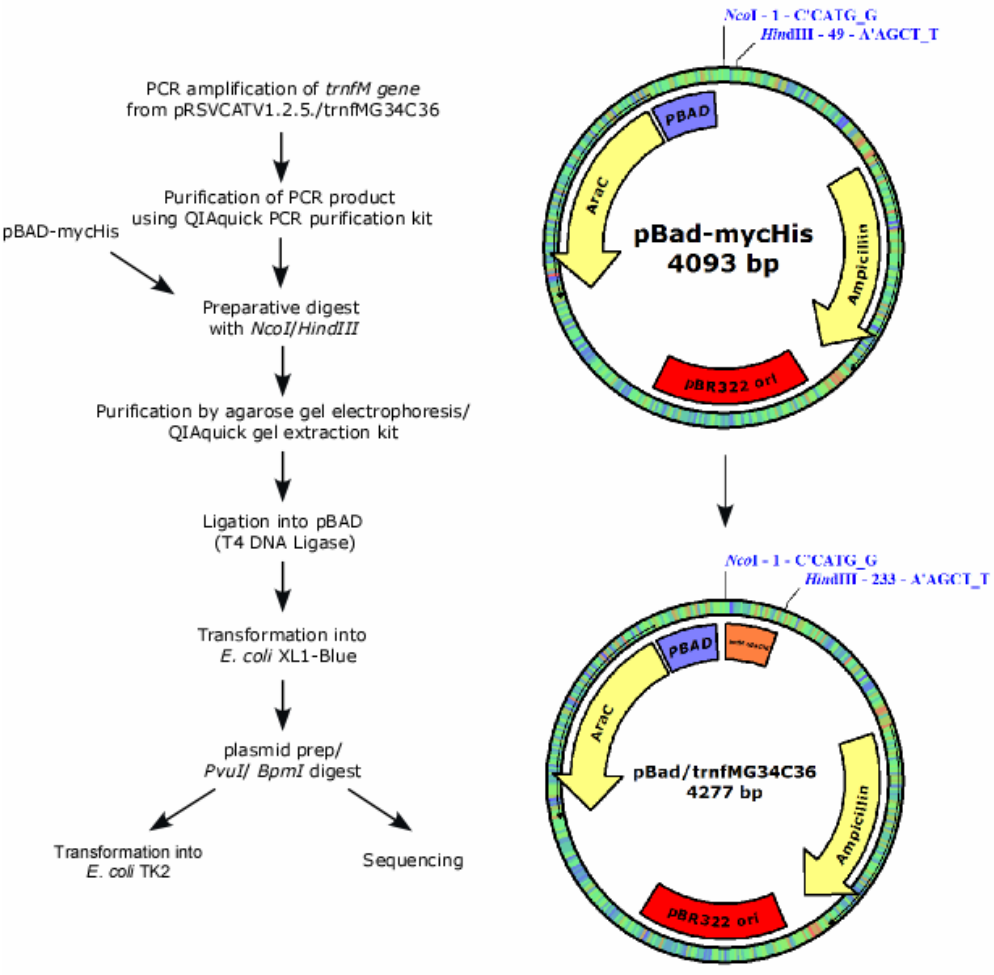

Fig. 3-3: Strategy of cloning of mutant *E. coli* initiator tRNA G34C36

Shown is a schematic illustration of the steps involved in cloning of the coding region of mutant *E. coli* $tRNA_2^{fMet}$ G34C36 into the expression vector pBAD-mycHis.

by addition of 0.1% arabinose (w/v). In the case of control cultures, arabinose was omitted. Cultures were further incubated for 4h and cell growth was monitored by measuring the culture density at various time points. No difference in cell growth was observed between cells transformed with the pBAD/trnfMG34C36 construct and empty vector in the presence or absence of arabinose (data not shown). Following cell growth, total RNA was isolated (3.3.1.3.3.) and samples were subjected to acid urea gel electrophoresis (2.3.1.1.2.3.) and analyzed by Northern blotting (2.3.1.2.). The blot was hybridized simultaneously with 5'-^{32}P-labelled oligonucleotides complementary to *E. coli* $tRNA_2^{fMet}$ carrying the G34C36 mutation and *E. coli* $tRNA^{Tyr}$, which was used as an internal control (Fig. 3-4). In case of empty vector and pBAD

constructs in the absence of arabinose (Fig. 3-4, lanes 1, 4, and 6) two bands were detectable, corresponding to $tRNA^{Tyr}$ in the uncharged and aminoacylated state. In the presence of arabinose, however, an additional band was observed in case of the pBAD construct containing the gene for mutant $tRNA_2^{fMet}$ G34C36. A similar band was detected in the sample obtained from *E. coli* CA274 transformed with plasmid pRSVCATV1.2.5./trnfMG34C36 (Fig. 3-4, lane 3), whereas no such band was observed in the control pBAD/trnfMU35A36 that expresses mutant initiator U35A36

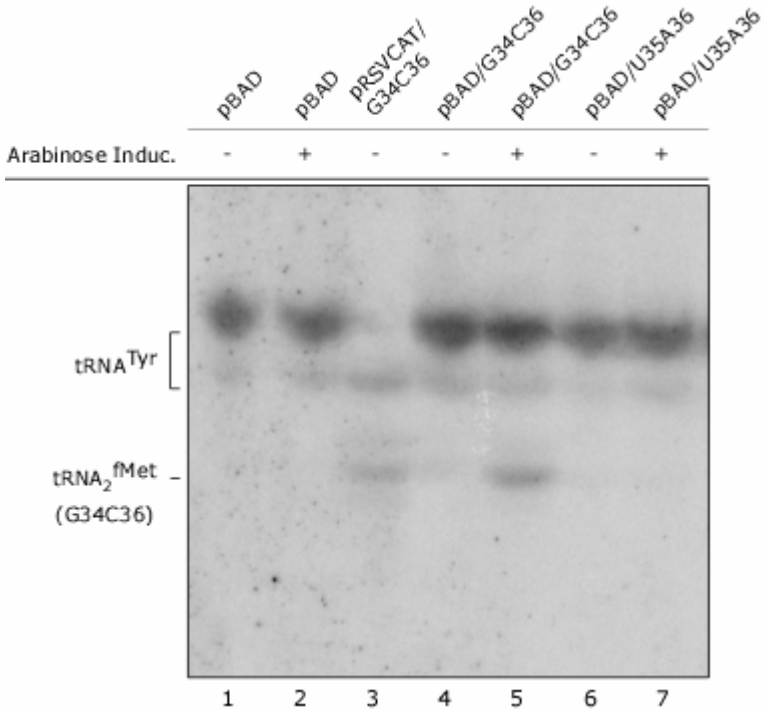

Fig. 3-4: Induced expression of mutant $tRNA_2^{fMet}$ G34C36

Cells of *E. coli* strain XL1-blue transformed with plasmids pBAD, pBAD/trnfMG34C36 and pBAD/trnfMG35A36, respectively, were grown in 5 ml LB broth at 37°C to a culture A_{600} of 0.5 and expression of mutant tRNAs was induced by addition of arabinose (0.1% (w/v), final concentration). Cells were further incubated for 4 h. Control cultures were grown in the absence of arabinose. Total RNA was isolated using Tri-Reagent (Sigma) under acetic conditions and analyzed by acid urea gel and Northern blot analysis. Each lane contained 0.025 A_{260} unit of total RNA. The blot was hybridized simultaneously with 5'-^{32}P-labelled oligonucleotides complementary to *E. coli* $tRNA_2^{fMet}$ carrying the G34C36 mutation: 5'-CCGACGATCTTCGGGTTGTCAG-3'; and *E. coli* $tRNA^{Tyr}$: 5'-CCTTTGGCCGCTCGGG-3'.

in the presence of arabinose (Fig. 3-4, lane 7). Since mutant $tRNA_2^{fMet}$ G34C36 is constitutively expressed from pRSVCAT, the additional band was accounted for as mutant initiator tRNA. The similar migration of the mutant $tRNA_2^{fMet}$ G34C36 in lane 3

and 5 (Fig. 3-4) further indicated that the mutant initiator tRNA is properly processed upon transcription. The fact that cells of *E. coli* XL1-blue showed normal cell growth following induction of expression of mutant $tRNA_2^{fMet}$ G34C36, recommended the use of construct pBAD/trnfMG34C36 for overexpression of the mutant in *E. coli* TK2.

3.4.2.2. Dose-dependent expression and steady-state levels of mutant initiator $tRNA_2^{fMet}$ G34C36 in *E. coli* TK2

For further characterization of dose-dependent expression of mutant $tRNA_2^{fMet}$, cells of *E. coli* TK2 were transformed with plasmid pBAD/trnfMG34C36. A single transformant was used to inoculate 5 ml LB broth supplemented with ampicillin. The primary culture was used to prepare glycerol stocks as well as inoculum for 7x 5 ml of LB broth supplemented with the same antibiotic. The cultures were incubated at 37°C until an A_{600} of 0.5 was reached followed by the addition of arabinose at final concentrations ranging from 0% to 0.5% (w/v). Cells were further incubated and 1 ml aliquots were taken at 3 and 6 h post-induction, respectively. Total RNA was isolated (3.3.1.3.3.) and samples were subjected to acid urea gel electrophoresis (2.3.1.1.2.3.) and analyzed by Northern blotting (2.3.1.2.). The blot was hybridized simultaneously with 5'-^{32}P-labelled oligonucleotides complementary to *E. coli* $tRNA_2^{fMet}$ carrying the G34C36 mutation and *E. coli* $tRNA^{Tyr}$. Figure 3-5 shows the dose-dependent expression of mutant $tRNA_2^{fMet}$ G34C36. Expression levels of the mutant tRNA were normalized to levels of endogenous $tRNA^{Tyr}$. In the absence of arabinose negligible traces of mutant $tRNA_2^{fMet}$ were detectable, probably due to leakage of the pBAD promoter. With increasing concentrations of arabinose, levels of expressed mutant $tRNA_2^{fMet}$ increased as well, reaching saturation at 0.5% of arabinose (w/v). Furthermore is was observed that expression levels after 3 h growth are higher than levels obtained after 6 h, suggesting a reduction in expression. Interesting enough, at a final concentration of 0.5% arabinose (w/v), three bands are visible for the mutant initiator tRNA corresponding to uncharged (bottom), formyaminoacylated (middle), and aminoacylated (top) species, thereby indicating that the mutant $tRNA_2^{fMet}$ G34C36 is solely present as formylaminoacyl-tRNA at lower concentrations. The fact that at higher concentrations the mutant initiator remains uncharged and aminoacylated, suggests that aminoacylation of G34C36 might be limited by native levels of ValRS and/or MTF, since the tRNA is overexpressed.

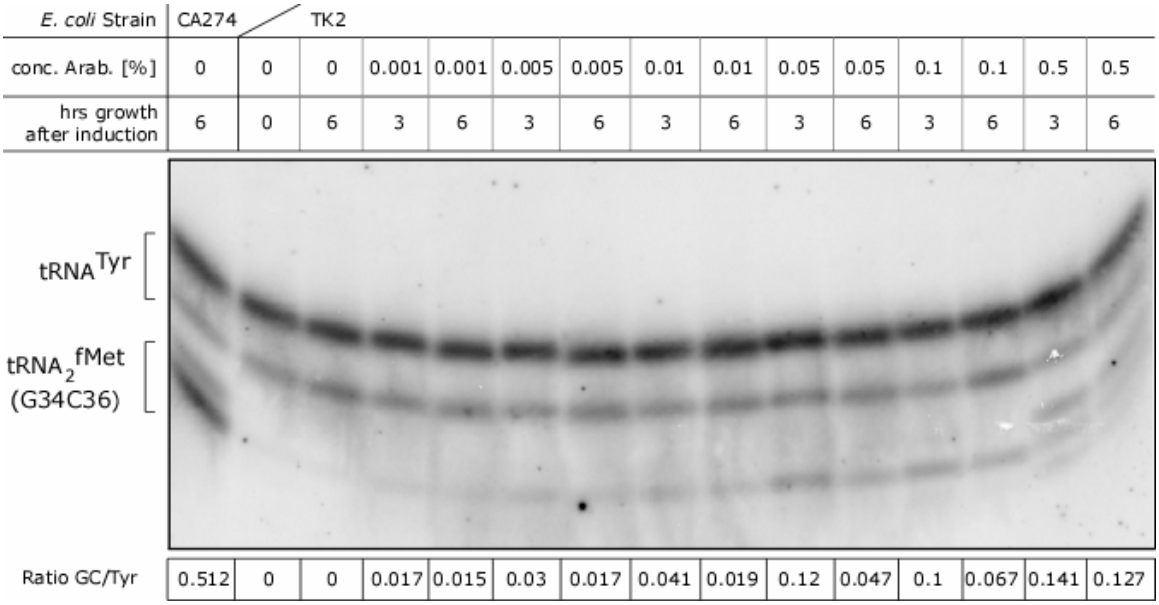

Fig. 3-5: Dose-dependent expression and steady-state levels of mutant initiator $tRNA_2^{fMet}$ G34C36

Cells of *E. coli* strain TK2 transformed with plasmid pBAD/trnfMG34C36, were grown in 5 ml LB broth at 37°C to an A_{600} of 0.5 and expression of mutant tRNAs was induced by addition of arabinose (0.001% to 0.5% (w/v), final concentration). Cells were further incubated for 6h. Control cultures were grown in the absence of arabinose. Total RNA was isolated using Tri-Reagent (Sigma) under acetic conditions and analyzed by acid urea gel and Northern blot analysis. Each lane contained 0.025 A_{260} unit of total RNA. The blot was hybridized simultaneously with 5'-^{32}P-labelled oligonucleotides complementary to *E. coli* $tRNA_2^{fMet}$ carrying the G34C36 mutation: 5'-CCGACGATCTTCGGGTTGTCAG-3'; and *E. coli* $tRNA^{Tyr}$: 5'-CCTTTGGCCGCTCGGG-3'

Furthermore, previous studies have shown that the mutant $tRNA_2^{fMet}$ G34C36 that is charged with valine, is a poor substrate for MTF (Mayer *et al.*, 2003; Wu and RajBhandary, 1997), thus an accumulation of the aminoacylated form can be expected at higher tRNA levels. In comparison with induced expression in TK2, levels of constitutive expression in CA274 are 4-fold higher. Since CA274 was the only *E. coli* strain that was able to grow after transformation with pRSVCAT1.2.5./trnfMG34C36, this result suggests that *E. coli* CA274 somehow can tolerate or compensate for higher amounts of formylvalyl-$tRNA^{fMet}$. Overall, based on the result of arabinose titration, a concentration of 0.05% (w/v) and a maximum incubation time between 3 and 4 h post-induction should be recommended for maximum overexpression of mutant $tRNA_2^{fMet}$ for the purpose of subsequent purification.

3.4.2.3. Usage of *E. coli* strain TK2 for the overexpression of mutant initiator tRNAs

Due to the lack of $tRNA_1^{fMet}$, *E. coli* strain TK2 seemed to be suitable as host strain for the overexpression of mutant intiator tRNAs G34C36 and G34A36, thereby enabling a single-step PAGE purification of these mutants without having to deal with the problem of any contamination by $tRNA_1^{fMet}$. For the preparation of total tRNA, TK2 cells harboring the plasmids pBAD/trnfMG34C36 and pRSVCATF1.2.5./trnfMG34 A36, respectively, were grown in 20 ml of LB broth at 37°C to saturation. The primary cultures where used to inoculate 1 L of LB broth. In case of mutant $tRNA_2^{fMet}$ G34A36 cells were grown overnight at 37°C, whereas in case of mutant $tRNA_2^{fMet}$ G34C36 once a culture A_{600} of 0.8 to 0.9 was reached, expression was induced by addition of 0.05% arabinose ((w/v), final concentration) followed by further cell growth for 3 h. Total tRNA samples of both mutant initiator tRNAs were obtained following the standard protocol (2.3.1.8.). Figure 3-6A shows a polyacrylamide gel electrophoresis pattern of tRNAs isolated from *E. coli* CA274, B105, and TK2, respectively, and further analysis by Northern blotting (Fig. 3-6B). The blot was hybridized with 5'-^{32}P-labelled oligonucleotides complementary to $tRNA_1^{fMet}$. As expected, comparison of lane 3 with lanes 1 and 2 (Fig. 3-6B), respectively, shows that the band corresponding to $tRNA_1^{fMet}$ in *E. coli* B105 and CA274 is absent in *E. coli* TK2. Similarly, overexpression of mutant $tRNA_2^{fMet}$ G34A36 (Fig. 3-6B, lane 5) and G34C36 (Fig. 3-6B, lane7) in *E. coli* TK2 leads to a clear separation of both mutants from all other tRNAs. This enables efficient recovery of mutant $tRNA_2^{fMet}$ from the gel free of any contamination.

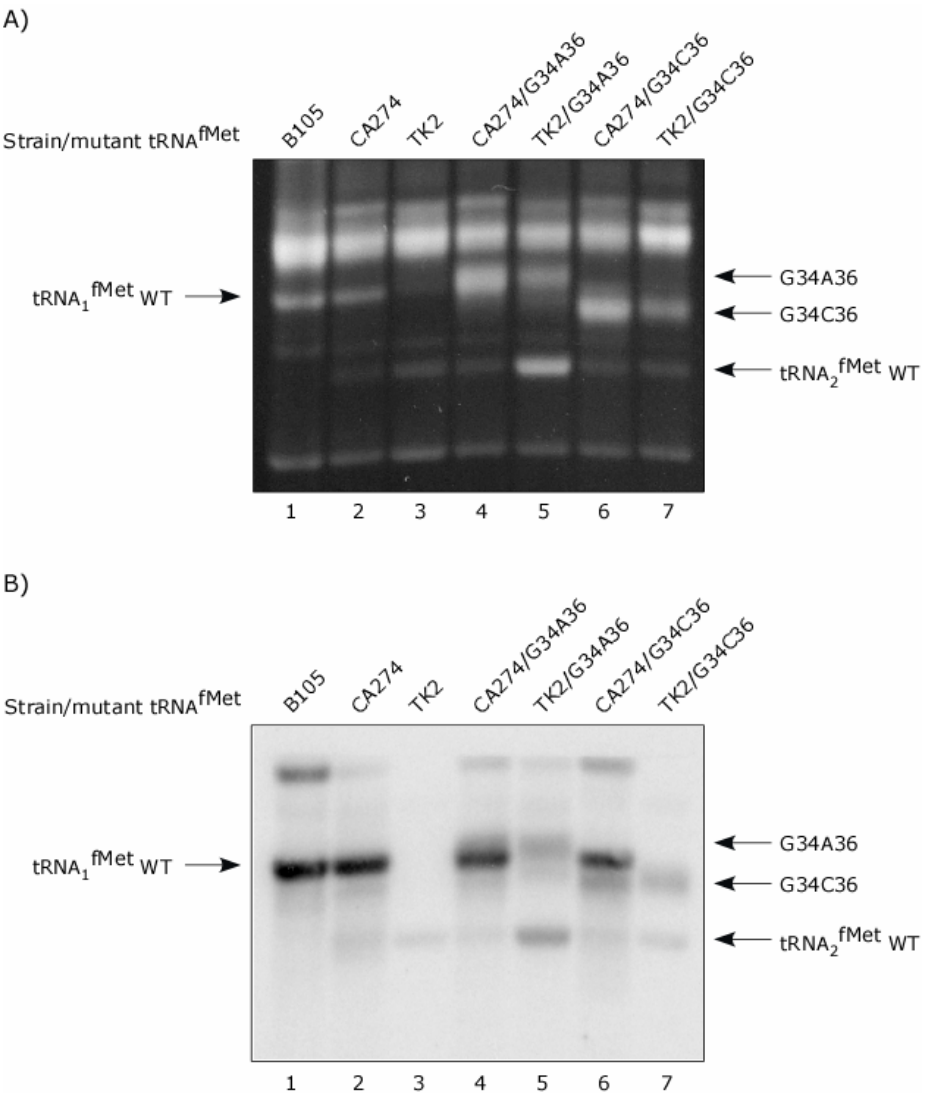

Fig. 3-6: PAGE and Northern blot analysis of mutant initiator tRNA expressed in *E. coli* strains CA274 or TK2

tRNA was isolated from untransformed *E. coli* strains B105 (lane 1), CA274 (lane 2), TK2 (lane 3), CA274 transformed with plasmid pRSVCATV1.2.5./trnfMG34C36 (lane 4) or pRSVCATF1.2.5./trnfMG34A36 (lane 6), and TK2 transformed with plasmid pBAD/trnfMG34C36 (lane 5) or pRSVCATF1.2.5./trnfMG34A36 (lane 7). 0.2 A_{260} units were loaded onto a 15% non-denaturing polyacrylamide gel. A) tRNAs were detected by staining with ethidium bromide (0.5 µg/ml); B) Northern blot analysis. The blot was hybridized with 5'-^{32}P-labelled oligonucleotides complementary to $tRNA_1^{fMet}$: 5'- ACCGACGACCTTCGGGT -3'.

3.4.3. Preparation of 3'-end radiolabelled formylaminoacyl-tRNA^{fMet}

Peptidyl-tRNA hydrolase (PTH) is an enzyme which hydrolyze the ester linkage in N-aminoacyl-tRNA and peptidyl-tRNAs (Lee *et al.*, 1992; Schulman and Pelka, 1975). To investigate the specificity of PTH for the amino acid attached to the initiator tRNA, wild-type and mutant initiator tRNAs had to be quantitatively aminoacylated and formylated. This was facilitated by using radiolabelled amino acid such as ^{35}S-methionine in case of wild-type and mutant tRNA^{fMet} G72 or ^{3}H-glutamine in case of mutant initiator tRNAs U35A36 and G72/U35A36, respectively. Preparative aminoacylation and subsequent formylation was carried out at 37°C for 30 min and 20 min in the presence of either MetRS or GlnRS and MTF, respectively. After the aminoacylation and formylation reaction, the enzymes were removed by phenol/chloroform extraction under acidic conditions. Subsequently, extensive dialysis was performed in order to remove excess amount of small molecules like amino acids and ATP, followed by ethanol precipitation. Final samples were analyzed by acid urea gel electrophoresis and Northern blot analysis (Fig. 3-7). In cases of wild-type (Fig. 3-7, lane 3) and mutant tRNA$_2^{fMet}$ U35A36 (Fig. 3-7, lane 9), the tRNAs were not completely aminoacylated and formylated. Phosphor imaging revealed that about 15% of tRNA in both samples was present in the uncharged state. However, the small fraction of uncharged tRNA was considered not to interfere in the subsequent PTH activity assay. In cases of mutant tRNA$_2^{fMet}$ G72 (Fig. 3-7, lane 6) and G72/U35A36 (Fig. 3-7, lane 12), tRNAs were aminoacylated and formylated to an extent greater than 97%.

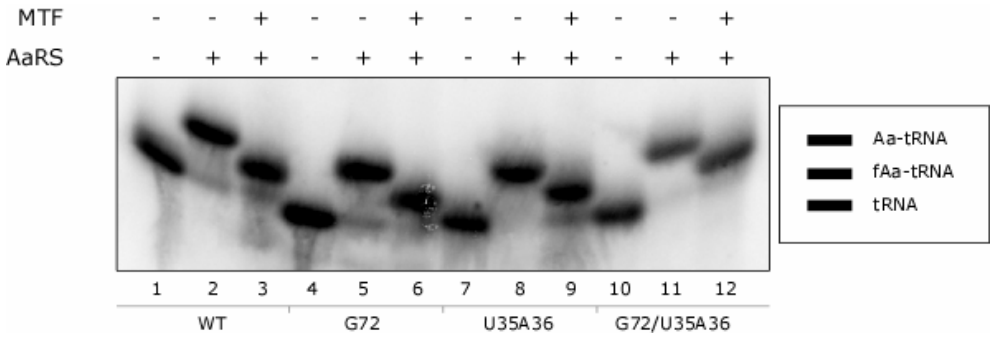

Fig. 3-7: Preparation of 3'-radiolabelled formylaminoacyl-tRNA$_2^{fMet}$

Progression of aminoacylation and formylation of wild-type and mutant tRNAs were analyzed by acid urea gel and Northern blot analysis. Aliquots after each reaction step were taken and added to 2x acid urea loading buffer containing 0.025 A_{260} units of yeast tRNA^{Tyr} as carrier. The blot was hybridized with 5'-^{32}P-labelled oligonucleotides complementary to tRNA$_2^{fMet}$: 5'- GAACCGACGATCTTCGG -3'; -OH: samples were treated with 0.1 M TrisHCl (pH 9.5) for 30 min at 37°C.

3.4.4. Cloning, expression and purification of recombinant *E. coli* peptidyl-tRNA hydrolase

3.4.4.1. Cloning and induced expression of *E. coli* PTH

In order to study the substrate specificity of PTH towards the initiator tRNA aminoacylated with different amino acids, the enzyme had to be overexpressed and purified to homogeneity. To purify PTH by single-step metal affinity chromatography the encoding gene had to be cloned into the pQE30 expression vector resulting in the

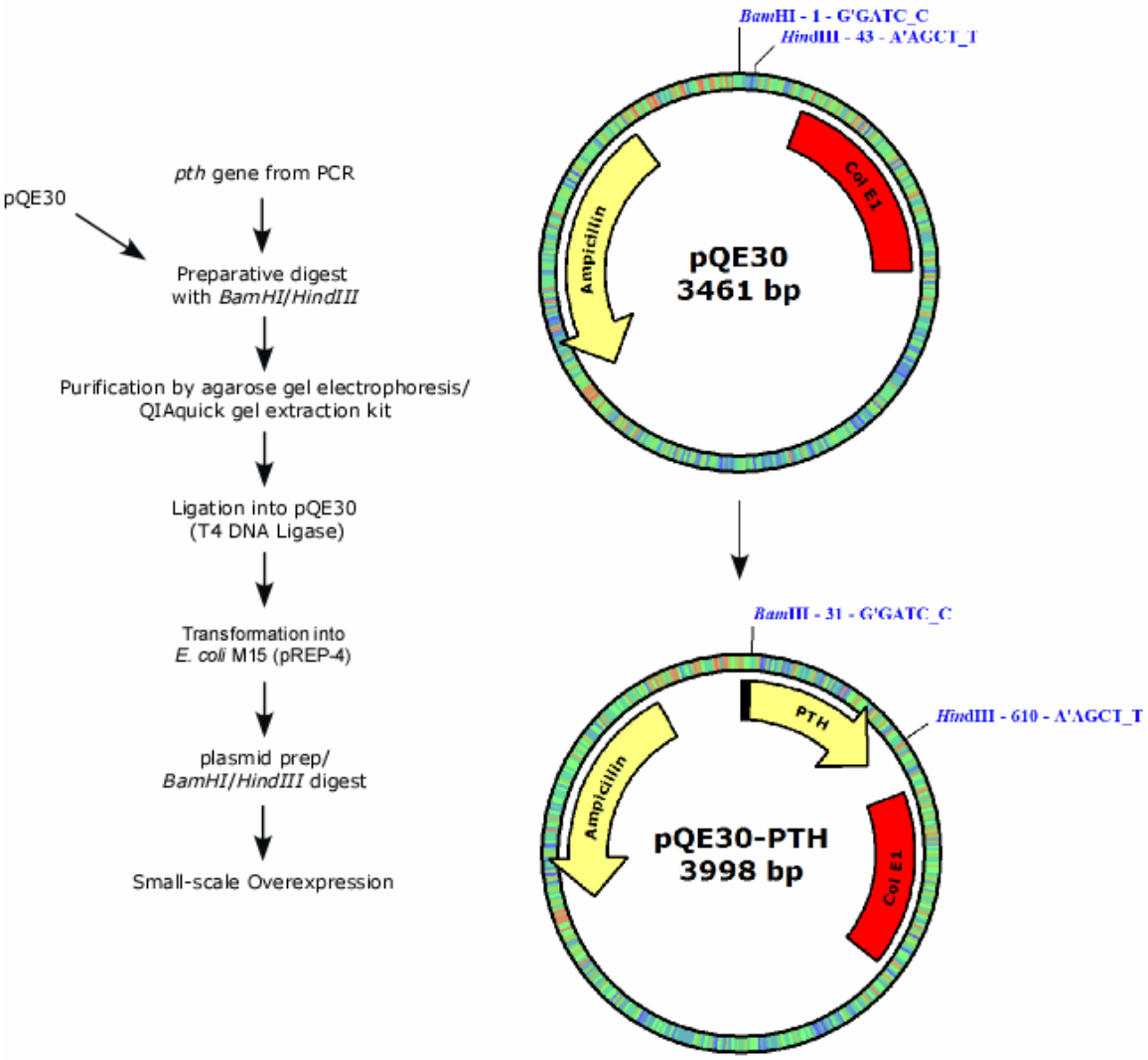

Fig. 3-8: Strategy of cloning of *E. coli pth* gene

Shown is a schematic illustration of the steps involved in cloning of the coding region of mutant *E. coli* $tRNA_2^{fMet}$ G34C36 into the expression vector pBAD-mycHis.

production of N-terminally polyhistidine tagged enzyme. The *E. coli pth* gene amplified by PCR was obtained from a laboratory stock. The DNA fragment was amplified in such a way that it contained a *BamHI* restriction site on the 5'-end and a *HindIII* restriction site on the 3'-end. Figure 3-8 outlines the steps involved cloning of the *E. coli pth* gene. The PCR product was subjected to restriction digestion using *BamHI* and *HindIII* restriction endonucleases, gel purified and subsequently cloned into the multiple cloning site of vector pQE30 digested with the same enzymes. Ligation reaction was used to transform *E. coli* M15 containing the pREP4 repression plasmid. Colonies were picked, plasmid DNA was isolated, and double digested with *BamH I* and *Hind III*. Since pREP4 (3740 bp) only contains a single *Hind III* site, double digestion should result in one smaller fragment of ~600 bp in size corresponding to the insert and two larger band representing pQE30 (~3,4 kb) and pREP4. Several positive constructs were identified. To confirm the presence of the *pth* gene in the pQE30 backbone, 5 ml cultures of positive clones were grown at 37°C until a culture A_{600} of 0.5 was reached and overexpression of PTH was induced by the addition of IPTG (1 mM final concentration). Aliquots were taken at different time points and analyzed by SDS-polyacrylamide gel electrophoresis (Fig. 3-9).

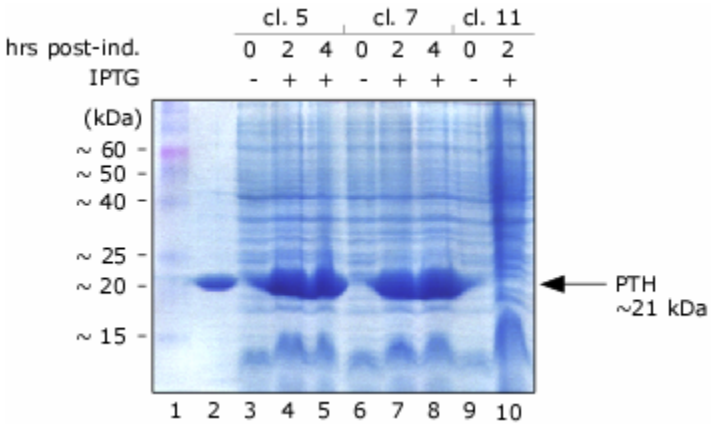

Fig. 3-9: Induced expression of *E. coli* PTH (small scale)

Overexpression of *E. coli* peptidyl-tRNA hydrolase (PTH) from single colonies analyzed by SDS-polyacrylamide gel electrophoresis. Overexpression was induced at an A_{600} of 0.6 to 0.7 by addition of IPTG (1mM final concentration). Cells of 1 ml aliquots were pelleted and resuspended in 1x SDS-loading buffer, boiled for 3 minutes and loaded onto a 12% SDS-PAGE. The gel was stained with coomassie blue stain after electrophoresis.

Clones 5 (Fig. 3-9, lanes 3 to 5) and 7 (Fig. 3-9, lanes 6 to 8) that contained an insert of expected size showed expression of a protein upon addition of IPTG,

whereas the control clone that lacked the insert showed no induction of such protein. Based on the expected molecular weight of 21 kDa, the expressed protein clearly corresponds to PTH. Thus clone 7 was chosen to be used for large scale expression and subsequent purification of polyhistidine tagged PTH.

3.4.4.2. Expression and purification of recombinant *E. coli* PTH

Cells of *E. coli* M15 harboring plasmids pREP4 and pQE30-PTH were grown in 10 ml of LB broth supplemented with ampicillin and kanamycin. The primary culture was used to inoculate 1 liter of LB broth and overexpression of PTH was induced by the addition of IPTG when the culture reached an A_{600} of 0.63. The cells were harvested, lysed by passage through a French pressure cell and the lysate was clarified by centrifugation. Although a minor fraction of PTH still remained in the pellet (Fig. 3-10, lane 4) great amounts of the enzyme was present in the supernatant (Fig. 3-10, lane 5). After applying the supernatant to the Talon resin, the polyhistidine tagged PTH was effectively bound, while non-tagged proteins did not bind or were washed

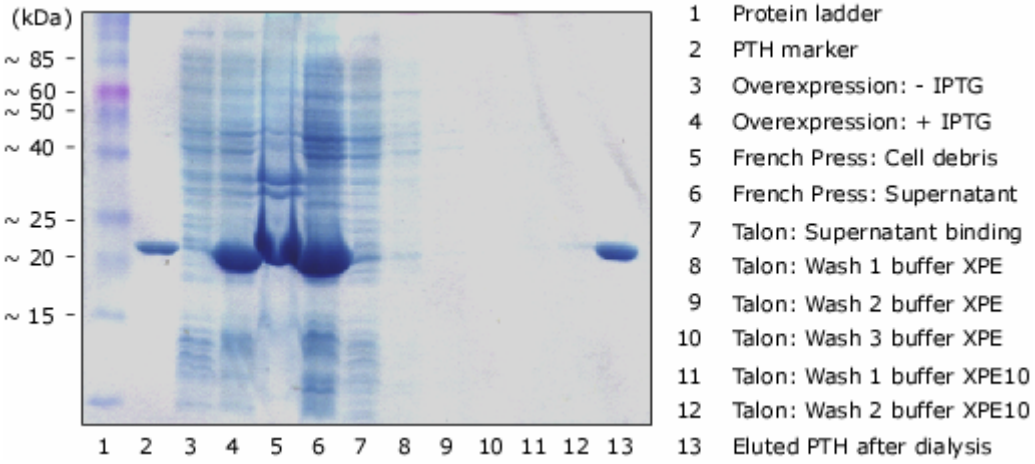

Fig. 3-10: Purification of *E. coli* PTH

Analysis of purification of *E. coli* peptidyl-tRNA hydrolase. Aliquots were taken after individual steps during the purification and were analyzed by SDS-PAGE electrophoresis. PTH marker was obtained from an older batch of purified PTH. The gel was stained with coomassie blue stain after electrophoresis.

off during extensive washing (Fig. 3-10, compare lane 6 with lanes 7 to 12). PTH was eluted from the Talon in the presence of 100 mM imidazole. PTH containing fractions were pooled and dialyzed against storage buffer. The purification yielded 44 mg of enzyme with a purity of >95%. Finally the purified PTH was tested for its hydrolytic

activity of wild-type fMet-tRNA^{fMet} (Fig. 3-11). The enzyme was found be highly active. The enzyme showed high activity at concentrations as low as 100 pM. At a concentration of 50 pM no activity was observed. The drastic drop in counts per minute within the first 5 minutes was accounted for defective substrate (several weeks old) since a similar pattern was observed in the absence of PTH.

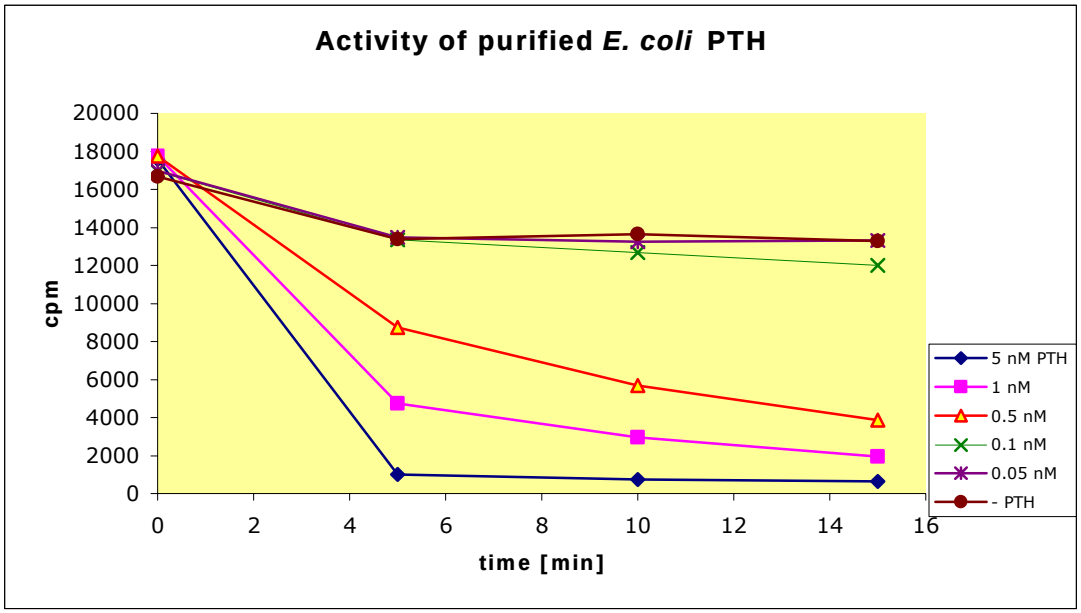

Fig. 3-11: Activity of purified *E. coli* PTH

Extent of hydrolysis of fMet-tRNA$_2^{fMet}$ was determined at various concentration of purified *E. coli* peptidyl-tRNA hydrolase (PTH). 166 µM of fMet-tRNA was used as substrate in the assay. Aliquots were taken at different time points and TCA precipitable counts were plotted as a function of time.

3.4.5. Substrate-specificity of peptidyl-tRNA hydrolase

Although it has been shown that the initiator tRNA is a poor substrate for PTH *in vivo*, choosing the appropriate concentration of PTH allows the measurement of substrate specificity of PTH towards the initiator tRNA charged with different amino acids. PTH was titrated over a broad range of concentration using wild-type fMet-tRNA^{fMet} as substrate (data not shown). The substrate specificity of PTH was measured by analyzing the extent of hydrolysis of formylaminoacyl-tRNA over time. The reactions were started by addition of an appropriate concentration of PTH to a reaction mixture pre-incubated for 10 min at 37°C containing wild-type or mutant f[^{35}S]-methionyl-tRNA$_2^{fMet}$ and f-[^{3}H]-glutaminyl-tRNA^{fMet}, respectively. The reactions

were incubated at 37° and aliquots were taken at various time points. Since PTH displays high specificity for tRNA containing a Watson-Crick base pair at positions

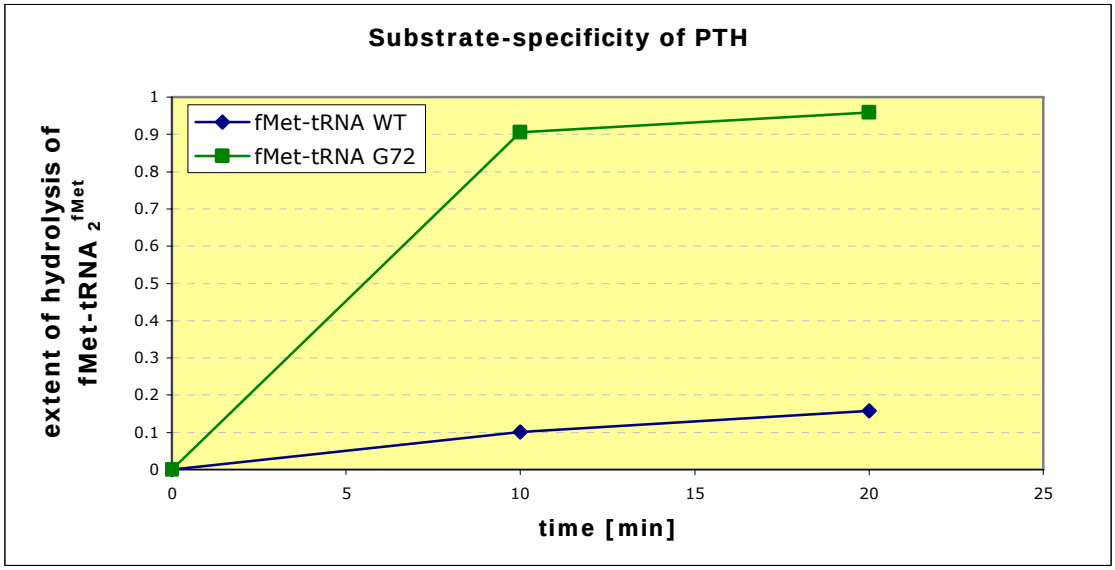

Fig. 3-12: Substrate-specificity of peptidyl-tRNA hydrolase

166 nM of either wild-type fMet-tRNA$_2^{fMet}$ or mutant fMet-tRNA$_2^{fMet}$ G72 were incubated with 1 nM of PTH at 37°C. Aliquots were taken at various time points and TCA precipitable counts were measured by scintillation counting. Extent of hydrolysis of substrate was plotted as a function of time. The data are an average of four separate measurements.

1-72, mutant fMet-tRNA$_2^{fMet}$ G72 (C1-G72) was used as control to ensure that the enzyme was active at the given concentration (Fig. 3-12). At a concentration of 1 nM, hydrolysis of wild-type fMet-tRNA$_2^{fMet}$ occurred at a slow rate. 10% of fMet-tRNA^{fMet} was hydrolyzed within 10 min whereas mutant fMet-tRNA$_2^{fMet}$ G72 was hydrolyzed to an extent of 90%, confirming that PTH favors tRNAs with a base pair at position 1-72 over mismatched initiator tRNA. Subsequent analysis of initiator tRNA charged with either methionine (wild-type) or glutamine (mutant U35A36) was carried out at 2 nM PTH. Unexpectedly, hydrolysis of formylmethionyl-tRNA^{fMet} by PTH was approximately 2 fold higher compared to initiator tRNA carrying formylglutamine (Fig. 3-13). Within 10 min of incubation at concentrations of 166 nM and 333 nM, 35% and 30% of fMet-tRNA^{fMet} were hydrolyzed by PTH, respectively. On the other hand, PTH hydrolyzed only 19% and 17% of fGln-tRNA^{fMet}, respectively. A similar result was obtained when comparing the substrate specificity of PTH towards fMet-tRNA^{fMet} and fGln-tRNA^{fMet} by using mutant tRNA$_2^{fMet}$ G72,

aminoacylated with methionine, and the double mutant G72/U35A36, which was aminoacylated with glutamine (Fig. 3-14). Within 10 min of incubation at a PTH concentration of 0.2 nM 32% of fMet-tRNA$_2^{fMet}$ G72 were hydrolyzed compared to

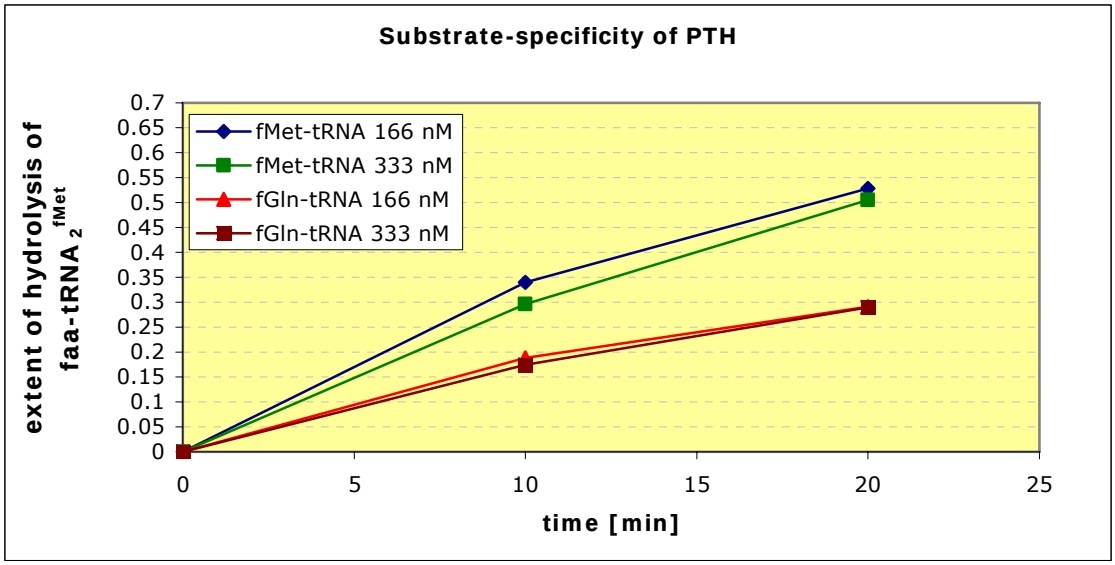

Fig. 3-13: Substrate-specificity of peptidyl-tRNA hydrolase

166 and 333 nM, respectively, of either wild-type fMet-tRNA$_2^{fMet}$ or mutant fGln-tRNA$_2^{fMet}$ U35A36 were incubated with 2 nM of PTH at 37°C. Aliquots were taken at various time points and TCA precipitable counts were measured by scintillation counting. Extent of hydrolysis of substrate was plotted as a function of time. The data are an average of four separate measurements.

17% of fGln-tRNA$_2^{fMet}$ G72/U35A36, indicating that PTH in the context of a similar tRNA backbone slightly favors methionine over glutamine.These obtained *in vitro* data are contrary to *in vivo* data published by Thanedar and co-workers (Thanedar *et al.*, 2000) who showed that initiator tRNAs were more resistant to PTH when they carried fMet than when they carried fGln.

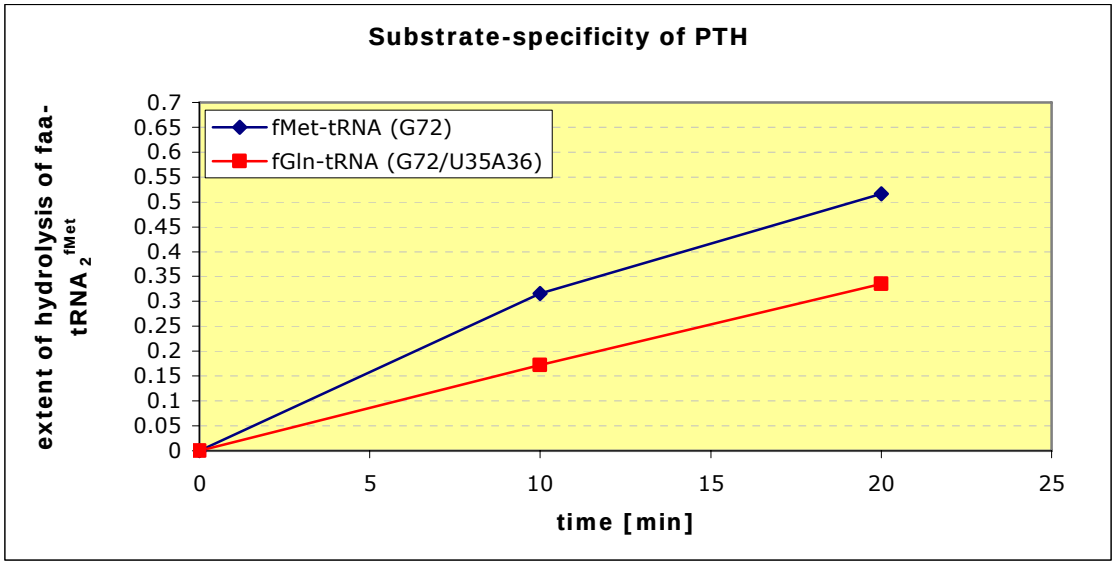

Fig. 3-14: Substrate-specificity of peptidyl-tRNA hydrolase

166 nM of either mutant fMet-$tRNA_2^{fMet}$ G72 or fGln-$tRNA_2^{fMet}$ G72/U35A36 were incubated with 0.2 nM of PTH at 37°C. Aliquots were taken at various time points and TCA precipitable counts were measured by scintillation counting. Extent of hydrolysis of substrate was plotted as a function of time. The data are an average of four separate measurements.

3.5. Discussion

Bacterial peptidyl-tRNA hydrolase (PTH) is thought to recycle aborted peptidyl-tRNA molecules resulting from premature termination by hydrolyzing the ester bond between the tRNA and the attached peptide, thereby regenerating the pool of free tRNA. The substrate specificity of PTH depends on both the peptidic and the nucleotidic moieties of the substrate (Cuzin *et al.*, 1967; Koessel and RajBhandary, 1968). It was shown that PTH hydrolyzes N-blocked aminoacyl-tRNAs, not aminoacyl-tRNA (Koessel and RajBhandary, 1968; Schulman and Pelka, 1975; Shiloach *et al.*, 1975), and that extension of the peptidic moiety to up to four residues increases the rate of hydrolysis in respect to N-amioacyl-tRNA (Shiloach *et al.*, 1975). On the other hand, aminoacylated and N-blocked initiator tRNA was found to be a very poor substrate for PTH (Koessel and RajBhandary, 1968; Schulman and Pelka, 1975). Considering its function in translation, formylmethionyl-$tRNA^{fMet}$ must be kept intact to be recruited by IF2 and to participate in the formation of the ribosomal initiation complex. The molecular basis for this resistance against PTH cleavage is the absence of a strong base pairing at positions 1-72, in the acceptor

stem of prokaryotic initiator tRNAs (Dutka *et al.*, 1993; Schulman and Pelka, 1975). Substitution of nucleotides at positions 1 and 72 of elongator tRNAs leading to a base mismatch, results in an increased resistance towards PTH hydrolysis. Schulman and Pelka further showed that the removal of the 5'-end phosphate group results in a drastic reduction in the rate of hydrolysis of N-acyl-aminoacyl-tRNA (Schulman and Pelka, 1975). X-ray crystallography and side-directed mutagenesis identified two cationic amino acid residues within the active center of PTH that function as receptor sites for the 5'-phosphate (Fromant *et al.*, 1999; Schmitt *et al.*, 1997), suggesting a role as relay between the enzyme and the status of the 1-72 base pair. Therefore, it was hypothesized that the mismatch at the top of the acceptor helix of initiator tRNA twists the position of the phosphate group such that it can no longer trigger the activity of the enzyme. Based on these finding the mismatch was considered to be the hallmark for resistance towards PTH hydrolysis. However, recent *in vivo* studies suggested that the nature of the amino acid attached to the tRNA might also play an important role in its recognition by PTH (Thanedar *et al.*, 2000). Thanedar and co-workers compared steady-state levels of wild-type and mutant initiator tRNAs aminoacylated with methionine and glutamine, respectively. Initiator tRNAs aminoacylated with glutamine were either present in the acylated or deacylated form upon overproduction of PTH, whereas in case of wild-type and mutant initiator tRNA only the formylated form was detected, suggesting that methionine of formylmethionine-tRNAs also prevents hydrolysis by PTH. This observation, however, could not be confirmed *in vitro*. In a first attempt to investigate the preference of PTH towards the nature of the amino acid attached to *E. coli* initiator tRNA, the rate of hydrolytic cleavage was assayed by using wild-type initiator tRNA aminoacylated with methionine, and a mutant initiator tRNA (U35A36) carrying mutations in the anticodon stem aminoacylated with glutamine (Fig. 3-13). Under the same conditions the extent of hydrolysis of formylmethionyl-tRNA^{fMet} was approximately 1.5 fold higher compared to formylglutaminylated initiator tRNA. A similar result was obtained when using mutant initiator tRNAs possessing a strong base pairing at positions 1-72 charged with formylmethionine (G72) and formylglutamine (G72/U35A36), respectively (Fig. 3-14), suggesting that PTH has a slightly higher preference for methionine than for glutamine, although marginal. This marginal difference is in agreement with the broad specificity of PTH towards the sequence of the peptidic moiety of a peptidy-tRNA, and is supported by X-ray crystallography (Schmitt *et al.*, 1997). The crystal structure of *E. coli* PTH showed that its active side

accommodates three amino acid residues of the C-terminal end of a neighboring PTH molecule. It was speculated that the C-terminal end of one PTH molecule bound to another one mimics the peptide product in the catalytic site (Schmitt *et al.*, 1997). Detailed analysis revealed that the contacts between the C-terminal end of PTH and the active site crevice only involves main chain atoms of the former, thus only the conformation of the amino acids should be of great importance in the interaction. Indeed, Koessel and RajBhandary showed that PTH is highly specific towards amino acids in the L-conformation (Koessel and RajBhandary, 1968). The lack of electrostatic interactions between residues of the active center of PTH and the side chains of the peptide attached to the tRNA could explain the low discrimination capacity of PTH. Accordingly, if PTH does not discriminate between the amino acids attached to the tRNA, what accounts for the relative resistance of fMet-tRNA^{fMet} against hydrolytic activity of PTH compared to fGln-tRNA^{fMet} as observed by Thanedar and colleagues (Thanedar *et al.*, 2000)? A likely explanation for the difference in steady-state levels of wild-type and mutant initiator tRNAs is rather an effect of substrate specificity of IF2 than that of PTH. Once the initiator tRNA is aminoacylated and formylated by aminoacyl-tRNA synthetase and MTF, respectively, it becomes a substrate for IF2 and PTH. Thus, PTH has to compete with IF2 for formylaminoacyl-tRNA. In case of IF2 it has been shown previously that the initiation factor discriminates the amino acid that is attached to the initiator tRNA (Mayer *et al.*, 2003), binding fMet-tRNA^{fMet} with a 30 fold higher affinity than fGln-tRNA^{fMet}. By comparison of the binding affinities of IF2 and PTH towards fMet-tRNA^{fMet} a binding inbalance occurs favoring IF2, which binds fMet-tRNA^{fMet} with an affinity of 1 µM (Mayer *et al.*, 2003) compared to 4.5 µM of PTH (Dutka *et al.*, 1993). A further inbalance favoring IF2 is reflected in the amounts of protein present in the cell, where as few as 25 molecules of PTH can occur (Dutka *et al.*, 1993) compared to an estimate of 10000 molecules of IF2 (Bremer, 1987). Furthermore it has to be considered that complete hydrolysis of fGln-tRNA only occurred when PTH alone was overproduced (Thanedar *et al.*, 2000), whereas simultaneous overproduction of IF2 completely annulled the effect of PTH overproduction. Taken together, this suggests that fMet-tRNA^{fMet} escapes PTH hydrolysis by the protection of IF2 whereas fGln-tRNA^{fMet} which is poorly bound by IF2 does not, thereby being efficiently hydrolyzed by PTH. In conclusion, the presented *in vitro* data suggests that the amino acid attached to the tRNA does not play a significant role in the recognition by PTH. The fact that formylmethionyl-tRNA was hydrolyzed more rapidly than formylglutaminyl-

tRNA might indicate a slight preference for hydrophobic amino acids, similar to the marked preference of leucine aminopeptidase of *Aeromonas proteolytica* (Wilkes *et al.*, 1973), with which *E. coli* PTH shares structural similarities within the central core (Chevrier *et al.*, 1994; Schmitt *et al.*, 1997). Further experiments could support this idea, nevertheless, the striking hierarchy for amino acid preference displayed by MTF, IF2 and EF-Tu should not be expected for PTH. Additional *in vivo* as well as *in vitro* experiments should be carried out using mutant initiator tRNA G34C36 which has formylvaline attached to it, and for which IF2 has also a high preference similar to that of methionine (Mayer *et al.*, 2003). Furthermore, *in vitro* analysis of PTH activity towards formylaminoacyl-$tRNA^{fMet}$ should be carried out in the presence of IF2, to investigate the "protective" effects of the latter protein.

Summary

The initiator tRNA contains several structural features that distinguish it from the elongator tRNA aiding in its role as initiator. The initiator tRNA determinants are located in the anticodon stem, the acceptor stem, and the dihydrouridine (D)-stem. Besides the three G:C base pairs in the anticodon stem that prevents the initiator tRNA from binding to the ribosomal A-side, a major structural feature is a mismatch at the end of the acceptor stem between nucleotides 1 and 72. The mismatch has been shown to be important in formylation of the initiator tRNA by methionyl-tRNA transformylase and in preventing it from being recognized by elongation factor Tu and peptidyl-tRNA hydrolase. Results of real-time binding studies have also suggested a role in the recognition of initiator tRNA by initiation factor 2.

To further investigate the molecular basis of IF2 interaction with the acceptor stem of the initiator tRNA, a set of mutant initiator tRNA harboring mutations at positions 1 and/or 72 were analyzed for their binding toward IF2. For *in vitro* analysis wild-type and acceptor stem mutants of initiator tRNAs as well as recombinant *E. coli* IF2 were overexpressed and purified to homogeneity. Electrophoretic mobility shift analysis of *E. coli* IF2·fMet-tRNA^{fMet} complexes did not reveal any significant discrimination by IF2. Furthermore, no discrimination in IF2 recognition towards fMet-tRNA^{fMet} and fGln-tRNA^{fMet} were observed, despite a 10 to 30-fold higher binding constant K_D for the IF2·fGln-tRNA^{fMet} in respect to IF2·fMet-tRNA^{fMet}, as demonstrated previous, indicating either a poor sensitivity of the assay or a general problem with the experimental setup. In addition, complex formations were analyzed by RNase protection assays. However, due to the weakness of the complexes no clear data could be obtained. To overcome possible nonspecific interactions of IF2 with other IF2 or tRNA molecules, IF2 from the thermo stable bacterium *Bacillus stearothermophilus* was further applied in the analysis. Utilization of *B. stearothermophilus* IF2 gave the advantage of higher concentrations of monovalent cations in the binding buffer, thereby reducing nonspecific interactions. *B. stearothermophilus* IF2 gene was isolated from genomic DNA, cloned, overexpressed in *E. coli* and purified to homogeneity. As for *E. coli* IF2, no distinct discrimination was observed in EMSA for *B. stearothermophilus* IF2·fMet-tRNA^{fMet} and IF2·fGln-tRNA^{fMet}, suggesting a general problem with the chosen experimental setup.

Besides sequence and structural feature of the initiator tRNA that are primary determinants for the interaction of MTF, IF2, EF-Tu, and PTH, there is increasing evidence that the amino acid attached to the initiator tRNA may also play an

important role in recognition and discrimination of aminoacylated and formylated tRNA by these proteins. As with MTF, a hierarchy of preferred amino acid was observed for IF2, indicating that the role of methionine has evolved in such a way that it is favored for initiation of protein synthesis. In line with these findings were the results obtained from *in vivo* studies showing that PTH hydrolyses the ester linkage of fGln-tRNA^{fMet} and not that of fMet-tRNA^{fMet} which appeared to be completely resistant to PTH.

To gain further insights in the role of the amino acid attached to the initiator tRNA in the hydrolytic activity of PTH, *in vitro* analysis of the substrate specificity of PTH using wild-type and mutant initiator tRNA aminoacylated with different amino acids was performed. Hydrolysis of formylmethionyl-tRNA^{fMet} by PTH was approximately 2 fold higher compared to initiator tRNA carrying formylglutamine. These data suggests that the amino acid attached to the tRNA does not play a significant role in the recognition by PTH. The fact that fMet-tRNA^{fMet} was hydrolyzed more rapidly than fGln-tRNA^{fMet} might indicate a slight preference for hydrophobic amino acids. The data are contrary to the aforementioned results from *in vivo* studies, and would suggest a competition for substrate between IF2 and PTH within in the cell. Thus, the observed *in vivo* discrimination would rather account for an effect of substrate specificity of IF2 than that of PTH.

In the course of purification of mutant initiator tRNA$_2^{fMet}$ the *E. coli* strain TK2, which lacks the isoacceptor 1 initiator tRNA$_1^{fMet}$, was introduced for overexpression. The utilization of the strain enables the efficient recovery of mutant tRNA$_2^{fMet}$ free of any contamination by wild-type tRNA$_1^{fMet}$ from polyacrylamide gels following electrophoretic separation of total tRNA.

Zusammenfassung

Die Initiator-tRNA enthaelt einige strukturelle Merkmale, die sie von Elongator-tRNAs unterscheidet, und sie so in Ihre Function in der Initiation der Proteinbiosynthese unterstuetzt. Die Determinanten der Initiator-tRNA sind im Anticodonstamm, im Akzeptorstamm und im Dihydrouridin (D)-Stamm lokalisiert. Neben den drei G:C Basenpaaren im Anticodonstamm, welche die Binding der Initiator-tRNA in der ribosomalen A-Seite verhinderen, ist ein ungleiches Basenpaar, zwischen den Positionen 1 und 72, am Ende des Akzeptorstammes, ein hervorgehobenes Merkmal, welches eine bedeutende Rolle in der Formylierung der Inititator-tRNA durch die

Methionyl-tRNA Transformylase spielt. Darueber hinaus verhindert das ungleiche Basenpaar die Erkennung und Bindung der Initiator-tRNA durch den Elongationsfaktor Tu und der Peptidyl-tRNA Hydrolase. Ergebnisse aus Echtzeit-Bindungsstudien haben desweiteren zeigen koennen, dass der Akzeptorstamm auch eine moegliche Rolle in der Erkennung der Initiator-tRNA durch den Inititionsfaktor 2 spielt.

Zur weiteren Klaerung der molekularen Grundlagen der IF2-Interaktion mit dem Akzeptorstamm wurde das Bindungsverhalten des Initiationsfaktors gegenueber muntanter Initiator-tRNAs, welche Mutationen an den Positionen 1 und/oder 72 aufweisen, untersucht. Hierfuer wurden Wildtype und Akzeptorstammmutanten der Initiator tRNA sowie eine rekombinante Version des *E. coli* IF2 aufgereinigt. Analyse der Komplexbildung mittels eines „Elektrophoretischer Mobilitaets Shift Assays" ergab jedoch keine signifikanten Diskriminierungen durch IF2. Darueber hinaus konnte keine eindeutigen Unterschiede zwischen der Erkennung von fMet-tRNA^{fMet} und fGln-tRNA^{fMet} aufgezeigt werden, obwohl der IF2·fGln-tRNA^{fMet}-Komplex eine 10- bis 30-mal hoehere Bindungskonstante K_D aufweist als der IF2·fMet-tRNA^{fMet}-Komplexes. Dies laesst auf ein schwache Sensitivitaet des Assays bzw. auf eine generelles Problem im experimentellen Aufbau schliessen. Zusaetzlich wurden die Komplexbildungen mittels eines RNase Protektions Assays untersucht, welches jedoch durch die Schwaeche der Komplexbildung unzureichende Ergebnisse lieferte. Um moegliche unspezifischen Wechselwirkungen zwischen einem Molekuel IF2 mit anderen IF2-Molekuelen oder anderer tRNAs zu umgehen, wurde die Verwendung des IF2 aus dem thermostabilen Bakterium *Bacillus stearothermophilus* erwogen, welches den Einsatz hoeherer Konzentrationen an monovalenten Kationen im Bindungspuffer ermoeglicht. Zu diesem Zweck wurde das IF2-Gen aus genomischer DNA von *B. stearothermophilus* isoliert, in entsprechende Expressionsvektoren kloniert und, nach Ueberexpression in *E. coli*, chromatographisch aufgereinigt. Wie fuer die *E. coli* Variante, so konnten keine Unterschiede in der Komplexbildung, zwischen IF2·fMet-tRNA^{fMet} und IF2·fGln-tRNA^{fMet}, beobachtet werden. Aufgrund dessen kann von einem generellen Problem im experimentellen Aufbau ausgegangen werden.

Neben sequenzspezifischen und strukturellen Merkmalen der Initiator-tRNA, welche die Hauptdeterminanten fuer die Interaktion mit MTF, IF2, EF-Tu und PTH sind, gibt es zunehmende Beweise fuer eine direkte Rolle der tRNA-gebundenen Aminosaure in der Erkennung und Unterscheidung von aminoacylierten und formylierten tRNAs

durch diese Proteine. So konnte gezeigt werden, dass IF2, aehnlich wie fuer MTF, eine Hierarchie bevorzugter Aminosaeuren aufweist, welches auf eine evolutionaere Bevorzugung der Aminosaeure Methioniens und dessen Bedeutung fuer die Initiation der Translation schliessen laesst. Desweiteren haben *in vivo* Experimente gezeigt, dass PTH die Esterbindung von fGln-tRNA^{fMet} hydrolysiert waehrend fMet-tRNA^{fMet} resistent gegen die hydrolytische Aktivitaet war.

Um einen tieferen Einblick in die Rolle der tRNA-gebundenen Aminosaeure gewinnen zu koennen, wurde die Substratspezifitaet der PTH unter der Verwendung von Wildtype und Mutanten der Initiator-tRNA, die mit unterschiedlichen Aminosaeuren beladen sind, *in vitr*o naeher charakterisiert. Dabei konnte gezeigt werden, dass die Rate der Hydrolyse von fMet-tRNA^{fMet} nur 2-mal hoeher ist als die von fGln-tRNA^{fMet}, was darauf schliessen laesst, dass die Natur der Aminosaeure kaum einen Einfluss auf die Aktivitaet der PTH hat. Der Umstand, dass fMet-tRNA^{fMet} schneller umgesetzt wurde als fGln-tRNA^{fMet} deutet auf eine leichte Bevorzugung von hydrophoben Aminosaeuren hin. Die gewonnenen Daten wiedersprechen den obengenannten *in vivo* Resultaten, und wuerden daher fuer einen Wettbewerb zwischen IF2 und PTH um entsprechende Substrate sprechen. Diesbezueglich weissen die gewonnen Erkenntnisse ehr auf einen direkten Einfluss der Substratspezifitaet von IF2 hin.

Im Rahmen der Aufreinigung von Initiator-tRNAs wurde ein neuer *E. coli* Stamm (TK2) eingefuehrt, in dem das Gen fuer die Isoakzeptor 1 Initiator-tRNA$_1^{fMet}$ substituiert wurde. Die Verwendung dieses Stammes ermoeglicht die effiziente Aufreinung von Initiator-tRNA Mutanten mittels elektrophoretischer Auftrennung der Gesamt-tRNA, unter der Vermeidung einer Kontamination durch Wildtype tRNA$_1^{fMet}$.

Bibliography

Agrawal, R. K., Sharma, M. R., Kiel, M. C., Hirokawa, G., Booth, T. M., Spahn, C. M., Grassucci, R. A., Kaji, A., and Frank, J. (2004). Visualization of ribosome-recycling factor on the Escherichia coli 70S ribosome: functional implications. Proc Natl Acad Sci U S A *101*, 8900-8905.

Allen, G. S., Zavialov, A., Gursky, R., Ehrenberg, M., and Frank, J. (2005). The cryo-EM structure of a translation initiation complex from Escherichia coli. Cell *121*, 703-712.

Antoun, A., Pavlov, M. Y., Andersson, K., Tenson, T., and Ehrenberg, M. (2003). The roles of initiation factor 2 and guanosine triphosphate in initiation of protein synthesis. Embo J *22*, 5593-5601.

Ausubel, F. M. (2001). Current protocols in molecular biology (New York: J. Wiley).

Ban, N., Nissen, P., Hansen, J., Moore, P. B., and Steitz, T. A. (2000). The complete atomic structure of the large ribosomal subunit at 2.4 A resolution. Science *289*, 905-920.

Benelli, D., Maone, E., and Londei, P. (2003). Two different mechanisms for ribosome/mRNA interaction in archaeal translation initiation. Mol Microbiol *50*, 635-643.

Binns, N., and Masters, M. (2002). Expression of the Escherichia coli pcnB gene is translationally limited using an inefficient start codon: a second chromosomal example of translation initiated at AUU. Mol Microbiol *44*, 1287-1298.

Biou, V., Shu, F., and Ramakrishnan, V. (1995). X-ray crystallography shows that translational initiation factor IF3 consists of two compact alpha/beta domains linked by an alpha-helix. Embo J *14*, 4056-4064.

Birnboim, H. C., and Doly, J. (1979). A rapid alkaline extraction procedure for screening recombinant plasmid DNA. Nucleic Acids Res *7*, 1513-1523.

Blattner, F. R., Plunkett, G., 3rd, Bloch, C. A., Perna, N. T., Burland, V., Riley, M., Collado-Vides, J., Glasner, J. D., Rode, C. K., Mayhew, G. F*., et al.* (1997). The complete genome sequence of Escherichia coli K-12. Science *277*, 1453-1474.

Boileau, G., Butler, P., Hershey, J. W., and Traut, R. R. (1983). Direct cross-links between initiation factors 1, 2, and 3 and ribosomal proteins promoted by 2-iminothiolane. Biochemistry *22*, 3162-3170.

Bradford, M. M. (1976). A rapid and sensitive method for the quantitation of microgram quantities of protein utilizing the principle of protein-dye binding. Anal Biochem *72*, 248-254.

Bremer, H. D., P. (1987). Modulation of chemical composition and other parameters of the cell by growth rate., In Escherichia coli and Salmonella typhimurium: Cellular and molecular biology., F. C. Neidhardt, ed. (Washington, D.C.: ASM Press), pp. 1527-1541.

Bretscher, M. S. (1968). Translocation in protein synthesis: a hybrid structure model. Nature *218*, 675-677.

Brombach, M., Gualerzi, C. O., Nakamura, Y., and Pon, C. L. (1986). Molecular cloning and sequence of the Bacillus stearothermophilus translational initiation factor IF2 gene. Mol Gen Genet *205*, 97-102.

Butler, J. S., Springer, M., Dondon, J., Graffe, M., and Grunberg-Manago, M. (1986). Escherichia coli protein synthesis initiation factor IF3 controls its own gene expression at the translational level in vivo. J Mol Biol *192*, 767-780.

Carter, A. P., Clemons, W. M., Jr., Brodersen, D. E., Morgan-Warren, R. J., Hartsch, T., Wimberly, B. T., and Ramakrishnan, V. (2001). Crystal structure of an initiation factor bound to the 30S ribosomal subunit. Science *291*, 498-501.

Cate, J. H., Yusupov, M. M., Yusupova, G. Z., Earnest, T. N., and Noller, H. F. (1999). X-ray crystal structures of 70S ribosome functional complexes. Science *285*, 2095-2104.

Celano, B., Pawlik, R. T., and Gualerzi, C. O. (1988). Interaction of Escherichia coli translation-initiation factor IF-1 with ribosomes. Eur J Biochem *178*, 351-355.

Chapeville, F., Lipmann, F., Von Ehrenstein, G., Weisblum, B., Ray, W. J., Jr., and Benzer, S. (1962). On the role of soluble ribonucleic acid in coding for amino acids. Proc Natl Acad Sci U S A *48*, 1086-1092.

Chen, H., Bjerknes, M., Kumar, R., and Jay, E. (1994). Determination of the optimal aligned spacing between the Shine-Dalgarno sequence and the translation initiation codon of Escherichia coli mRNAs. Nucleic Acids Res *22*, 4953-4957.

Chen, H., Pomeroy-Cloney, L., Bjerknes, M., Tam, J., and Jay, E. (1994). The influence of adenine-rich motifs in the 3' portion of the ribosome binding site on human IFN-gamma gene expression in Escherichia coli. J Mol Biol *240*, 20-27.

Chevrier, B., Schalk, C., D'Orchymont, H., Rondeau, J. M., Moras, D., and Tarnus, C. (1994). Crystal structure of Aeromonas proteolytica aminopeptidase: a prototypical member of the co-catalytic zinc enzyme family. Structure *2*, 283-291.

Choi, S. K., Olsen, D. S., Roll-Mecak, A., Martung, A., Remo, K. L., Burley, S. K., Hinnebusch, A. G., and Dever, T. E. (2000). Physical and functional interaction between the eukaryotic orthologs of prokaryotic translation initiation factors IF1 and IF2. Mol Cell Biol *20*, 7183-7191.

Clark, B. F., Dube, S. K., and Marcker, K. A. (1968). Specific codon-anticodon interaction of an initiator-tRNA fragment. Nature *219*, 484-485.

Crick, F. (1970). Central dogma of molecular biology. Nature *227*, 561-563.

Cromie, G. A., Connelly, J. C., and Leach, D. R. (2001). Recombination at double-strand breaks and DNA ends: conserved mechanisms from phage to humans. Mol Cell *8*, 1163-1174.

Cummings, H. S., Sands, J. F., Foreman, P. C., Fraser, J., and Hershey, J. W. (1991). Structure and expression of the infA operon encoding translational initiation factor IF1. Transcriptional control by growth rate. J Biol Chem *266*, 16491-16498.

Cuzin, F., Kretchmer, N., Greenberg, R. E., Hurwitz, R., and Chapeville, F. (1967). Enzymatic hydrolysis of N-substituted aminoacyl-tRNA. Proc Natl Acad Sci U S A *58*, 2079-2086.

Dahlquist, K. D., and Puglisi, J. D. (2000). Interaction of translation initiation factor IF1 with the E. coli ribosomal A site. J Mol Biol *299*, 1-15.

de Cock, E., Springer, M., and Dardel, F. (1999). The interdomain linker of Escherichia coli initiation factor IF3: a possible trigger of translation initiation specificity. Mol Microbiol *32*, 193-202.

de Smit, M. H., and van Duin, J. (1994). Translational initiation on structured messengers. Another role for the Shine-Dalgarno interaction. J Mol Biol *235*, 173-184.

Delk, A. S., and Rabinowitz, J. C. (1974). Partial nucleotide sequence of a prokaryote initiator tRNA that functions in its non-formylated form. Nature *252*, 106-109.

Dottavio-Martin, D., Suttle, D. P., and Ravel, J. M. (1979). The effects of initiation factors IF-1 and IF-3 on the dissociation of Escherichia coli 70 S ribosomes. FEBS Lett *97*, 105-110.

Dube, S. K., Marcker, K. A., Clark, B. F., and Cory, S. (1968). Nucleotide sequence of N-formyl-methionyl-transfer RNA. Nature *218*, 232-233.

Dube, S. K., Rudland, P. S., Clark, B. F., and Marcker, K. A. (1969). A structural requirement for codon-anticodon interaction on the ribosome. Cold Spring Harb Symp Quant Biol *34*, 161-166.

Dutka, S., Meinnel, T., Lazennec, C., Mechulam, Y., and Blanquet, S. (1993). Role of the 1-72 base pair in tRNAs for the activity of Escherichia coli peptidyl-tRNA hydrolase. Nucleic Acids Res *21*, 4025-4030.

Egan, B. Z., Weiss, J. F., and Kelmers, A. D. (1973). Separation and comparison of primary structures of three formylmethionine tRNAs from E. coli K-12 MO. Biochem Biophys Res Commun *55*, 320-327.

Fortier, P. L., Schmitter, J. M., Garcia, C., and Dardel, F. (1994). The N-terminal half of initiation factor IF3 is folded as a stable independent domain. Biochimie *76*, 376-383.

Freistroffer, D. V., Pavlov, M. Y., MacDougall, J., Buckingham, R. H., and Ehrenberg, M. (1997). Release factor RF3 in E.coli accelerates the dissociation of release factors RF1 and RF2 from the ribosome in a GTP-dependent manner. Embo J *16*, 4126-4133.

Fromant, M., Plateau, P., Schmitt, E., Mechulam, Y., and Blanquet, S. (1999). Receptor site for the 5'-phosphate of elongator tRNAs governs substrate selection by peptidyl-tRNA hydrolase. Biochemistry *38*, 4982-4987.

Garcia, C., Fortier, P. L., Blanquet, S., Lallemand, J. Y., and Dardel, F. (1995). 1H and 15N resonance assignments and structure of the N-terminal domain of Escherichia coli initiation factor 3. Eur J Biochem *228*, 395-402.

Ghosh, G., Pelka, H., and Schulman, L. H. (1990). Identification of the tRNA anticodon recognition site of Escherichia coli methionyl-tRNA synthetase. Biochemistry *29*, 2220-2225.

Giuliodori, A. M., Brandi, A., Gualerzi, C. O., and Pon, C. L. (2004). Preferential translation of cold-shock mRNAs during cold adaptation. Rna *10*, 265-276.

Goodman, H. M., Abelson, J., Landy, A., Brenner, S., and Smith, J. D. (1968). Amber suppression: a nucleotide change in the anticodon of a tyrosine transfer RNA. Nature *217*, 1019-1024.

Grill, S., Gualerzi, C. O., Londei, P., and Blasi, U. (2000). Selective stimulation of translation of leaderless mRNA by initiation factor 2: evolutionary implications for translation. Embo J *19*, 4101-4110.

Grill, S., Moll, I., Hasenohrl, D., Gualerzi, C. O., and Blasi, U. (2001). Modulation of ribosomal recruitment to 5'-terminal start codons by translation initiation factors IF2 and IF3. FEBS Lett *495*, 167-171.

Grunberg-Manago, M., Dessen, P., Pantaloni, D., Godefroy-Colburn, T., Wolfe, A. D., and Dondon, J. (1975). Light-scattering studies showing the effect of initiation factors on the reversible dissociation of Escherichia coli ribosomes. J Mol Biol *94*, 461-478.

Gualerzi, C., Risuleo, G., and Pon, C. L. (1977). Initial rate kinetic analysis of the mechanism of initiation complex formation and the role of initiation factor IF-3. Biochemistry *16*, 1684-1689.

Gualerzi, C. O., and Pon, C. L. (1990). Initiation of mRNA translation in prokaryotes. Biochemistry *29*, 5881-5889.

Guenneugues, M., Caserta, E., Brandi, L., Spurio, R., Meunier, S., Pon, C. L., Boelens, R., and Gualerzi, C. O. (2000). Mapping the fMet-tRNA(f)(Met) binding site of initiation factor IF2. Embo J *19*, 5233-5240.

Haggerty, T. J., and Lovett, S. T. (1997). IF3-mediated suppression of a GUA initiation codon mutation in the recJ gene of Escherichia coli. J Bacteriol *179*, 6705-6713.

Hanahan, D. (1983). Studies on transformation of Escherichia coli with plasmids. J Mol Biol *166*, 557-580.

Hartz, D., Binkley, J., Hollingsworth, T., and Gold, L. (1990). Domains of initiator tRNA and initiation codon crucial for initiator tRNA selection by Escherichia coli IF3. Genes Dev *4*, 1790-1800.

Hartz, D., McPheeters, D. S., and Gold, L. (1989). Selection of the initiator tRNA by Escherichia coli initiation factors. Genes Dev *3*, 1899-1912.

Hirokawa, G., Kiel, M. C., Muto, A., Selmer, M., Raj, V. S., Liljas, A., Igarashi, K., Kaji, H., and Kaji, A. (2002). Post-termination complex disassembly by ribosome recycling factor, a functional tRNA mimic. Embo J *21*, 2272-2281.

Hirokawa, G., Nijman, R. M., Raj, V. S., Kaji, H., Igarashi, K., and Kaji, A. (2005). The role of ribosome recycling factor in dissociation of 70S ribosomes into subunits. Rna *11*, 1317-1328.

Ho, Y. S., and Kan, Y. W. (1987). In vivo aminoacylation of human and Xenopus suppressor tRNAs constructed by site-specific mutagenesis. Proc Natl Acad Sci U S A *84*, 2185-2188.

Holley, R. W., Apgar, J., Everett, G. A., Madison, J. T., Marquisee, M., Merrill, S. H., Penswick, J. R., and Zamir, A. (1965). Structure Of A Ribonucleic Acid. Science *147*, 1462-1465.

Howe, J. G., and Hershey, J. W. (1983). Initiation factor and ribosome levels are coordinately controlled in Escherichia coli growing at different rates. J Biol Chem *258*, 1954-1959.

Hua, Y., and Raleigh, D. P. (1998). On the global architecture of initiation factor IF3: a comparative study of the linker regions from the Escherichia coli protein and the Bacillus stearothermophilus protein. J Mol Biol *278*, 871-878.

Ikemura, T., and Ozeki, H. (1977). Gross map location of Escherichia coli transfer RNA genes. J Mol Biol *117*, 419-446.

Inoue-Yokosawa, N., Ishikawa, C., and Kaziro, Y. (1974). The role of guanosine triphosphate in translocation reaction catalyzed by elongation factor G. J Biol Chem *249*, 4321-4323.

Ishii, S., Kuroki, K., and Imamoto, F. (1984). tRNAMetf2 gene in the leader region of the nusA operon in Escherichia coli. Proc Natl Acad Sci U S A *81*, 409-413.

Janiak, F., Dell, V. A., Abrahamson, J. K., Watson, B. S., Miller, D. L., and Johnson, A. E. (1990). Fluorescence characterization of the interaction of various transfer RNA species with elongation factor Tu.GTP: evidence for a new functional role for elongation factor Tu in protein biosynthesis. Biochemistry *29*, 4268-4277.

Kaji, A., Teyssier, E., and Hirokawa, G. (1998). Disassembly of the post-termination complex and reduction of translational error by ribosome recycling factor (RRF)-A possible new target for antibacterial agents. Biochem Biophys Res Commun *250*, 1-4.

Karimi, R., Pavlov, M. Y., Buckingham, R. H., and Ehrenberg, M. (1999). Novel roles for classical factors at the interface between translation termination and initiation. Mol Cell *3*, 601-609.

Kenri, T., Imamoto, F., and Kano, Y. (1994). Three tandemly repeated structural genes encoding tRNA(f1Met) in the metZ operon of Escherichia coli K-12. Gene *138*, 261-262.

Kenri, T., Kohno, K., Goshima, N., Imamoto, F., and Kano, Y. (1991). Construction and characterization of an Escherichia coli mutant with a deletion of the metZ gene encoding tRNA (f1Met). Gene *103*, 31-36.

Khaitovich, P., Mankin, A. S., Green, R., Lancaster, L., and Noller, H. F. (1999). Characterization of functionally active subribosomal particles from Thermus aquaticus. Proc Natl Acad Sci U S A *96*, 85-90.

Kisselev, L., Ehrenberg, M., and Frolova, L. (2003). Termination of translation: interplay of mRNA, rRNAs and release factors? Embo J *22*, 175-182.

Koessel, H., and RajBhandary, U. L. (1968). Studies on polynucleotides. LXXXVI. Enzymic hydrolysis of N-acylaminoacyl-transfer RNA. J Mol Biol *35*, 539-560.

Kozak, M. (1983). Comparison of initiation of protein synthesis in procaryotes, eucaryotes, and organelles. Microbiol Rev *47*, 1-45.

Kozak, M. (1999). Initiation of translation in prokaryotes and eukaryotes. Gene *234*, 187-208.

Kozak, M. (2005). Regulation of translation via mRNA structure in prokaryotes and eukaryotes. Gene *361*, 13-37.

Krafft, C., Diehl, A., Laettig, S., Behlke, J., Heinemann, U., Pon, C. L., Gualerzi, C. O., and Welfle, H. (2000). Interaction of fMet-tRNA(fMet) with the C-terminal domain of translational initiation factor IF2 from Bacillus stearothermophilus. FEBS Lett *471*, 128-132.

La Teana, A., Pon, C. L., and Gualerzi, C. O. (1996). Late events in translation initiation. Adjustment of fMet-tRNA in the ribosomal P-site. J Mol Biol *256*, 667-675.

Laalami, S., Timofeev, A. V., Putzer, H., Leautey, J., and Grunberg-Manago, M. (1994). In vivo study of engineered G-domain mutants of Escherichia coli translation initiation factor IF2. Mol Microbiol *11*, 293-302.

Laemmli, U. K. (1970). Cleavage of structural proteins during the assembly of the head of bacteriophage T4. Nature *227*, 680-685.

Lancaster, L., Kiel, M. C., Kaji, A., and Noller, H. F. (2002). Orientation of ribosome recycling factor in the ribosome from directed hydroxyl radical probing. Cell *111*, 129-140.

Lander, E. S., Linton, L. M., Birren, B., Nusbaum, C., Zody, M. C., Baldwin, J., Devon, K., Dewar, K., Doyle, M., FitzHugh, W*., et al.* (2001). Initial sequencing and analysis of the human genome. Nature *409*, 860-921.

Larigauderie, G., Laalami, S., Nyengaard, N. R., Grunberg-Manago, M., Cenatiempo, Y., Mortensen, K. K., and Sperling-Petersen, H. U. (2000). Mutation of Thr445 and Ile500 of initiation factor 2 G-domain affects Escherichia coli growth rate at low temperature. Biochimie *82*, 1091-1098.

LaRiviere, F. J., Wolfson, A. D., and Uhlenbeck, O. C. (2001). Uniform binding of aminoacyl-tRNAs to elongation factor Tu by thermodynamic compensation. Science *294*, 165-168.

Laursen, B. S., de, A. S. S. A., Hedegaard, J., Moreno, J. M., Mortensen, K. K., and Sperling-Petersen, H. U. (2002). Structural requirements of the mRNA for intracistronic translation initiation of the enterobacterial infB gene. Genes Cells *7*, 901-910.

Laursen, B. S., Kjaergaard, A. C., Mortensen, K. K., Hoffman, D. W., and Sperling-Petersen, H. U. (2004). The N-terminal domain (IF2N) of bacterial translation initiation factor IF2 is connected to the conserved C-terminal domains by a flexible linker. Protein Sci *13*, 230-239.

Laursen, B. S., Mortensen, K. K., Sperling-Petersen, H. U., and Hoffman, D. W. (2003). A conserved structural motif at the N terminus of bacterial translation initiation factor IF2. J Biol Chem *278*, 16320-16328.

Lee, C. P., Dyson, M. R., Mandal, N., Varshney, U., Bahramian, B., and RajBhandary, U. L. (1992). Striking effects of coupling mutations in the acceptor stem on recognition of tRNAs by Escherichia coli Met-tRNA synthetase and Met-tRNA transformylase. Proc Natl Acad Sci U S A *89*, 9262-9266.

Lee, C. P., Mandal, N., Dyson, M. R., and RajBhandary, U. L. (1993). The discriminator base influences tRNA structure at the end of the acceptor stem and possibly its interaction with proteins. Proc Natl Acad Sci U S A *90*, 7149-7152.

Lee, C. P., Seong, B. L., and RajBhandary, U. L. (1991). Structural and sequence elements important for recognition of Escherichia coli formylmethionine tRNA by methionyl-tRNA transformylase are clustered in the acceptor stem. J Biol Chem *266*, 18012-18017.

Lelong, J. C., Grunberg-Manago, M., Dondon, J., Gros, D., and Gros, F. (1970). Interaction between guanosine derivatives and factors involved in the initiation of protein synthesis. Nature *226*, 505-510.

Leon, M., Dondon, J., Labouesse, J., Grunberg-Manago, M., and Buckingham, R. H. (1979). Recognition of tRNA Trp by initiation factors from Escherichia coli. Eur J Biochem *98*, 149-154.

Lesage, P., Truong, H. N., Graffe, M., Dondon, J., and Springer, M. (1990). Translated translational operator in Escherichia coli. Auto-regulation in the infC-rpmI-rplT operon. J Mol Biol *213*, 465-475.

Li, S., Kumar, N. V., Varshney, U., and RajBhandary, U. L. (1996). Important role of the amino acid attached to tRNA in formylation and in initiation of protein synthesis in Escherichia coli. J Biol Chem *271*, 1022-1028.

Liao, H. X., and Spremulli, L. L. (1991). Initiation of protein synthesis in animal mitochondria. Purification and characterization of translational initiation factor 2. J Biol Chem *266*, 20714-20719.

Lingelbach, K., and Dobberstein, B. (1988). An extended RNA/RNA duplex structure within the coding region of mRNA does not block translational elongation. Nucleic Acids Res *16*, 3405-3414.

Lockwood, A. H., Sarkar, P., and Maitra, U. (1972). Release of polypeptide chain initiation factor IF-2 during initiation complex formation. Proc Natl Acad Sci U S A *69*, 3602-3605.

Louie, A., and Jurnak, F. (1985). Kinetic studies of Escherichia coli elongation factor Tu-guanosine 5'-triphosphate-aminoacyl-tRNA complexes. Biochemistry *24*, 6433-6439.

Lucchini, G., and Bianchetti, R. (1980). Initiation of protein synthesis in isolated mitochondria and chloroplasts. Biochim Biophys Acta *608*, 54-61.

Luchin, S., Putzer, H., Hershey, J. W., Cenatiempo, Y., Grunberg-Manago, M., and Laalami, S. (1999). In vitro study of two dominant inhibitory GTPase mutants of Escherichia coli translation initiation factor IF2. Direct evidence that GTP hydrolysis is necessary for factor recycling. J Biol Chem *274*, 6074-6079.

Mandal, N., and RajBhandary, U. L. (1992). Escherichia coli B lacks one of the two initiator tRNA species present in E. coli K-12. J Bacteriol *174*, 7827-7830.

Mangroo, D., and RajBhandary, U. L. (1995). Mutants of Escherichia coli initiator tRNA defective in initiation. Effects of overproduction of methionyl-tRNA transformylase and the initiation factors IF2 and IF3. J Biol Chem *270*, 12203-12209.

Marcker, K., and Sanger, F. (1964). N-Formyl-Methionyl-S-Rna. J Mol Biol *12*, 835-840.

Marzi, S., Knight, W., Brandi, L., Caserta, E., Soboleva, N., Hill, W. E., Gualerzi, C. O., and Lodmell, J. S. (2003). Ribosomal localization of translation initiation factor IF2. Rna *9*, 958-969.

Matthaei, J. H., and Nirenberg, M. W. (1961). Characteristics and stabilization of DNAase-sensitive protein synthesis in E. coli extracts. Proc Natl Acad Sci U S A *47*, 1580-1588.

Mayer, C., Kohrer, C., Kenny, E., Prusko, C., and RajBhandary, U. L. (2003). Anticodon sequence mutants of Escherichia coli initiator tRNA: effects of overproduction of aminoacyl-tRNA synthetases, methionyl-tRNA formyltransferase, and initiation factor 2 on activity in initiation. Biochemistry *42*, 4787-4799.

Mayer, C., Stortchevoi, A., Kohrer, C., Varshney, U., and RajBhandary, U. L. (2001). Initiator tRNA and its role in initiation of protein synthesis. Cold Spring Harb Symp Quant Biol *66*, 195-206.

McClain, W. H. (1993). Rules that govern tRNA identity in protein synthesis. J Mol Biol *234*, 257-280.

McCutcheon, J. P., Agrawal, R. K., Philips, S. M., Grassucci, R. A., Gerchman, S. E., Clemons, W. M., Jr., Ramakrishnan, V., and Frank, J. (1999). Location of translational initiation factor IF3 on the small ribosomal subunit. Proc Natl Acad Sci U S A *96*, 4301-4306.

Meinnel, T., Sacerdot, C., Graffe, M., Blanquet, S., and Springer, M. (1999). Discrimination by Escherichia coli initiation factor IF3 against initiation on non-canonical codons relies on complementarity rules. J Mol Biol *290*, 825-837.

Meunier, S., Spurio, R., Czisch, M., Wechselberger, R., Guenneugues, M., Gualerzi, C. O., and Boelens, R. (2000). Structure of the fMet-tRNA(fMet)-binding domain of B. stearothermophilus initiation factor IF2. Embo J *19*, 1918-1926.

Misselwitz, R., Welfe, K., Krafft, C., Gualerzi, C. O., and Welfle, H. (1997). Translational initiation factor IF2 from Bacillus stearothermophilus: a spectroscopic and microcalorimetric study of the C-domain. Biochemistry *36*, 3170-3178.

Misselwitz, R., Welfle, K., Krafft, C., Welfle, H., Brandi, L., Caserta, E., and Gualerzi, C. O. (1999). The fMet-tRNA binding domain of translational initiation factor IF2: role and environment of its two Cys residues. FEBS Lett *459*, 332-336.

Moazed, D., and Noller, H. F. (1989). Interaction of tRNA with 23S rRNA in the ribosomal A, P, and E sites. Cell *57*, 585-597.

Moazed, D., and Noller, H. F. (1989). Intermediate states in the movement of transfer RNA in the ribosome. Nature *342*, 142-148.

Moazed, D., Samaha, R. R., Gualerzi, C., and Noller, H. F. (1995). Specific protection of 16 S rRNA by translational initiation factors. J Mol Biol *248*, 207-210.

Moll, I., Grill, S., Gualerzi, C. O., and Blasi, U. (2002). Leaderless mRNAs in bacteria: surprises in ribosomal recruitment and translational control. Mol Microbiol *43*, 239-246.

Moll, I., Hirokawa, G., Kiel, M. C., Kaji, A., and Blasi, U. (2004). Translation initiation with 70S ribosomes: an alternative pathway for leaderless mRNAs. Nucleic Acids Res *32*, 3354-3363.

Monro, R. E. (1967). Catalysis of peptide bond formation by 50 S ribosomal subunits from Escherichia coli. J Mol Biol *26*, 147-151.

Mora, L., Heurgue-Hamard, V., Champ, S., Ehrenberg, M., Kisselev, L. L., and Buckingham, R. H. (2003). The essential role of the invariant GGQ motif in the function and stability in vivo of bacterial release factors RF1 and RF2. Mol Microbiol *47*, 267-275.

Moreau, M., de Cock, E., Fortier, P. L., Garcia, C., Albaret, C., Blanquet, S., Lallemand, J. Y., and Dardel, F. (1997). Heteronuclear NMR studies of E. coli translation initiation factor IF3. Evidence that the inter-domain region is disordered in solution. J Mol Biol *266*, 15-22.

Moreno, J. M., Drskjotersen, L., Kristensen, J. E., Mortensen, K. K., and Sperling-Petersen, H. U. (1999). Characterization of the domains of E. coli initiation factor IF2 responsible for recognition of the ribosome. FEBS Lett *455*, 130-134.

Moreno, J. M., Kildsgaard, J., Siwanowicz, I., Mortensen, K. K., and Sperling-Petersen, H. U. (1998). Binding of Escherichia coli initiation factor IF2 to 30S ribosomal subunits: a functional role for the N-terminus of the factor. Biochem Biophys Res Commun *252*, 465-471.

Mortensen, K. K., Hajnsdorf, E., Regnier, P., and Sperling-Petersen, H. U. (1995). Improved recombinant tandem expression of translation initiation factor IF2 in RNASE E deficient E. coli cells. Biochem Biophys Res Commun *214*, 1254-1259.

Mortensen, K. K., Kildsgaard, J., Moreno, J. M., Steffensen, S. A., Egebjerg, J., and Sperling-Petersen, H. U. (1998). A six-domain structural model for Escherichia coli translation initiation factor IF2. Characterisation of twelve surface epitopes. Biochem Mol Biol Int *46*, 1027-1041.

Muramatsu, T., Nishikawa, K., Nemoto, F., Kuchino, Y., Nishimura, S., Miyazawa, T., and Yokoyama, S. (1988). Codon and amino-acid specificities of a transfer RNA are both converted by a single post-transcriptional modification. Nature *336*, 179-181.

Nakamura, Y., Plumbridge, J., Dondon, J., and Grunberg-Manago, M. (1985). Evidence for autoregulation of the nusA-infB operon of Escherichia coli. Gene *36*, 189-193.

Nakanishi, K., Ogiso, Y., Nakama, T., Fukai, S., and Nureki, O. (2005). Structural basis for anticodon recognition by methionyl-tRNA synthetase. Nat Struct Mol Biol *12*, 931-932.

Nishimura, S., Jones, D. S., and Khorana, H. G. (1965). Studies on polynucleotides. 48. The in vitro synthesis of a co-polypeptide containing two amino acids in alternating sequence dependent upon a DNA-like polymer containing two nucleotides in alternating sequence. J Mol Biol *13*, 302-324.

Nissen, P., Hansen, J., Ban, N., Moore, P. B., and Steitz, T. A. (2000). The structural basis of ribosome activity in peptide bond synthesis. Science *289*, 920-930.

Noller, H. F., Kop, J., Wheaton, V., Brosius, J., Gutell, R. R., Kopylov, A. M., Dohme, F., Herr, W., Stahl, D. A., Gupta, R., and Waese, C. R. (1981). Secondary structure model for 23S ribosomal RNA. Nucleic Acids Res *9*, 6167-6189.

Noller, H. F., and Woese, C. R. (1981). Secondary structure of 16S ribosomal RNA. Science *212*, 403-411.

Nyengaard, N. R., Mortensen, K. K., Lassen, S. F., Hershey, J. W., and Sperling-Petersen, H. U. (1991). Tandem translation of E. coli initiation factor IF2 beta: purification and characterization in vitro of two active forms. Biochem Biophys Res Commun *181*, 1572-1579.

O'Donnell, S. M., and Janssen, G. R. (2002). Leaderless mRNAs bind 70S ribosomes more strongly than 30S ribosomal subunits in Escherichia coli. J Bacteriol *184*, 6730-6733.

Ogle, J. M., Brodersen, D. E., Clemons, W. M., Jr., Tarry, M. J., Carter, A. P., and Ramakrishnan, V. (2001). Recognition of cognate transfer RNA by the 30S ribosomal subunit. Science *292*, 897-902.

Ogle, J. M., Carter, A. P., and Ramakrishnan, V. (2003). Insights into the decoding mechanism from recent ribosome structures. Trends Biochem Sci *28*, 259-266.

Ogle, J. M., and Ramakrishnan, V. (2005). Structural insights into translational fidelity. Annu Rev Biochem *74*, 129-177.

Olsson, C. L., Graffe, M., Springer, M., and Hershey, J. W. (1996). Physiological effects of translation initiation factor IF3 and ribosomal protein L20 limitation in Escherichia coli. Mol Gen Genet *250*, 705-714.

Pape, T., Wintermeyer, W., and Rodnina, M. (1999). Induced fit in initial selection and proofreading of aminoacyl-tRNA on the ribosome. Embo J *18*, 3800-3807.

Petersen, H. U., Roll, T., Grunberg-Manago, M., and Clark, B. F. (1979). Specific interaction of initiation factor IF2 of E. coli with formylmethionyl-tRNA f Met. Biochem Biophys Res Commun *91*, 1068-1074.

Petrelli, D., Garofalo, C., Lammi, M., Spurio, R., Pon, C. L., Gualerzi, C. O., and La Teana, A. (2003). Mapping the active sites of bacterial translation initiation factor IF3. J Mol Biol *331*, 541-556.

Petrelli, D., LaTeana, A., Garofalo, C., Spurio, R., Pon, C. L., and Gualerzi, C. O. (2001). Translation initiation factor IF3: two domains, five functions, one mechanism? Embo J *20*, 4560-4569.

Pioletti, M., Schlunzen, F., Harms, J., Zarivach, R., Gluhmann, M., Avila, H., Bashan, A., Bartels, H., Auerbach, T., Jacobi, C*., et al.* (2001). Crystal structures of complexes of the small ribosomal subunit with tetracycline, edeine and IF3. Embo J *20*, 1829-1839.

Plumbridge, J. A., Dondon, J., Nakamura, Y., and Grunberg-Manago, M. (1985). Effect of NusA protein on expression of the nusA,infB operon in E. coli. Nucleic Acids Res *13*, 3371-3388.

Plumbridge, J. A., Springer, M., Graffe, M., Goursot, R., and Grunberg-Manago, M. (1980). Physical localisation and cloning of the structural gene for E. coli initiation factor IF3 from a group of genes concerned with translation. Gene *11*, 33-42.

Pon, C. L., and Gualerzi, C. (1974). Effect of initiation factor 3 binding on the 30S ribosomal subunits of Escherichia coli. Proc Natl Acad Sci U S A *71*, 4950-4954.

Pon, C. L., and Gualerzi, C. O. (1984). Mechanism of protein biosynthesis in prokaryotic cells. Effect of initiation factor IF1 on the initial rate of 30 S initiation complex formation. FEBS Lett *175*, 203-207.

Pon, C. L., Paci, M., Pawlik, R. T., and Gualerzi, C. O. (1985). Structure-function relationship in Escherichia coli initiation factors. Biochemical and biophysical characterization of the interaction between IF-2 and guanosine nucleotides. J Biol Chem *260*, 8918-8924.

Pon, C. L., Pawlik, R. T., and Gualerzi, C. (1982). The topographical localization of IF3 on Escherichia coli 30 S ribosomal subunits as a clue to its way of functioning. FEBS Lett *137*, 163-167.

Potapov, A. P. (1982). A stereospecific mechanism for the aminoacyl-tRNA selection at the ribosome. FEBS Lett *146*, 5-8.

Ramakrishnan, V. (2002). Ribosome structure and the mechanism of translation. Cell *108*, 557-572.

Rawat, U. B., Zavialov, A. V., Sengupta, J., Valle, M., Grassucci, R. A., Linde, J., Vestergaard, B., Ehrenberg, M., and Frank, J. (2003). A cryo-electron microscopic study of ribosome-bound termination factor RF2. Nature *421*, 87-90.

Rich, A., and Kim, S. H. (1978). The three-dimensional structure of transfer RNA. Sci Am *238*, 52-62.

Rich, A., and RajBhandary, U. L. (1976). Transfer RNA: molecular structure, sequence, and properties. Annu Rev Biochem *45*, 805-860.

Ringquist, S., Shinedling, S., Barrick, D., Green, L., Binkley, J., Stormo, G. D., and Gold, L. (1992). Translation initiation in Escherichia coli: sequences within the ribosome-binding site. Mol Microbiol *6*, 1219-1229.

Rodnina, M. V., Fricke, R., Kuhn, L., and Wintermeyer, W. (1995). Codon-dependent conformational change of elongation factor Tu preceding GTP hydrolysis on the ribosome. Embo J *14*, 2613-2619.

Rodnina, M. V., Gromadski, K. B., Kothe, U., and Wieden, H. J. (2005). Recognition and selection of tRNA in translation. FEBS Lett *579*, 938-942.

Rodnina, M. V., Savelsbergh, A., Katunin, V. I., and Wintermeyer, W. (1997). Hydrolysis of GTP by elongation factor G drives tRNA movement on the ribosome. Nature *385*, 37-41.

Rodnina, M. V., Stark, H., Savelsbergh, A., Wieden, H. J., Mohr, D., Matassova, N. B., Peske, F., Daviter, T., Gualerzi, C. O., and Wintermeyer, W. (2000). GTPases mechanisms and functions of translation factors on the ribosome. Biol Chem *381*, 377-387.

Rodnina, M. V., and Wintermeyer, W. (2001). Fidelity of aminoacyl-tRNA selection on the ribosome: kinetic and structural mechanisms. Annu Rev Biochem *70*, 415-435.

Rodnina, M. V., and Wintermeyer, W. (2001). Ribosome fidelity: tRNA discrimination, proofreading and induced fit. Trends Biochem Sci *26*, 124-130.

Roll-Mecak, A., Cao, C., Dever, T. E., and Burley, S. K. (2000). X-Ray structures of the universal translation initiation factor IF2/eIF5B: conformational changes on GDP and GTP binding. Cell *103*, 781-792.

Sacerdot, C., Fayat, G., Dessen, P., Springer, M., Plumbridge, J. A., Grunberg-Manago, M., and Blanquet, S. (1982). Sequence of a 1.26-kb DNA fragment containing the structural gene for E.coli initiation factor IF3: presence of an AUU initiator codon. Embo J *1*, 311-315.

Sacerdot, C., Vachon, G., Laalami, S., Morel-Deville, F., Cenatiempo, Y., and Grunberg-Manago, M. (1992). Both forms of translational initiation factor IF2 (alpha and beta) are required for maximal growth of Escherichia coli. Evidence for two translational initiation codons for IF2 beta. J Mol Biol *225*, 67-80.

Sambrook, J., and Russell, D. W. (2001). Molecular cloning: a laboratory manual, 3rd edn (Cold Spring Harbor, N.Y.: Cold Spring Harbor Laboratory Press).

Sands, J. F., Cummings, H. S., Sacerdot, C., Dondon, L., Grunberg-Manago, M., and Hershey, J. W. (1987). Cloning and mapping of infA, the gene for protein synthesis initiation factor IF1. Nucleic Acids Res *15*, 5157-5168.

Schimmel, P. (1989). Parameters for the molecular recognition of transfer RNAs. Biochemistry *28*, 2747-2759.

Schluenzen, F., Tocilj, A., Zarivach, R., Harms, J., Gluehmann, M., Janell, D., Bashan, A., Bartels, H., Agmon, I., Franceschi, F., and Yonath, A. (2000). Structure of functionally activated small ribosomal subunit at 3.3 angstroms resolution. Cell *102*, 615-623.

Schmeing, T. M., Moore, P. B., and Steitz, T. A. (2003). Structures of deacylated tRNA mimics bound to the E site of the large ribosomal subunit. Rna *9*, 1345-1352.

Schmitt, E., Fromant, M., Plateau, P., Mechulam, Y., and Blanquet, S. (1997). Crystallization and preliminary X-ray analysis of Escherichia coli peptidyl-tRNA hydrolase. Proteins *28*, 135-136.

Schmitt, E., Panvert, M., Blanquet, S., and Mechulam, Y. (1998). Crystal structure of methionyl-tRNAfMet transformylase complexed with the initiator formyl-methionyl-tRNAfMet. Embo J *17*, 6819-6826.

Schulman, L. H., and Pelka, H. (1975). The structural basis for the resistance of Escherichia coli formylmethionyl transfer ribonucleic acid to cleavage by Escherichia coli peptidyl transfer ribonucleic acid hydrolase. J Biol Chem *250*, 542-547.

Schulman, L. H., and Pelka, H. (1988). Anticodon switching changes the identity of methionine and valine transfer RNAs. Science *242*, 765-768.

Schuwirth, B. S., Borovinskaya, M. A., Hau, C. W., Zhang, W., Vila-Sanjurjo, A., Holton, J. M., and Cate, J. H. (2005). Structures of the bacterial ribosome at 3.5 A resolution. Science *310*, 827-834.

Selmer, M., Al-Karadaghi, S., Hirokawa, G., Kaji, A., and Liljas, A. (1999). Crystal structure of Thermotoga maritima ribosome recycling factor: a tRNA mimic. Science *286*, 2349-2352.

Seong, B. L., Lee, C. P., and RajBhandary, U. L. (1989). Suppression of amber codons in vivo as evidence that mutants derived from Escherichia coli initiator tRNA can act at the step of elongation in protein synthesis. J Biol Chem *264*, 6504-6508.

Seong, B. L., and RajBhandary, U. L. (1987). Escherichia coli formylmethionine tRNA: mutations in GGGCCC sequence conserved in anticodon stem of initiator tRNAs affect initiation of protein synthesis and conformation of anticodon loop. Proc Natl Acad Sci U S A *84*, 334-338.

Seong, B. L., and RajBhandary, U. L. (1987). Mutants of Escherichia coli formylmethionine tRNA: a single base change enables initiator tRNA to act as an elongator in vitro. Proc Natl Acad Sci U S A *84*, 8859-8863.

Sette, M., Spurio, R., van Tilborg, P., Gualerzi, C. O., and Boelens, R. (1999). Identification of the ribosome binding sites of translation initiation factor IF3 by multidimensional heteronuclear NMR spectroscopy. Rna *5*, 82-92.

Sette, M., van Tilborg, P., Spurio, R., Kaptein, R., Paci, M., Gualerzi, C. O., and Boelens, R. (1997). The structure of the translational initiation factor IF1 from E.coli contains an oligomer-binding motif. Embo J *16*, 1436-1443.

Severini, M., Choli, T., La Teana, A., and Gualerzi, C. O. (1992). Proteolysis of Bacillus stearothermophilus IF2 and specific protection by fMet-tRNA. FEBS Lett *297*, 226-228.

Shiba, K., and Schimmel, P. (1992). Functional assembly of a randomly cleaved protein. Proc Natl Acad Sci U S A *89*, 1880-1884.

Shiloach, J., Bauer, S., de Groot, N., and Lapidot, Y. (1975). The influence of the peptide chain length on the activity of peptidyl-tRNA hydrolase from E. coli. Nucleic Acids Res *2*, 1941-1950.

Shine, J., and Dalgarno, L. (1974). The 3'-terminal sequence of Escherichia coli 16S ribosomal RNA: complementarity to nonsense triplets and ribosome binding sites. Proc Natl Acad Sci U S A *71*, 1342-1346.

Sigler, P. B. (1975). An analysis of the structure of tRNA. Annu Rev Biophys Bioeng *4*, 477-527.

Silberklang, M., Gillum, A. M., and RajBhandary, U. L. (1979). Use of in vitro 32P labeling in the sequence analysis of nonradioactive tRNAs. Methods Enzymol *59*, 58-109.

Silberklang, M., Prochiantz, A., Haenni, A. L., and Rajbhandary, U. L. (1977). Studies on the sequence of the 3'-terminal region of turnip-yellow-mosaic-virus RNA. Eur J Biochem *72*, 465-478.

Sorensen, M. A., Kurland, C. G., and Pedersen, S. (1989). Codon usage determines translation rate in Escherichia coli. J Mol Biol *207*, 365-377.

Spahn, C. M., Penczek, P. A., Leith, A., and Frank, J. (2000). A method for differentiating proteins from nucleic acids in intermediate-resolution density maps: cryo-electron microscopy defines the quaternary structure of the Escherichia coli 70S ribosome. Structure Fold Des *8*, 937-948.

Spirin, A. S. (1969). A model of the functioning ribosome: locking and unlocking of the ribosome subparticles. Cold Spring Harb Symp Quant Biol *34*, 197-207.

Sprinzl, M., Hartmann, T., Meissner, F., Moll, J., and Vorderwulbecke, T. (1987). Compilation of tRNA sequences and sequences of tRNA genes. Nucleic Acids Res *15 Suppl*, r53-188.

Spurio, R., Brandi, L., Caserta, E., Pon, C. L., Gualerzi, C. O., Misselwitz, R., Krafft, C., Welfle, K., and Welfle, H. (2000). The C-terminal subdomain (IF2 C-2) contains the entire fMet-tRNA binding site of initiation factor IF2. J Biol Chem *275*, 2447-2454.

Steitz, J. A. (1969). Polypeptide chain initiation: nucleotide sequences of the three ribosomal binding sites in bacteriophage R17 RNA. Nature *224*, 957-964.

Steitz, J. A., and Jakes, K. (1975). How ribosomes select initiator regions in mRNA: base pair formation between the 3' terminus of 16S rRNA and the mRNA during initiation of protein synthesis in Escherichia coli. Proc Natl Acad Sci U S A *72*, 4734-4738.

Steitz, T. A., and Moore, P. B. (2003). RNA, the first macromolecular catalyst: the ribosome is a ribozyme. Trends Biochem Sci *28*, 411-418.

Stortchevoi, A., Varshney, U., and RajBhandary, U. L. (2003). Common location of determinants in initiator transfer RNAs for initiator-elongator discrimination in bacteria and in eukaryotes. J Biol Chem *278*, 17672-17679.

Stringer, E. A., Sarkar, P., and Maitra, U. (1977). Function of initiation factor 1 in the binding and release of initiation factor 2 from ribosomal initiation complexes in Escherichia coli. J Biol Chem *252*, 1739-1744.

Sundari, R. M., Stringer, E. A., Schulman, L. H., and Maitra, U. (1976). Interaction of bacterial initiation factor 2 with initiator tRNA. J Biol Chem *251*, 3338-3345.

Sussman, J. K., Simons, E. L., and Simons, R. W. (1996). Escherichia coli translation initiation factor 3 discriminates the initiation codon in vivo. Mol Microbiol *21*, 347-360.

Szkaradkiewicz, K., Zuleeg, T., Limmer, S., and Sprinzl, M. (2000). Interaction of fMet-tRNAfMet and fMet-AMP with the C-terminal domain of Thermus thermophilus translation initiation factor 2. Eur J Biochem *267*, 4290-4299.

Takeuchi, N., Vial, L., Panvert, M., Schmitt, E., Watanabe, K., Mechulam, Y., and Blanquet, S. (2001). Recognition of tRNAs by Methionyl-tRNA transformylase from mammalian mitochondria. J Biol Chem *276*, 20064-20068.

Tedin, K., Moll, I., Grill, S., Resch, A., Graschopf, A., Gualerzi, C. O., and Blasi, U. (1999). Translation initiation factor 3 antagonizes authentic start codon selection on leaderless mRNAs. Mol Microbiol *31*, 67-77.

Thanedar, S., Kumar, N. V., and Varshney, U. (2000). The fate of the initiator tRNAs is sensitive to the critical balance between interacting proteins. J Biol Chem *275*, 20361-20367.

Tomsic, J., Vitali, L. A., Daviter, T., Savelsbergh, A., Spurio, R., Striebeck, P., Wintermeyer, W., Rodnina, M. V., and Gualerzi, C. O. (2000). Late events of translation initiation in bacteria: a kinetic analysis. Embo J *19*, 2127-2136.

Towbin, H., Staehelin, T., and Gordon, J. (1979). Electrophoretic transfer of proteins from polyacrylamide gels to nitrocellulose sheets: procedure and some applications. Proc Natl Acad Sci U S A *76*, 4350-4354.

Udagawa, T., Shimizu, Y., and Ueda, T. (2004). Evidence for the translation initiation of leaderless mRNAs by the intact 70 S ribosome without its dissociation into subunits in eubacteria. J Biol Chem *279*, 8539-8546.

Varshney, U., Lee, C. P., and RajBhandary, U. L. (1991). Direct analysis of aminoacylation levels of tRNAs in vivo. Application to studying recognition of Escherichia coli initiator tRNA mutants by glutaminyl-tRNA synthetase. J Biol Chem *266*, 24712-24718.

Varshney, U., and RajBhandary, U. L. (1992). Role of methionine and formylation of initiator tRNA in initiation of protein synthesis in Escherichia coli. J Bacteriol *174*, 7819-7826.

Vestergaard, B., Van, L. B., Andersen, G. R., Nyborg, J., Buckingham, R. H., and Kjeldgaard, M. (2001). Bacterial polypeptide release factor RF2 is structurally distinct from eukaryotic eRF1. Mol Cell *8*, 1375-1382.

Vetter, I. R., and Wittinghofer, A. (2001). The guanine nucleotide-binding switch in three dimensions. Science *294*, 1299-1304.

Vila-Sanjurjo, A., Ridgeway, W. K., Seymaner, V., Zhang, W., Santoso, S., Yu, K., and Cate, J. H. (2003). X-ray crystal structures of the WT and a hyper-accurate ribosome from Escherichia coli. Proc Natl Acad Sci U S A *100*, 8682-8687.

Wakao, H., Romby, P., Westhof, E., Laalami, S., Grunberg-Manago, M., Ebel, J. P., Ehresmann, C., and Ehresmann, B. (1989). The solution structure of the Escherichia coli initiator tRNA and its interactions with initiation factor 2 and the ribosomal 30 S subunit. J Biol Chem *264*, 20363-20371.

Warburg, O., and Christian, W. (1942). Isolierung und Kristallisation des Gaerungsferments Enolase. Biochemische Zeitschrift *310*, 384-421.

Weyens, G., Charlier, D., Roovers, M., Pierard, A., and Glansdorff, N. (1988). On the role of the Shine-Dalgarno sequence in determining the efficiency of translation initiation at a weak start codon in the car operon of Escherichia coli K12. J Mol Biol *204*, 1045-1048.

Weygand-Durasevic, I., Schwob, E., and Soll, D. (1993). Acceptor end binding domain interactions ensure correct aminoacylation of transfer RNA. Proc Natl Acad Sci U S A *90*, 2010-2014.

Wilkes, S. H., Bayliss, M. E., and Prescott, J. M. (1973). Specificity of aeromonas aminopeptidase toward oligopeptides and polypeptides. Eur J Biochem *34*, 459-466.

Wimberly, B. T., Brodersen, D. E., Clemons, W. M., Jr., Morgan-Warren, R. J., Carter, A. P., Vonrhein, C., Hartsch, T., and Ramakrishnan, V. (2000). Structure of the 30S ribosomal subunit. Nature *407*, 327-339.

Winkler, H. (1920). Verbreitung und Ursache der Parthenogenesis im Pflanzen- und Tierreich. *1*, 231.

Wintermeyer, W., and Gualerzi, C. (1983). Effect of Escherichia coli initiation factors on the kinetics of N-Acphe-tRNAPhe binding to 30S ribosomal subunits. A fluorescence stopped-flow study. Biochemistry *22*, 690-694.

Wintermeyer, W., Peske, F., Beringer, M., Gromadski, K. B., Savelsbergh, A., and Rodnina, M. V. (2004). Mechanisms of elongation on the ribosome: dynamics of a macromolecular machine. Biochem Soc Trans *32*, 733-737.

Woo, N. H., Roe, B. A., and Rich, A. (1980). Three-dimensional structure of Escherichia coli initiator tRNAfMet. Nature *286*, 346-351.

Wrede, P., Woo, N. H., and Rich, A. (1979). Initiator tRNAs have a unique anticodon loop conformation. Proc Natl Acad Sci U S A *76*, 3289-3293.

Wu, X. Q., and RajBhandary, U. L. (1997). Effect of the amino acid attached to Escherichia coli initiator tRNA on its affinity for the initiation factor IF2 and on the IF2 dependence of its binding to the ribosome. J Biol Chem *272*, 1891-1895.

Yusupov, M. M., Yusupova, G. Z., Baucom, A., Lieberman, K., Earnest, T. N., Cate, J. H., and Noller, H. F. (2001). Crystal structure of the ribosome at 5.5 A resolution. Science *292*, 883-896.

Yusupova, G., Reinbolt, J., Wakao, H., Laalami, S., Grunberg-Manago, M., Romby, P., Ehresmann, B., and Ehresmann, C. (1996). Topography of the Escherichia coli initiation factor 2/fMet-tRNA(f)(Met) complex as studied by cross-linking. Biochemistry *35*, 2978-2984.

Yusupova, G. Z., Yusupov, M. M., Cate, J. H., and Noller, H. F. (2001). The path of messenger RNA through the ribosome. Cell *106*, 233-241.

Zavialov, A. V., Buckingham, R. H., and Ehrenberg, M. (2001). A posttermination ribosomal complex is the guanine nucleotide exchange factor for peptide release factor RF3. Cell *107*, 115-124.

Zavialov, A. V., and Ehrenberg, M. (2003). Peptidyl-tRNA regulates the GTPase activity of translation factors. Cell *114*, 113-122.

Zavialov, A. V., Hauryliuk, V. V., and Ehrenberg, M. (2005). Guanine-nucleotide exchange on ribosome-bound elongation factor G initiates the translocation of tRNAs. J Biol *4*, 9.

Zavialov, A. V., Hauryliuk, V. V., and Ehrenberg, M. (2005). Splitting of the posttermination ribosome into subunits by the concerted action of RRF and EF-G. Mol Cell *18*, 675-686.

Zavialov, A. V., Mora, L., Buckingham, R. H., and Ehrenberg, M. (2002). Release of peptide promoted by the GGQ motif of class 1 release factors regulates the GTPase activity of RF3. Mol Cell *10*, 789-798.

Zuleeg, T., Vogtherr, M., Schubel, H., and Limmer, S. (2000). The C-A mismatch base pair and the single-strand terminus in the E. coli initiator tRNA(fMet) acceptor stem adopt unusual conformations. FEBS Lett *472*, 247-253.

Part II

Antimicrobial peptides in the hemolymph of the honey bee Apis mellifera

Chapter I

General introduction

1.1. Innate immunity

All metazoan organisms are continuously exposed to potentially pathogenic microorganisms, but most of them can be successfully fended off by complex and highly conserved biological mechanisms as well as structures that separate the interior from the exterior of an organism. The epithelial tissue represents the first and non-specific obstacle, which pathogens have to overcome in order to cause an infection. The mechanical, protective function of these cell layers becomes most obvious when the cuticles of insects are considered (Andersen *et al.*, 1995). Not only do they encase the outside of insects but they also line up most parts of the integument or gut (Scholz *et al.*, 1999). Epithelia's also inhibit non-pathogenic flora that competes with pathogenic microorganisms for nutrients and places to adhere on the cell surface, and in some cases produce antimicrobial substances, e.g. colicines in case of *Escherichia coli* (Janeway, 2005). Thus, the epithelium also represents a microbiological barrier which prevents the colonization of the epithelia itself.

In order to cause harm, intruders have to brake through these physical barriers. During evolution organisms have developed different strategies to prevent, to resist and to overcome microbial and parasitic infection. In vertebrates, especially in mammalians, the immune system has a two-stage defensive system with an innate and an acquired, or adaptive immune component. Adaptive immunity is based on receptors that are generated by somatic gene rearrangement and clonal selection during the life of each individual organism (Medzhitov and Janeway, 1997). This system leads to high specificity, but the immune reactions need time to be generated. On the other hand invertebrates, especially insects lack an acquired immune system but have a well-developed innate, or natural, so-called non-clonal system. The term innate immunity literally means germ-line encoded anti-infection tool of the host (Boman, 1995) and refers to phylogenetically ancient defense mechanisms that are inherited present and active from birth (Irving *et al.*, 2001; Medzhitov and Janeway, 1997). They are found in all metazoan organism studied to date. The immune reactions are mediated by immunologically active cells and germ-

line encoded molecules, with the latter either already present or induced upon infection. Thus, the task of the innate immune system is to quickly locate and destroy the invaders, neutralize their virulence factors, and prohibit their spread inside the organism.

In insects the innate immune system can be divided into three branches: the cellular response, the action of the pro/phenoloxidase enzyme cascade, and the humoral response. However, the division is somewhat arbitrary, as many humoral factors affect hemocyte functions and hemocytes are an important source of many humoral molecules (Lavine and Strand, 2002). In the following sections the innate immune system of insects will be discussed in more detail.

1.2. The cellular immune response

The cellular insect immune responses are mediated by the insect blood cells, collectively called hemocytes. Hemocytes first develop in insects during embryogenesis from head or dorsal mesoderm and are further produced during larval or nymphal stages via division of stem cells in mesoderminally derived hematopoetic organs and/or by continued division of hemocytes already in circulation (Lavine and Strand, 2002). Despite the normally low mitotic index in circulating hemocytes, mitosis probably plays an important role in maintaining high hemocyte numbers under stress conditions (Gupta, 1985). Hemocytes can be classified in seven major types on the basis of their morphology (Gupta, 1979): prohemocytes (PRO), plasmatocytes (PL), granulocytes (GR), spherulocytes (SP), adipohemocytes (AD), oenocytoids (OE), and coagulocytes. However the numbers of hemocyte types can vary from organism to organism. Apart from being very dissimilar in their morphological appearance, different hemocyte types can handle the same infectious agent, probably due to a different distribution of responsible receptors on the surface of the various cell types (Trenczek, 1998). The main functions of hemocytes are sealing wounds, phagocytosis of bacteria, as well as nodulation and encapsulation of large eukaryotic parasites or parasitoids (Trenczek, 1998).

Two hemocyte types, granulocytes and plasmatocytes are involved in phagocytosis and encapsulation. Phagocytosis is the endocytic process of ingestion performed by single cells, and is the primary response of hemocytes to small foreign biotic particles such as viruses, bacteria, fungi, and protozoa. It is accomplished in three stages, first by the attachment to the particle and its recognition as non-self,

followed by the activation of pseudopodium formation via signal transduction and ingestion of the foreign body, and finally its disposal or clearance from the host (Ratcliffe and Rowley, 1979). Nodulation and encapsulation on the other hand are highly coordinated multicellular immune responses towards larger aggregations of bacteria and targets like parasitoids and nematodes, respectively, during which a multilayered sheet of hemocytes is formed around the invaders, thereby isolating the invaders from the rest of the body. These processes are thought to be the earliest, and quantitatively, the predominant cellular reaction in response to bacterial infections in insects (Miller and Stanley, 1998). Both processes usually start with individual granular cells that randomly contact the foreign particles and thereafter secrete a flocculent material, known as opsonins, surrounding and tightly binding all participants together. With increase numbers of granulocytes in complex, they have lost their shape, thereby inducing plasmatocytes to change from non-adhesive to strongly adhesive cells. In the cellular encapsulation reaction these activated plasmatocytes form the majority of the capsule. While the core of the capsule begins to melanize, capsule formation ends with a monolayer of apoptotic granular cells that constitute the periphery. Once complex formation is finished the entrapped invader is killed and degraded through the action of several factors including the production of toxic quinines or hydroquinones via the pro/phenoloxidase enzyme cascade, as well as secreted molecules like peroxidases, hydrolytic enzymes and antimicrobial peptides (Gillespie *et al.*, 1997; Trenczek, 1998).

1.3. The Pro/Phenoloxidase enzyme cascade

In insects the primary and most obvious function of the copper-containing phenoloxidase enzyme family (Mason, 1965) is the pigmentation and sclerotization of the cuticle before or after ecdysis (Andersen *et al.*, 1995; Hopkins and Kramer, 1992). Additionally the enzyme plays an important role in innate immunity. In invertebrates, mechanical injuries or presence of foreign objects such as parasites and microorganisms result in melanin deposition around the damage tissue or intruding object. The melanin will physically contain an intruder and therefore prevent or retard its growth. Even more importantly highly reactive and toxic quinine intermediates are produced during melanin formation, which play a fundamental role in the killing of non-phagocytosed microbes and parasites (Soderhall and Cerenius, 1998). Responsible for these dramatic activities is the active form of phenoloxidase

(PO). Upon proteolysis of the inactive zymogen prophenoloxidase (PPO), PO catalyzes the hydroxylation of tyrosine to dopa and the subsequent oxidation of dopa to the corresponding quinine, which leads to melanin in a non-enzymatic manner (Ashida and Brey, 1998). Prophenoloxidase is present in hemolymph, plasma or cuticle (Ashida and Brey, 1995; Marmaras *et al.*, 1996) and has been localized by immunofluorescence on the cell surface of hemocytes of *Cerratitis capitata* (Marmaras *et al.*, 1996). In addition PPO has also been detected in midgut epithelial cells (Brey *et al.*, 1993). All arthropod PPOs, with one exception (Parkinson *et al.*, 2001), are synthesized without a hydrophobic signal sequence for endoplasmatic reticulum localization and are therefore commonly assumed to be released from the cell upon rupture of the cell membrane (Cerenius and Soderhall, 2004). In most cases, subsets of hemocytes are responsible for the bulk production of the proenzyme (Waltzer *et al.*, 2002). After being released from the hemocyte, hemocyte-derived PPO can be post-translationally modified and transported through the cuticle by an unknown mechanism (Asano and Ashida 2001a, 2001b). Although further evidence is lacking these findings suggest that hemocytes might be responsible for PPO synthesis in many tissues (Cerenius and Soderhall, 2004). Activation of PPO through limited proteolysis is facilitated by serine proteinases (Satoh 1999; Lee 1998; Lee 1998), also known as PPO-activating enzymes (ppA) (Cerenius and Soderhall, 2004), and is triggered by minute quantities of microbial carbohydrates, such as glycans, peptidoglycans, or lipopolysaccharids via binding to specific pattern-recognition molecules (Lee *et al.*, 2000; Yoshida *et al.*, 1996). Thus far, all characterized ppAs are produced as zymogens and become proteolytically active in the presence of such microbial products in complex with their recognition protein. Furthermore, to avoid excessive or premature activation of phenoloxidase, proteinase inhibitors also play an important role in tightly regulating the activity of ppAs (Hergenhahn *et al.*, 1987; Liang *et al.*, 1997).

1.4. The humoral immune response

Besides the cellular and the PPO-system that can be recruited very rapidly upon invasion of pathogens, insects also respond to infections by synthesizing an assortment of so-called anti-microbial peptides (AMPs) which possess both antibacterial and anti-fungal activities. AMPs work in concert to halt the infection process and to provide a short period of protection from further pathogenic invasion.

These peptides or polypeptides that often contain less than 150 to 200 amino acids are produced mainly in the insect's fat body, the equivalent to the mammalian kidney, and are secreted into the hemolymph. Smaller contributions are made by hemocytes and other tissues such as dial cells, Malphigian tubulus, and midgut (Dickinson *et al.*, 1988; Dunn *et al.*, 1994; Mulnix and Dunn, 1994; Russell and Dunn, 1991; Russell and Dunn, 1996). Depending on the organism considered, they are either constitutively present within secretory cells or induced at the time of infection (Hancock and Diamond, 2000). Since the isolation and characterization of the first inducible anti-bacterial peptide from an insect, the cecropin from bacterial-challenged diapausig pupae of the moth *Hyalophora cecropia* by Steiner and coworkers (Steiner *et al.*, 1981), more than 170 antimicrobial peptides have been found in insects. Most of these AMPs are of low molecular weight (<10 kDa) and have alkaline character, meaning that they have a positive net charge at physiological pH due to the presence of higher content in arginine and lysine. Furthermore, this cationic character can be reinforced by a C-terminal amidation.

AMPs can be tentatively classified into two broad classes based on sequence and structural similarities (Bulet *et al.*, 2004): i) cyclic and open-cyclic AMPs that contain one to four disulfide bridges and form β-hairpin-like, β-sheet, or a mixed α-helical/ β-sheet structure, and ii) linear peptides that are forming α-helical structures and are deprived of cysteine residues that can further be divided into two subfamilies on the basis of their higher content in proline and glycine, respectively.

In the former class, the defensins with three to four disulfide bridges represent the most widespread family of invertebrate AMPs with more than 70 members (Bulet *et al.*, 2004). Typically defensins are 36 to 46 amino acid long with few exceptions found in hymenopteran insects that possess a 12-amino acid C-terminal extension (Bulet *et al.*, 1999). Most of the insect defensins were isolated from the hemolymph of experimentally infected animals, whereas in scorpions, mollusks, and the termite, defensins are present in granular hemocytes of non-infected animals. Other than the vertebrate defensins which can be classified based on the cysteine disulfide pattern (Boman, 1995), the classification of the invertebrate especially insect defensins in subfamilies is based on their biological properties, anti-bacterial versus anti-fungal. Almost all insect defensins have the same cysteine pairing: Cys1-Cys4, Cys2-Cys5, and Cys3-Cys6 (Bulet *et al.*, 1999). Furthermore they display a high specificity in killing gram$^+$ bacteria through cell lysis, with rather limited activity on gram$^-$ bacteria and filamentous fungi. The only insect defensin found with four disulfide bridges is

the anti-fungal drosomycin in the fruitfly *Drosophila melanogaster* (Fehlbaum *et al.*, 1994; Michaut *et al.*, 1996), which shares striking similarities with anti-fungal peptides from plants (Fant *et al.*, 1998). So far only three other solely anti-fungal defensins have been described, namely heliomicin from *Heliothis virescens* (Lamberty *et al.*, 2001), termicin from *Pseudacanthothermes spiniger* (Lamberty *et al.*, 2001), and gallerimycin from *Galleria mellonella* (Schuhmann *et al.*, 2003).

The second class of anti-microbial peptides consists of linear amphipatic peptides with an α-helical structure rich in proline and glycine, respectively. Proline-rich peptides were first described in the *honey bee Apis mellifera* (Casteels *et al.*, 1989; Casteels *et al.*, 1990), but since then were also found in other hymenopteran, dipteran and hemipteran species. They vary from 15 to 39 residues in size and proline makes up more than 25% of the amino acid composition of these peptides. Furthermore, the proline residues are often associated in doublets and triplets with basic residues like arginine and lysine. A major subgroup of the proline-rich peptides are the short-chained apidaecins that were only found in Hymenoptera. So far 17 isoforms have been isolated which all show a highly conserved C-terminal octapeptide (Bulet *et al.*, 1999). Furthermore the octapeptide contains a Pro-Arg-Pro motif that is also found in other apidaecin-like AMPs (Bulet *et al.*, 1993; Chernysh *et al.*, 1996). Besides the apidaecins, a group of long-chain AMPs were isolated from hymenopteran species, the so-called abaecins (Casteels *et al.*, 1990; Rees *et al.*, 1997). They show structural similarities with two classes of anti-microbial peptides found in *D. melanogaster* and the silkworm *B. mori* (Hara and Yamakawa, 1995; Levashina *et al.*, 1995), namely metchikowins and lebocins, respectively. Similar to the PRP-motif present in apidaecin, these anti-microbial peptides share a highly conserved Pro-Phe-Asn-Pro motif in the C-terminal part. Thus, it was suggested that these evolutionary conserved sequences represent a functionally important domain (Bulet *et al.*, 1999). Indeed, studies of the biological activities of wild type and mutant variants of apidaecins indicated that the major activity of apidaecin-type peptides resides within in the C-terminal core (Taguchi *et al.*, 1996). Furthermore, Taguchi and colleagues showed that the proline and arginine residues are of great importance for the biological activity of apidaecins. As a general feature, most of the short-chain proline-rich peptides are active against gram$^-$ bacteria while gram$^+$ bacteria remain mostly unaffected. However, variability in antibacterial spectra und specificity exists that can be correlated to very subtle sequence modifications in the variable N-terminal part as observed for the isoforms of apidaecins (Casteels *et al.*,

1994; Taguchi *et al.*, 1996). Abaecins on the other hand are active against both gram$^-$ and gram$^+$ bacteria. Unlike defensins and cecropins which kill the microorganism within minutes through lytic, non-stereospecific mechanisms, killing of bacteria by apidaecins is found to take several hours. In addition, all D-enantiomers of the peptides are completely inactive, suggesting a reaction mechanism involving a stereospecific interaction of the peptide with a bacterial target (Casteels and Tempst, 1994).

Besides anti-microbial peptides rich in proline, several antibacterial polypeptides with high glycine content have been isolated from various insect species belonging to the Diptera, Lepidoptera and Hymenoptera families. Depending on the organism considered, they are either active against gram$^-$ or gram$^+$ or both. In the hymenopteran species *Apis mellifera* and *Bombus pascuorum* one such glycine-rich anti-microbial peptide, known as hymenoptaecin, is induced upon immunization (Casteels *et al.*, 1993; Rees *et al.*, 1997).

1.5. Recognition of pathogens and activation of the insect immune system

In order for the immune system to act specifically against invading pathogens it has to identify the intruder as non-self. The innate immune system uses a set of sensors, so-called pattern-recognition receptors (PRRs) that recognize conserved molecular patterns present on the pathogens surface and which are absent in the host itself (Janeway, 1989). Such pathogen associated molecular patterns (PAMPs) are peptidoglycans (PG) unique to bacterial cell walls, lipopolysaccharids (LPS) from the outer membrane of gram$^-$ bacteria, and β-1,3-glycans and β-1,3-mannans from fungal cell walls. Pattern-recognition receptors can be divided into three types: i) proteins circulating in the bloodstream, ii) endocytic receptors expressed on the cell surface, and iii) signaling receptors that can be expressed either on the cell surface or intracellularly (Medzhitov and Janeway, 1997). After recognition, the PRRs stimulate immune response by activating cellular reactions, including phagocytosis, and humoral reactions, such as activation of proteolytic cascades in the hemolymph and intracellular signaling pathways in immune-responsive tissues.

Lipopolysaccharids derived from different groups of Gram-negative bacteria have a common basic structure, consisting of a covalently bound lipid component, termed

lipid A, and a hydrophilic heteropolysaccharide. Lipid A provides the anchor that secures the molecule within the membrane, while the polysaccharide component interacts with the external environment, including the defenses of the animal or plant host species. Lipid A is a unique and distinctive phosphoglycolipid, the structure of which is highly conserved among bacterial species. LPS are recognized by the host defense through so-called lectins or immuno lectins (IML), which have been isolated from hemolymph of various insects (Chen *et al.*, 1993; Koizumi *et al.*, 1999; Shin *et al.*, 2000; Yu and Kanost, 2000). Lectins participate in the clearing from the hemolymph probably by triggering phagocytosis of hemocytes upon binding of the lectins to bacterial surfaces (Gillespie *et al.*, 1997). Furthermore there is evidence that lectins play a role in the activation of the prophenoloxidase cascade (Yu and Kanost, 2000).

Peptidoglycan, the major pattern molecule, shows large heterogeneity both in composition and in structure among bacterial species. It consists of long carbohydrate chains of alternating N-acetylglucosamine and N-acetylmuramic acid residues that are connected via stem peptides bound to the lactic acid group on N-acetylmuramic acid. Gram$^-$ bacteria have cell walls with one to three layers of peptidoglycans, whereas gram$^+$ bacteria can have an up to 70-layer thick and exposed PG wall. There are two major types of of peptidoglycans found in bacterial cell walls: the Lys-type found in gram$^+$ bacteria, and the diaminopilemic acid-type (DAP) in gram$^-$ bacteria. A protein recognizing peptidoglycans was first isolated from silk moth (*Bombyx mori*) hemolymph based on the affinity to bacterial peptidoglycans (Yoshida *et al.*, 1996). Since then major contributions on characterization of peptidoglycan recognition proteins (PGRPs) are based on genetically and biochemical studies on the fruit fly *D. melanogaster*. In Drosophila, PGRP genes are expressed in immune-reactive tissues such as hemocytes, the fat body, the gut, and the epidermis (Werner *et al.*, 2000). All PGRPs identified so far have a C-terminal PGRP-domain that it highly conserved from insects to mammals (Kurata, 2004). PGRPs are grouped into two classes: short PGRPs (PGRP-S) are encoded by short transcripts, and long PGRPs (PGRP-L) are encoded by long transcripts. Proteins of the former class all have N-terminal signal sequences, and thus, being secretory proteins. The other class code for long proteins with potential transmembrane segments and a variable intracellular part in addition to the conserved PGRP domain. The expression of most PGRP-S is upregulated in response to bacterial infection, whereas the longer PGRPs are expressed constitutively, with

few exceptions (Werner *et al.*, 2000). Genetic screens for *D. melanogaster* mutants deficient in immune functions identified several PGRPs that can be directly correlated to two signaling pathways that regulate the expression of different anti-microbial peptides (Choe *et al.*, 2002; Michel *et al.*, 2001), known as Toll and *imd* pathways. Toll was shown to predominantly activate the expression of drosomycin in response to fungal and of gram$^+$ bacteria infections (Lemaitre *et al.*, 1996). Mutations in the gene coding for PGRP-SA resulted in an impaired resistance against gram$^+$ bacteria, while mutant flies were as resistant as wild type flies to gram$^-$ bacteria and to one fungus. On the other hand, genetic screening for mutants that showed a similar phenotype as *imd* mutants, i.e. they do not synthesize anti-microbial peptides such as dipericin, cecropin, or defensin, localized a mutation to the PGRP-LC locus. Furthermore, these mutants were sensitive to gram$^-$ but not to tested gram$^+$ bacteria (Gottar *et al.*, 2002). A second activator of the *imd* pathway was identified in PGRP-LE, which specifically activates this signal transduction cascade upon overexpression, while the Toll pathway was not activated (Takehana *et al.*, 2002). In addition to its role in *imd* activation, Takehana and colleagues demonstrated that the overexpression of PGRP-LE also stimulated the proteolytic activation of the prophenoloxidase cascade in the hemolymph. The ability of PGRP to activate the PPO-cascade was shown early on by in vitro experiments of purified PGRP of *B. mori* (Yoshida *et al.*, 1996).

As mentioned above, there are two separate pathways regulating the genes involved in humoral insect immunity (Hultmark, 2003), one of them being the Toll pathway. The Toll protein acts as a membrane-bound receptor, which activates Dif, a member of the Rel family which are similar to the human transcription factor NF-κB. At the resting stage Dif forms an inactive complex with Cactus, an IκB-like inhibitor. Upon activation of Toll, a relay of phosphorylation involving several kinases leads to the proteosome-dependent degradation of the inhibitor. Dif then translocates into the nucleus where it participates in the transcriptional activation of target genes such as anti-microbial peptides. The second system for activation of anti-microbial peptide genes is the *imd* pathway. It leads to the activation of the Rel factor Relish via a series of kinases. Within seconds after an infection, Relish is cleaved into two parts. The N-terminal REL-68 fragment translocates into the nucleus where it binds to κB-like enhancer elements in the promoters of target genes. Activation of this pathway results in a general humoral response comprising most anti-microbial peptides.

Chapter II

Identification and characterization of c-type lysozymes from A. mellifera

2.1. Introduction

Probably the most universal antibacterial peptide known is lysozyme, also known as muramidase, which was first discovered by Alexander Fleming in 1922. Lysozyme is widely distributed among eukaryotic and prokaryotic organisms. The enzyme hydrolyses the β-1,4-glycosidic linkage between altering N-acetylglucosamine (NAG) and N-acetylmuramic acid (NAM) residues in the peptidoglycan (PGN) layer of bacterial cell walls, resulting in cell lysis (Fig. 2-1).

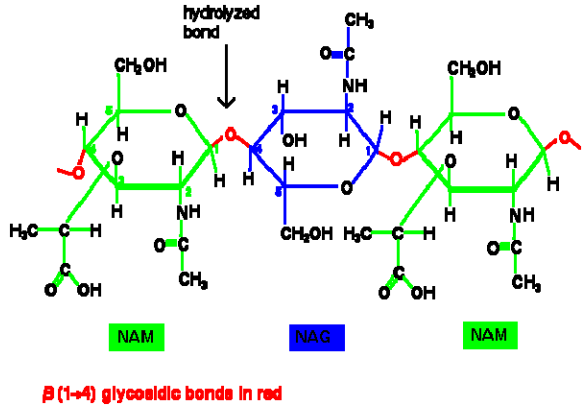

Fig. 2-1: Schematic presentation of the hydrolytic site in the NAM-NAG backbone of peptidoglycan

Lysozyme can be classified into six types according to physico-chemical properties such as primary structure and the molecular mass, as well as the biological sources in which it is found, namely chicken (c-type), which includes stomach lysozymes and calcium-binding lysozymes, goose (g-type), plants, bacteria, phages (p-type), and invertebrate lysozymes (i-type) (Beintema and Terwisscha van Scheltinga, 1996; Holtje, 1996; Hultmark, 1996; Jolles and Jolles, 1975; Prager and Jolles, 1996; Qasba and Kumar, 1997).

The structure of the lysozyme extracted from the chicken egg-white was the first ever to be solved for an enzyme (Phillips, 1966), and has become a favorite subject for research because of its abundance and ease of crystallization. Two carboxylic acid residues in chicken egg-white lysozyme, Glu35 and Asp52, were identified to be involved in the catalytic hydrolysis which led to the proposed mechanism for c-type lysozymes by Phillips (illustrated in Fig. 2-2). Both residues are in vicinity of hexose 4 and 5 of the hexasaccharide substrate which occupies the binding site. Glutamic acid 35 acts as a general base by transferring a proton to the O1 position which results in an oxonium ion intermediate. Ionized carbons are normally very unstable, but the attraction of the negative charged carboxyl group of

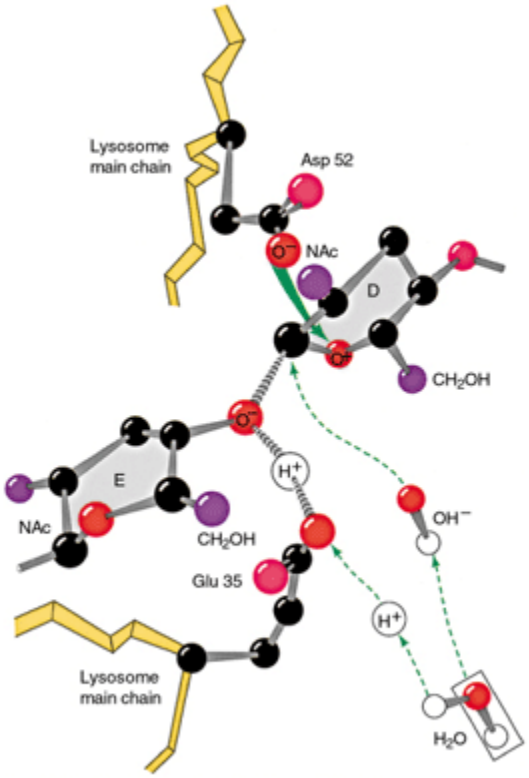

From D. Voet and J. G. Voet, *Biochemistry*, 2d ed., copyright © 1995, John Wiley & Sons, Inc. Reprinted by permission of John Wiley & Sons, Inc. Copyright 1999 John Wiley and Sons, Inc. All rights reserved.

Fig. 2-2: Illustration of the catalytic mechanism of chicken-type lysozyme

aspartic acid 52 stabilizes the intermediate long enough for a hydroxide ion to unit with the carbon which eventually breaks the polysaccharide chain. The hydrogen ion left over replaces that lost by Glu35.

C-type lysozymes are also found in insects as shown by the sequences from a variety of species in the orders Lepidoptera, Orthoptera, and Diptera, that have been characterized (Hultmark, 1996). It was hypothized that lysozyme plays a dual role in insects: i) in a digestive manner to break down ingested bacteria in the gut, and ii) as a defense response against pathogens that enter the hemocoel (Ursic Bedoya *et al.*, 2005). Lysozyme function has been widely described in species that ingest or harbor bacteria in the digestive tract throughout their life cycles, such as *Musca domestica* and *Drosophila melanogaster*, and thus were characterized as digestive enzymes (Daffre *et al.*, 1994; Lemos and Terra, 1991; Regel *et al.*, 1998). Furthermore, it was shown that the enzyme in these insects is solely expressed in tissues of the gut. On the other hand, lysozymes have been implicated in the antimicrobial defense of insects for over 40 years (Malke, 1965; Mohrig and Messner, 1968). Lee and Brey (Lee and Brey, 1995) demonstrated that lysozyme is expressed in epidermal cuticle tissue and conclude to be an important first line of defense. In several lepidopteran species such as *B. mori*, *H. virescens* and *M. sexta*, production of lysozyme occurs in the fat body as primary source in which expression of the enzyme is induced in response to bacterial challenge (Engstrom *et al.*, 1985; Lockey and Ourth, 1996; Morishima *et al.*, 1995; Mulnix and Dunn, 1994). In the hymenopteran species *A. mellifera* (honey bee) lytic activity was observed in the venom which was attributed to lysozyme (Mohrig and Messner, 1968), however, isolation and further characterization of the enzyme from other tissues failed. With the progress in sequencing of the honey bee genome new data become available which allows the search and identification of genes coding for homologous proteins found in other organism. The presented work describes the *in silico* identification of lysozyme-encoding genes in *A. mellifera* and further characterization of the enzyme.

2.2. Methods

2.2.1. Database searches

Blast searches of the *honey bee* genome assembly database (as of 2005/01/20) were done with the protein sequence of *Drosophila melanogaster* lysozyme D (gi:48429242) on the Human Genome Sequencing Center server (http://www.hgsc.bcm.tmc.edu/projects/honeybee/) using the tBLASTn search algorithm (Altschul *et al.*, 1997).

2.2.2. Sequence alignments

Related sequences were aligned with Clustal-X 1.8 software designed for multiple-sequence alignment (Jeanmougin *et al.*, 1998). Aligned sequences were subjected to phylogenetic analysis using the neighbor-joining method implemented within Clustal X. Branch stability was tested by bootstrap analysis (1000 repetitions) (http://www.ch.embnet.org/software/BOX_form.html). Furthermore, dendrograms were drawn using the Phylodendron server (http://iubio.bio.indiana.edu/treeapp/treeprint-form.html).

2.2.3. Sequence analysis

The amino acid sequences of lysozymes from *A. mellifera* were inferred from the genomic DNA sequence using the TRANSLATE program available in the GCG package 10.3 (http://www.accelrys.com/). Transcription factor binding sites in the upstream part of gene were identified using software TFSEARCH (http://www.cbrc.jp/research/db/TFSEARCH.html). Prediction of the TATA-box consensus sequences was done using software HCtata (http://l25.itba.mi.cnr.it/~webgene/wwwHC_tata.html). Physico-chemical analysis of protein sequences were carried out using the ProtParam tool (Gasteiger *et al.*, 2005) on the EXPASY proteomics server (http://www.expasy.org/). Signal peptidase cleavage sites were predicted using the SignalP 3.0 server (http://www.cbs.dtu.dk/services/SignalP/) (Bendtsen *et al.*, 2004). SignalP 3.0 incorporates a prediction of cleavage sites and a signal peptide/non-signal peptide prediction based on a combination of several artificial neural networks and hidden Markov models.

2.2.4. Comparative protein modeling

3-D models of lysozyme 2 from *A. mellifera* were generated based on homology-modeling (Guex and Peitsch, 1997; Peitsch, 1995; Schwede *et al.*, 2003) using the SWISS-MODEL server (http://swissmodel.expasy.org//SWISS-MODEL.html).

2.3. Results

2.3.1. Identification of lyszozyme-encoding genes in the genome of *A. mellifera*

In recent years much effort was made to sequence the genome of the honey bee *Apis mellifera*. The genome assembly of the genome is accessible via the internet and supports an online-based BLAST search for comparison against homologous sequences found in other organisms. Here, the protein sequence of *Drosophila melanogaster* lysozyme D was used to search for genes coding for lysozyme in the honey bee. The result of this query is shown in figure 2-3. Two proteins were identified that share 30% of identical amino acids in respect to *D. melanogaster* lysozyme D. If amino acids are taken into account that share similar properties the homology increases to 45%.

Both genes are located on chromosome 13. Further analysis of the genomic region (Fig. 2-4) revealed that both of the lysozymes-encoding genes are located within a region of 2000 nucleotides and are arranged in tandem. The upstream regions do not share any significant similarities. Furthermore, no binding sites for a member of the NF-κB-family of transcription factors were found upstream of the corresponding lysozyme genes. Of further interest is the absence of any introns within either gene. Based on the order of arrangement, the first gene (highlighted in blue) will hereby be defined as *lyz1* encoding for lysozyme 1 (Lys-1), whereas the second gene (highlighted in green) will be defined as *lyz2* encoding for lysozyme 2 (Lys-2) of *A. mellifera*.

```
>gnl|Amel_2.0|Group13.6
          Length = 772051

Score = 76.3 bits (186), Expect = 4e-14
Identities = 41/135 (30%), Positives = 62/135 (45%), Gaps = 2/135 (1%)
Frame = -1

Query: 7     LVALACAAPAFGRTMDRCSLAREMSNLGVPRDQLARWACIAEHESSYRTGVVGPENYNGS 66
              +VA+        R + +C   +E+    +PR  ++ W C+ + ES   T +V       S
Sbjct: 96625 IVAILIDNHVEARILTQCEAVQELQKAQIPRTYISNWVCLMQSESGMNTRLVTGPKTASS 96446

Query: 67    NDYGIFQINDYYWCAPPSGRFSYNECGLSCNALLTDDITHSVRCAQKVLSQQGWSAWSTW 126
                +GIFQIN   WC   S   S   C   C     DDI   + CA+K+ + +G+ AW  W
Sbjct: 96445 YSFGIFQINSAKWC---SRGHSGGICNKRCEDFADDDIRDDIECAKKIQAMEGFKAWDGW 96275

Query: 127   -HYCSGW-LPSIDDC 139
                 C    LP+I +C
Sbjct: 96274 MKKCKNKPLPNIGNC 96230


Score = 73.9 bits (180), Expect = 2e-13
Identities = 37/124 (29%), Positives = 57/124 (45%), Gaps = 2/124 (1%)
Frame = -2

Query: 18    GRTMDRCSLAREMSNLGVPRDQLARWACIAEHESSYRTGVVGPENYNGSNDYGIFQINDY 77
              G+ +  C + +++    + R  ++ W C+ + ES   T ++       S  YGIFQIN
Sbjct: 95223 GKILTECEIVQQLQQARISRSDISSWICLMQSESGLNTNLITGPKTASSYSYGIFQINSA 95044

Query: 78    YWCAPPSGRFSYNECGLSCNALLTDDITHSVRCAQKVLSQQGWSAWSTW--HYCSGWLPS 135
               WC   S   S   C   C     DDI   + CA+K+ S +G+ AW  W  +     LP+
Sbjct: 95043 KWC---SRGHSGGICKKRCEDFANDDIRDDIACAKKIQSLEGFKAWDGWVKNCKKKPLPN 94873

Query: 136   IDDC 139
              I  C
Sbjct: 94872 IQKC 94861
```

Fig. 2-3: BLAST search of lysozyme-encoding genes in the genome of *A. mellifera*

Blast searches of the honey bee genome assembly database (as of 2005/01/20) were done with the protein sequence of *Drosophila melanogaster* lysozyme D (gi:48429242) on the Human Genome Sequencing Center server using the tBLASTn search algorithm (Altschul et al., 1997).

```
   1 gtataactcg cctgcaattt ctactaataa agttttaaaa gattacaggc atcatttcct
  61 taaattgctg cgaattagtt aattggaagc ggaaattagc tcaaatatta attgttgtag
 121 agaaataaca attattcgta atccatgtcc aatcttatcg gcgcttctcg gtcgtaaaac
 181 gaaaaaagtt ttaaaactta tacgagtaaa aaaagcaatt tatcgtgaag aaaaagatca
 241 aattgattgg aaatttatcg agtcaacctg tctcgaagac gactggcgcc aaattgccta
 301 taaaagaaga aagaacgaag aaacgagaca acagacatta tttccggcca cgcagtgcct
 361 aggaaattat aatttatcag tgaagcttaa tgacgtcgtg cgtcgtttgt acgacacaca
 421 gtatggcaca aacggcgaag taagtcgcgt gatatttaag tgcgaatctt tatattacgc
 481 cgtaattgca cgcgataaag ttggaacatc attcgaccct ggttcatttc tcgatcaata
 541 aaggaattaa tcttaaagga aggATGATCA AACTGTGCTT AATTCTCCCG GCTATTGTGG
 601 CTATTTTGAT CGACAACCAC GTGGAGGCGA GGATTCTGAC TCAATGCGAA GCCGTGCAAG
 661 AGCTTCAAAA AGCTCAAATC CCGAGAACCT ACATCAGCAA CTGGGTCTGC CTGATGCAGA
 721 GCGAGAGCGG AATGAACACA CGGTTGGTCA CTGGTCCAAA AACAGCCTCG AGCTACAGTT
 781 TCGGAATCTT CCAGATCAAC AGCGCGAAAT GGTGCTCCAG GGGGCACAGC GGAGGGATAT
 841 GCAACAAACG TTGCGAGGAT TTCGCGGACG ACGATATAAG GGACGATATC GAATGCGCCA
 901 AGAAGATTCA GGCTATGGAG GGATTCAAAG CGTGGGACGG TTGGATGAAG AAATGCAAGA
 961 ACAAGCCGTT GCCGAATATT GGAAACTGCA AACGACGAAA ACGATGGTTG GAAATATTAT
1021 TGGAATTGGA GCAATAAaat ttcttcgtcg ttgaattatc gggtatcggt taattaacga
1081 aaattgtaaa ttacaaatat gatgtaagat gattgttcgt acatcgccat cattcgataa
1141 ttaattgttc aatagagatg aaaatataaa gcgttttatc tattattttc ccaatattct
1201 tacttgagct tgaaataata ccgcctcttt gtgaaaagag ttgaatgttt acaatttcgc
1261 tggttactca actcttatcg gctctcctta atatcatttt ttacgataat attaaaatgt
1321 tcacagcgac aacaaagttc gcgaaactat ctatcgatat ttgttatagc ccaatgatta
1381 gatactttcg aagctaatat tatcttgaat aattaacctc tcgtgtcagt ttgaaagact
1441 ttagagggca ataactaatc tgacaagtcg tatagacgaa cgtaaaaata ttacatgcct
1501 cttgtggcga tgaacaatcc cgtcttcaat tacgcgttga aaggtacaat tcaaattaat
1561 ttcaagttaa ttgaataata ttcacccggc gggaataaac ctcgaaataa aggcgaaaat
1621 aaagatgtac ggtacggaac aaagcgaaca ttcatgttgt cgaaccgttt cgttccgttc
1681 cgtttcatga tgacaattag aaaaattaca atttatcgtg caatttattg cgacgcgatt
1741 tattgcatac acagaatcga tcgacagtat aacataacca gcagcgtggc aagtcgtctc
1801 tattacttaa gacgaattct cgccacggtg catacagtaa caggcgatag tgtttcgcgt
1861 cgaaacgatc gttcgatctg tcttattatt atagatcgat aacgggtcgg catcgaggaa
1921 caaacgtaag agaagATGGA GAAATCGTGG CTGATATCGC TGTTCCTCGT CGTTCTGATC
1981 GACGGCCGGG TGGCAGGCAA AATTCTAACG GAATGCGAAA TCGTGCAACA ACTCCAACAA
2041 GCTAGAATCT CAAGGAGCGA CATAAGCAGT TGGATCTGTT TGATGCAGAG CGAGAGCGGA
2101 TTGAACACGA ATTTGATAAC TGGGCCGAAG ACGGCCTCCA GCTACAGCTA CGGGATCTTC
2161 CAAATTAACA GCGCCAAGTG GTGTTCCAGG GGACATAGCG GGGGTATTTG CAAAAAACGT
2221 TGCGAGGATT TCGCGAATGA CGATATCAGA GACGATATCG CGTGCGCTAA GAAGATTCAA
2281 AGTTTGGAAG GGTTCAAGGC GTGGGATGGT TGGGTGAAGA ATTGCAAAAA AAAGCCTTTG
2341 CCGAATATAC AGAAATGCTC ACGATGAtga cagtatatag ttttatcgaa gccagtacct
2401 tgaaacgagg taaatagaaa tatttttgtg aaacaaatct ggagatctct ttttaaaaaa
2461 aagagaaatt ttttgaattt aagaggaaaa aattgtaaag tatcttgatt gaaatgacga
2521 tatattacat ttttcaggtg gattttccaa agacgtggta aaaataatta ataattaaac
2581 attggacctc gcctgaattt tcatatatcg attctcatta tgtgtttctt ttcgaagaaa
2641 aaaaaatcgt tttcgtaatt ttgattttta aaatctgtta ataataataa tccttattgt
2701 aagtgaatca ttagctgttt tttatcgata ttgaaaaaag gaaaaaagaa attctctact
2761 agtcttccac tctttctctt cttcaccaat cttgatgatt ttaatataca aattttattt
2821 gttccggaaa tcatattgat cctcgataaa gttaaatgat gttatttatc aaaccaaaga
```

Fig. 2-4: Sequence of the genomic region harboring lysozyme-encoding genes

Chromosome 13 of *A. mellifera* harbors both genes encoding for lysozymes. Genomic regions harboring lysozyme-encoding genes were identified by BLAST search of the assembled *A. mellifera* genome. Blue and green labeled sequences represent the coding regions for lysozyme 1 and lysozyme 2, respectively. Underline: transcription start site, double underline: TATA-box

2.3.2. Protein sequence and physico-chemical properties of *A. mellifera* lysozymes

The amino acid sequences of both lysozymes were obtained by translation of the DNA sequences (Fig. 2-5). Lys-1 consists of 157 amino acids, whereas Lys-2 is slightly shorter (143 amino acids), lacking the C-terminal extension found in Lys-1 (Fig. 2-6). Both proteins share a sequence similarity of 90% with 78% of identical amino acid residues. Lys-1 and Lys-2 have 27 and 21 strongly basic amino acids (K and R), respectively, accounting for nearly 15% of the total number of residues. This confers the basic nature of these proteins with an estimated isoelectric point of 8.74 and 9.07. The N-terminus of each protein is hydrophobic, suggesting the presence of a signal peptide, with a predicted signal peptidase cleavage site between A22 and R23 in Lys-1 and G21 and K22 in Lys-2 (SignalP v3.0). Cleavage of the signal peptide produces potentially active peptides of 14.9 and 13.4 kDa with an isoelectric point of 8.95 and 9.09, respectively.

A) Lysozyme 1

```
   1  CCTGGTTCATTTCTCGATCAATAAAGGAATTAATCTTAAAGGAAGGATGATCAAACTGTG   60
   1                                                M  I  K  L  C   5

  61  CTTAATTCTCCCGGCTATTGTGGCTATTTTGATCGACAACCACGTGGAGGCGAGGATTCT   120
   6   L  I  L  P  A  I  V  A  I  L  I  D  N  H  V  E  A  R  I  L   25

 121  GACTCAATGCGAAGCCGTGCAAGAGCTTCAAAAAGCTCAAATCCCGAGAACCTACATCAG   180
  26   T  Q  C  E  A  V  Q  E  L  Q  K  A  Q  I  P  R  T  Y  I  S   45

 181  CAACTGGGTCTGCCTGATGCAGAGCGAGAGCGGAATGAACACACGGTTGGTCACTGGTCC   240
  46   N  W  V  C  L  M  Q  S  E  S  G  M  N  T  R  L  V  T  G  P   65

 241  AAAAACAGCCTCGAGCTACAGTTTCGGAATCTTCCAGATCAACAGCGCGAAATGGTGCTC   300
  66   K  T  A  S  S  Y  S  F  G  I  F  Q  I  N  S  A  K  W  C  S   85

 301  CAGGGGGCACAGCGGAGGGATATGCAACAAACGTTGCGAGGATTTCGCGGACGACGATAT   360
  86   R  G  H  S  G  G  I  C  N  K  R  C  E  D  F  A  D  D  D  I   105

 361  AAGGGACGATATCGAATGCGCCAAGAAGATTCAGGCTATGGAGGGATTCAAAGCGTGGGA   420
 106   R  D  D  I  E  C  A  K  K  I  Q  A  M  E  G  F  K  A  W  D   125

 421  CGGTTGGATGAAGAAATGCAAGAACAAGCCGTTGCCGAATATTGGAAACTGCAAACGACG   480
 126   G  W  M  K  K  C  K  N  K  P  L  P  N  I  G  N  C  K  R  R   145

 481  AAAACGATGGTTGGAAATATTATTGGAATTGGAGCAATAAAATTTCTTCGTCGTTGAATT   540
 146   K  R  W  L  E  I  L  L  E  L  E  Q  *

 541  ATCGGGTATCG  551
```

B) Lysozyme 2

```
   1  GAACAAACGTAAGAGAAGATGGAGAAATCGTGGCTGATATCGCTGTTCCTCGTCGTTCTG   60
   1                      M  E  K  S  W  L  I  S  L  F  L  V  V  L   14

  61  ATCGACGGCCGGGTGGCAGGCAAAATTCTAACGGAATGCGAAATCGTGCAACAACTCCAA  120
  15  I  D  G  R  V  A  G  K  I  L  T  E  C  E  I  V  Q  Q  L  Q   34

 121  CAAGCTAGAATCTCAAGGAGCGACATAAGCAGTTGGATCTGTTTGATGCAGAGCGAGAGC  180
  35  Q  A  R  I  S  R  S  D  I  S  S  W  I  C  L  M  Q  S  E  S   54

 181  GGATTGAACACGAATTTGATAACTGGGCCGAAGACGGCCTCCAGCTACAGCTACGGGATC  240
  55  G  L  N  T  N  L  I  T  G  P  K  T  A  S  S  Y  S  Y  G  I   74

 241  TTCCAAATTAACAGCGCCAAGTGGTGTTCCAGGGGACATAGCGGGGGTATTTGCAAAAAA  300
  75  F  Q  I  N  S  A  K  W  C  S  R  G  H  S  G  G  I  C  K  K   94

 301  CGTTGCGAGGATTTCGCGAATGACGATATCAGAGACGATATCGCGTGCGCTAAGAAGATT  360
  95  R  C  E  D  F  A  N  D  D  I  R  D  D  I  A  C  A  K  K  I  114

 361  CAAAGTTTGGAAGGGTTCAAGGCGTGGGATGGTTGGGTGAAGAATTGCAAAAAAAAGCCT  420
 115  Q  S  L  E  G  F  K  A  W  D  G  W  V  K  N  C  K  K  K  P  134

 421  TTGCCGAATATACAGAAATGCTCACGATGATGACAGTATATAGTTTTATCGAAGCCAGTA  480
 135  L  P  N  I  Q  K  C  S  R  *

 481  CCTTGAAACGAGGTAAATAGA  501
```

Fig. 2-5: Nucleotide and amino acid sequences of *A. mellifera* lysozymes

Shown are the nucleotide and inferred amino acid sequences of lysozyme 1 (A) and lysozyme 2 (B). The amino acid sequences were inferred from the genomic DNA sequence using the TRANSLATE program (GCG package v10.3). Arrows show possible signal peptidase cleavage sites as predicted by SignalP 3.0. Predicted hydrophobic signal peptides are underlined. * STOP codon.

Fig. 2-6: Amino acid alignment of *A. mellifera* lysozymes

Amino acid sequences of A. mellifera lysozymes were aligned with Clustal-X 1.8 software (Jean-Mougin et al., 1998}. The sequence alignment was edited using BOXSHADE 3.21. Identical and similar amino acids are boxed in black or grey, respectively.

2.3.3. Phylogenetic analysis of *A. mellifera* lysozymes

To date, lysozymes have been identified in many organisms from eubacteria to vertebrates. Thus, the obtained amino acid sequences of Lys-1 and Lys-2 allows further characterization of these proteins in respect to their relationship to lysozymes from other organisms. A protein sequence alignment between *A. mellifera* and other

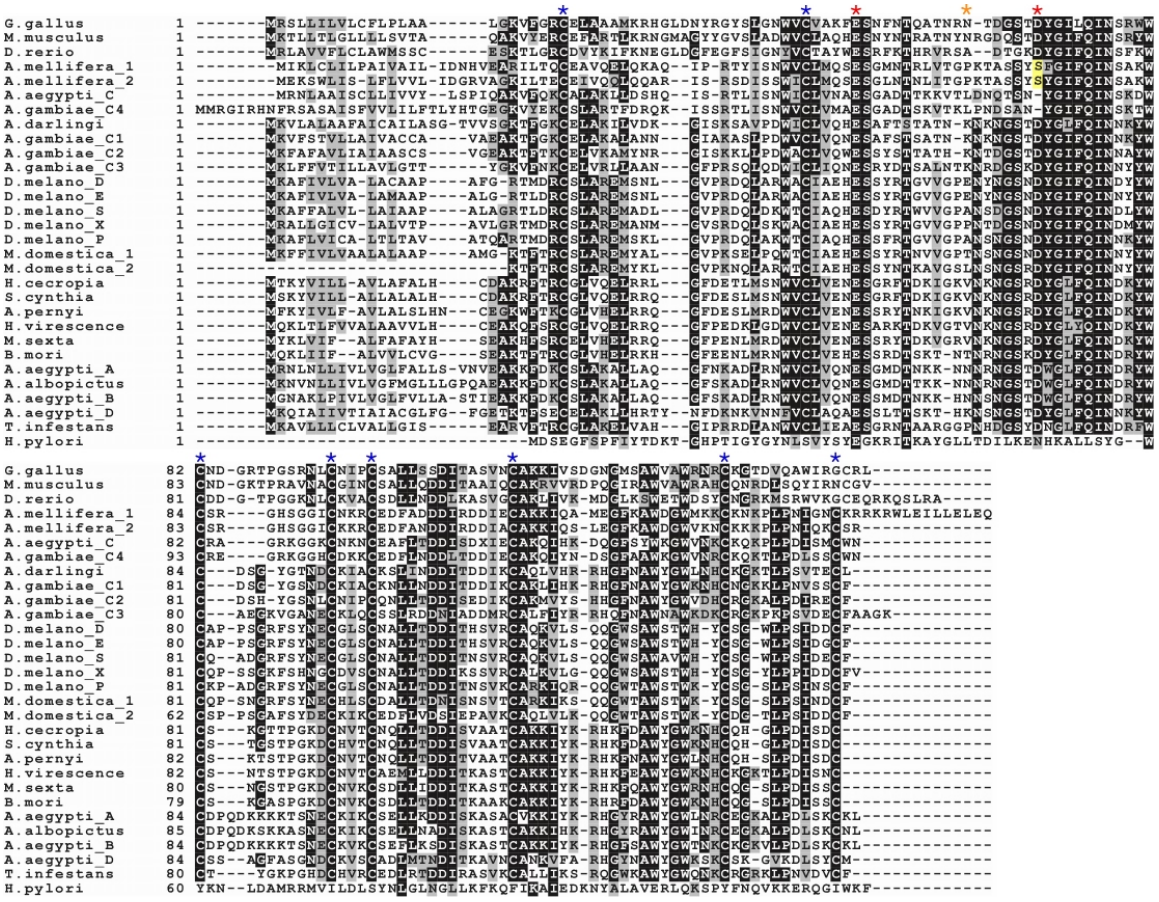

Fig. 2-7: Alignment of *A. mellifera* lysozymes with other selected c-type lysozyme sequences

Alignments were made using Clustal-X 1.8 software designed for multiple-sequence alignment (Jean-Mougin et al., 1998). Gaps used to maintain optimal alignment are indicated by dashes. Sequence alignments were edited using BOXSHADE 3.21. Identical and similar amino acids are boxed in black and grey, respectively. Blue and red stars indicate conserved cysteine and catalytic residues of c-type lysozymes, respectively. Orange star indicates important asparagine. D52S substitution in *Apis mellifera* is denoted by yellow box. The sequences used in the alignment are: *G. gallus* (gi:45384212), *M. musculus* (gi:8393739), *D. rerio* (gi:23308613), *A. aegypti* A, B, C and D (gi:12044523, gi:51702892, gi:42763735, gi:18568288); *A. albopictus* (gi:20159661); *A. gambiae* C1, C2, C3 and C4 (gi:62997710, gi:49089569, gi:49089577, gi:62997712); *A. darlingi* (gi:2198832); *A. pernyi* (gi:85687538); *B. mori* (gi:567099); *D. melanogaster* D, E, S, X and P (gi:48429242, gi:12644241, gi:12644242, gi:12644243, gi:266492); *H. cecropia* (gi:159204); *H. virescence* (gi:4097239); *M. domestica* 1 and 2 (gi:33504660, gi:33504658); *M. sexta* (gi:7327646); *S. cynthia* (gi:12082298); *T. infestans* (gi:32454476); *H. pylori* (gi:15723741)

lysozymes from selected species was performed using the software Clustal-X (Fig. 2-7). The sequence alignment indicates that both lysozymes belong to the chicken c-

type family, with eight highly conserved cysteine residues (blue stars) at positions 28, 49, 84, 93, 97, 111, 131, 142 in Lys-1 and positions 27, 48, 83, 92, 96, 110, 130, 141 in Lys-2. Furthermore, the highly conserved active site glutamic acid (1st red star), which has been shown to be essential for the enzyme's catalytic activity (Malcolm *et al.*, 1989), is also well preserved in *A. mellifera* at position 32 of mature

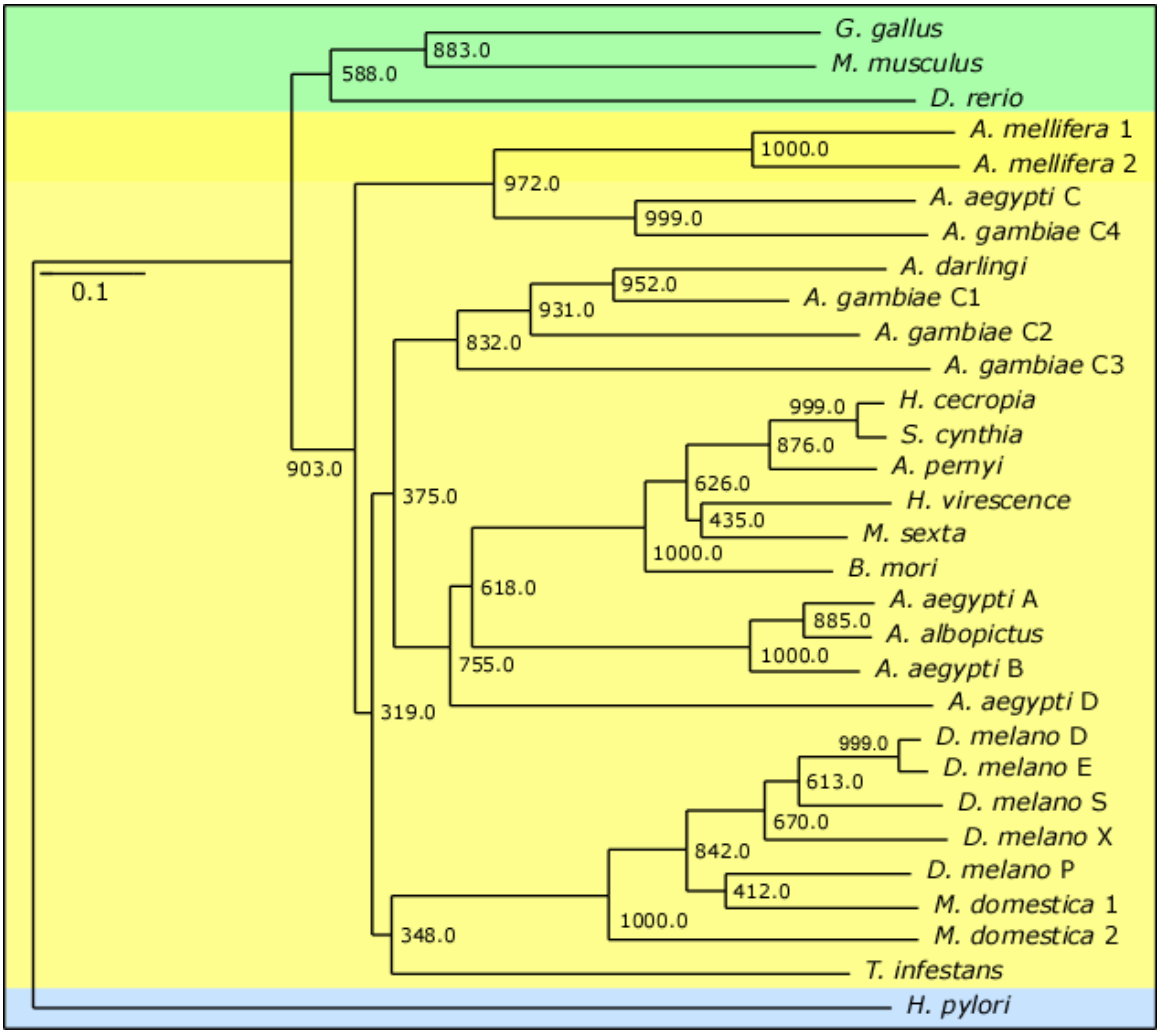

Fig. 2-8: Phylogenetic analysis of c-type lysozymes

A rooted phylogenetic tree was constructed with aligned amino acid sequences of lysozymes from selected organisms using neighbor joining. Branch stability was tested by bootstrap analysis (1000 repetitions). Lysozyme from *H. pylori* (eubacteria) was set as outgroup. Green, yellow and blue boxes represents the phyla chordata, arthropoda (class: insecta) and eubacteria, respectively.

Lys-1 and Lys-2. On the other hand, an important aspartic acid in the active site (2nd red star) that helps to stabilize a substrate intermediate during catalysis is replaced

by a serine residue in the lysozymes of *A. mellifera* (S72 and S71, highlighted in yellow). Furthermore, the active site asparagine (orange star) that in concert with the aspartic acid helps to distort the pyranose ring of N-acetymuramic acid into the reactive half-chair conformation is lacking as well. This is very interesting since almost all c-type lysozymes characterized to date have both residues conserved at the corresponding positions, with the exceptions of *Aedes aegypti* C and *Anophilis gambiae* C4. On the basis of the sequence alignment, a rooted phylogentic tree was constructed using the neighbor-joining method (Fig. 2-8), using the lysozyme of *H. pylori* as outgroup, if we start with the assumption that bacterial lysozymes respresent the most ancient ancestors of this family of proteins. The data suggests an early divergence of the lysozymes of *A. mellifera* from a common ancestor of insects, building a defined subgroup together with the two lysozymes of *Aedes aegypti* and *Anophilis gambiae* mentioned above. Furthermore, Lys-1 and Lys-2 have evolved from one common ancestor, probably through gene duplication which is supported by the finding that their corresponding genes are arranged in tandem (2.3.1).

2.3.4. Comparative 3D-models of *A. mellifera* lysozymes

C-type lysozymes are the preferred model enzymes for structural analysis with over a thousand entries in the Protein Data Bank (PDB). The 3D structure of lysozyme extracted from the chicken egg white was the first structure ever to be determined for an enzyme (Phillips, 1966). Since then the protein structures of lysozymes from various organisms ranging from phage to human have been obtained by NMR and X-ray crystallography. Based on the sequence similarity of *A. mellifera* lysozymes with other c-type lysozymes it is possible to generate 3D-models of both proteins. The template structure is used as scaffold to model the structure of the target sequence. The published 3D structure of the lysozyme from the silkmoth *Bombyx mori* (Matsuura *et al.*, 2002), which shares the highest sequence similarity of all available structures with *A. mellifera* lysozymes (36%), was used as template for the construction of a 3D-model of Lys-1 and Lys-2 (Fig. 2-9 and Fig. 2-10, respectively).

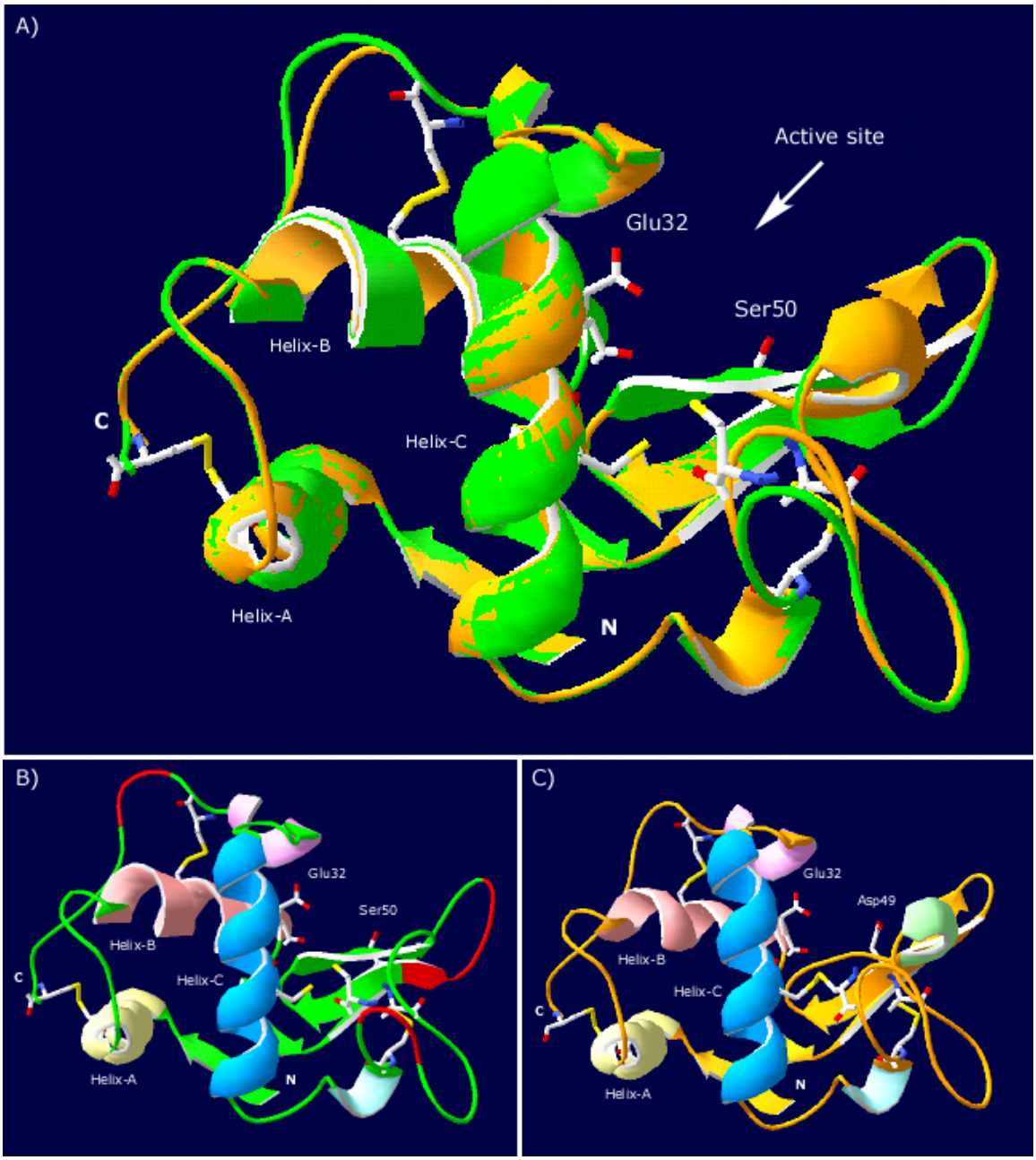

Fig. 2-9: Ribbon model of *A. mellifera* Lys-1

The model was generated by sequence alignment using SWISS-MODEL. The 3D-structure of *B. mori* (1gd6) was used as template. A) The model of Lys-1 (green) superimposed onto the 3D-structure of *B. mori* (orange) is shown. The highly conserved cysteines and active site glutamic acid (Glu32) as well as the Ser50 substitution are displayed; B) Isolated model of Lys-1. Regions of the model that appear in red have been completely rebuild; C) 3D-structure of *B. mori* lysozyme. The highly conserved cysteines and active site Glu32 and Asp49 are displayed.

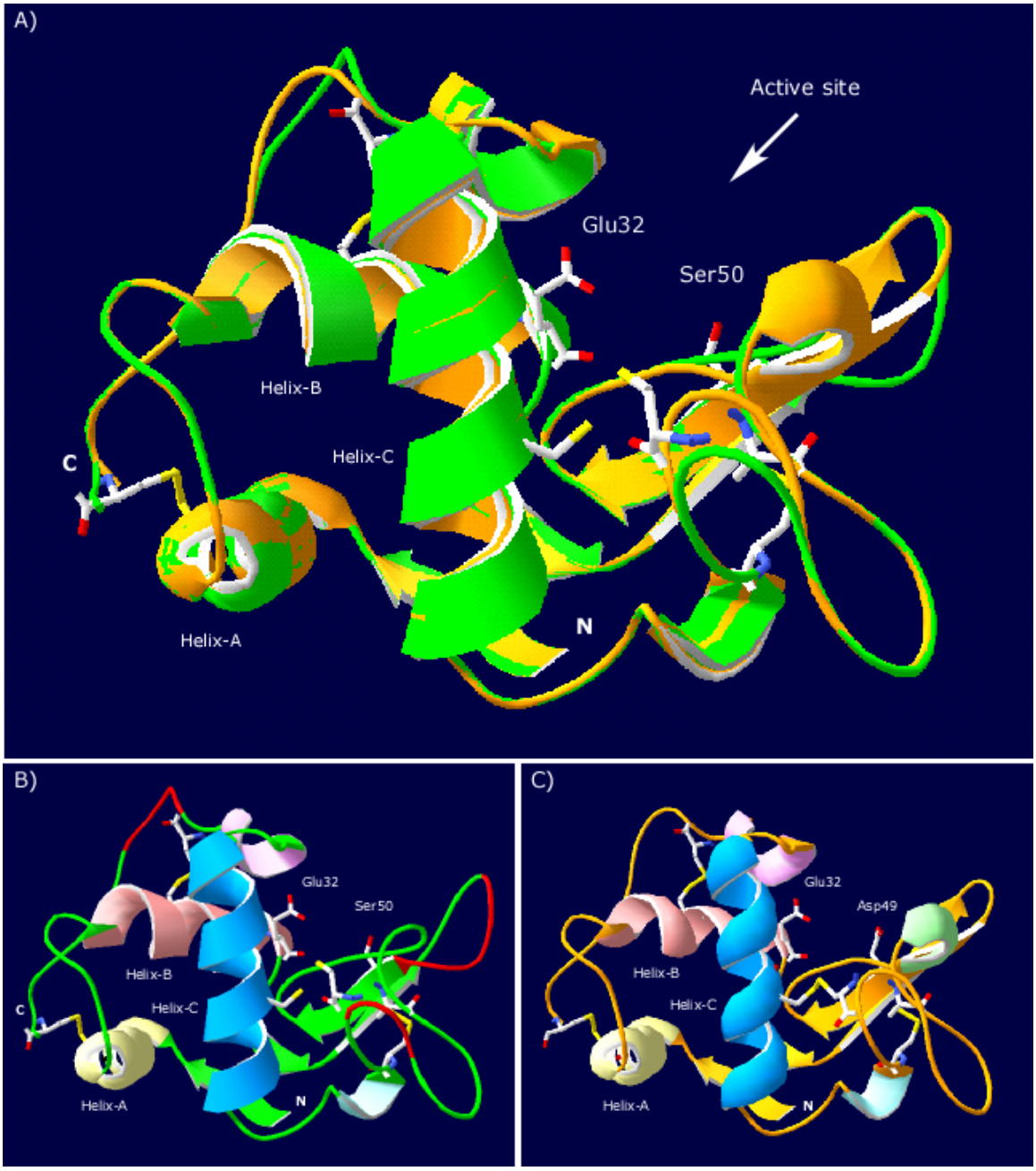

Fig. 2-10: Ribbon model of *A. mellifera* Lys-2

The model was generated by sequence alignment using SWISS-MODEL. The 3D-structure of *B. mori* (1gd6) was used as template. A) The model of Lys-2 (green) superimposed onto the 3D-structure of *B. mori* (orange) is shown. The highly conserved cysteines and active site glutamic acid (Glu32) as well as the Ser50 substitution are displayed; B) Isolated model of Lys-2. Regions of the model that appear in red have been completely rebuild; C) 3D-structure of *B. mori* lysozyme. The highly conserved cysteines and active site Glu32 and Asp49 are displayed.

The models of Lys-1 and Lys-2 suggest that both enzymes resemble, in large part, the structure of *B. mori* lysozyme. The structure of the large domain containing helices A, B, and C fits remarkably well into the experimentally determined structure of *B. mori*. The positioning of the active site glutamic acid E32 at the end of helix B is also conserved. Furthermore, all cysteines in this part of the molecule are predicted to be able to build disulfide bridges similar to those found in *B. mori*, which indicates the conservation of this domain. On the other hand, the smaller domain comprised of the characteristic β-sheet and loop region, displays some differences in the structural arrangement with respect to the *B. mori* lysozyme (Fig. 2-9/2-10 B: regions are highlighted in red). The β-sheet harboring the active site aspartic acid 49 (*B. mori*) is found to be shorter in both *A. mellifera* lysozymes. However, it should be noted that this observation may not reflect the structural arrangement in the native enzyme. In addition, the loop region following the β-sheet shows an altered conformation which is also reflected in the inability of cysteines 71 and 89 to build a proper disulfide bridge. In general, almost every protein model contains non-conserved loops which are expected to be the least reliable portion of a protein model (Schwede *et al.*, 2003). Furthermore, loops also correspond to the most flexible part of the structure which suggests that the small domain in the *A. mellifera* lysozyme slightly differs from the structure of the *B. mori* enzyme. Conversely, core residues are found to be in essentially the same orientation as the experimental control structure, since they are generally well conserved.

2.4. Discussion

The bacteriolytic enzyme lysozyme which hydrolyses the β-1,4-glycosidic linkage between altering N-acetylglucosamine and N-acetylmuramic acid residues in the peptidoglycan layer of bacterial cell walls, is widely distributed among eukaryotic and prokaryotic organisms (Beintema and Terwisscha van Scheltinga, 1996; Holtje, 1996; Hultmark, 1996; Jolles and Jolles, 1975; Prager and Jolles, 1996; Qasba and Kumar, 1997). Lysozymes have been identified and characterized in a variety of insect species in the orders Lepidoptera, Orthoptera, and Diptera (Hultmark, 1996) where the enzyme plays a role as a digestion enzyme in the digestive tract (Daffre *et al.*, 1994; Lemos and Terra, 1991; Regel *et al.*, 1998) and/or in the defense response against pathogens that have entered the hemocoel (Engstrom *et al.*, 1985; Lockey and Ourth, 1996; Morishima *et al.*, 1995; Mulnix and Dunn, 1994). In *A.*

mellifera, which belongs to the order hymenoptera, lytic activity was observed in the venom which was attributed to lysozyme (Mohrig and Messner, 1968), however, investigations to properly isolate and characterize the enzyme had been lacking. The successful sequencing and assembly of the honey bee genome provides a new source of information to the scientific community which allows the screening for homologues proteins from other organisms. This work details the *in silico* identification and characterization of the enzyme lysozyme from *A. mellifera*.

The program BLAST (Basic Local Alignment Search Tool) (Altschul *et al.*, 1997) that finds regions of local similarity between sequences was applied on the honey bee genome assembly using the protein sequence of *Drosophila melanogaster* lysozyme D. The database query indicated the presence of two genes in the genome of *A. mellifera* that code for lysozymes (Fig. 2-3). The two genes are arranged in tandem on chromosome 13 and are devoid of introns. The only insect species identified this far to lack introns in its lysozyme genes is *D. melanogaster* (Daffre *et al.*, 1994), whereas in all other insect species studied to date the *lyz* genes contain at least one intron (Bae and Kim, 2003; Kang *et al.*, 1996; Liu *et al.*, 2004; Ursic Bedoya *et al.*, 2005).

Alignment of the deduced protein sequences of Lys-1 and Lys-2 (Fig. 2-6) showed that they share over 90% in sequence similarity and more than 78% identity in amino acid sequence. The major difference between the two lysozymes is the absence of a 13 amino acid long extension at the C-terminal end of Lys-2 compared to Lys-1. No obvious function can be assigned to this extension as it is not associated with any functional domains. Therefore, the absence of the extension in Lys-2 would suggest that it is not essential. However, it might play a role in regulating Lys-1 function by blocking the substrate binding cleft. The fact that the two genes are highly conserved in sequence suggests that the second copy probably arose by a gene duplication event. Both proteins display a relatively high content of the basic amino acids lysine and arginine which contribute strongly to their basic nature, characteristic for lysozymes. Furthermore, the N-terminus of each protein is hydrophobic, suggesting the presence of a signal peptide that directs the translocation of synthesized secretory proteins into the lumen of the rough endoplasmatic reticulum. Prediction of a signal peptidase cleavage site using the server-based prediction tool SignalP v3.0 (Bendtsen *et al.*, 2004) identified one distinct cleavage site in each protein. Sequence alignment between both *A. mellifera* lysozymes and lysozymes from other organisms indicates that these positions are

highly conserved (Fig. 2-7). Based on the sequence alignment, eight cysteine residues and the active site glutamic acid that are highly conserved in chicken-type lysozymes were identified in *A. mellifera* lysozymes. Thus, both proteins can be attributed to this enzyme family. However, the conserved aspartic acid in the active site of c-type lysozyme is substituted for serine in both *A. mellifera* lysozymes. The Asp to Ser substitution is the first to be reported for a c-type lysozyme. Furthermore, the sequence alignment revealed that Asp is replaced by its corresponding amide, asparagine, in lysozyme C and C4 of *Aedes aegypti* and *Anophilis gambiae*, respectively. This is very interesting since it is generally thought that the aspartic acid at this position plays two important roles in the catalytic mechanism of c-type lysozymes; It provides electrostatic stabilization of the oxonium ion intermediate (Phillips, 1966; Vernon, 1967) and helps to strain the substrate into a more reactive conformation (Strynadka and James, 1991). Based on the X-ray structure of chicken egg-white lysozyme (ChEWL) Strynadka and James further suggested that an adjacent asparagine (N46) stabilizes the negative charge of the aspartic acid (D52) by hydrogen-bonding. This asparagine residue is also absent in the active site of *A. mellifera* lysozymes. The importance of the ionized aspartic acid for the catalytic activity of ChEWL was demonstrated by site-directed mutagenesis. When Asp52 was altered to asparagine the resulting mutant exhibited biphasic kinetics, with fast and slow phase velocities equal to 5% and 0.5% of the wild type rate, respectively (Malcolm *et al.*, 1989). In addition, when Asp52 is replaced by serine, the corresponding mutant exhibits an even lower catalytic activity equal to ≤1% of the wild type enzyme (Lumb *et al.*, 1992). Thus one would expect a highly reduced catalytic activity for both lysozymes of *A. mellifera* in respect to ChEWL.

The replacement of the active site aspartic acid in the honey bee lysozymes would further suggest a different catalytic mechanism. Similar to the *A. mellifera* lysozymes, goose-type lysozymes (Weaver *et al.*, 1995) as well as some phage lysozymes (Garvey *et al.*, 1986) and the distantly related *Escherichia coli* soluble lytic transglycosylase (Thunnissen *et al.*, 1995) do not have an equivalent to Asp52. Although the goose-type lysozymes lack a second catalytic carboxylate, they facilitate hydrolysis by interacting with the peptide side chains attached to N-acetylmuramic acid unit of the peptidoglycan which lead to the proposal of a substrate-assisted mechanism (Matsumura and Kirsch, 1996). Furthermore, g-type lysozymes utilize the free energy of association with the peptide to strain the D-subsite N-acetylmuramic acid unit into the more reactive half-chair or sofa

conformation (Weaver *et al.*, 1995). According to Matsumura and Kirsch (Matsumura and Kirsch, 1996) the substrate-assisted mechanism depends on the availability of glycine carboxylate groups of un-cross-linked peptides. Based on model-building, they have shown that a correctly positioned carboxylate group of certain substrates can be rotated into the location that is normally occupied by the carboxyl group of Asp52 in ChEWL. Since N-acetylmuramic acid units differ among bacterial species in respect to the state of substitution and the amino acid composition of the peptidic residue, a narrowed spectrum of potential target bacteria is the consequence of this mechanism.

Furthermore, as a result of the substrate-assisted mechanism, the bound product possesses an alternate chirality in respect to the substrate. While the product retains the β-configuration of the substrate in c-type lysozymes, the chirality of the product is inversted to a α-configuration in lysozymes of the g-type (Kuroki *et al.*, 1999). The ability for anomer-inversion is also found in the phage T4 lysozyme which, in contrast to the g-type lysozymes, possesses an equivalent to Asp52 of ChEWL. However, based on their mutation analysis, Kuroki and colleagues presumed that the native phage enzyme displays a single-displacement mechanism in which a well coordinated H_2O molecule attacks from the α-site of the substrate (Kuroki *et al.*, 1999). They further proposed that the single-displacement mechanism requires two carboxylates separated by 7.2 to 9.5 Å that lead to an intervention of a H_2O molecule; however, emphasizing that in some cases a single carboxylate might be sufficient for catalysis. The fact that the product bound to the D52S mutant of chicken egg-white lysozyme adopts preferentially the α-configuration (Hadfield *et al.*, 1994) as well as the lack of a second catalytic carboxylate in both *A. mellifera* lysozymes suggests that the catalytic activity underlies either a similar substrate-assisted mechanism as observed for g-type lysozymes or follows a single-displacement mechanism displayed by T4 phage. Based on structural modeling of Lys-1 and Lys-2 (Fig. 2-9 and 2-10), one can assume that the honey bee lysozymes resemble, in large part, the structure of other c-type lysozymes. Superimposition of the experimentally determined structure of the silk moth *Bombx mori* and the modeled structure of *A. mellifera* lysozymes indicates that the active site glutamic acid and the substituted serine are located at the same positions as Glu32 and Asp49 in *B. mori*. If one assumes that the positioning is true for the native structure, a substrate-assisted mechanism is less likely because Ser50 would stericly hinder the correct placement of a carboxylate group of the substrate into the location that is

normally occupied by the carboxyl group of aspartic acid. This assumption is supported by the observation that the relative velocity of the assisted catalysis of ChEWL mutant D52A is four fold higher (~20%) than that of mutant D52N (~5%) which possesses a larger side chain (Malcolm *et al.*, 1989; Matsumura and Kirsch, 1996). In case of the presumed single-displacement mechanism of T4 lysozyme, two carboxylic acids, Glu11 and Asp20, as well as the hydrophilic residue Thr26 are involved in catalysis. It is thought that Asp20 and Thr26 coordinate a H_2O molecule through hydrogen-binding that acts as a nucleophile in attacking the C-1 carbon of N-acetylmuramic acid (Kuroki *et al.*, 1999). Although the second carboxylate is

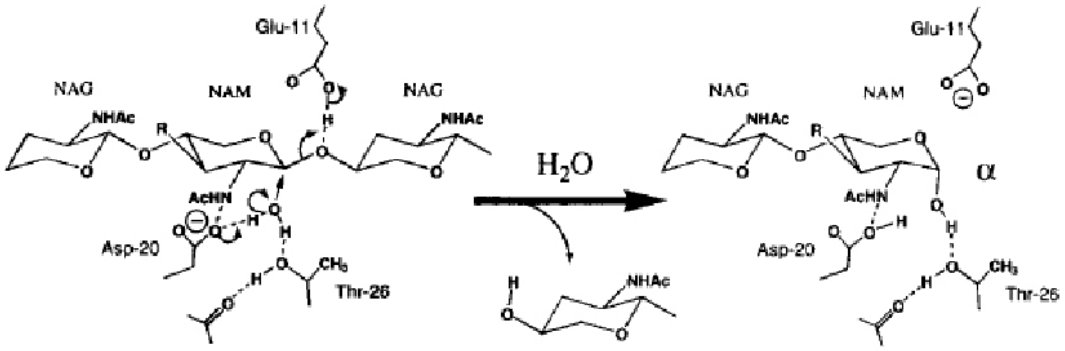

Fig. 2-11: Catalytic mechanism of phage T4 lysozyme

Shown is the overall relationship between active-site structures and the presumed mechanism of phage T4 lysozyme (figure taken from Kuroki *et al.*, 1999)

lacking, the mechanism of catalysis in *A. mellifera* lysozymes might resemble that of T4 lysozyme in which the hydroxyl group of Ser50, similar to Thr26 in T4 lysozyme, is involved in the coordination of a water molecule. A similar single-displacement inverting mechanism was also proposed for the family 18 chitinases, a class of antifungal proteins expressed in plants which catalyze the hydrolysis of chitin. Chitin, a β1,4-linked N-acetyl-glucosamine polysaccharide, is a major structural component of many organisms including fungi, insects, and crustaceans. The detailed mechanism was revealed by molecular dynamics simulations on the barley seed endochitinase complexed with a hexaNAG on the basis of the crystal structure of NAG-NAM-NAG/ChEWL complex (Brameld and Goddard, 1998). Two carboxylic amino acids were identified to be involved in catalysis. Glu67 is located on the β-site

of the hexaNAG substrate and is thought to act as a general acid similar to Glu35 in ChEWL. The second carboxylic residue (Glu89) is located within a flexible loop on the α-site of the substrate which is brought closer to the oxocarbenium ion intermediate by conformational change of the active site. Similar to the mechanism proposed for T4 lysozyme, Glu89 is involved in the concert coordination of a nucleophilic H_2O molecule. In the case of chitinase the coordination is supported by a serine residue (Fig. 2-12). It just can be speculated whether or not the lysozymes from *A. mellifera*

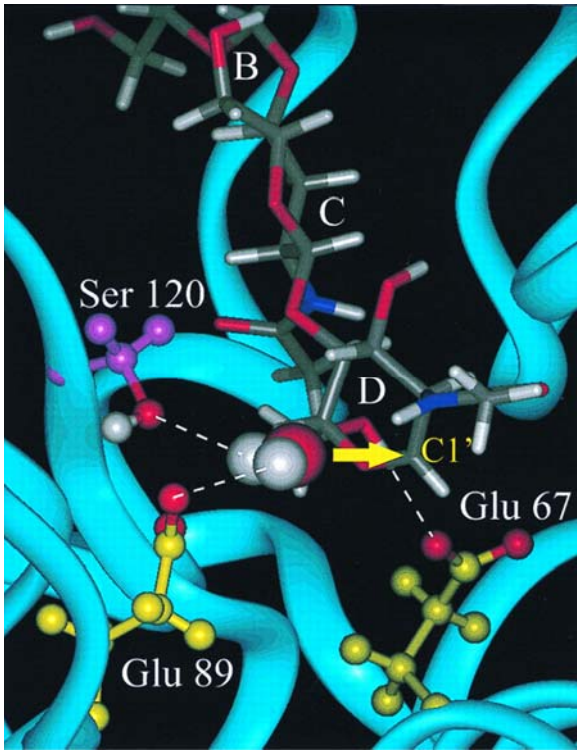

Fig. 2-12: 3D-model of the active site of barley seed endochitinase

Snapshot from the dynamic simulation of a tri-NAG oxocarbenium ion intermediate bound to barley chitinase. An arrow marks the α face of the oxocarbenium ion. Figure from *Brameld et al.*, 1998.

follow a similar mode-of-action. Noteworthy is the observed variability of the β-sheet and loop regions in the obtained lysozymes models (Fig. 2-9 and Fig. 2-10). Based on the amino acid sequences only two potential residues can be assigned for the loop region that are in close proximity to Ser50 and might act as a hydrogen acceptor, Gln55 and Asn57. However, for the hydrolytic reaction to go to completion either of these residues would need further hydrogen bonding in order to compensate the positive charge. Nevertheless, the imagination that both lysozymes could act as chitinases would suggest a new role in the humoral immune response of *A. mellifera* as an antimicrobial peptide with antifungal activity.

Although the *A. mellifera* lysozymes can be classified as c-type lysozymes, the question arises why they would differ greatly from other c-type lysozymes in respect

to mechanism and substrate-specificity. A possible answer could be that the *A. mellifera* lysozymes resemble an ancient c-type ancestor that followed a single-displacement mechanism with a limited set of catalytic activities. This would imply that the binding cleft and the catalytic site of all other c-type lysozymes have been optimized during evolution in which the catalytic activity has progressively increased by acquisition of amino acids serving a function in catalysis. Acquisition of catalytic amino acids would have brought about a considerable evolutionary advantage for individuals requiring a lysozyme with higher catalytic activity. The presence of two acidic amino acids in the active site of lysozymes or glycosylases is the consequence of the convergent evolution of these enzymes in the acquisition of a more efficient double-displacement mechanism. The absence of the active site aspartic acid in some lysozymes and the different levels of activity shown by several ChEWL mutants where Asp52 was substituted for asparagine and serine (Lumb *et al.*, 1992; Malcolm *et al.*, 1989), would support this hypothesis. Based on the observed catalytic rates an evolutionary pathway out going from serine via asparagines can be drawn for Asp52. Indeed, a single G→A transition in the serine reading codons AGT and AGC followed by an A→G transition in the codons of asparagine would be sufficient to

Amino acid	**Codon**		**Activity**
Ser	A **G** T	A **G** C	≤1 %
↓	↓	↓	↓
Asn	**A** A T	**A** A C	5%
↓	↓	↓	↓
Asp	**G A** T	**G A** C	100%*

Fig. 2-13: Mutagenic pathway of Asp52 in chicken egg-white lysozyme

Codons used in this figure reading for serine correspond to the codons found in *A. mellifera* Lys-1 and Lys-2 at position 50, respectively.

* refers to activity of wild type ChEWL

obtain codons reading for aspartic acid (Fig. 2-13). The codons AGT and AGC are found in the coding sequence of Lys-1 and Lys-2 corresponding to Ser50, and thus, could be considered as a starting point of such a mutagenic pathway. Besides the serine substitution in *A. mellifera*, asparagine replacements are found in some lysozymes of *A. aegypti* and *A. gambiae* which would support this idea. The existence of such mutagenic pathways in the evolution of catalytic domains that lead to a

progressive increase in catalytic rate and substrate-specificity was demonstrated for serine proteases (Carter and Wells, 1988).

To confirm the proposed hypothesis it is necessary to clone and purify the lysozymes of *A. mellifera* and to carry out intensive kinetic studies in respect to catalytic activity and substrate-specificity. The fact that both lysozyme-encoding genes are devoid of introns makes it easy to amplify the genes from genomic DNA. The proteins could then be overexpressed in *Saccharomyces cerevisiae* and further purified as demonstrated for other c-type lysozymes (Koganesawa *et al.*, 2001; Kumagai and Miura, 1989; Matsumura and Kirsch, 1996). Furthermore, mutational analysis involving the active site serine could reveal a mutagenic pathway which leads to a double-displacement mechanism. In addition, NMR and X-ray crystallography of wild type and mutant *A. mellifera* lysozymes could be performed to dissect the catalytic mode-of-action of the proposed ancient ancestor of modern c-type lysozymes.

Chapter III

Identification and characterization of antimicrobial peptides in the hemolymph of A. mellifera

3.1. Introduction

The honey bee *A. mellifera* plays an important economic role as pollinator of many fruits and crops enhancing their productivity by an order of magnitude (Carreck and Williams, 1998) and an estimated indirect economic value to the German agriculture of 1.5 to 2.5 billion euros. Thus the health of the bee has been in the focus of intense research in past years. Like other animals, the honey bee is susceptible to infections by a variety of organisms, including viruses, bacteria, fungi and parasites. Some of these pathogens affect the adult bee, while others affect the brood, or immature stages. During evolution the honey bee has developed different strategies to prevent, resist and overcome microbial and parasitic infections. Once the pathogen has breached the physical barrier, i.e. the cuticle, and has entered the hemocoel, it induces cellular and humoral immune reactions, which results in the rapid elimination of the invader. In *A. mellifera* the humoral part of the immune system is comprised of a defined set of antimicrobial peptides (AMPs) that are mainly produced by the fat body upon infection. To date four classes of AMPs have been isolated and characterized from immunized bees that provide a broad-spectrum of antibacterial defense through complementarity. Apidaecins, a family of short non-helical peptides (18 amino acids) inhibit the viability of gram$^-$ bacteria and are overproduced by a combination of low threshold transcriptional activation as well as a unique, genetically encoded amplification mechanism (Casteels-Josson *et al.*, 1993; Casteels *et al.*, 1989; Casteels and Tempst, 1994). On the other hand, defensin 1 (51 amino acids) was found to be solely bactericidal against gram$^+$ bacteria. Gene expression is induced upon bacterial infection, however transcription is minimal and delayed, and only minute quantities of corresponding peptide are produced (Casteels-Josson *et al.*, 1994; Casteels *et al.*, 1993). The inducible polypeptides abaecin and hymenoptaecin (34 and 93 amino acids long, respectively) are the predominantly produced AMPs and display a more diverse spectrum of antibacterial activity affecting the growth of gram$^+$ and gram$^-$ bacteria (Casteels *et al.*, 1993; Casteels *et al.*, 1990).

Furthermore, the bacteriolytic enzyme lysozyme, which hydrolyzes the β-1,4-glycosidic linkages in the peptidoglycan layer of bacterial cell walls, is thought to complete the set of AMPs (Mohrig and Messner, 1968). Direct evidence of the presence in the hemolymph and other tissues however is still outstanding.

As part of the ongoing research on the immune system of the honey bee this chapter describes the identification of the antimicrobial peptides abaecin, defensin 1, hymenoptaecin and lysozyme 2 in the hemolymph by mass spectrometry. The effect of pathogenic dose and the timeline of peptide induction were studied by SDS-polyacrylamide gel electrophoresis. Furthermore, the induction pattern of these peptides was studied in respect to age of the worker honey bee.

3.2. Material

3.2.1. Chemicals

CHEMICALS

Acrylamide solution (Gel A)	Carl Roth GmbH, Karlsruhe, Germany
Ammonium Persulfate	Carl Roth GmbH, Karlsruhe, Germany
Apiinvert®	Suedzucker AG, Ochsenfurt, Germany
Bisacrylamide solution (Gel B)	Carl Roth GmbH, Karlsruhe, Germany
Bacto-Agar	DIFCO, BD Bioscience, San Jose, CA
Bacto-Trypton	DIFCO, BD Bioscience, San Jose, CA
Bacto-Yeast-Extract	DIFCO, BD Bioscience, San Jose, CA
Coomassie blue (R250)	Serva Electroph. GmbH, Heidelberg, Germany
Coomassie blue (G250)	Serva Electroph. GmbH, Heidelberg, Germany
Glycerin (86%)	Carl Roth GmbH, Karlsruhe, Germany
Glycin	Carl Roth GmbH, Karlsruhe, Germany
2-Mercaptoethanol	Carl Roth GmbH, Karlsruhe, Germany
Methanol	Merck KGaA, Darmstadt, Germany
Phenylthiourea	Sigma-Aldrich Corp., St. Louis, MO
Potassium Chloride	Carl Roth GmbH, Karlsruhe, Germany
Potassium phosphate mono	Carl Roth GmbH, Karlsruhe, Germany
Sodium Chloride	Carl Roth GmbH, Karlsruhe, Germany
Sodium Dodecyl Sulfate	Carl Roth GmbH, Karlsruhe, Germany
Sodium phosphate di	Carl Roth GmbH, Karlsruhe, Germany
Tricine	Serva Electroph. GmbH, Heidelberg, Germany
Tris Base	Carl Roth GmbH, Karlsruhe, Germany

MOLECULAR WEIGHT MARKERS

High Molecular Weight	Serva Electroph. GmbH, Heidelberg, Germany
Low Molecular Weight	Serva Electroph. GmbH, Heidelberg, Germany

3.2.2. Biological material

3.2.2.1. Bacterial strains

Bacillus subtilis	Courtesy of Dr. Rdest, Institute of Microbiology, Wuerzburg, Germany
Escherichia coli K12	Courtesy of Dr. Rdest, Institute of Microbiology, Wuerzburg, Germany

Micrococcus flavus	Courtesy of Dr. Rdest, Institute of Microbiology, Wuerzburg, Germany

3.2.2.2. Other organisms

Honey bee *Apis mellifera ligustica*	Bee group, University of Wuerzburg, Wuerzburg, Germany

3.2.3. Instruments and equipment

Autoclave	H+P Labortechnik AG, Oberschleissheim, Germany
Biofuge 22R	Heraeus Instruments GmbH, Hanau, Germany
Electrophoresis System, vertical	Institute of Biochemistry, Wuerzburg, Germany
Hamilton syringe 75RN	Hamilton Company, Reno, NV
Incubator	Heraeus Instruments GmbH, Hanau, Germany
Needles, Point 4, Gauge 26	Hamilton Company, Reno, NV

3.3. Methods

3.3.1. Immunization of honey bees

3.3.1.1. Preparation of bacterial suspensions

Solutions were prepared according to Sambrook *et al.* (Sambrook and Russell, 2001).

Luria-Bertani broth

	Per 1000 ml
Bacto-Tryptone	10 g
Bacto-Yeast-Extract	5 g
NaCl	10 g

10x PBS

	Per 1000 ml
Na_2HPO_4	14.4 g
KH_2PO_4	2.4 g
NaCl	80.0 g
KCl	2.0 g
ddH_2O	→pH 7.4 w/ HCl

The desired bacterial strain was grown in Luria-Bertani broth overnight in a shaking incubator at 37°C. The preculture was used to inoculate 5 ml of LB broth. The culture was further incubated at 37°C until it reached A_{600} = 0.6. 1 ml of culture was

transferred into a sterile tube and cells were pelleted by centrifugation. After washing 3x with sterile 1x PBS a suspension of 10^5 cells per µl PBS was prepared and stored at 4°C for up to 3 days.

3.3.1.2. Bacterial infections

3.3.1.2.1. General procedure

Newly emerged *honey bee*s were obtained by removing sealed brood combs from a hive and further incubation at 35°C and 70% humidity. Upon emergence, worker bees (0-18 h old) of all combs were pooled (N= 200 to 800 bees), color coded and subjected to further treatment. In case of conducted age series, emerged bees were color labeled conveying the date of emergence. The marked bees were given back into a visually healthy colony and sampled either after 7, 14, 21, and 28 days post-emergence (July 2005) or every other day (September 2005).
Prior to injection, groups of 10 to 20 bees were anesthetized on ice and the injection site was treated with 70% ethanol. Subsequently, 1 µl of either sterile 1x PBS (control) or 1x PBS containing bacteria (typically 10^4 to 10^5 cells per µl) were injected into the hemocoel between the third and forth abdominal tergite using a sterile micro syringe. Bees of each group were transferred in a sterile metal cage and maintained at 35°C and 70% humidity for 24 h. During this incubation period bees were fed Apiinvert®. Following incubation the bees were anesthetized on ice and hemolymph was collected (3.3.2).

3.3.1.2.2. Dose-dependent induction

Basically as described in 3.3.1.2.1.. Bees were injected with 1 µl of either sterile 1x PBS or 1x PBS containing *E. coli* ranging from 10^1 to 10^5 cells per µl.

3.3.1.2.3. Time-dependent induction

Basically as described in 3.3.1.2.1.. Bees were injected with 1 µl of either sterile 1x PBS or 1x PBS containing 10^4 or 10^5 cells per µl. When applied, cells were killed by autoclaving the PBS suspension at 121° for 15 min. After injection bees were kept at 35°C and 70% humidity for 3 to 96 h.

3.3.2. Collection of hemolymph

Bees were anesthetized on ice and fixed to a wax plate with four crossed needles ventral site up. Under a dissecting microscope, both legs of the first pair were removed with a sharp scalpel at the level of the coxa. Outpouring hemolymph was immediately taken up with a glass micro capillary which had been pulled to a fine point with a glass electrode puller. Collected hemolymph (5 to 10 µl) was pooled on ice in a sterile tube containing phenylthiourea to prevent melanization (final concentration: 10 µg/ml).

3.3.3. Analysis of hemolymph

3.3.3.1. Pre-treatment of hemolymph samples

Collected hemolymph was subjected to heat-treatment by incubation of the samples at 100°C for 2 min. The precipitate was spun down by centrifugation for 10 min at 4°C and 17,000 rpm (Biofuge R22). The supernatant was transferred into a fresh tube and stored at -20°C until further use.

3.3.3.2. SDS-polyacrylamide gel electrophoretic analysis of hemolymph

Hemolymph of immunized bees was analyzed for the presence of inducible antimicrobial peptides by SDS-polyacrylamide gel electrophoresis (Laemmli, 1970). Alternatively, for better separation of proteins with low molecular weight (<20 kDa) gel electrophoresis was carried out using the electrophoresis buffer system as described by Schagger *et al.* (Schagger and von Jagow, 1987). Throughout the course of this study protein samples were analyzes on either a 10% or 17.5% polyacrylamide gel. Typically 2.5 to 5 µl of untreated or pretreated hemolymph samples (3.3.3.1.) were subjected to SDS-polyacrylamide gel electrophoresis.

3.3.3.2.1. SDS-polyacrylamide gel electrophoresis

First, the resolving gel (composition see below) was poured vertically between two bottom sealed glass plates, followed by carefully pouring ddH_2O on top of the gel solution. After polymerization of the resolving gel for 20 min, the water was removed and the stacking gel (composition see below) was poured on top of the resolving gel.

An appropriate comb was applied and the stacking gel was allowed to polymerize for 10 min. The comb was immediately removed and wells were thoroughly flushed with electrophoresis buffer. The ready-to-use gel was clamped into electrophoresis apparatus, which was subsequently filled with electrophoresis buffer. Protein samples were prepared by addition of 2x SDS-loading buffer and heating the samples for 5 min at 100°C. The samples were loaded onto the gel along with an appropriate protein ladder serving as a molecular mass marker. The apparatus was attached to a power supply and electrophoresis was started at 60V. After the BPB dye moved into the resolving gel, the voltage was increased to 120 V. Electrophoresis was continued until the bromphenol blue (BPB) dye reached the bottom of the gel.

Resolving gel	**7.5 %**	**10 %**	**12.5 %**	**15 %**	**17.5 %**
	per 30 ml				
Acrylamide (30%)	7.5 ml	10 ml	12.5 ml	15 ml	17.5 ml
Bisacrylamide (2%)	3.0 ml	4.0 ml	5.0 ml	6.0 ml	7.0 ml
Tris·HCl, 1.5 M (pH 8.8)	7.5 ml	7.5 ml	7.5 ml	7.5 ml	7.5 ml
ddH_2O	11.5 ml	8.0 ml	4.5 ml	1.0 ml	-
degassing for 5 min					
SDS (10%)	300 µl	300 µl	300 µl	300 µl	300 µl
APS (20%)	200 µl	200 µl	200 µl	200 µl	200 µl
TEMED	20 µl	20 µl	20 µl	20 µl	20 µl

Stacking gel	**5 %**
	per 15 ml
Acrylamide (30%)	2.5 ml
Bisacrylamide (2%)	1.0 ml
Tris·HCl, 0.5 M (pH 6.8)	3.7 ml
ddH_2O	7.5 ml
degassing for 5 min	
SDS (10%)	150 µl
APS (20%)	200 µl
TEMED	10 µl

SDS-Sample buffer	**1x SP**	**2x SP**
	per 5 ml	
Tris·HCl, 0.5 M (pH 6.8)	0.5 ml	1.0 ml
SDS (10%)	1.0 ml	2.0 ml
Glycerol (86%)	0.5 ml	1.0 ml
2-mercaptoethanol, 14 M	0.15 ml	0.3 ml
BPB (1%)	0.25 ml	0.5 ml
ddH_2O	ad	ad

Buffer system (Laemmli)	
Electrophoresis buffer	
Glycine	250 mM
Tris base	25 mM
SDS	0.15% (w/v)

Buffer system (Schagger *et al.*)		
Electr. buffers	**Cathode**	**Anode**
Tris base	0.1 M	0.2 M
Tricine	0.1 M	-
SDS	0.1 % (w/v)	-
ddH_2O	→pH 8.3 w/ HCl	→pH 8.9 w/ HCl

3.3.3.2.2. Staining of protein gels

Following gel electrophoresis, gels were incubated in staining solution A overnight at room temperature. Subsequently, they were destained with methanol/acetic acid destaining solution until the blue protein bands appeared against a clear background. For preservation, the gels were placed between appropriate sized Whatman 3MM paper and a sheet of cellophane and dried on a gel drying apparatus for 1.5 h at 80°C. For mass spectrometric analysis, gels were incubated overnight in staining solution B and destained in ddH_2O several times.

Staining solution A	
methanol	45% (v/v)
Acetic acid	10% (v/v)
Coomassie R-250	0.05% (w/v)
ddH_2O	45%

Destaining solution	
methanol	45% (v/v)
Acetic acid	10% (v/v)
ddH_2O	45%

Staining solution B	
methanol	34% (v/v)
Phosphoric acid	2% (v/v)
Ammonium sulfate	17% (w/v)
Coomassie G-250	0.066% (w/v)
ddH_2O	Add to 100 ml

3.3.3.3. Inhibition-zone assay

The presence of induced antimicrobial peptides was analyzed by inhibition zone assay. The principle of this method is dependent upon the inhibition of reproduction of a microorganism on the surface of a solid medium by an antimicrobial agent which diffuses into the medium, e.g. from a filter paper disc. Thus, for an organism which is truly sensitive (susceptible) to an antimicrobial agent one expects to see a zone of inhibition around the disc impregnated with the agent; Beyond this zone an unaffected, area of normal growth (lawn) of the organism is present.
Antimicrobial activity against two different microbes was analyzed: the gram$^+$ bacteria *Micrococcus flavus* and the gram$^-$ bacterium *Escherichia coli*. 150 µl of fresh overnight cultures ($2 \cdot 10^9$ microbes/ml) were spread on appropriate agar plates and were kept for 15 min at room temperature. Subsequently, 1 µl of each hemolymph samples was spotted onto the plates followed by incubation overnight at 37°C.

3.4. Results

3.4.1. Identification of bacteria inducible peptides and proteins in the hemolymph of *A. mellifera*

3.4.1.1. Induction of peptides and proteins after bacterial challenge

The humoral immune system of *A. mellifera acts* specifically against invading pathogens by transcriptional activation of genes encoding for antimicrobial peptides (AMPs) such as apidaecins, abaecin, defensins and hymenoptaecin. Theses peptides are mainly synthesized in the fat body and secreted into the hemolymph. In order to identify these and other bacterial induced peptides and proteins by mass spectrometry, the induction of the full set of AMPs was undertaken. This was accomplished by the infection of newly emerged bees with a bacterial suspension containing the gram$^-$ and gram$^+$ bacteria *Escherichia coli* and *Bacillus subtilis*, respectively (3.3.1.2.). PBS injection was employed as an "aseptic" treatment while untreated bees were included as controls for baseline expression. Following infection, treated and control bees were incubated for 24 and 48 h at 35°C (bee hive temperature). Due to the fact that all antimicrobial peptides of *A. mellifera* characterized to date remain soluble at high temperatures the collected hemolymph was incubated at 100°C and clarified by centrifugation. The supernatants and pellets

A)

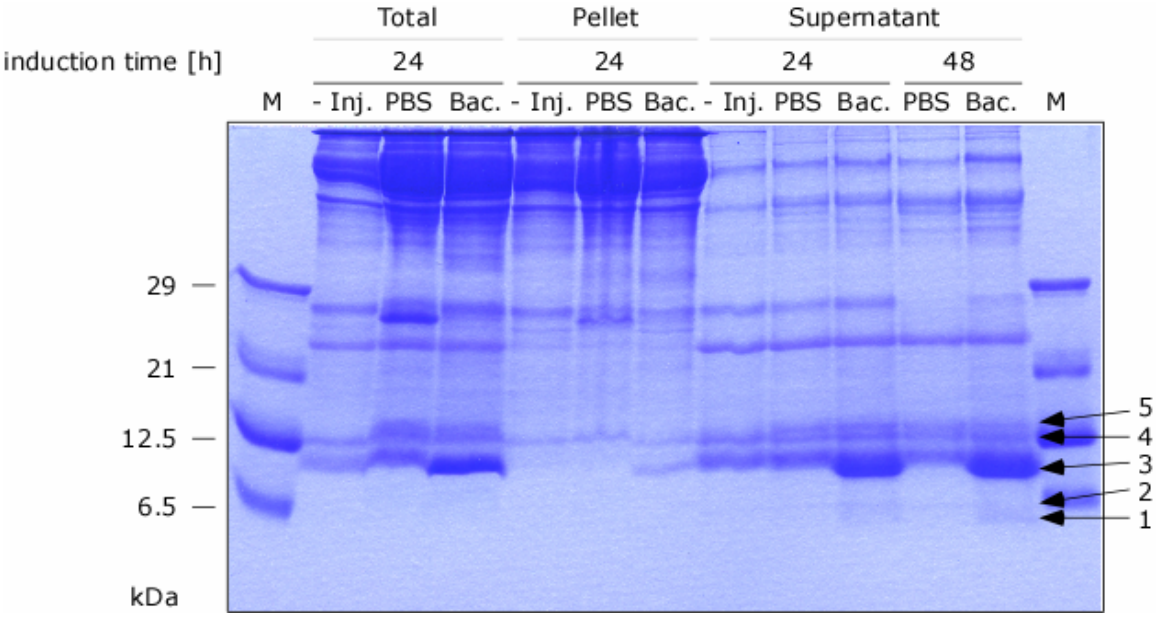

B)

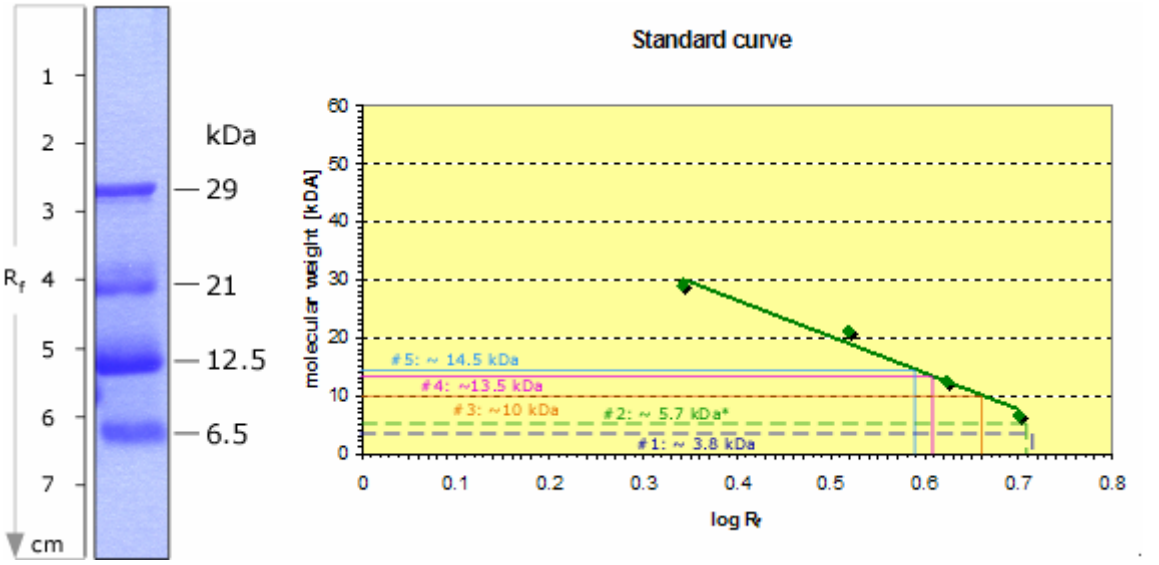

Fig. 3-1: Induction of AMPs in the hemolymph of *A. mellifera*

A) SDS-PAGE analysis of inducible antimicrobial peptides (AMP) in the hemolymph following bacterial infections. Newly emerged bees (0-18 h) were injected with 1 µl of either sterile 1xPBS (control) or 1xPBS containing 10^4 cells of *E. coli* and *B. subtilis* per µl PBS. Bees were incubated at 35°C and 70% humidity for 24 h. Hemolymph was taken from a pool of 5 to 7 bees and subjected to 100°C for 2 min followed by centrifugation. Pelles were washed several times and resuspended in 100 µl of 1xPBS. 5 µl of each sample were analyzed on a 17.5% SDS-polyacrylamide gel using a Tricine containing buffer system. –Inj.: non-injected bees (control). B) Molecular weight standard curve. *: estimation with reservation

were subsequently analyzed by SDS-polyacrylamide gel electrophoresis (3.3.3.2.) using a Tricine-containing buffer system (Schagger and von Jagow, 1987) which allows a good separation of proteins smaller than 20 kDa (Fig. 3-1). Injection of bacteria resulted in a clear induction of at least three peptides compared to the non-injected and PBS- injected control bees. The strongest induction level was observed for a peptide with a molecular weight between 6.5 and 12.5 kDa (#3). Based on the standard curve (Fig. 3-1B) protein #3 has an estimated molecular mass of 10 kDa. An inducible antimicrobial peptide with such a molecular weight, known as hymenoptaecin, was identified by Casteels and colleagues (Casteels *et al.*, 1993). Lower levels were observed for two peptides smaller than 6.5 kDa in size (#1 and 2) which could indicate the presence of abaecin and defensin 1 (Casteels *et al.*, 1993; Casteels *et al.*, 1990; Fujiwara *et al.*, 1990). As expected these peptides were found solely in the supernatant of heat-treated hemolymph. Expression levels observed for peptides 1 and 3 after 24 h post-injection appeared to increase slightly upon further incubation (48 h).
For further characterization, the inducible peptides were selected for mass spectrometry (3.4.1.2.). In addition, two proteins with estimated molecular weights of approximately 13.5 and 14.5 kDa were in the focus of interest (#4 and 5) in order to find both lysozymes of *A. mellifera* (see chapter 2).

3.4.1.2. Sequencing of bacteria induced peptides and proteins

Mass spectrometry or so-called mass mapping is a convenient method for determining the identity of proteins. It can provide sequencing data from any Coomassie stained band or gel spot. The protein of interest is digested with trypsin in the gel, peptide fragments are eluted and fractionated by reverse-phase chromatography followed by introduction into the mass spectrometer. The mass spectrometer determines the mass of the peptides and the sequence by collision-induced dissociation. The obtained mass spectrometric profile is used to accurately identify the protein by comparison with known sequences available through public or local databases. The mass mapping was carried out at the laboratories of Prof. Dr. Mueller (Lehrstuhl fuer Pharmazeutische Biologie) and Dr. Sickmann (Virchow-Zentrum) at the University of Wuerzburg.

1: Abaecin

MKVVIFIFALLATICAAFAYVPLPNVPQPGRRPFPTFPGQGPFNPKIKWPQG
Y

2: Defensin 1

MKIYFIVGLLFMAMVAIMAAPVEDEFEPLEHFENEERADRHRRVTCDLLSFK
GQVNDSACAANCLSLGKAGGHCEKGVCICRKTSFKDLWDKRFG

3: Hymenoptaecin

MKFIVLVLFCAVAYVSAQAELEPEDTMDYIPTRFRRQERGSIVIQGTKEGKS
RPSLDIDYKQRVYDKNGMTGDAYGGLNIRPGQPSRQHAGFEFGKEYKNGFIK
GQSEVQRGPGGRLSPYFGINGGFRF

4: Lysozyme 2

MEKSWLISLFLVVLIDGRVAGKILTECEIVQQLQQARISRSDISSWICLMQS
ESGLNTNLITGPKTASSYSYGIFQINSAKWCSRGHSGGICKKRCEDFANDDI
RDDIACAKKIQSLEGFKAWDGWVKNCKKKPLPNIQKCSR

5: FABP-like protein

MVQFEGKFQFVSQNNFEEFAKVLGDQNLVNTVLQPRPSFELSKNGDEWTFTS
SSGDNTYTKTFKMNVPFEETLPSLPDRKFQTVTSIEGNTFKTETQVNDSLKV
TRLYEFSDNELLVHISTNKSDVKATRVYKRV

6: Transferrin

MMLRCNIWTLAVNVLFVNSFLFVIAAQDSSGRIFTICVPEIYSKECDEMKKD
SAVKGIPVSCISGRDRYECIEKVGKKEADVVAVDPEDMYLAVKDNKLASNAG
YNVIEQVRTKEEPHAPYRYEAVAVIHKDLPINNVQGLRGLKSCHTGVGRNVG
YKIPITKLTAMGVLNNLHDPEYSARENELRALSSLFSKGCLVGTWSPDPAIN
RRLKETYSNMCALCEKPEVCDYPDIYSGYEGALRCLAHNGGEIAWTKVIYVK
RFFGLPVGVTAAIPTSENPADYRYFCPDGSKVPIDANTKPCTWAARPWQGYM
TNNGVNNVEAVQKELTDLGKLGEEEKADWWKDIMLLNEKTLAVPAPPVLPEN
HLKNAKYLDVIERNSGATDKIIRWCTWSEGDLEKCKALTRAAYSRDVRPKYD
CTLEKSQDDCLKAIKENNADLTVVSGGSVLRATKEYNTVPIIAESYGSGSTN
FNERPAVAVVSKSSSINKLEDLRNKKSCHSGYKDSFAGWTAPIYTLKRKGLI
KSENEAADFFSGSCAPGAPLDSKLCQQCVGNLASNNDRIRQVTKCKATNEET
YRGGKGALSCLLDGKGDVAFVPLTALSEEGVQSKDLALICPDGGRAEINEWE
RCNLGLEPPRVILSSGAKSPTVLEELTHGTLAASTLYSKRPDLLHLFGSWSN
RPNLLFKDEAKDLVSVNKSWNKWNDWQETQNNYGAA

Fig. 3-2: Listing of antimicrobial peptides identified by mass spectrometry

Shown are the sequences of the identified proteins. The order is according to the appearance in Fig. 3-1. The corresponding tryptic fragments identified by MS are highlighted in blue and orange. Underlining indicates the presence of a signal peptide sequence. A dashed underline indicates the presence of a pre-pro-sequence in the corresponding protein.

Results of mass mapping are shown in figure 3-2. Peptides 1, 2 and 3 were identified to be abaecin, defensin 1 and hymenoptaecin, respectively. In these cases, almost all of the expected tryptic fragments of the mature peptides were determined by mass spectrometry. Database query of the MS profile of proteins 4 and 5 identified the proteins to be lysozyme 2 (Lys-2) and a FABP-like protein (fatty-acid binding protein). In case of Lys-2, one distinct tryptic fragment (orange) was detected for this peptide, whereas a second fragment (blue) should be considered with caution since it refers to the theoretical signal peptide, and thus, should not be present in the mature protein. Nevertheless, the MS data strongly suggests the presence of lys-2 in the hemolymph of *A. mellifera*. The observed molecular mass of 13 to 14 kDA also corresponds to the theoretical mass of 13.4 kDa. Last but not least, a bacterial induced protein (#6, Fig. 3-5) with an observed molecular mass greater than 68 kDa was identified as transferrin, an iron-binding protein that has been implicated in innate immunity in the honey bee (Kucharski and Maleszka, 2003).

3.4.2. Dose-dependent induction of antimicrobial peptides and transferrin

The dose-effect of injected bacterial cells on the levels of induced peptides in the hemolymph was determined by injection of *E. coli* ranging from 10^1 to 10^5 cells per µl bacterial suspension. Injected and control bees were incubated for 24 h. For further analysis a fraction of the collected hemolymph was subjected to heat-treatment.

3.4.2.1. Inhibition-zone Assay

The increased antibacterial activity in the hemolymph was analyzed by an agar-diffusion or inhibition-zone-assay (3.3.3.3.). This assay is one of the most widely used methods to determine the susceptibility of microorganisms to antimicrobial agents. Antimicrobial activity against two different microbes was analyzed: the gram$^-$ bacterium *E. coli* and the gram$^+$ bacterium *Micrococcus flavus*. The bacteria were spread on appropriate agar plates and 1 µl of supernatant was spotted onto the plates followed by incubation overnight at 37°C. Figure 3-3 shows the susceptibility of *E. coli* and *M. flavus* to the induced antimicrobial peptides in the hemolymph of bacteria challenged bees. For both bacteria, no inhibition was observed for hemolymph of non-treated bees (-Inj.) indicating that no potentially active

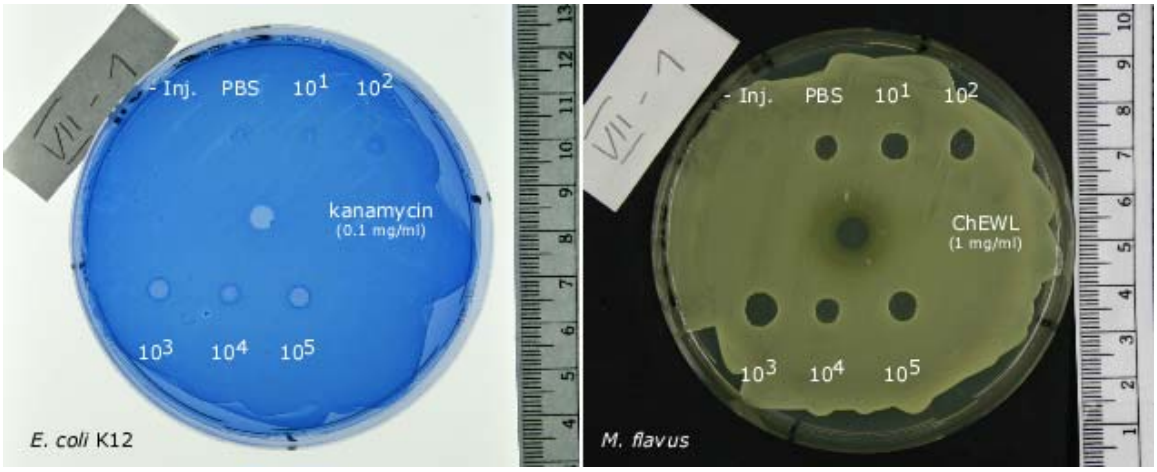

Fig. 3-3: Inhibition-zone assay

The presence of induced antimicrobial peptides was analyzed by inhibition zone assay. Antimicrobial activity against *E. coli* K12 (gram$^-$) and *M. flavus* (gram$^+$) was analyzed. 150 µl of fresh overnight cultures ($2 \cdot 10^9$ microbes/ml) were spread on appropriate agar plates and were kept for 15 min at room temperature. 1 µl of each hemolymph samples was spotted onto the plates followed by incubation overnight at 37°C. Controls: Kanamycin, Chicken egg-white lysozyme.

antimicrobial peptides are present. While growth inhibition was only observed for hemolymph samples of bees challenged with 10^3 to 10^5 cells in case of *E. coli*, *M. flavus* displays a somewhat high sensitivity towards antimicrobial peptides even at low levels. Comparable growth inhibition was observed for all samples of treated bees including the control bees injected with PBS, which was employed as an "aseptic" treatment. This result suggests that *E. coli* is more resistant against the mode of action of these peptides compared to *M. flavus*, therefore higher concentrations of antimicrobial peptides are necessary to eliminate the former.

3.4.2.2. SDS-PAGE analysis of hemolymph accumulation of AMPs and transferrin

The collected supernatants were further analyzed by SDS-PAGE (Fig. 3-4). Abeacin and hymenoptaecin are highly induced upon bacterial infection and the amount of each peptide increases linearly with the amount of injected bacterial cells. On the other hand, expression levels of defensin 1 hardly increased with increasing amounts of bacterial cells injected. Furthermore, the protein levels of Lys-2 were not affected by bacterial injection at all and remained at the baseline level observed in untreated

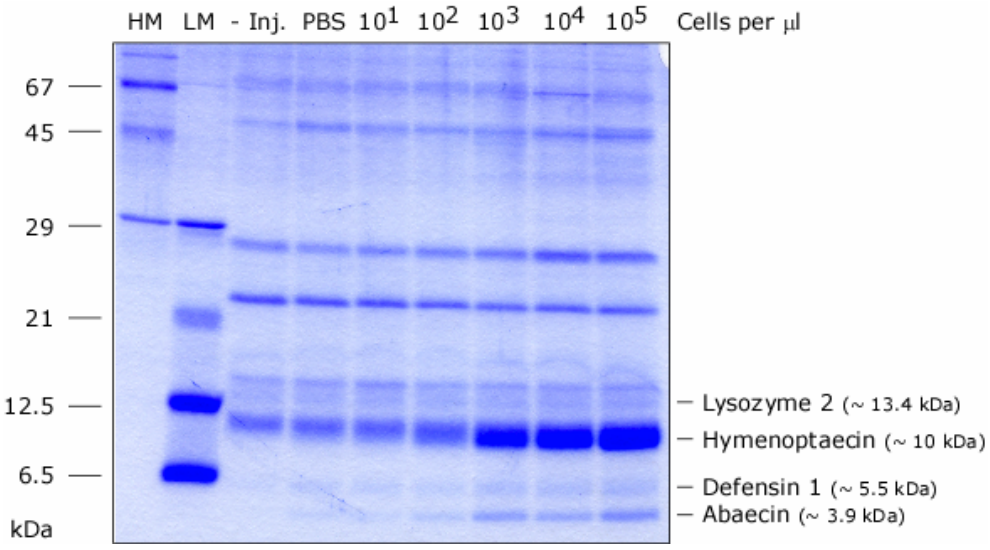

Fig. 3-4: Dose-dependent induction of antimicrobial peptides

SDS-PAGE analysis of AMP levels in the hemolymph of bacterial challenged bees. Newly emerged bees (0-18 h) were injected with 1 µl of either sterile 1xPBS (control) or 1xPBs containing *E. coli* ranging from 10^1 to 10^5 cells per µl. Bees were incubated at 35C and 70% humidity for 24 h. Hemolymph was taken from a pool of 7 to 10 bees and subjected to 100°C for 2 min followed by centrifugation. 5 µl of supernatants were analyzed on a 17.5% SDS-polyacrylamide gel. –Inj.: non-injected bees (control).

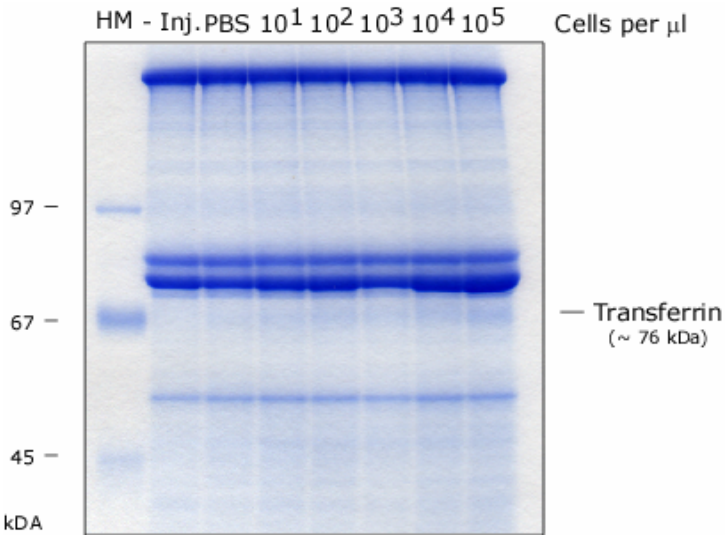

Fig. 3-5: Dose-dependent induction of transferrin

SDS-PAGE analysis of transferrin levels in the hemolymph of bacterial challenged bees. Newly emerged bees (0-18 h) injected with 1 µl of either sterile 1x PBS (control) or 1x PBS containing *E. coli* ranging from 10^1 to 10^5 cells per µl PBS. Bees were incubated at 35°C and 70% humidity for 24 h. Hemolymph was taken from a pool of 7 to 10 bees and 2.5 µl of each sample was analyzed on a 10% SDS-PAGE. –Inj.: non-injected bees (control).

bees. In addition, untreated hemolymph samples were analyzed on a 10% SDS-polyacrylamide gel to determine the expression levels of transferrin (Fig. 3-5). Low levels of transferrin were detected after aseptic injury of the cuticle (PBS) and further increased with increasing amounts of bacterial cells injected into the hemocoel.

3.4.3. Time-dependent induction of AMPs and transferrin

In order to investigate the accumulation of AMPs and transferrin in respect to post-injection time, groups of bees were injected with either heat-killed or untreated bacteria. Killing of bacteria was confirmed by spreading the remaining bacterial suspension onto an agar plate followed by incubation overnight at 37°. No growth was observed whereas untreated bacteria exhibited normal growth (data not shown). Following infection, groups of 10 bees were incubated for several hours (short term) to several days (long term) at 35°C. For further analysis a fraction of the collected hemolymph was subjected to heat-treatment.

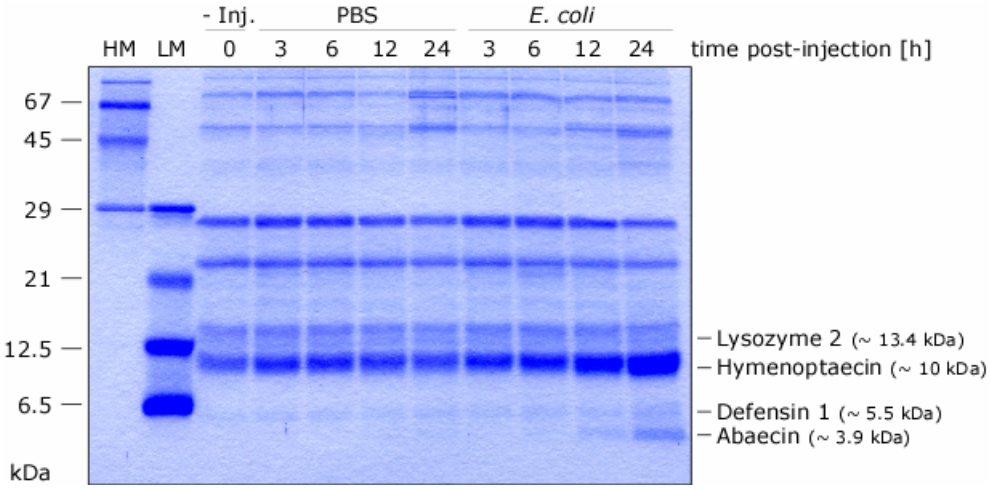

Fig. 3-6: Short term accumulation of antimicrobial peptides in the hemolymph

SDS-PAGE analysis of AMP levels in the hemolymph following bacterial infections. Newly emerged bees (0-18 h) were injected with 1 µl of either sterile 1xPBS (control) or 1xPBs containing 10^4 cells of *E. coli* per µl PBS. Bees were incubated at 35°C and 70% humidity for 3 to 24h. Hemolymph was taken from a pool of 7 to 10 bees and subjected to 100°C for 2 min followed by centrifugation. 5 µl of supernatants were analyzed on a 17.5% SDS-polyacrylamide gel. –Inj.: non-injected bees (control).

Supernatants of heat-treated hemolymph were analyzed on a 17.5% SDS-PA gel (Fig. 3-6). Traces of abaecin and hymenoptaecin were detected after 6 h post-induction and the amount of both peptides increased further with time. On the other hand expression of defensin 1 is hardly induced which is reflected in a slow rate of peptide accumulation in the hemolymph. As expected for Lys-2 protein, levels are not affected by bacterial infection. In case of long term kinetic studies, bees were

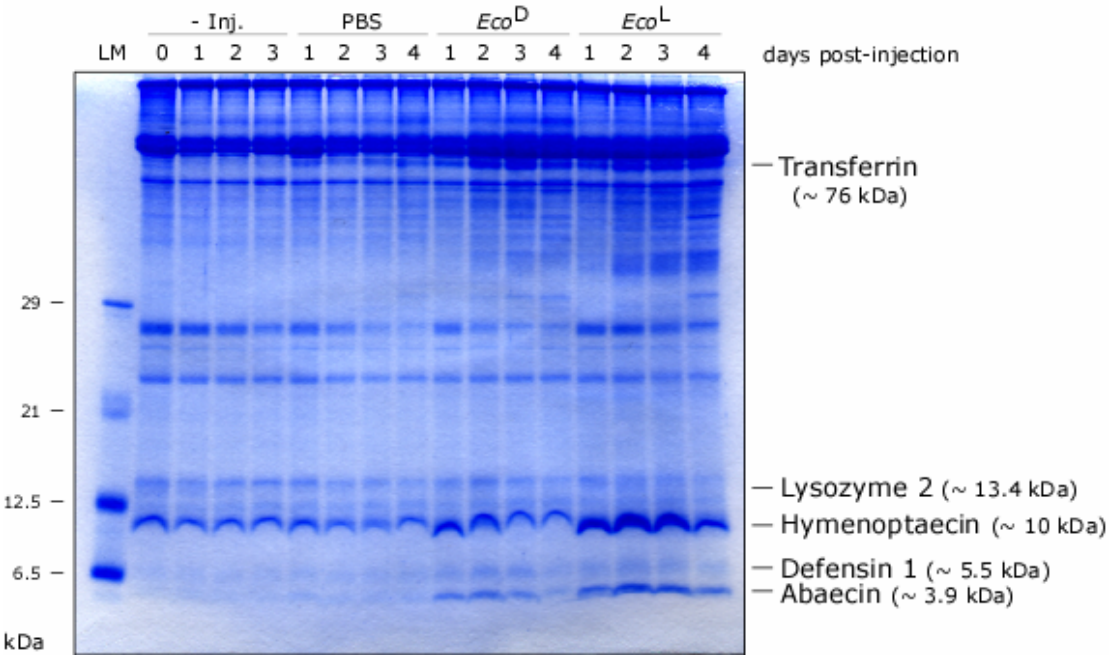

Fig. 3-7: Long term accumulation of antimicrobial peptides in the hemolymph

SDS-PAGE analysis of AMP levels in the hemolymph following bacterial infections. Newly emerged bees (0-18 h) were injected with 1 µl of either sterile 1xPBS (control) or 1xPBs containing 10^5 cells of *E. coli* per µl PBS. Bees were incubated at 35°C and 70% humidity for 24 to 96h. Hemolymph was taken from a pool of 7 to 10 bees and 2.5 µl of each sample were analyzed on a 17.5% SDS-polyacrylamide gel. –Inj.: non-injected bees (control); Eco^D: cells were heat-killed (15 min at 120°C) prior to injection; Eco^L: untreated cells.

injected with either heat-killed or untreated bacteria and incubated for 24 to 96 h before hemolymph was collected. The untreated samples were then analyzed on 17.5% and 10% SDS-PA gels (Fig. 3-7 and Fig. 3-8). Injection of heat-killed bacteria (Eco^D) lead to a moderate induction of abaecin and hymenoptaecin with accumulation reaching a maximum after 2 days followed by a decline in peptide

amounts in the hemolymph. Only small traces were detectable on day 4. A similar pattern was observed for bees injected with untreated bacteria (*Eco*^{L}), however, peptide expression appeared to be 2 to 4 fold higher compared to heat-killed bacteria. Induction of defensin 1 expression remained at equally low levels in both cases with an estimated expression maximum after 2 days. As observed above, Lys-2 expression was not affected. In case of transferrin (Fig. 3-8), aseptic injury of the cuticle (PBS) induced low expression of the protein with constant levels observed even after four days post-injection. Injection of heat-killed and untreated bacteria resulted in higher expression levels of similar intensity as compared with PBS injection. The peak accumulation was observed after 2 days and appeared to remain at constant levels on the following days with a slight decrease after day 4.

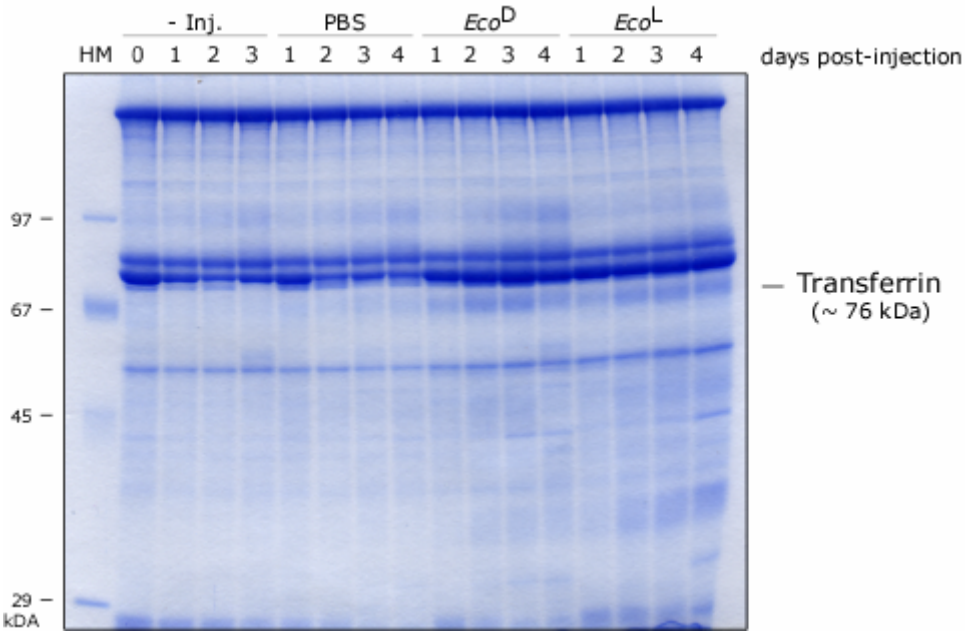

Fig. 3-8: Long term accumulation of transferrin in the hemolymph

SDS-PAGE analysis of transferrin levels in the hemolymph following bacterial infections. Newly emerged bees (0-18 h) were injected with 1 µl of either sterile 1xPBS (control) or 1xPBs containing 10^5 cells of *E. coli* per µl PBS. Bees were incubated at 35°C and 70% humidity for 24 to 96 h. Hemolymph was taken from a pool of 7 to 10 bees and 2.5 µl of each sample were analyzed on a 10% SDS-polyacrylamide gel. –Inj.: non-injected bees (control); *Eco*^{D}: cells were heat-killed (15 min at 120°C) prior to injection; *Eco*^{L}: untreated cells.

3.4.4. Induction of AMPs and transferrin by different bacterial species

The innate immune system uses a set of pattern-recognition receptors that recognize conserved molecular patterns on the surface of pathogens such as peptidoglycan unique to bacterial cell walls and lipopolysaccharids from the outer membrane of gram$^-$ bacteria. Since the cell wall composition differs greatly among bacteria species each organism is recognized differently which induces an immune response in a species specific manner. To investigate the induction of antimicrobial peptides with respect to the type of bacterium injected bees were treated with, either *E. coli* (similar to 3.4.3.) or *M. flavus*, a gram$^+$ type bacterium was used. Following injection and incubation over a period of four days the collected hemolymph samples were analyzed by SDS-PAGE (Fig. 3-9 and Fig. 3-10).

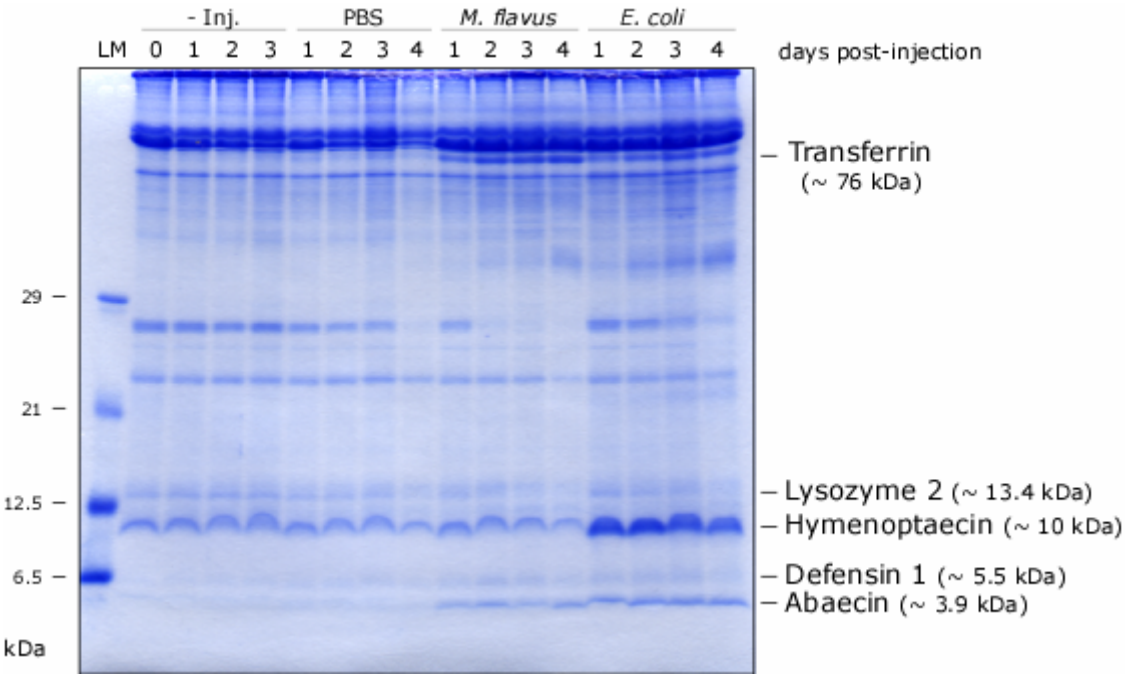

Fig. 3-9: Induction of antimicrobial peptides by *M. flavus* and *E. coli*

SDS-PAGE analysis of AMP levels in the hemolymph following bacterial infections. Newly emerged bees (0-18 h) were injected with 1 µl of either sterile 1xPBS (control) or 1xPBs containing either 10^5 cells of *M. flavus* or *E. coli* per µl PBS. Bees were incubated at 35°C and 70% humidity for 24 to 96 h. Hemolymph was taken from a pool of 7 to 10 bees and 2.5 µl of each sample were analyzed on a 17.5% SDS-polyacrylamide gel. - Inj.: non-injected bees (control).

A difference in expression levels was observed for hymenoptaecin which is hardly induced upon infection with *M. flavus* compared to a high induction rate when

treated with *E. coli*. On the other hand, expression of abaecin and defensin 1 was equally induced by both bacteria with little deviations in the peptide accumulation. As for Lys-2, expression levels were not affected by the infection of *M. flavus* when compared to *E. coli*. Furthermore, expression of transferrin was induced to a much greater extent when bees were injected with *M. flavus* than observed for *E. coli* (Fig. 3-9; Fig. 3-10).

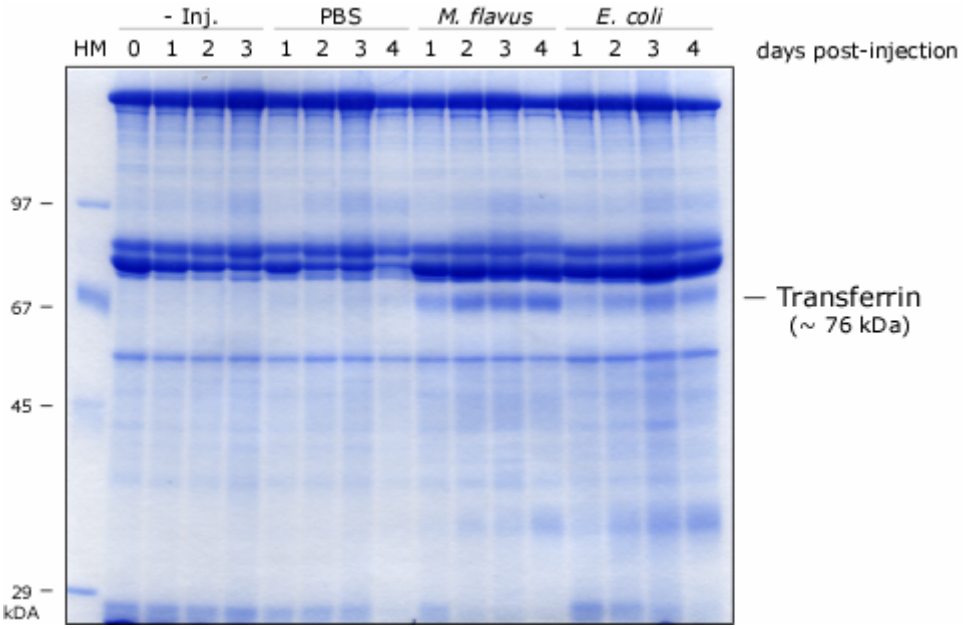

Fig. 3-10: Induction of transferrin by *M. flavus* and *E. coli*

SDS-PAGE analysis of transferrin levels in the hemolymph following bacterial infections. Newly emerged bees (0-18 h) were injected with 1 µl of either sterile 1xPBS (control) or 1xPBs containing either 10^5 cells of *M. flavus* or *E. coli* per µl PBS. Bees were incubated at 35°C and 70% humidity for 24 to 96 h. Hemolymph was taken from a pool of 7 to 10 bees and 2.5 µl of each sample were analyzed on a 10% SDS-polyacrylamide gel. - Inj.: non-injected bees (control).

3.4.5. Age-related regulation of AMPs and transferrin

Worker bees have a short life span of approximately 30 days in the summer, but may live several months during the winter. During this time they will undergo different developmental stages which dictate their role in the hive. Worker bees typically start there lives with cell cleaning (first 2 days), then perform brood rearing, so-called nursing (3 to 10 days of age), followed by a period of hive maintenance duties (11 to 20 days of age) and finally switch to colony defense and foraging when

they are about three weeks old (>21 days of age) (Page and Peng, 2001). To investigate a possible age-dependent regulation of the inducible antimicrobial peptides, several age series were performed. Newly emerged bees were color-labeled conveying the date of emergence and were given back into a visually healthy colony. Groups of 10 bees were sampled after 7, 14, 21, and 28 days post-emergence and were infected with *E. coli*. Following a 24 h incubation period,

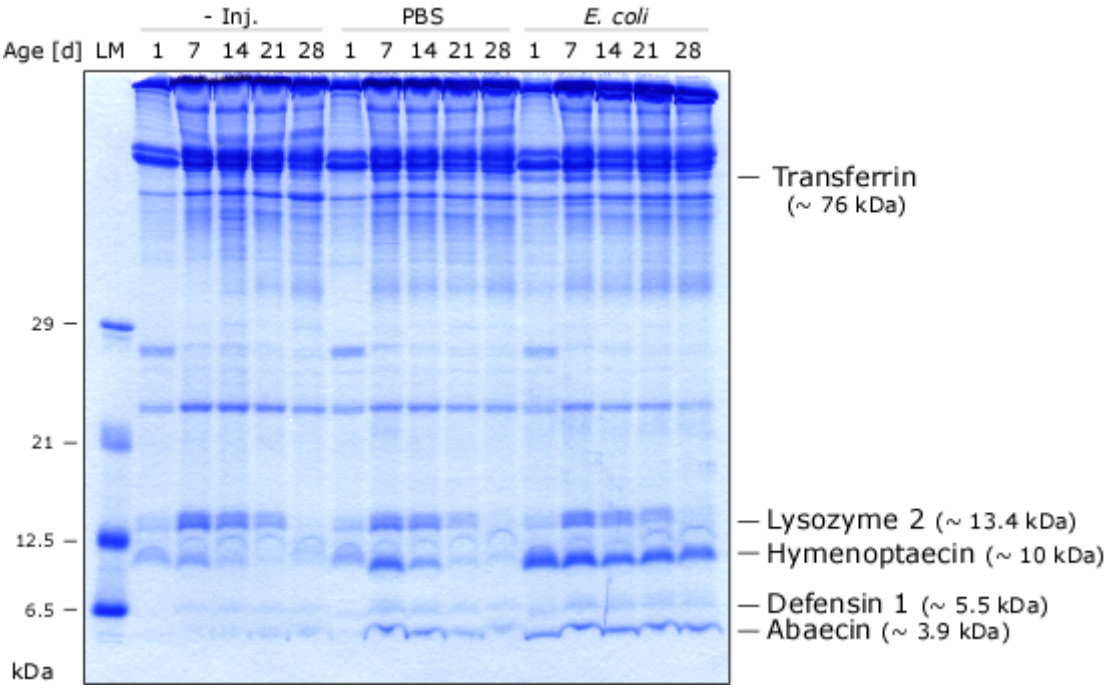

Fig. 3-11: Age-dependent induction of antimicrobial peptides

SDS-PAGE analysis of AMP levels in the hemolymph of different aged bees following bacterial infections. Bees of different ages (1-28 d) were taken out of a visually healthy colony and injected with 1 µl of either sterile 1xPBS (control) or 1xPBs containing 10^5 cells of *E. coli* per µl PBS. Bees were incubated at 35°C and 70% humidity for 24 h. Hemolymph was taken from a pool of 5 to 7 bees and 2.5 µl of each sample were analyzed on a 17.5% SDS-polyacrylamide gel. - Inj.: non-injected bees (control). Age series was performed in July 2005.

hemolymph was collected and stored until further use. The collected samples were finally analyzed by SDS-PAGE. Figure 3-11 shows the analysis of one such age series. Induced expression levels of abaecin and hymenoptaecin upon *E. coli* infection were observed to be comparably independent of the bee's age. Similarly, expression of defensin 1 remained at low levels and was not up-regulated at a particular age. However, an age-related effect on AMP induction was observed after injection of sterile PBS. While newly emerged bees did not show any induced

expression upon aseptic injury of the cuticle (similar to previous observations), abaecin, defensin 1 and hymenoptaecin were greatly induced in 7-day old bees. Furthermore, the intensity of induced expression declined with increasing age (days 14 to 28). Also noteworthy is the accumulation of Lys-2 in the hemolymph of untreated control bees (-Inj). Independent of injury and bacterial infection an increased accumulation of the enzyme was observed with a maximum reached in 7-day old bees followed by a linear decrease of induction levels with ongoing age. In case of transferrin a similar induction pattern following injections was observed as for abaecin, defensin and hymenoptaecin (Fig. 3-12). While bacterial infections induced the expression of comparable protein levels, PBS injections induced the highest level of transferrin at day 7 followed by an observed decline in protein induction.

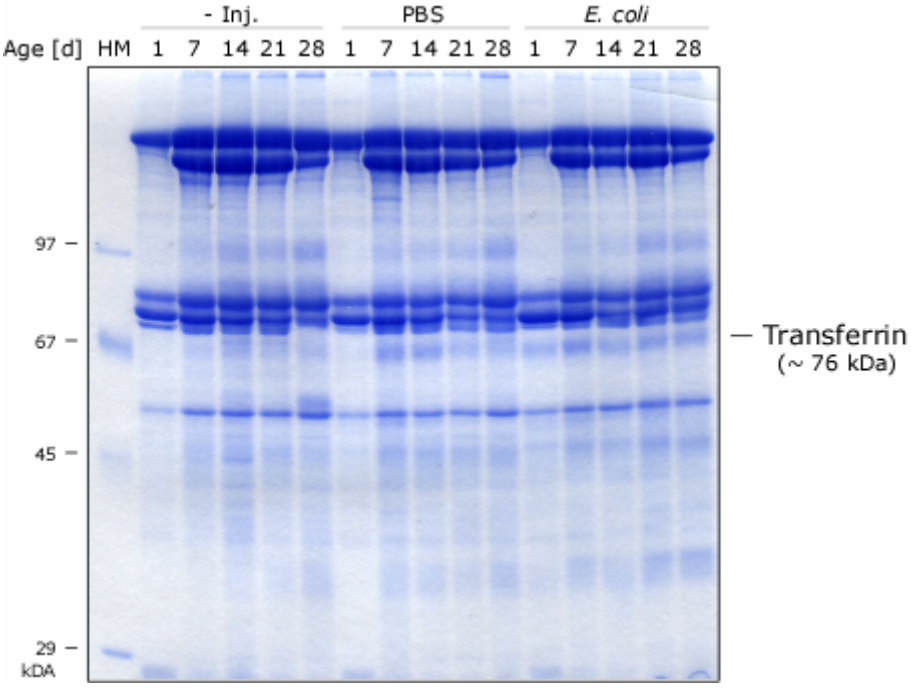

Fig.3-12: Age-dependent induction of transferrin

SDS-PAGE analysis of transferrin levels in the hemolymph of different aged bees following bacterial infections. Bees (1-28 d) were taken out of a visually healthy colony and injected with 1 µl of either sterile 1xPBS (control) or 1xPBS containing 10^5 cells of *E. coli* per µl PBS. Bees were incubated at 35°C and 70% humidity for 24 h. Hemolymph was taken from a pool of 5 to 7 bees and 2.5 µl of each sample were analyzed on a 10% SDS-polyacrylamide gel. - Inj.: non-injected bees (control). Age series was performed in July 2005.

3.4.6. Age-related accumulation of lysozyme 2 in winter bees

Based on the obtained results for Lys-2, a final age series was set up with the intention to analyze the accumulation of the enzyme in more detail. Due to the near ending of the bee season (April to August) it was not possible to obtain a brood of bees that can be truly be classified as summer bees, thus, in September 2005 emerged bees were considered to be winter bees that display a different physiology compared to their summer counterpart. Similar to the earlier age series, the newly emerged bees were color-labeled and transferred back into a visually healthy colony. Bees were sampled every other day. Hemolymph of 7 to 10 bees was directly collected and stored until the final sample was taken. Subsequently, the samples were analyzed on a 17.5% SDS-PA gel (Fig. 3-13). As expected, Lys-2 accumulated within the first week (days 1 to 7), however, a followed decline in protein levels was not observed. Moreover the protein accumulated further reaching levels of saturation after 11 days.

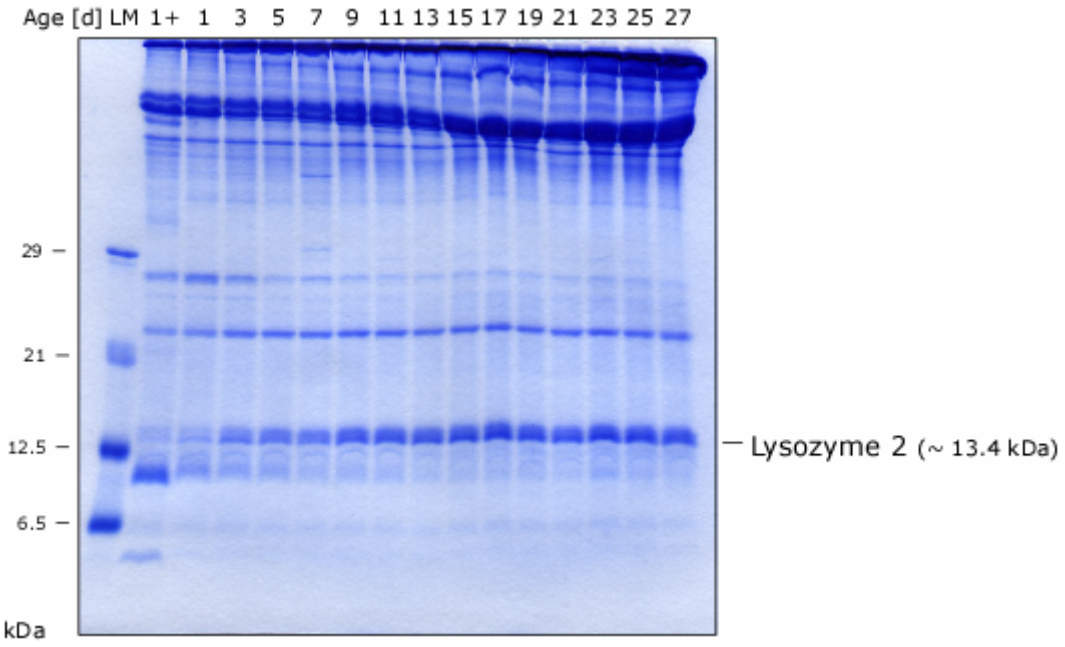

Fig. 3-13: Accumulation of lysozyme 2

SDS-PAGE analysis of lysozyme 2 levels in the hemolymph. Bees of different ages (1-27 d) were taken out of a visually healthy colony. Hemolymph was taken from a pool of 7 to 10 bees and 2.5 µl of each sample were analyzed on a 17.5% SDS-polyacrylamide gel. 1+: hemolymph from bacterial challenged bees. Age series was performed in September 2005.

3.5. Discussion

During evolution, the honey bee has developed different strategies to prevent, resist and overcome microbial and parasitic infections. Once the pathogen has breached the physical barrier, i.e. the cuticle, it is recognized by the immune system as non-self that triggers an induced cellular and humoral immune response. Part of this immune response is the production of four different antimicrobial peptides that are secreted into the hemolymph of *A. mellifera* upon infection (Casteels-Josson *et al.*, 1994). Applying SDS-polyacrylamide gel electrophoresis and mass spectrometry on hemolymph from immunized bees, three out of the four peptides were identified, i.e. abaecin, defensin 1 and hymenoptaecin (Fig. 3-1 and Fig. 3-2). Detection of the 2.1 kDa small apidaecins by SDS-PAGE was not possible. A likely explanation could be that the peptides were too small in order to be retained by gel fixation and thus diffused from the gel during the staining procedure. Besides the above mentioned antimicrobial peptides, a 76 kDa large inducible protein was identified which turned out to be transferrin. *A. mellifera* transferrin is a multifunctional iron-binding protein expressed under a wide range of developmental and physiological conditions (Kucharski and Maleszka, 2003). In insects, expression of transferrin was demonstrated to be up-regulated upon bacterial infection, suggesting a role in the innate immune system (Kucharski and Maleszka, 2003; Yoshiga *et al.*, 1999; Yoshiga *et al.*, 1997). Furthermore, the 13.4 kDa large lysozyme 2 (Lys-2) was identified in the hemolymph by mass spectrometry (Fig. 3-1, band 4), conclusively demonstrating the presence of a lysozyme in the hemolymph of *A. mellifera* for the first time.

Further characterization of the abovementioned peptides and proteins showed that the intensity of expression of the antibacterial peptides, abaecin, defensin 1, and hymenoptaecin as well as transferrin increased proportionally with the amount of bacteria injected into the hemocoel (Fig. 3-4 and Fig. 3-5). No such effect was observed for the protein levels of Lys-2, which remained at basal levels at any stage of infection, indicating that the gene expression of the putative antibacterial protein is not under the regulatory control of the Imd and Toll pathways. Both pathways have been assigned to be in control of expression of genes encoding antimicrobial peptides for humoral response in *Drosophila melanogaster* (Hoffmann, 2003; Hultmark, 2003). Based on homologues of both pathways found in the *A. mellifera* genome, the Imd and Toll pathways can be considered to be conserved in the honey bee, suggesting a direct role in the induced expression of abaecin, defensin 1 and hymenoptaecin. Whether expression of transferrin is also regulated by either of the

two pathways has not been elucidated, yet. Up-regulation of the three antibacterial peptides was observed within the first 24 h following infection (Fig. 3-6), with amounts of protein detectable after 6 and 12 h for hymenoptaecin and abaecin, respectively, while a minimal increase in the protein level was observed for defensin 1 after 24 h. Furthermore, it appears that protein levels reached saturation after 24 h and remained at relatively high levels for up to 36 h (Fig. 3-7). These results are in line with observations on the kinetics of mRNA accumulation following bacterial infections made by Casteels-Josson and colleagues (Casteels-Josson *et al.*, 1994). Applying Northern blot analysis they showed that transcripts of abaecin and hymenoptaecin accumulated constantly within the first 12 h post-infection and continued to accumulate for more than 36 h. In case of defensin 1 transcription was minimal and delayed with small traces detectable as late as 12 h after infection, supporting the observed minute quantities of peptide in the hemolymph. In terms of bacterial viability it was demonstrated that the number of bacteria once injected rapidly increased during the first hours of infection and than drastically decreased between 5 and 10 h post-infection. Due to the constant accumulation of antibacterial peptides for more than 36 h, it was further concluded that not all of the bacteria were eliminated within the first 10 h post-infection and thus minimal remaining traces of pathogen were sufficient to maintain a continuous activation of the humoral immune system (Casteels-Josson *et al.*, 1994). In case of transferrin, a similar pattern of protein accumulation in the hemolymph was observed as for abaecin and hymenoptaecin, with levels of saturation reached after 48 h (Fig. 3-8). However, slight differences in the expression patterns of abaecin and transferrin compared to hymenoptaecin were observed when heat-killed bacteria were injected. While substantial amounts of abaecin and transferrin were detectable over several days, injection of heat-killed bacteria resulted in a much weaker accumulation of hymenoptaecin. A similar observation was made after infection with the gram$^+$ bacterium *Micrococcus flavus* (Fig. 3-9 and Fig. 3-10). High and moderate protein levels were detectable for transferrin and abaecin upon infection, whereas hardly any accumulation of hymenoptaecin was observed. These results indicate that the gene expression of abaecin and transferrin is somehow positively correlated, and would suggest a shared regulatory pathway that differs from that of hymenoptaecin. This assumption finds support by the work of Yang and Cox-Foster, who investigated the suppression of antibacterial peptide genes in bees infested by the mite *varroa destructor* (Yang and Cox-Foster, 2005). They showed that in mite-infested bees the

pattern of gene expression of hymenoptaecin following bacterial infection greatly differs from the patterns observed for abaecin and defensin 1 which shared the same trend. These results indicated that expression of abaecin and defensin 1 are positively correlated, whereas hymenoptaecin expression is not correlated to either of the former two, leading to the conclusion that hymenoptaecin must use a different regulatory pathway than abaecin and defensin 1. In addition to the three antimicrobial peptides Yang and Cox-Foster also analyzed the expression patterns of four immune-related enzymes, i.e. phenoloxidase, glucose dehydrogenase, glucose oxidase, and lysozyme, which appears to be Lys-1 based on the sequences of PCR primers used. Expression of the genes encoding for the four enzymes was significantly positively correlated, suggesting a commonly shared transcriptional regulation that differs from those of the three antimicrobial peptides abaecin, defensin and hymenoptaecin. Noteworthy is the observation that gene expression levels of Lys-1 upon bacterial infected remained at the levels found in untreated bees. Despite the fact that Lys-1 was not identified in the hemolymph (Fig. 3-2) the results of Yang and Cox-Foster are inline with the herein described findings. Accumulation levels of Lys-2 in the hemolymph were not affected or stimulated by bacterial infection (Fig. 3-4, Fig. 3-9 and Fig. 3-11). This is most astonishing since almost all insect lysozymes isolated to date were found to be up-regulated upon bacterial infection (Bae and Kim, 2003; Fujimoto *et al.*, 2001; Gao and Fallon, 2000; Kang *et al.*, 1996; Lee and Brey, 1995; Lockey and Ourth, 1996; Morishima *et al.*, 1995; Mulnix and Dunn, 1994). These lysozymes are predominantly synthesized in the fat body and secreted into the hemolymph, thus considered to play a role in the immune response. The only exceptions are the lysozymes of *D. melanogaster* and *M. domestica* that are not expressed in the fat body or in hemocytes. The enzymes are constitutively expressed and solely found in the digestive tract of these insects, suggesting a change of function of lysozyme as a digestive enzyme (Daffre *et al.*, 1994; Ito *et al.*, 1995; Lemos and Terra, 1991).

Although bacterial infections don't seem to stimulate the production of Lys-2, different concentrations in the hemolymph were observed in bees of different ages, regardless of the applied treatment (Fig. 3-11). Levels of Lys-2 greatly increased within the first week post-emergence, followed by a decline in protein accumulation (days 7 to 28) with little to no levels detectable at 28 days. This result in itself is very interesting, for it suggests a correlation between the expression of Lys-2 and the age-related division of labor of adult worker honey bees. The age-related division

of labor is a key feature of many eusocial hymenopteran species and is based on a form of behavioral development by workers also known as age polyethism (Hoelldobler and Wilson, 1990). In *A. mellifera*, female workers typically begin with cell cleaning (first 2 days), then perform brood rearing, so-called nursing (3 to 10 days of age), followed by a period of hive maintenance duties (11 to 20 days of age) and finally switch to colony defense and foraging when they are about three weeks old (>21 days of age) (Page and Peng, 2001). The "behavioral pacemaker" in this age polyethism is the gonotrophic juvenile hormone (JH) (Robinson and Vargo, 1997). Radio immune assays and measurements of JH biosynthesis showed that JH titers are low in bees that work in hive performing brood care and other activities, and high in foragers (Fig. 3-14) (Huang *et al.*, 1994; Huang *et al.*, 1991; Robinson *et al.*, 1992). Huang and colleagues further showed that the JH titer in the hemolymph increases constantly at a slow rate from day one to day 14 followed by a drastic increase thereafter.

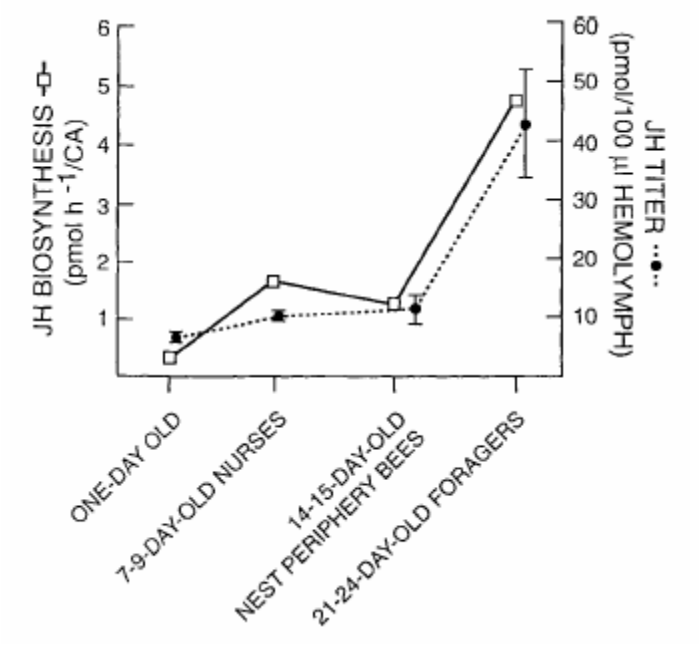

Fig. 3-14: Rates of juvenile hormone biosynthesis and hemolymph titer of JH in worker honey bees (Figure from Huang et al., 1991)

In terms of the gene expression of Lys-2 and other proteins, the JH titer might have an important regulatory function. Based on the observed pattern of Lys-2

accumulation one might assume that increasing hemolymph concentrations of JH up to a certain threshold could up-regulate the expression of Lys-2 (within the first 10 days), whereas concentrations above this threshold have a contrary effect by down-regulating the gene expression proportional to the levels of JH. This assumption would also explain the observation made for bees emerged in September (Fig. 3-13) were Lys-2 accumulated linearly within the first two weeks and remained at a constant level with ongoing age. Huang and Robinson revealed a seasonal related phenomenon in which the JH titer levels in younger, pre-foraging bees declined in the fall and then increased in the following spring as colony activity arose (Huang and Robinson, 1995). They further showed that these so-called "winter bees" have lower JH levels compared to summer nurse bees, which would support the hypothesis of a threshold mediated regulation of Lys-2 expression by JH. The observation that the expression of both lysozyme genes is not under the control of the two immune-related pathways, Imd and Toll, as well as a hydrolytic mechanism that differs from other insect lysozymes as proposed earlier (chapter 2) raises the overall question about the role of lysozymes in *A. mellifera*. A plausible answer might be that the lysozymes belong to a part of the innate immune system that can be modulated in accordance with the functional behavior of the individual worker bee within the colonial society. Having a correlation between the hemolymph titer of JH and the age-related accumulation of Lys-2 in the hemolymph would suggest such ability. A regulatory function of JH on parts of the honey bee immune system was previously suggested for the cellular defense machinery (Amdam *et al.*, 2004). Based on their and others observation, that in-hive bees possess higher numbers of hemocytes but low levels of JH compared to foragers (Fluri *et al.*, 1977; Huang and Robinson, 1995; Rutz *et al.*, 1974), Amdam and colleagues proposed a causal relationship between an increasing JH titer and a reduction in the number of functional hemocytes. In general the activation and the use of the immune system are thought to be costly and therefore cannot be sustained simultaneously with other demanding activities such as flying (Moret and Schmid-Hempel, 2000). Furthermore, healthy nurse bees are of greater importance to the overall survival of the colony than foragers, therefore high levels of lysozyme in the hemolymph of the former might be considered as precautious immunization to maximize the resistance against potential pathogens. This idea would further explain the observation that nurse bees were more sensitive towards an aseptic injury which led to an induction of the antimicrobial peptides abaecin, defensin and hymenoptaecin, compared to foragers

were no such induction was observed (Fig. 3-12). In this case it only can be speculated whether this phenomenon can also be correlated to the distinct JH titer found in nurse bees.

In order to further investigate the role of JH in the regulation of the immune system in general and the transcriptional activation of lysozyme expression in particular, one might consider experiments under conditions where the colony is deprived of a certain group of workers. In these so-called single-cohort colonies bee of a given age perform precocious tasks which has a direct effect on the JH titer (Huang and Robinson, 1992; Robinson *et al.*, 1989). According to Huang and Robinson, young bees show precocious foraging in colonies that lack a normal complement of foragers, and these precocious foragers have JH titers that are comparable to those of normal-age foragers. Vise versa, behavioral reversion of foragers that perform nursing occurs if there are no other nurses in the colony (Page, 1992; Robinson *et al.*, 1992), and these "reverted nurses" showed correspondingly lower JH titers. Therefore one would expect increasing and decreasing levels of lysozyme in "reversed nurses" and precocious forager, respectively, compared to same aged bee that perform their normal task. Furthermore, treatment of bees with the hormone would demonstrate that the transcriptional regulation of lysozyme and/or other immune-related peptides is directly affected by JH. Such injection of synthetic JH was demonstrated earlier to induce worker bees to forage precociously (Jaycox, 1976; Jaycox *et al.*, 1974). In terms of further characterization of the two lysozymes one might consider Northern blot or RT-PCR analysis to determine the tissue specific expression as well as the profile of transcriptional regulation. Furthermore, a tissue specific localization could be confirmed by Western blot analysis using commercially available antibodies against chicken egg-white lysozymes. This seems to be a cheap and promising approach since ChEWL antibodies have been demonstrated successfully in the detection of c-type lysozymes in insects (Gao and Fallon, 2000).

Summary

During evolution the honey bee *A. mellifera* has developed different strategies to prevent, resist and overcome microbial and parasitic infections. Once the pathogen has breached the physical barrier, i.e. the cuticle, and has entered the hemocoel, it induces cellular and humoral immune reactions, which results in the rapid elimination of the invader. In *A. mellifera* the humoral part of the immune system is comprised of a defined set of antimicrobial peptides that are mainly produced by the fat body upon infection. To date four classes of AMPs have been isolated and characterized from immunized bees that provide a broad-spectrum of antibacterial defense through complementarity. Furthermore, the bacteriolytic enzyme lysozyme, which hydrolyzes the β-1,4-glycosidic linkages in the peptidoglycan layer of bacterial cell walls, is thought to complete the set of AMPs. Direct evidence of the presence in the hemolymph and other tissues however is still outstanding.

With the progress in sequencing of the honey bee genome new data become available which allows the search and identification of genes coding for homologous proteins found in other organism. Two genes coding for c-type lysozymes were identified in the genome of *A. mellifera* through an online-based BLAST search. Expression of both intron-less genes seems not to be under the regulatory control of either of the two pathways involved in humoral insect immunity, i.e. Toll and Imd, since no NF-κB transcription factor binding sites are found upstream of the genes. The encoded Lys-1 and Lys-2 are 157 and 143 amino acid long, respectively, and share a sequence similarity of 90%. Further *in silico* analysis revealed a signal peptidase cleavage site at the N-terminus of each amino acid sequence, strongly suggesting a secretion of the enzymes into the surrounding environment of the producing cells. Sequence alignments of both amino acid sequences with other c-type lysozymes identified the highly conserved active site glutamic acid (Glu32) as well as eight highly conserved cysteine residues. However, an important aspartic acid (Asp50) in the active site that helps to stabilize a substrate intermediate during catalysis is replaced by a serine residue in the lysozymes of *A. mellifera*. The replacement of the active site aspartic acid in the honey bee lysozymes suggests a different catalytic mechanism and/or a different substrate-specificity in respect to other c-type lysozymes. Furthermore, 3D-models of Lys-1 and Lys-2 were generated based on the sequence similarity of *A. mellifera* lysozymes with other c-type lysozymes. The published 3D structure of the lysozyme from the silkmoth *Bombyx mori*, which shares the highest sequence similarity of all available structures with *A.*

mellifera lysozymes, was used as template for the construction of the 3D-models. The models of Lys-1 and Lys-2 suggest that both enzymes resemble, in large part, the structure of *B. mori* lysozyme.

In order to identify the set of AMPs in the hemolymph of *A. mellifera*, hemolymph of immunized bees was analyzed. Applying SDS-polyacrylamide gel electrophoresis and mass spectrometry on hemolymph from immunized bees, three out of the four peptides were identified, i.e. abaecin, defensin 1 and hymenoptaecin. Furthermore, Lys-2 was identified in the hemolymph by mass spectrometry, conclusively demonstrating the presence of a lysozyme in the hemolymph of *A. mellifera* for the first time. However, the protein levels of Lys-2 were not affected by bacterial injection, suggesting that the gene expression of the putative antibacterial protein is not under the regulatory control of the Imd and/or Toll pathway. Besides the abovementioned antimicrobial peptides, the 76 kDa large transferrin was also identified. Transferrin is an iron-binding protein that has been implicated in innate immunity in the honey bee. Furthermore, the effect of pathogenic dose, the timeline of peptide induction and the age-related accumulation of the aforementioned AMPs were studied. The intensity of expression of the antimicrobial peptides, abaecin, defensin 1, and hymenoptaecin as well as transferrin increased proportionally with the amount of bacteria injected into the hemocoel. No such effect was observed for the protein levels of Lys-2. Furthermore, up-regulation of the three antibacterial peptides and transferrin was observed within the first 24 h following infection with *E. coli* ($gram^-$). Infection with the $gram^+$ bacterium *Micrococcus flavus* resulted in high and moderate protein levels for transferrin and abaecin, respectively, whereas hardly any accumulation of hymenoptaecin was observed, indicating that the gene expression of abaecin and transferrin is somehow positively correlated, and would suggest a shared regulatory pathway that differs from that of hymenoptaecin. Although bacterial infections didn't seem to stimulate the production of Lys-2, different concentrations in the hemolymph were observed in bees of different ages, suggesting a correlation between the expression of Lys-2 and the age-related division of labor of adult worker honey bees, also known as age polyethism. The results further allow a proposed causal connection between the age-dependent accumulation of Lys-2 and the hemolymph titer of the gonotrophic hormone juvenile hormone, which is the "behavioral pacemaker" in adult honey bees, and thus, should be further investigated.

Zusammenfassung

Im Laufe der Evolution hat die Honigbiene *A. mellifera* verschiedene Strategien entwickelt, mikrobialle und parasitaere Infektion zu bekaempfen. Hat der pathogene Eindringling die physikalische Barriere, also die Kutikula, einmal durchbrochen, ruft er eine zellulaere und humorale Immunantwort hervor, welche zu einer rapiden Eliminierung des Pathogens fuehren. Der humorale Teil des Immunsystems der Honigbiene besteht aus einem definierten Satz von antimikrobiellen Peptiden, welche vornehmlich, nach erfolgter Infektion, im Fettkoerper gebildet werden. Bisher wurden vier Klassen solcher AMPs isoliert und charakterisiert. Durch die Komplementaritaet in ihrer Wirkungsweise ermoeglichen diese AMPs ein breites Spektrum an antimikrobieller Abwehr. Im allgemeinen wird auch das baktriolytische Enzym Lysozym, welches die β-1,4-glykosidische Bindung in der Peptidoglykanschicht bakterieller Zellwaende hydrolysiert, dem humoralen Immunsystem zugeschrieben. Jedoch fehlte bisher der direkte Beweis fuer eine Existenz des Lysozyms in der Hemolymphe oder anderen Gewebe der Honigbiene.
Mit der fortschreitenden Sequenzierung des Bienengenoms werden staendig neue Daten zur Verfuegung gestellt, die eine gezielte Suche und Identifizierung von homologen Protein in der Honigbiene ermoeglichen. Mittels einer web-basierenden BLAST-Suche konnten im Genom zwei Gene identifiziert werden, welche fuer Lysozyme des C-typs kodieren. Genauere Untersuchung der Genloci konnten zeigten, dass beide Geneabschnitte keine Bindestellen fuer Transkriptionsfaktoren der NF-κB-Familie aufweisen, und daher davon auszugehen ist, dass die Lysozyme-Gene nicht unter der Kontrolle der beiden regulatroischen Pathways Toll bzw. Imd, von denen man annimmt, dass sie die humorale Immunantwort regulieren, stehen. Die beiden Gene *lyz1* und *lyz2* kodieren ein 157 bzw. ein 143 Aminosaeure langes Protein, welche zu 90% sequenzielle Aehnlichkeiten aufweisen. Durch weitere *in silico* Analyse der Protein konnten an den N-termini Erkennungssignale der Signalpeptidase gefunden werden, welche darauf schliessen lassen, dass beide Lysozyme in die Zellumgebung sezerniert werden. Mittels Sequenzvergleiche beider *A. mellifera* Lysozyme mit anderen C-typ Lysozymen konnte die hochkonservierte und fuer den katalytische Aktivitaet essentielle Aminosaeure Glutamat 32 (Glu32), sowie acht konservierte Cysteine identifiziert werden. Erstaunlicherweise fehlt das fuer den katalytischen Mechanismus essentielle Aspartat 50 (Asp50), welches fuer die Stabilizierung von Intermediaerprodukten wichtig ist. In *A. mellifera* Lysozymen ist dieses Aspartat durch ein Serin substituiert, was darauf schliessen laesst, dass die

beiden Enzyme einen anderen Mechanism und/oder eine andere Substratspezifitaet aufweissen als dies fuer die C-typ Familie der Fall ist. In diesem Zusammenhang wurde ein evolutionaerer Pathway vorgesschlagen, der eine moegliche Transition von Serin zu Aspartat erklaert. Schliesslich konnten aufgrund der Sequenzhomologien zu anderen C-typ Lysozyme und anhand von bestehende Strukturen, 3D-Strukturmodelle der beiden Lysozyme erstellt werde. Die Modelle haben gezeigt, dass die Struktur der beide Enzyme groessenteils den Strukturen andere C-typ Lysozyme gleicht.

Zur Identifiezung vom AMPs in *A. mellifera*, wurde die Hemoplymphe immunisierte Bienen elektrophoretisch und massenspektrometrisch analysisiert. Die drei AMPs Abaecin, Defensin 1 und Hymenoptaecin konnten dabei verifiziert werden. Darueber hinaus wurde zum ersten Mal das Lys-2 in der Hemolymphe nachgewiessen. Anders als bei den drei Oben erwaehnten AMPs, wurde das Lys-2 jedoch nicht durch bakterielle Infektion induziert. Die konstitutive Expression des Lys-2 laesst darauf schliessen, dass es nicht, wie bereits erwaehnt, unter der Kontrolle der beiden immunspezifischen, regulatorischen Pathways Toll und Imd steht. Zusaetlich zu den AMPs wurde das 76 kDa grosse Transferrin, ein Eisen-bindendes Protein, identifiziert, welches eine Rolle in der angeborenen Immunitaet zugesprochen wird. Anhand der genauen Bestimmung der Peptide wurde desweiteren der Effekt der bakteriellen Dosis, der Zeitverlauf der Induktion und die alterabhaengige Induktion naeher untersucht. Die Intensitaet der Expression der AMPs Abaecin, Defensin 1 und Hymenoptaecin sowie Transferrin nahm proportional mit der Menge an injezierten Bakterien zu. Die Akkumulation von Lys-2 wurde dagegen nicht beeinflusst. Desweiteren konnte eine Hochregulierung der Expressionslevel der drei AMPs und Transferrin, nach erfolgter Infektion mit *E. coli*, innerhalb der ersten 24 Stunden beobachtet werden. Infektion mit dem gram$^+$ Bakterium *Micrococcus flavus* resultiert dagegen in hoch bzw. moderate Expression von Transferin und Abaecin, jedoch war kaum ein Anstieg der Expression von Hymenoptaecin zu verzeichnen. Dies laesst daraus schliessen, dass die Expression von Abaecin und Transferrin positiv korrelieren sind und spricht fuer einen gemeinsamen regulatorischen Pathway, der sich von dem des Hymenoptaecin unterscheidet. Trotz der Beobachtung, dass die Expression von Lys-2 nicht durch bakterielle Infection induziert wird, konnten unterschiedliche Expressionsmuster in Bienen unterschiedlichen Alters beobachtet werden, welche auf eine Korrelation zwischen der Expression des Lys-2 und der altersabhaengigen Arbeitsteilung adulter Honigbienen, dem sogenennten

Alterspolythismus, schliessen lassen. Aufgrund dessen, koennte man einen kausalen Zusammenhang zwischen der alterabhaengigen Akkumulation des Lys-2 und dem Hemolymphtiter des gonotrophen Juvenilhormons, welches fuer die Verhaltensaenderung adulter Bienen verantwortlich ist, sehen, welcher weiterer Untersuchungen bedarf.

Bibliography

Altschul, S. F., Madden, T. L., Schaffer, A. A., Zhang, J., Zhang, Z., Miller, W., and Lipman, D. J. (1997). Gapped BLAST and PSI-BLAST: a new generation of protein database search programs. Nucleic Acids Res *25*, 3389-3402.

Amdam, G. V., Simoes, Z. L., Hagen, A., Norberg, K., Schroder, K., Mikkelsen, O., Kirkwood, T. B., and Omholt, S. W. (2004). Hormonal control of the yolk precursor vitellogenin regulates immune function and longevity in honeybees. Exp Gerontol *39*, 767-773.

Andersen, S. O., Hojrup, P., and Roepstorff, P. (1995). Insect cuticular proteins. Insect Biochem Mol Biol *25*, 153-176.

Ashida, M., and Brey, P. T. (1995). Role of the integument in insect defense: pro-phenol oxidase cascade in the cuticular matrix. Proc Natl Acad Sci U S A *92*, 10698-10702.

Ashida, M., and Brey, P. T. (1998). Resent advances on the research of the insect prophenoloxidase cascade, In Molecular Mechanism of Immune Response in Insects, P. T. H. Brey, D., ed. (London: Chapman & Hall), pp. 135-172.

Bae, S., and Kim, Y. (2003). Lysozyme of the beet armyworm, *Spodoptera exigua*: activity induction and cDNA structure. Comp Biochem Physiol B Biochem Mol Biol *135*, 511-519.

Beintema, J. J., and Terwisscha van Scheltinga, A. C. (1996). Plant lysozymes. Exs *75*, 75-86.

Bendtsen, J. D., Nielsen, H., von Heijne, G., and Brunak, S. (2004). Improved prediction of signal peptides: SignalP 3.0. J Mol Biol *340*, 783-795.

Boman, H. G. (1995). Peptide antibiotics and their role in innate immunity. Annu Rev Immunol *13*, 61-92.

Brameld, K. A., and Goddard, W. A., 3rd (1998). The role of enzyme distortion in the single displacement mechanism of family 19 chitinases. Proc Natl Acad Sci U S A *95*, 4276-4281.

Brey, P. T., Lee, W. J., Yamakawa, M., Koizumi, Y., Perrot, S., Francois, M., and Ashida, M. (1993). Role of the integument in insect immunity: epicuticular abrasion and induction of cecropin synthesis in cuticular epithelial cells. Proc Natl Acad Sci U S A *90*, 6275-6279.

Bulet, P., Dimarcq, J. L., Hetru, C., Lagueux, M., Charlet, M., Hegy, G., Van Dorsselaer, A., and Hoffmann, J. A. (1993). A novel inducible antibacterial peptide of *Drosophila* carries an O-glycosylated substitution. J Biol Chem *268*, 14893-14897.

Bulet, P., Hetru, C., Dimarcq, J. L., and Hoffmann, D. (1999). Antimicrobial peptides in insects; structure and function. Dev Comp Immunol *23*, 329-344.

Bulet, P., Stocklin, R., and Menin, L. (2004). Anti-microbial peptides: from invertebrates to vertebrates. Immunol Rev *198*, 169-184.

Carreck, N. L., and Williams, I. H. (1998). The economic value of bees in the UK. Bee World *79*, 115-123.

Carter, P., and Wells, J. A. (1988). Dissecting the catalytic triad of a serine protease. Nature *332*, 564-568.

Casteels-Josson, K., Capaci, T., Casteels, P., and Tempst, P. (1993). Apidaecin multipeptide precursor structure: a putative mechanism for amplification of the insect antibacterial response. Embo J *12*, 1569-1578.

Casteels-Josson, K., Zhang, W., Capaci, T., Casteels, P., and Tempst, P. (1994). Acute transcriptional response of the honeybee peptide-antibiotics gene repertoire and required post-translational conversion of the precursor structures. J Biol Chem *269*, 28569-28575.

Casteels, P., Ampe, C., Jacobs, F., and Tempst, P. (1993). Functional and chemical characterization of Hymenoptaecin, an antibacterial polypeptide that is infection-inducible in the honeybee (*Apis mellifera*). J Biol Chem *268*, 7044-7054.

Casteels, P., Ampe, C., Jacobs, F., Vaeck, M., and Tempst, P. (1989). Apidaecins: antibacterial peptides from honeybees. Embo J *8*, 2387-2391.

Casteels, P., Ampe, C., Riviere, L., Van Damme, J., Elicone, C., Fleming, M., Jacobs, F., and Tempst, P. (1990). Isolation and characterization of abaecin, a major antibacterial response peptide in the honeybee (*Apis mellifera*). Eur J Biochem *187*, 381-386.

Casteels, P., Romagnolo, J., Castle, M., Casteels-Josson, K., Erdjument-Bromage, H., and Tempst, P. (1994). Biodiversity of apidaecin-type peptide antibiotics. Prospects of manipulating the antibacterial spectrum and combating acquired resistance. J Biol Chem *269*, 26107-26115.

Casteels, P., and Tempst, P. (1994). Apidaecin-type peptide antibiotics function through a non-poreforming mechanism involving stereospecificity. Biochem Biophys Res Commun *199*, 339-345.

Cerenius, L., and Soderhall, K. (2004). The prophenoloxidase-activating system in invertebrates. Immunol Rev *198*, 116-126.

Chen, C., Ratcliffe, N. A., and Rowley, A. F. (1993). Detection, isolation and characterization of multiple lectins from the haemolymph of the cockroach *Blaberus discoidalis*. Biochem J *294 (Pt 1)*, 181-190.

Chernysh, S., Cociancich, S., Briand, J.-P., Hetru, C., and Bulet, P. (1996). The inducible antibacterial peptides of the hemipteran insect *Palomena prasina*: identification of a unique family of proline-rich peptids and of a novel insect defensin. Journal of Insect Physiology *42*, 81-89.

Choe, K. M., Werner, T., Stoven, S., Hultmark, D., and Anderson, K. V. (2002). Requirement for a peptidoglycan recognition protein (PGRP) in Relish activation and antibacterial immune responses in *Drosophila*. Science *296*, 359-362.

Daffre, S., Kylsten, P., Samakovlis, C., and Hultmark, D. (1994). The lysozyme locus in *Drosophila melanogaster*: an expanded gene family adapted for expression in the digestive tract. Mol Gen Genet *242*, 152-162.

Dickinson, L., Russell, V., and Dunn, P. E. (1988). A family of bacteria-regulated, cecropin D-like peptides from *Manduca sexta*. J Biol Chem *263*, 19424-19429.

Dunn, P. E., Bohnert, T. J., and Russell, V. (1994). Regulation of antibacterial protein synthesis following infection and during metamorphosis of *Manduca sexta*. Ann N Y Acad Sci *712*, 117-130.

Engstrom, A., Xanthopoulos, K. G., Boman, H. G., and Bennich, H. (1985). Amino acid and cDNA sequences of lysozyme from *Hyalophora cecropia*. Embo J *4*, 2119-2122.

Fant, F., Vranken, W., Broekaert, W., and Borremans, F. (1998). Determination of the three-dimensional solution structure of *Raphanus sativus* antifungal protein 1 by 1H NMR. J Mol Biol *279*, 257-270.

Fehlbaum, P., Bulet, P., Michaut, L., Lagueux, M., Broekaert, W. F., Hetru, C., and Hoffmann, J. A. (1994). Insect immunity. Septic injury of *Drosophila* induces the synthesis of a potent antifungal peptide with sequence homology to plant antifungal peptides. J Biol Chem *269*, 33159-33163.

Fluri, P., Wille, H., Gerig, L., and Luescher, M. (1977). Juvenile hormone, vitellogenin and heamocyte composition in winter worker honeybees (*Apis meliffera*). Experientia *33*, 1240-1241.

Fujimoto, S., Toshimori-Tsuda, I., Kishimoto, K., Yamano, Y., and Morishima, I. (2001). Protein purification, cDNA cloning and gene expression of lysozyme from eri-silkworm, *Samia cynthia ricini*. Comp Biochem Physiol B Biochem Mol Biol *128*, 709-718.

Fujiwara, S., Imai, J., Fujiwara, M., Yaeshima, T., Kawashima, T., and Kobayashi, K. (1990). A potent antibacterial protein in royal jelly. Purification and determination of the primary structure of royalisin. J Biol Chem *265*, 11333-11337.

Gao, Y., and Fallon, A. M. (2000). Immune activation upregulates lysozyme gene expression in *Aedes aegypti* mosquito cell culture. Insect Mol Biol *9*, 553-558.

Garvey, K. J., Saedi, M. S., and Ito, J. (1986). Nucleotide sequence of *Bacillus phage phi 29* genes 14 and 15: homology of gene 15 with other phage lysozymes. Nucleic Acids Res *14*, 10001-10008.

Gasteiger, E., Hoogland, C., Gattiker, A., Duvaud, S., Wilkins, M. R., Appel, R. D., and Bairoch, A. (2005). Protein Identification and Analysis Tools on the ExPASy Server, In The Proteomics Protocols Handbook, J. M. Walker, ed. (Humana Press), pp. 571-607.

Gillespie, J. P., Kanost, M. R., and Trenczek, T. (1997). Biological mediators of insect immunity. Annu Rev Entomol *42*, 611-643.

Gottar, M., Gobert, V., Michel, T., Belvin, M., Duyk, G., Hoffmann, J. A., Ferrandon, D., and Royet, J. (2002). The *Drosophila* immune response against Gram-negative bacteria is mediated by a peptidoglycan recognition protein. Nature *416*, 640-644.

Guex, N., and Peitsch, M. C. (1997). SWISS-MODEL and the Swiss-PdbViewer: an environment for comparative protein modeling. Electrophoresis *18*, 2714-2723.

Gupta, A. P. (1979). Hemocyte types: their structure, synonymies, interrelations, and taxonomic significants, In Insect Hemocytes, A. P. Gupta, ed. (Cambridge Univ Press), pp. 85-127.

Gupta, A. P. (1985). Cellular elements of the heamolymph, In Comprehensive Insect Physiology, Biochemistry and Pharmacology, G. A. G. Kerkut, L. I., ed. (Oxfort: Pergamon Press), pp. 401-451.

Hadfield, A. T., Harvey, D. J., Archer, D. B., MacKenzie, D. A., Jeenes, D. J., Radford, S. E., Lowe, G., Dobson, C. M., and Johnson, L. N. (1994). Crystal structure of the mutant D52S hen egg white lysozyme with an oligosaccharide product. J Mol Biol *243*, 856-872.

Hancock, R. E., and Diamond, G. (2000). The role of cationic antimicrobial peptides in innate host defences. Trends Microbiol *8*, 402-410.

Hara, S., and Yamakawa, M. (1995). A novel antibacterial peptide family isolated from the silkworm, *Bombyx mori*. Biochem J *310 (Pt 2)*, 651-656.

Hergenhahn, H. G., Aspan, A., and Soderhall, K. (1987). Purification and characterization of a high-Mr proteinase inhibitor of pro-phenol oxidase activation from crayfish plasma. Biochem J *248*, 223-228.

Hoelldobler, B., and Wilson, E. O. (1990). The ants (Cambridge, Mass.: Belknap Press of Harvard University Press).

Hoffmann, J. A. (2003). The immune response of *Drosophila*. Nature *426*, 33-38.

Holtje, J. V. (1996). Bacterial lysozymes. Exs *75*, 65-74.

Hopkins, T. L., and Kramer, K. J. (1992). Insect cuticle sclerotization. Annu Rev Entomol *32*, 71-93.

Huang, Z. Y., and Robinson, G. E. (1992). Honeybee colony integration: worker-worker interactions mediate hormonally regulated plasticity in division of labor. Proc Natl Acad Sci U S A *89*, 11726-11729.

Huang, Z. Y., and Robinson, G. E. (1995). Seasonal changes in juvenile hormone titers and rates of biosynthesis in honey bees. J Comp Physiol [B] *165*, 18-28.

Huang, Z. Y., Robinson, G. E., and Borst, D. W. (1994). Physiological correlates of division of labor among similarly aged honey bees. J Comp Physiol [A] *174*, 731-739.

Huang, Z. Y., Robinson, G. E., Tobe, S. S., Yagi, K. J., Strambi, C., and Stay, B. (1991). Hormonal regulation of behavioural development in the honey bee is based on changes in the rate of juvenile hormone biosynthesis. J Insect Physiol *37*, 733-741.

Hultmark, D. (1996). Insect lysozymes, In Lysozymes: Model Enzymes in Biochemistry and Biology, P. Jolles, ed. (Basel), pp. 87-102.

Hultmark, D. (2003). Drosophila immunity: paths and patterns. Curr Opin Immunol *15*, 12-19.

Irving, P., Troxler, L., Heuer, T. S., Belvin, M., Kopczynski, C., Reichhart, J. M., Hoffmann, J. A., and Hetru, C. (2001). A genome-wide analysis of immune responses in *Drosophila*. Proc Natl Acad Sci U S A *98*, 15119-15124.

Ito, Y., Nakamura, M., Hotani, T., and Imoto, T. (1995). Insect lysozyme from house fly (*Musca domestica*) larvae: possible digestive function based on sequence and enzymatic properties. J Biochem (Tokyo) *118*, 546-551.

Janeway, C. (2005). Immunobiology: the immune system in health and disease, 6th edn (New York: Garland Science).

Janeway, C. A., Jr. (1989). Approaching the asymptote? Evolution and revolution in immunology. Cold Spring Harb Symp Quant Biol *54 Pt 1*, 1-13.

Jaycox, E. R. (1976). Behavioral changes in worker honey bees (*Apis mellifera* L.) after injection with synthetic juvenile hormone (*Hymenoptera: Apidae*). J Kansas Entomol Soc *49*, 165-170.

Jaycox, E. R., Skowronek, W., and Gwynn, G. (1974). Behavioral changes in worker honey bees (*Apis mellifera*) induced by injections of a juvenile hormone mimic. Ann Entomol Soc Am *67*, 529-534.

Jeanmougin, F., Thompson, J. D., Gouy, M., Higgins, D. G., and Gibson, T. J. (1998). Multiple sequence alignment with Clustal X. Trends Biochem Sci *23*, 403-405.

Jolles, J., and Jolles, P. (1975). The losozyme from *Asterias rubens*. Eur J Biochem *54*, 19-23.

Kang, D., Romans, P., and Lee, J. Y. (1996). Analysis of a lysozyme gene from the malaria vector mosquito, *Anopheles gambiae*. Gene *174*, 239-244.

Koganesawa, N., Aizawa, T., Masaki, K., Matsuura, A., Nimori, T., Bando, H., Kawano, K., and Nitta, K. (2001). Construction of an expression system of insect lysozyme lacking thermal stability: the effect of selection of signal sequence on level of expression in the *Pichia pastoris* expression system. Protein Eng *14*, 705-710.

Koizumi, N., Imai, Y., Morozumi, A., Imamura, M., Kadotani, T., Yaoi, K., Iwahana, H., and Sato, R. (1999). Lipopolysaccharide-binding protein of *Bombyx mori* participates in a hemocyte-mediated defense reaction against gram-negative bacteria. J Insect Physiol *45*, 853-859.

Kucharski, R., and Maleszka, R. (2003). Transcriptional profiling reveals multifunctional roles for transferrin in the honeybee, *Apis mellifera*. J Insect Sci *3*, 27.

Kumagai, I., and Miura, K. (1989). Enhanced bacteriolytic activity of hen egg-white lysozyme due to conversion of Trp62 to other aromatic amino acid residues. J Biochem (Tokyo) *105*, 946-948.

Kurata, S. (2004). [Recognition of infectious non-self and activation of immune responses by peptidoglycan recognition protein (PGRP)--family members in *Drosophila*]. Tanpakushitsu Kakusan Koso *49*, 1174-1178.

Kuroki, R., Weaver, L. H., and Matthews, B. W. (1999). Structural basis of the conversion of T4 lysozyme into a transglycosidase by reengineering the active site. Proc Natl Acad Sci U S A *96*, 8949-8954.

Laemmli, U. K. (1970). Cleavage of structural proteins during the assembly of the head of *bacteriophage T4*. Nature *227*, 680-685.

Lamberty, M., Caille, A., Landon, C., Tassin-Moindrot, S., Hetru, C., Bulet, P., and Vovelle, F. (2001). Solution structures of the antifungal heliomicin and a selected variant with both antibacterial and antifungal activities. Biochemistry *40*, 11995-12003.

Lamberty, M., Zachary, D., Lanot, R., Bordereau, C., Robert, A., Hoffmann, J. A., and Bulet, P. (2001). Insect immunity. Constitutive expression of a cysteine-rich antifungal and a linear antibacterial peptide in a termite insect. J Biol Chem *276*, 4085-4092.

Lavine, M. D., and Strand, M. R. (2002). Insect hemocytes and their role in immunity. Insect Biochem Mol Biol *32*, 1295-1309.

Lee, S. Y., Wang, R., and Soderhall, K. (2000). A lipopolysaccharide- and beta-1,3-glucan-binding protein from hemocytes of the freshwater crayfish *Pacifastacus leniusculus*. Purification, characterization, and cDNA cloning. J Biol Chem *275*, 1337-1343.

Lee, W. J., and Brey, P. T. (1995). Isolation and characterization of the lysozyme-encoding gene from the silkworm *Bombyx mori*. Gene *161*, 199-203.

Lemaitre, B., Nicolas, E., Michaut, L., Reichhart, J. M., and Hoffmann, J. A. (1996). The dorsoventral regulatory gene cassette spatzle/Toll/cactus controls the potent antifungal response in *Drosophila* adults. Cell *86*, 973-983.

Lemos, F. J., and Terra, W. R. (1991). *Digestion* of bacteria and the role of midgut lysozyme in some insect larvae. Comp Biochem Physiol B *100*, 265-268.

Levashina, E. A., Ohresser, S., Bulet, P., Reichhart, J. M., Hetru, C., and Hoffmann, J. A. (1995). Metchnikowin, a novel immune-inducible proline-rich peptide from *Drosophila* with antibacterial and antifungal properties. Eur J Biochem *233*, 694-700.

Liang, Z., Sottrup-Jensen, L., Aspan, A., Hall, M., and Soderhall, K. (1997). Pacifastin, a novel 155-kDa heterodimeric proteinase inhibitor containing a unique transferrin chain. Proc Natl Acad Sci U S A *94*, 6682-6687.

Liu, F., Cui, L., Cox-Foster, D., and Felton, G. W. (2004). Characterization of a salivary lysozyme in larval *Helicoverpa zea*. J Chem Ecol *30*, 2439-2457.

Lockey, T. D., and Ourth, D. D. (1996). Purification and characterization of lysozyme from hemolymph of *Heliothis virescens* larvae. Biochem Biophys Res Commun *220*, 502-508.

Lumb, K. J., Aplin, R. T., Radford, S. E., Archer, D. B., Jeenes, D. J., Lambert, N., MacKenzie, D. A., Dobson, C. M., and Lowe, G. (1992). A study of D52S hen lysozyme-GlcNAc oligosaccharide complexes by NMR spectroscopy and electrospray mass spectrometry. FEBS Lett *296*, 153-157.

Malcolm, B. A., Rosenberg, S., Corey, M. J., Allen, J. S., de Baetselier, A., and Kirsch, J. F. (1989). Site-directed mutagenesis of the catalytic residues Asp-52 and Glu-35 of chicken egg white lysozyme. Proc Natl Acad Sci U S A *86*, 133-137.

Malke, H. (1965). [On the presence of lysozyme in insects]. Z Allg Mikrobiol *5*, 42-47.

Marmaras, V. J., Charalambidis, N. D., and Zervas, C. G. (1996). Immune response in insects: the role of phenoloxidase in defense reactions in relation to melanization and sclerotization. Arch Insect Biochem Physiol *31*, 119-133.

Mason, H. S. (1965). Oxidases. Annu Rev Biochem *34*, 595-634.

Matsumura, I., and Kirsch, J. F. (1996). Is aspartate 52 essential for catalysis by chicken egg white lysozyme? The role of natural substrate-assisted hydrolysis. Biochemistry *35*, 1881-1889.

Matsuura, A., Yao, M., Aizawa, T., Koganesawa, N., Masaki, K., Miyazawa, M., Demura, M., Tanaka, I., Kawano, K., and Nitta, K. (2002). Structural analysis of an insect lysozyme exhibiting catalytic efficiency at low temperatures. Biochemistry *41*, 12086-12092.

Medzhitov, R., and Janeway, C. A., Jr. (1997). Innate immunity: impact on the adaptive immune response. Curr Opin Immunol *9*, 4-9.

Michaut, L., Fehlbaum, P., Moniatte, M., Van Dorsselaer, A., Reichhart, J. M., and Bulet, P. (1996). Determination of the disulfide array of the first inducible antifungal peptide from insects: drosomycin from Drosophila melanogaster. FEBS Lett *395*, 6-10.

Michel, T., Reichhart, J. M., Hoffmann, J. A., and Royet, J. (2001). *Drosophila* Toll is activated by Gram-positive bacteria through a circulating peptidoglycan recognition protein. Nature *414*, 756-759.

Miller, J. S., and Stanley, D. W. (1998). Techniques for Assaying Nodulation in Insects, In Techniques in Insect Immunity, A. D. Wiesner, G. B.; Marmaras, V. J.; Morishima, I.; Sugumaran, M.; Yamakawa, M, ed. (Fair Haven, NJ: SOS Pub.), pp. 265-270.

Mohrig, W., and Messner, B. (1968). [Lysozyme as antibacterial agent in honey and bees venom]. Acta Biol Med Ger *21*, 85-95.

Moret, Y., and Schmid-Hempel, P. (2000). Survival for immunity: the price of immune system activation for bumblebee workers. Science *290*, 1166-1168.

Morishima, I., Horiba, T., Iketani, M., Nishioka, E., and Yamano, Y. (1995). Parallel induction of cecropin and lysozyme in larvae of the silkworm, *Bombyx mori*. Dev Comp Immunol *19*, 357-363.

Mulnix, A. B., and Dunn, P. E. (1994). Structure and induction of a lysozyme gene from the tobacco hornworm, *Manduca sexta*. Insect Biochem Mol Biol *24*, 271-281.

Page, R. E., Jr., and Peng, C. Y. (2001). Aging and development in social insects with emphasis on the honey bee, *Apis mellifera* L. Exp Gerontol *36*, 695-711.

Page, R. E., Jr.; Robinson, G. E.; Britton, D. S.; Fondrk, M. K. (1992). Genotypic variability for rates of behavioral development in worker honey bees (*Apis mellifera* L.). Behav Ecol *3*, 173-180.

Parkinson, N., Smith, I., Weaver, R., and Edwards, J. P. (2001). A new form of arthropod phenoloxidase is abundant in venom of the parasitoid wasp Pimpla hypochondriaca. Insect Biochem Mol Biol *31*, 57-63.

Peitsch, M. C. (1995). Protein modeling by E-mail. Bio/Technology *13*, 658-660.

Phillips, D. C. (1966). The three-dimensional structure of an enzyme molecule. Sci Am *215*, 78-90.

Prager, E. M., and Jolles, P. (1996). Animal lysozymes c and g: an overview. Exs *75*, 9-31.

Qasba, P. K., and Kumar, S. (1997). Molecular divergence of lysozymes and alpha-lactalbumin. Crit Rev Biochem Mol Biol *32*, 255-306.

Ratcliffe, N. A., and Rowley, A. F. (1979). A comparative synopsis of the structure and function of the blood cells of insects and other invertebrates. Dev Comp Immunol *3*, 189-221.

Rees, J. A., Moniatte, M., and Bulet, P. (1997). Novel antibacterial peptides isolated from a European bumblebee, *Bombus pascuorum* (*Hymenoptera, Apoidea*). Insect Biochem Mol Biol *27*, 413-422.

Regel, R., Matioli, S. R., and Terra, W. R. (1998). Molecular adaptation of *Drosophila melanogaster* lysozymes to a digestive function. Insect Biochem Mol Biol *28*, 309-319.

Robinson, G. E., Page, R. E. j., Strambi, A., and Strambi, C. (1989). Hormonal and genetic control of behavioral integration in honey bee colonies. Science *246*, 109-112.

Robinson, G. E., Strambi, C., Strambi, A., and Huang, Z. Y. (1992). Reproduction in worker honey bees is associated with low juvenile hormone titers and rates of biosynthesis. Gen Comp Endocrinol *87*, 471-480.

Robinson, G. E., and Vargo, E. L. (1997). Juvenile hormone in adult eusocial Hymenoptera: gonadotropin and behavioral pacemaker. Arch Insect Biochem Physiol *35*, 559-583.

Russell, V. W., and Dunn, P. E. (1991). Lysozyme in the midgut of *Manduca sexta* during metamorphosis. Arch Insect Biochem Physiol *17*, 67-80.

Russell, V. W., and Dunn, P. E. (1996). Antimicrobial proteins in the midgut of *Manduca sexta* during metamorphosis. J Insect Physiol *42*, 65-72.

Rutz, W., Luzio, G., Wille, H., and Luescher, M. (1974). A bio-assay for juvenile hormone (JH) effects of insect growth regulators (IGR) on adult worker honeybees. Bull Soc Entomol Sueisse *47*, 307-313.

Sambrook, J., and Russell, D. W. (2001). Molecular cloning: a laboratory manual, 3rd edn (Cold Spring Harbor, N.Y.: Cold Spring Harbor Laboratory Press).

Schagger, H., and von Jagow, G. (1987). Tricine-sodium dodecyl sulfate-polyacrylamide gel electrophoresis for the separation of proteins in the range from 1 to 100 kDa. Anal Biochem *166*, 368-379.

Scholz, F. R., Beetz, S., Lesch, C., Holthusen, T. K., and Trenczek, T. (1999). Wie wehren sich Insekten gegen Krankheitserreger? Spiegel der Forschung *16*, 46-54.

Schuhmann, B., Seitz, V., Vilcinskas, A., and Podsiadlowski, L. (2003). Cloning and expression of gallerimycin, an antifungal peptide expressed in immune response of greater wax moth larvae, *Galleria mellonella*. Arch Insect Biochem Physiol *53*, 125-133.

Schwede, T., Kopp, J., Guex, N., and Peitsch, M. C. (2003). SWISS-MODEL: An automated protein homology-modeling server. Nucleic Acids Res *31*, 3381-3385.

Shin, S. W., Park, D. S., Kim, S. C., and Park, H. Y. (2000). Two carbohydrate recognition domains of *Hyphantria cunea* lectin bind to bacterial lipopolysaccharides through O-specific chain. FEBS Lett *467*, 70-74.

Soderhall, K., and Cerenius, L. (1998). Role of the prophenoloxidase-activating system in invertebrate immunity. Curr Opin Immunol *10*, 23-28.

Steiner, H., Hultmark, D., Engstrom, A., Bennich, H., and Boman, H. G. (1981). Sequence and specificity of two antibacterial proteins involved in insect immunity. Nature *292*, 246-248.

Strynadka, N. C., and James, M. N. (1991). Lysozyme revisited: crystallographic evidence for distortion of an N-acetylmuramic acid residue bound in site D. J Mol Biol *220*, 401-424.

Taguchi, S., Ozaki, A., Nakagawa, K., and Momose, H. (1996). Functional mapping of amino acid residues responsible for the antibacterial action of apidaecin. Appl Environ Microbiol *62*, 4652-4655.

Takehana, A., Katsuyama, T., Yano, T., Oshima, Y., Takada, H., Aigaki, T., and Kurata, S. (2002). Overexpression of a pattern-recognition receptor, peptidoglycan-recognition protein-LE, activates imd/relish-mediated antibacterial defense and the prophenoloxidase cascade in *Drosophila* larvae. Proc Natl Acad Sci U S A *99*, 13705-13710.

Thunnissen, A. M., Isaacs, N. W., and Dijkstra, B. W. (1995). The catalytic domain of a bacterial lytic transglycosylase defines a novel class of lysozymes. Proteins *22*, 245-258.

Trenczek, T. (1998). Endogenous defense mechanism of insects. Zoology *101*, 298-315.

Ursic Bedoya, R. J., Mitzey, A. M., Obraztsova, M., and Lowenberger, C. (2005). Molecular cloning and transcriptional activation of lysozyme-encoding cDNAs in the mosquito *Aedes aegypti*. Insect Mol Biol *14*, 89-94.

Vernon, C. A. (1967). The mechanisms of hydrolysis of glycosides and their revelance to enzyme-catalysed reactions. Proc R Soc Lond B Biol Sci *167*, 389-401.

Waltzer, L., Bataille, L., Peyrefitte, S., and Haenlin, M. (2002). Two isoforms of Serpent containing either one or two GATA zinc fingers have different roles in *Drosophila haematopoiesis*. Embo J *21*, 5477-5486.

Weaver, L. H., Grutter, M. G., and Matthews, B. W. (1995). The refined structures of goose lysozyme and its complex with a bound trisaccharide show that the "goose-type" lysozymes lack a catalytic aspartate residue. J Mol Biol *245*, 54-68.

Werner, T., Liu, G., Kang, D., Ekengren, S., Steiner, H., and Hultmark, D. (2000). A family of peptidoglycan recognition proteins in the fruit fly *Drosophila melanogaster*. Proc Natl Acad Sci U S A *97*, 13772-13777.

Yang, X., and Cox-Foster, D. L. (2005). Impact of an ectoparasite on the immunity and pathology of an invertebrate: evidence for host immunosuppression and viral amplification. Proc Natl Acad Sci U S A *102*, 7470-7475.

Yoshida, H., Kinoshita, K., and Ashida, M. (1996). Purification of a peptidoglycan recognition protein from hemolymph of the silkworm, *Bombyx mori*. J Biol Chem *271*, 13854-13860.

Yoshiga, T., Georgieva, T., Dunkov, B. C., Harizanova, N., Ralchev, K., and Law, J. H. (1999). *Drosophila melanogaster* transferrin. Cloning, deduced protein sequence, expression during the life cycle, gene localization and up-regulation on bacterial infection. Eur J Biochem *260*, 414-420.

Yoshiga, T., Hernandez, V. P., Fallon, A. M., and Law, J. H. (1997). Mosquito transferrin, an acute-phase protein that is up-regulated upon infection. Proc Natl Acad Sci U S A *94*, 12337-12342.

Yu, X. Q., and Kanost, M. R. (2000). Immulectin-2, a lipopolysaccharide-specific lectin from an insect, *Manduca sexta*, is induced in response to gram-negative bacteria. J Biol Chem *275*, 37373-37381.